UNIVERSIDAD AUTÓNOMA DE MADRID

Programa de Doctorado en Biociencias Moleculares

Facultad de Ciencias

Control of Potato Tuberization by Gl and Proteins of the FT Family

TESIS DOCTORAL

Eduard Cruz Oró

Madrid, 2017

UNIVERSIDAD AUTÓNOMA DE MADRID

Programa de Doctorado en Biociencias Moleculares

Facultad de Ciencias

Control of Potato Tuberization by GI and Proteins of the FT Family

Memoria presentada por **Eduard Cruz Oró**

Licenciado en Biotecnología

para optar al grado de doctor en Biociencias Moleculares

Vº Bº del Director: Vº Bº del Tutor:

Salomé Prat Monguió **Marta Martín Basanta**

CENTRO NACIONAL DE BIOTECNOLOGÍA – CSIC

Madrid, 2017

Als meus pares i a la meva germana

"Una fructa hay en aquella tierra, por donde anduvo el mariscal don Diego de Almagro, de la otra parte del Cuzco, que la produçe de sí mesma la tierra; é son como ajes, redondos é tan gruessos como el puño, é llamánlos papas, é quieren paresçer turmas de tierra."

Gonzalo Fernández de Oviedo y Valdés
Primer Cronista del Nuevo Mundo

Historia Natural y General de las Indias,
Islas y Tierra-firme del Mar Océano (1535)

Aquest treball no hauria estat possible sense la gent que m'ha acompanyat durant aquests casi 7 anys de tesis, els quals m'han fet créixer científicament però sobretot m'han fet millor persona. A tots vosaltres, companys, amics, família, us vull donar les gràcies.

Gràcies Salomé per donar-me la oportunitat de fer la tesis al teu laboratori, per tot el que m'has ensenyat durant aquest anys, per creure en mi i estar sempre disposada a trobar solucions. Malgrat que en alguns moments la tesis no ha estat idíl·lica, sempre he sentit que podia comptar amb tu per tirar-la endavant.

A mis compañeros de piso, Marco, Isa y Guille, Rubén y Alex, por ser mi familia en Madrid y compartir mucho más que un simple alquiler.

Gràcies Alba per acompanyar-me en els inicis d'aquesta aventura madrilenya.

Gràcies a la colla de Molle, per fer-me sentir Mollerussenc malgrat la distància, i als "Masqueperros", Octavi, Jordi i Dani, per les escapades europees i els moments èpics. Who let the dogs out!

Gracias Lucía, la mejor "hater" cántabra, y Albert, "el punyeta", por ser un oasis de UdL en Madrid y compartir desde viajes locos a Salamanca hasta el estrés pre-tesis. Aunque tomemos caminos separados siempre nos quedarán esos lunes de Juego de Tronos.

A todo GMP, en especial al grupo de predocs por ser un grupo donde impera el buen rollo y donde las pequeñas cosas como los viernes en Psicología hacen mucho más llevaderos los días duros en el laboratorio.

Gracias al equipo de los PNAS por las pachangas de los jueves y los partidos de los domingos, en especial a Enrique, "el coach", que siempre ha tirado del carro para que el equipo siguiera adelante.

Al grupo de teatro NokAut, por las risas y el cachondeo escribiendo guiones, montando videos, ensayando y durante la propia obra. Espero que sigáis haciendo reír al CNB durante muchas fiestas más.

A la gente de mi laboratorio, a los nuevos y a los que se fueron. Gracias Abe y Cris Navarro por ayudarme a dar mis primeros pasos científicos. Gracias Cris Martínez por las risas, el "Wall of Shame" y las discusiones sobre "els Països". Gracias Pilar por transmitirme un poco de tu pensamiento "Alemán", por decir las cosas directas, por compartir estos años de tesis juntos. Gracias Cris Ni, has sido como una hermana para mí, gracias por los chistes, los viajes, las bromas de vestuario, por aguantar mis quejas…has hecho que una parte de mí no quiera irse nunca de Madrid.

A Carlos, “el tomate”, por ser un verdadero amigo. Gracias por el vacile, los chascarrillos y las noches de juerga, pero también por los consejos y el apoyo en los momentos difíciles. Pasarán los años, pero los trovadores seguirán cantando la de los gemelos golpean dos veces.

A Eli, por estar a mi lado en los momentos importantes siempre con una sonrisa. Por todos los momentos inolvidables juntos, gracias.

A la meva família, des de la iaia fins al padrí, però sobretot als meus pares Domingo i Neus, i a la meva germana Sònia, per donar-m’ho tot i fer-me sentir afortunat de tenir-los al meu costat. Tot el que he aconseguit és gràcies a vosaltres.

I would like to thank Dr. Salomé Prat for directing and supervising the work presented in this PhD thesis. Thanks also to all CNB facilities, especially to genomics, photography, *in vitro* culture and glasshouse. I also thank my colleague Dr. Ruth Sanz for performing the GUS staining experiments and sprout-length measurements. I would like to show my gratitude to Dr. Sophia Sonnewald and Uwe Sonnewald's group in University of Erlangen for performing the hybridization of all microarrays showed in this thesis. Thanks also to Dr. Christian Bachem for providing us 35S::StCDF1.2 transgenic lines. Finally, I would like to thank the CNAG-CRG lab. for performing the RNA-seq experiments and Dr. Glenn Bryan for giving me the opportunity to join his group at the James Hutton Institute and perform RNA-seq data analysis.

This work was carried out in the Plant Molecular Genetics Department of the Spanish National Center for Biotechnology and was supported by the Spanish Minister of Economy and Competitiveness (PhD Fellowship Ref. BES-2012-053812).

Summary

Potato is the fifth most important crop worldwide and is a staple food of critical relevance in terms of food security. The FT protein StSP6A is the main component of the "tuberigen" signal that is produced in the leaves and transported to the stolon to trigger tuber formation. In non-inductive LD photoperiodic conditions, StCOL1 inhibits tuberization by activating the FT protein StSP5G, engaged in repressing *StSP6A* transcription in the leaves. Identification of the *earliness* locus showed that expression of *StCOL1* is repressed by StCDF1. Allelic variants of *StCDF1* lacking the C-terminal StFKF1-interaction domain are not destabilized by the StFKF1-StGI complex and constitutively repress *StCOL1*.

Here, we have demonstrated that StGI plays a critical role in the photoperiodic tuberization pathway and in the control of plant maturity by mediating destabilization of StCDF1. Transgenic potato plants silenced in *StGI* expression accumulate higher levels of the StCDF1 protein and show reduced levels of expression of the *StCOL1*, *StCOL2* and *StSP5G* genes in LDs. Moreover, we show that silencing of *StGI* leads to activation of *StSP6A* and to changes in levels of expression of a large group of MADS-box factors, which act downstream of StSP6A in inducing tuberization and in conferring early maturity traits in potato. Furthermore, our studies revealed that, besides repressing *StSP6A* expression in the leaves, StSP5G regulates tuber shape likely by restricting cells undergoing differentiation, and its function is also required in mature tubers to preserve the shoot identity of tuber sprouts. Analysis of the gene regulatory network controlled by StSP5G demonstrates that this FT-like protein suppresses CK biosynthesis by repressing multiple isopentenyl transferase (*IPT*) genes, in addition to modulate a big set of MADS-box proteins in the leaves, tubers and in tuber sprouts. We have also demonstrated that warm temperatures inhibit tuberization by directly suppressing *StSP6A* expression in the leaves, while other regulators of the day-length pathway were not affected. We show that plants overexpressing *StSP6A* not only exhibit much higher tuber yields under warm temperatures but also show a reduced thermomorphogenic response. The transcriptomic analyses of these transgenic plants showed that StSP6A confers heat tolerance by repressing auxin, ethylene and jasmonic acid signalling, in addition to up-regulate photosynthesis and sugar export-related genes, thus evidencing an increased source capacity of leaves.

Overall, these studies provide important insights regarding function of the StGI, StSP5G and StSP6A proteins in photoperiod and temperature-dependent control of tuber formation, and show that MADS-box transcription factors are downstream activation targets of StSP6A. We showed that StSP6A overexpression largely overcomes negative effects of temperature on tuber yield, quality, and dormancy. Hence, these findings provide a basis for improvement of potato heat tolerance by selecting cultivars where *StSP6A* expression is not reduced under warm temperatures.

La patata es el quinto cultivo más importante a nivel mundial y es un alimento básico en términos de seguridad alimentaria. La proteína StSP6A es el principal componente de la señal de tuberización que se produce en las hojas y que posteriormente es transportada al estolón para inducir la tuberización. En condiciones no inductivas de días largos, StCOL1 inhibe la tuberización al activar la transcripción de *StSP5G*, que actúa como un inhibidor de la expresión de *StSP6A* en las hojas. La identificación del locus "*earliness*" ha demostrado que StCDF1 reprime a *StCOL1*. Variantes alélicas de *StCDF1* truncadas en el dominio C-terminal o de interacción con StFKF1 no son desestabilizadas por el complejo StFKF1-StGI y en consecuencia promueven una represión constitutiva del gen *StCOL1*.

En este trabajo, hemos demostrado que StGI juega un papel crítico en la vía fotoperiódica de tuberización y en el control de la madurez de la planta, al promover la desestabilización de StCDF1. Plantas transgénicas silenciadas en la expresión de StGI acumulan altos niveles de la proteína StCDF1 y muestran una inhibición de los genes *StCOL1*, *StCOL2* y *StSP5G* en días largos. Además, el silenciamiento de StGI activa el gen *StSP6A* y promueve cambios en los niveles de expresión de un gran número de factores MADS-box que actúan aguas abajo de StSP6A en la inducción de la tuberización y de caracteres de madurez. Nuestros estudios también han revelado que, además de reprimir la expresión de *StSP6A*, StSP5G regula la morfología del tubérculo y su función es necesaria para preservar la identidad de tallo de los brotes del tubérculo. El análisis de la red de genes controlados por StSP5G demuestra que este represor homólogo de *FT* suprime la biosíntesis de CKs mediante la represión de múltiples isopentenil transferasas (IPT), además de regular la expresión de un gran número de genes MADS-box en hojas, tubérculos y brotes. Además, hemos demostrado que las temperaturas elevadas inhiben la tuberización debido a que reprimen a *StSP6A* en las hojas, aunque no afectan a los demás reguladores de la vía fotoperiódica. Hemos visto que plantas que sobreexpresan StSP6A producen más tubérculos a altas temperaturas y muestran una menor termomorfogénesis. Los análisis de expresión génica muestran que StSP6A confiere termotolerancia debido a que reprime las vías de auxinas, etileno y ácido jasmónico, además de activar genes relacionados con la fotosíntesis y el exporte de azúcares, por lo que la capacidad de las hojas como fuente de carbono es mayor.

En conjunto, estos estudios proporcionan datos relevantes acerca de la función de StGI, StSP5G y StSP6A en el control de la tuberización, y muestran que los factores MADS-box actúan aguas abajo de StSP6A. Hemos demostrado que StSP6A revierte los efectos negativos de la temperatura sobre la producción, calidad del tubérculo y tiempo de dormición. Así, estos hallazgos indican que los genotipos en los que la expresión de StSP6A no se vea reducida por calor, debieran ser más tolerantes a temperatura.

Index

Abbreviations

ABA – Abscisic acid

AG – AGAMOUS

AGL – AGAMOUS-LIKE

AOS – Allene oxide synthase

AP – APETALA

ARF– AUXIN RESPONSE FACTOR

BAM – β-amylase

bHLH – Basic helix-loop-helix

BiFC – Bimolecular Fluorescence Complementation

BLAST – Basic local alignment search tool

bp – Base pairs

BRC1 – BRANCHED 1

bZIP – Basic leucine zipper domain

CAB – Chlorophyll a/b binding protein

CAPS – Cleavage amplified polymorphic sequence

CCA1 – CIRCADIAN CLOCK ASSOCIATED 1

CCD – Carotenoid cleavage dioxygenase

CCT – CO, CO-LIKE and TOC1

CDF – CYCLING DOF FACTOR

cDNA – complementary DNA

CDPK – Calcium-dependent protein kinase

CEN – CENTRORADIALIS

CETS – CENTRORADIALIS, TERMINAL FLOWER 1 and SELF-PRUNING

CK – Cytokinin

CKX – Cytokinin oxidase

CO – CONSTANS

COI – CORONATIVE INSENSITIVE 1

COL – CO-LIKE

COP1 – CONSTITUTIVE PHOTOMORPHOGENIC 1

CRISPR – Clustered regularly interspaced short palindromic repeats

CRY – CRYPTOCHROME

cv – cultivar

DEF – DEFICIENS

DEGs – Differentially expressed genes

DNA – Deoxyribonucleic acid

DNP – Day-neutral plant

Ehd1 – EARLY HEADING DATE 1

ELF3 – EARLY FLOWERING 3

ERF – ETHYLENE RESPONSE FACTOR

ET – Ethylene

FAC – Florigen activator complex

FC – Fold change

FD – FLOWERING LOCUS D

FIP1 – FT-INTERACTING PROTEIN 1

FKF1 – FLAVIN-BINDING, KELCH REPEAT, F-box 1

FLC – FLOWERING LOCUS C

FQC – Floral quartet-like complex

FR – Far red light

FT – FLOWERING LOCUS T

FUL – FRUITFULL

GA – Gibberellin

GAox – Gibberellin oxidase

Ghd7 – GRAIN NUMBER, PLANT HEIGHT AND HEADING DATE 7G

GI – GIGANTEA

GUS – β-Glucuronidase

HA – Hemagglutinin

Hd1 – HEADING DATE 1

Hd3a – HEADING DATE 3A

HOS1 – HIGH EXPRESSION OF OSMOTICALLY RESPONSE GENE 1

HSF – Heat shock factor

HSP – Heat shock protein

i – RNA interference

IAA –INDOLE-3-ACETIC ACID INDUCIBLE

ID1 – INDETERMINATE 1

IPT– Isopentenyltransferase

JA – Jasmonic acid

JAZ – JASMONATE-SIM-DOMAIN PROTEIN

LAX – LIKE AUX1

LD – Long day

LDP – Long day-plant

LFY – LEAFY

LHY – LATE ELONGATED HYPOCOTHYL

LKP2 – LOV KELCH REPEAT PROTEIN 2

LOB – LATERAL ORGAN BOUNDARIES

LOG1 – LONELY GUY 1

MADS – MCM1, AG, DEF and SRF

MC – MACROCALYX

MCM1 – MINICHROMOSOME MAINTENANCE FACTOR 1

MEX – MALTOSE EXCESS

MFT – MOTHER OF FT

miR – microRNA

NB – Night break

NF-Y – NUCLEAR FACTOR Y

ox – overexpression

P2P – PANICLE PHYTOMER 2

PCR – Polymerase chain reaction

PEBP – Phosphatidylethanolamine-binding protein

Pfr – Phytochrome far red

PHL – PHYTOCHROME-DEPENDENT LATE-FLOWERING

PHY – PHYTOCHROME

PI – PISTILATA

PIF4 – PHYTOCHROME INTERACTING FACTOR 4

PIM – PROLIFERATING INFLORESCENCE MERISTEM

PIN – PIN-FORMED

POTM1 – Potato MADS box 1

Pr – Phytochrome red

PRR – PSEUDO-RESPONSE REGULATOR

PSII – Photosystem II

qPCR – Quantitative PCR

QTL – Quantitative trait locus

R – Red light

RFT1 – RICE FT-LIKE1

RNA – Ribonucleic acid

RPT5 – REGULATORY PARTICLE TRIPLE-A ATPASE 5

RQ – Relative quantification

SAUR – Small auxin-up RNA

SBPase – SEDOHEPTULOSE-BISPHOSPHATASE

SD – Short day

SDP – Short-day plant

SEP – SEPALLATA

SEX – STARCH EXCESS

SFT – SINGLE FLOWER TRUSS

SL – Strigolactone

SNP – Single nucleotide polymorphism

SOC1 – SUPPRESSOR OF OVEREXPRESSION OF CO 1

SP – SELF-PRUNING

SPA1 – SUPRESSOR of PHYTOCHROME A

SPP – Sucrose phosphatase

SPS – Sucrose-phosphate synthase

SQUA – SQUAMOSA

SRF – SERUM RESPONSE FACTOR

SRG1 – SENESCENCE RELATED GENE 1

SUS – Sucrose synthase

SVP – SHORT VEGETATIVE PHASE

TEM – TEMPRANILLO

TFL1 – TERMINAL FLOWER 1

TOC1 – TIMING OF CAB EXPRESSION 1

tRNA – transfer RNA

UNS – UNSHAVEN

WT – Wild type

ZT – Zeitgeber time

ZTL – ZEITLUPE

Introduction

1. The potato crop

Potato (*Solanum tuberosum* L.) is an herbaceous annual plant belonging to the *Solanaceae* family which is cultivated worldwide for its edible tubers. The *Solanaceae*, commonly called nightshades, is a family of flowering plants globally distributed that include cultivated species of unquestionable agricultural interest. Besides potato, tomato (*Solanum lycopersicum* L.), aubergine (*Solanum melongena* L.), pepper (*Capsicum annuum* L.) and tobacco (*Nicotiana tabacum* L.) are nightshades with substantial agronomic and economic importance.

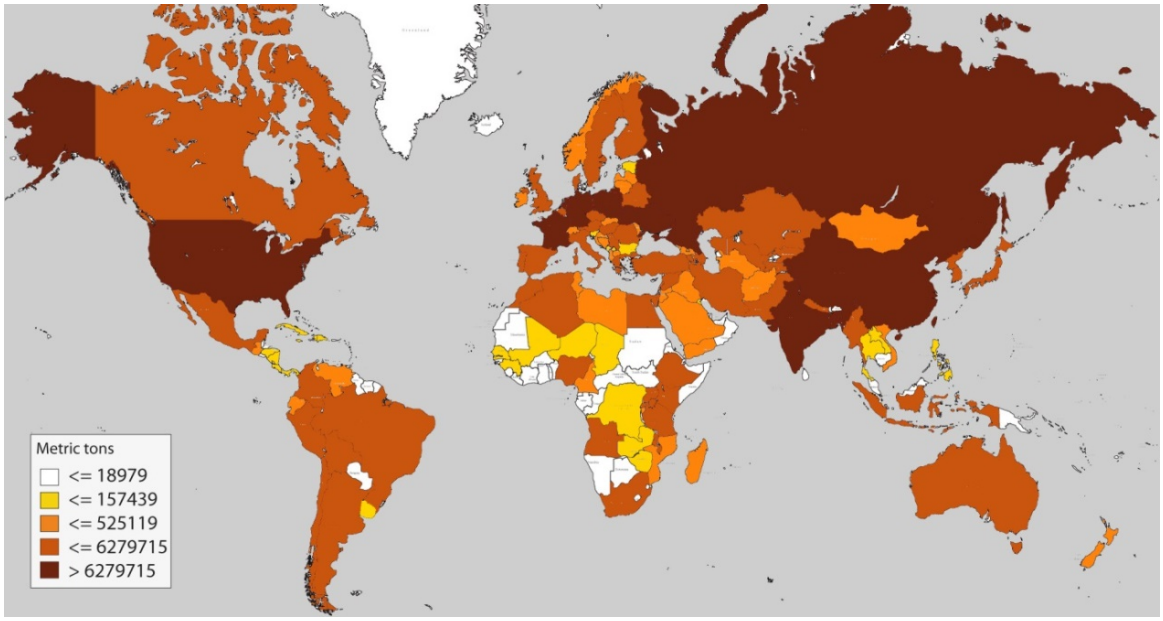

Figure 1. Global potato production. World map representing the metric tons of potato tubers produced by each country in 2014 (adapted from http://faostat3.fao.org/).

Potato is indigenous from the Andean regions of South America and it was first domesticated in the highlands Peru by pre-Columbian civilizations around 10000 years ago (Spooner et al., 2005). Potato was brought to Europe in the 16th century during the Spanish conquest of Meso- and South America and since then, its cultivation has been growing and has spread all over the world. In 2014, potato production reached more than 380 million metric tons, being the fifth most important crop in terms of global production after wheat (*Triticum aestivum* L.), rice (*Oryza sativa* L.), maize (*Zea mays* L.) and sugar cane (*Saccharum officinarum* L.) (http://faostat3.fao.org/). Nowadays, Asia produces almost half the global harvest of potato tubers; however, potato remains an essential crop in Europe where its production per capita is still the highest in the world (http://faostat3.fao.org/) (Figure 1).

Potato tubers accumulate high amounts of starch, are a good source of vitamins B1, B3 and B6, are low fat and, with respect to cereals, are richer in vitamin C while show a more equilibrated composition in essential aminoacids (US Department of Agriculture, National Nutrient Database). As such, they are used for human and animal consumption, and also to obtain alcohol or starch for multiple industrial applications.

Due to its nutritional properties and relative low farming demands, potato is currently a staple food in several developing countries and is considered a critical crop in terms of food security (Birch et al., 2012). Thus, understanding how initiation and growth of potato tubers is regulated is an important goal to meet the nutritional demands of a rising world population, besides being a fundamental question in developmental biology.

2. Tuber formation

During evolution, several plant species have acquired the capacity of differentiate their leaves, stems or roots into storage organs. Formation of these organs is induced by adverse environmental conditions that compromise plant viability and usually provides a survival strategy to the plant, as a system of asexual propagation. In most cases, storage organs remain dormant in soil during the cold or dry season to be reactivated in the next favourable season and generate a new plant that is genetically identical to the mother plant. Thus, in order to sustain initial growth of these shoots, tubers accumulate a large amount of metabolic resources in the form of starch or soluble sugars.

Out of 1500 species of *Solanaceae*, 150 have the ability to produce tuber-like storage organs being potato the most extendedly cultivated (Bohs, 2007). Potato tubers are swollen underground stems with short internodes and scale leaves subtending the dormant axillary buds, commonly called tuber eyes. These storage organs develop from specialized stems called stolons, which grow diagravitropically in the soil from the base of the main stem. Tuber formation is promoted by long nights, cool temperatures and low rates of nitrogen fertilization (Rodriguez-Falcon et al., 2006). However, endogenous factors as the physiological age of the seed tuber or the genetic background have also remarkable effects on tuberization time (Asiedu et al., 2003).

At the onset of tuberization, stolons cease their longitudinal growth and start to radially expand in their subapical region (Cutter, 1978). This involves an initial enlargement and longitudinal division of the pith and cortex cells located below the stolon apical meristem, followed by an enlargement and randomly oriented division of the cells at the perimedullary region (Xu et al., 1998b). After the first visible signs of tuber formation, a switch in the mechanism of sucrose phloem unloading from apoplastic to symplastic is observed in the

stolon, and this is accompanied with a reduction in cell wall invertase activity and an increase in the sucrose synthase and fructokinase enzymes (Appeldoorn et al., 2002; Viola et al., 2001). During the bulking phase, tubers accumulate large amount of starch and storage proteins, and massive transcriptomic changes are observed in these organs including the activation of multiple starch biosynthetic enzymes, storage glycoproteins and proteinase inhibitor genes (Kloosterman et al., 2008; Prat et al., 1990; Visser et al., 1994).

New formed tubers undergo a period of dormancy characterized by the absence of any bud growth. Length of this endodormancy period is determined by multiple environmental, physiological and hormonal factors (Sonnewald and Sonnewald, 2014), acquisition of bud break competence leading to sprouting and the generation of new shoots. With the onset of sprouting, multiple transcriptomic and metabolic changes are again induced in the tuber, as the activation of enzymes involved in photorespiration and starch breakdown, which promote the remobilization of stored reserves to support bud growth and the development of a new plant (Campbell et al., 2008; Sonnewald and Sonnewald, 2014; Viola et al., 2007).

3. Photoperiodic control of tuberization

Photoperiod is defined as the amount of light and dark hours in a daily cycle of 24 h. The angle of rotation of the earth in its orbit around the sun makes photoperiod to change during the year in all latitudes except in the equator. Photoperiod is therefore a highly reliable indicator of the time of the year and is used by plants to schedule their developmental processes to environmental conditions (Jackson, 2009). Based on their response to photoperiod, plants can be divided into three major groups. Long-day plants (LDP), in which response is induced when the day exceeds a critical length; Short-day plants (SDP) in which response is induced when the day is shorter than a critical length; and Day-neutral plants (DNP) which do not respond to photoperiod.

Besides flowering and bud set, tuberization is one of the most important developmental processes regulated by photoperiod in plants. In their natural habitat, potato tubers are formed between autumn and early winter, and remain dormant in soil until next spring in which they sprout and generate a new plant. Hence, to ensure that dormancy overlaps with the cold winter, tuber formation is triggered in response to day-length shortening (Figure 2).

Andean potatoes landraces (*Solanum tuberosum* L. ssp. *andigena*) are native from highlands Peru, where day-length remains close to 12 h all over the year due to proximity to the equator and temperatures are low at night. These plants are adapted to short days (SDs)

and cool temperatures and do not produce tubers under the longer summer days of temperate zones or warm temperatures of tropic lowlands. Chilean potato landraces (*Solanum tuberosum* L. ssp. *tuberosum*) originally from lowlands of South-Central Chile, are more adapted to long days (LDs) and are best suited for cultivation in temperate zones of Europe or North America. Modern potato cultivars were generated by crossing Andean and Chilean landraces, and ability to tuberize under long days probably was one of the first selected traits. Repetitive selection for tuber formation in long days led to the Neo-tuberosum genotypes, more closely related to the Chilean than Andean landraces (Ghislain et al., 2009). Short days and cool temperatures, however, still accelerate tuber formation in most of these cultivars.

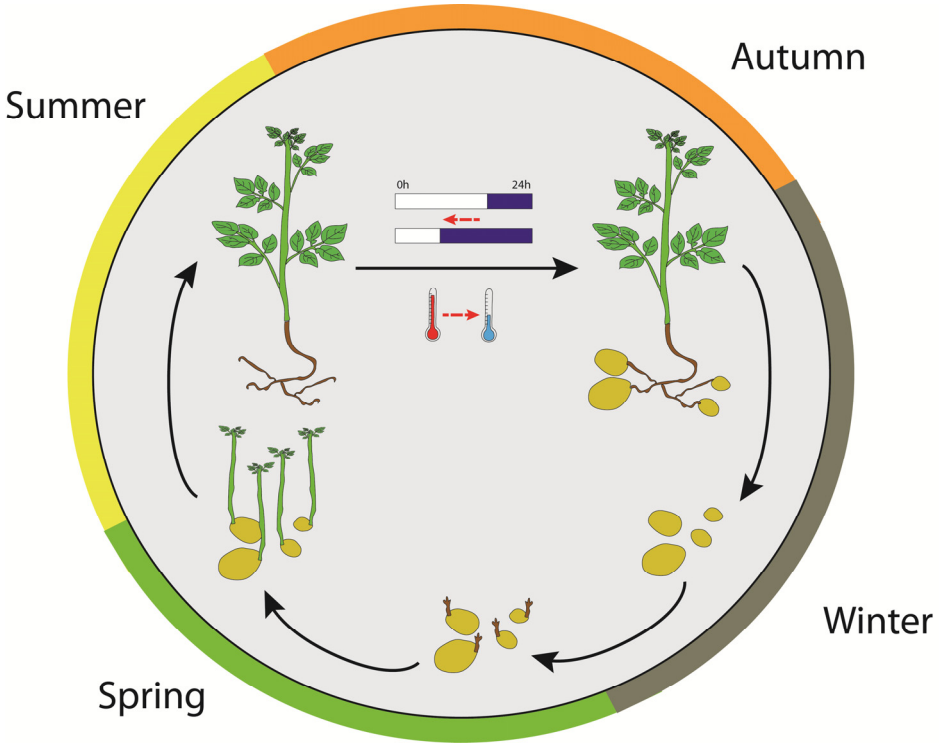

Figure 2. Potato life cycle. Schematic representation of the life cycle of potato and tuberization induction. Tuber formation is usually induced between autumn and early winter in response to day-length shortening and cool temperatures. Tubers remain dormant in soil during the cold winter and after bud break regenerate new shoots in the next spring.

Because of their tight day-length control of tuberization, *Andigena* plants are an excellent model to the study of the signalling mechanisms controlling tuber formation in potato. These plants are strictly dependent on SDs for tuberization (8 h light/ 16 h dark) and do not produce tubers when grown under LD conditions (16 h light/ 8h dark) or when long nights are interrupted with a pulse of light, which is called a night break (NB) (Rodriguez-

Falcon et al., 2006). Among all light qualities, red light (R) is the most effective in repressing tuber formation in a night break. Also, the repressive effect of a R light pulse is reversed by the immediate application of an additional pulse of far red light (FR), evidencing that length of the night is mostly sensed by phytochromes (Batutis and Ewing, 1982).

Phytochromes are soluble dimeric proteins with a tetrapyrrole chromophore linked to an invariant Cys located to the N-terminal half the protein. Intrinsic photochemical activity of this prosthetic group allows conversion between two forms of different biological activity. Phytochromes are synthesized in the inactive (Pr) form that localizes in the cytosol. Upon light irradiation, R light absorption converts these proteins to the active (Pfr) form, that is translocated into the nucleus, rapidly activating light-responsive gene expression. Phytochromes may function as light-regulated serine/threonine kinases, and *in vitro* can phosphorylate several substrates, including themselves. In darkness, the nuclear Pfr form is slowly converted back to Pr and this reversion is faster in response to FR or low R/FR ratios, which allows these photoreceptors to function as R/FR-dependent molecular switches (Li et al., 2011; Viczian et al., 2016).

Andigena lines with reduced levels of *PHYB* are almost day-length insensitive and tuberize under non-inductive LD and NB conditions (Jackson et al., 1996). Moreover, reduced levels of *PHYA* in the cv.*Desiree* leads to an early tuberization response when days are extended with FR+R light, evidencing that both PHYA and PHYB play an important role in the photoperiodic control of tuberization (Yanovsky et al., 2000).

4. FT-like proteins

Initial grafting experiments using *Andigena* plants showed that day-length is perceived in the leaves and that, under inductive SD conditions, a mobile signal or “tuberigen” is synthesized in these organs and transported to the underground stems to induce tuber formation (Chapman, 1958). Flowering tobacco scions were shown to promote tuber formation when grafted onto non-induced *Andigena* stocks, indicating that the mobile tuberization signal shares conserved elements with the mobile flowering signal or “florigen” (Chailakhyan et al., 1981).

Studies in the model plant *Arabidopsis thaliana* (L.) Heynh., which is facultative LD for flowering, showed that the small protein FLOWERING LOCUS T (FT) is a major component of the “florigen” signal. FT is activated in the leaves in LD conditions and is transported via the phloem to the shoot apical meristem, where it interacts with the bZIP factor FLOWERING LOCUS D (FD) to promote expression of the floral meristem genes *AP1* and *SOC1* (Andres and Coupland, 2012; Turck et al., 2008).

FT belongs to the CETS (CENTRORADIALIS (CEN), TERMINAL FLOWER 1 (TFL1) and SELF-PRUNING (SP)) protein family, a group of proteins that share similitude with phosphatidylethanolamine-binding proteins (PEBPs) (Karlgren et al., 2011). PEBPs are present in all taxa from bacteria to animals and plants, and act in most cases as regulators of signalling pathways controlling growth and differentiation (Chautard et al., 2004; Yeung et al., 1999). Whereas *Arabidopsis* CETS proteins are encoded by six genes; this family appears to have undergone a preferential expansion in the *Solanaceae*, 15 and 13 different CETS-coding genes being identified in potato and tomato respectively (Abelenda et al., 2014). Members of this family are divided into 3 major clades, the FT clade, the TFL1 clade and the MOTHER OF FT (MFT) clade. Phylogenetic studies revealed that MFT-like proteins are the ancestral form of these genes in plants, whereas FT- and TFL1-like proteins are the result of two gene duplication events, one occurred before the appearance of seed-producing plants, and a second one that occurred exclusively in the angiosperm lineage (Karlgren et al., 2011). Despite sharing a high degree of protein identify, FT-like and TFL1-like proteins play opposite roles in floral transition, promoting or preventing flowering respectively (Kobayashi et al., 1999; Pnueli et al., 1998). This functional divergence lies on specific motifs in the protein, such as amino acid position 85 in exon 2, and the external P-loop segment B region in exon 4, apparently involved in protein partner interactions (Ahn et al., 2006; Hanzawa et al., 2005) (Figure 3B).

The FT-like SINGLE FLOWER TRUSS (SFT) protein in tomato and its potato ortholog StSP3D, promote flowering in day-neutral tomato and potato plants (Lifschitz and Eshed, 2006; Molinero-Rosales et al., 2004; Navarro et al., 2011). Noteworthy, potato is a SD plant for tuberization but is able to flower in LDs if grown under high light irradiance conditions, and this correlates with activation of StSP3D.

The potato *StSP6A* protein, groups into the FT clade, and studies in *Andigena* showed that it corresponds to the mobile tuberization signal (Navarro et al., 2011). In *Andigena* plants, *StSP6A* is exclusively expressed under SD conditions and is regulated by an autorelay mechanism that activates its own expression in underground stolons (Navarro et al., 2011). In *Neo-tuberosum* genotypes, a second allele, *StSP6A-a2*, differing from the *Andigena StSP6A* gene in intron size and in various nucleotide polymorphisms was identified. In contrast to *StSP6A*, *StSP6A-a2* is expressed in LDs, hence suggesting that this gene contributes to the ability of the *Neo-tuberosum* germplasm to tuberize in LDs (Morris et al., 2014).

The potato StSP5G FT-like protein has been recently described as a tuberization repressor (Abelenda et al., 2016). *StSP5G* is expressed in *Andigena* plants only under LD or NB conditions and its inhibition results in mild activation of *StSP6A* in leaves and in tuber

formation under non-inductive LDs (Abelenda et al., 2016). Although FT-like proteins have long been considered to act as flowering promotors, additional FT-like genes with a repressive role in flowering have been by now identified in several plant species. In sugar beet (*Beta vulgaris* L.), the FT-like gene *BvFT1* is highly expressed in leaves before vernalization and represses expression of another FT-like gene, *BvFT2*, which is a floral inducer (Pin et al., 2010). Notably, antagonistic function of *BvFT1* and *BvFT2* rely upon divergent amino acidic residues within their external segment B region, as reported for the *FT* and *TFL1* clade proteins in *Arabidopsis* (Ahn et al., 2006; Pin et al., 2010). In tobacco, four FT-like proteins act also antagonistically to regulate floral initiation, *NtFT-1*, *NtFT-2* and *NtFT-3* being shown to act as floral repressors while *NtFT-4* has a flowering promoter function (Harig et al., 2012). Flowering and bulb formation are likewise regulated by independent FT-like proteins in onion (*Allium cepa* L.). In this monocot species, flowering is regulated by the FT-like protein *AcFT2* which is activated by vernalization, whereas bulb formation is regulated by two FT-like proteins, *AcFT1* and *ActFT4*, with antagonistic functions. *AcFT4* expression is regulated by photoperiod and suppresses activation of *AcFT1* in leaves, shown to encode the mobile signal for bulb formation (Lee et al., 2013). A repressive *FT* paralog, *GmFT4*, also controls flowering in soybean (*Glicine max* L.), apparently by preventing activation in leaves of the two FT-like flowering activators, *GmFT2a* and *GmFT5a* (Zhai et al., 2014). Furthermore, domesticated sunflower (*Helianthus annuus* L.) carries a frame-shift mutation in the *HaFT1* gene, which in WT represses flowering by interfering with the FT flowering inducer *HaFT4* (Blackman et al., 2010).

In tomato, three FT family genes, *SlSP5G*, *SlSP5G2* and *SlSP5G3*, have been shown to have flowering repressing activity, *SlSP5G* being mainly expressed under LDs, while *SlSP5G2* and *SlSP5G3* are induced under SDs (Cao et al., 2015). CRISPR/cas9-induced mutations in *SlSP5G* were recently shown to result in early flowering and slight activation of *SFT* expression in leaves, providing evidence that tomato *SlSP5G* and *SFT* show a similar antagonistic function as that reported for *StSP5G* and *StSP6A* in potato (Abelenda et al., 2016; Soyk et al., 2017).

As seen for *BvFT1*, FT-like proteins with a repressive function differ from those promoting flowering, tuberization or bulb formation, in several residues at the external P-loop segment or B region, suggesting that plasticity in this part of the protein contributes to their different activity (Figure 3A). Sequence alignment revealed two conserved sites that determine inducer function of FT-like proteins; a tyrosine at position 134 and a tryptophan at position 138, in the *Arabidopsis* FT protein (Abelenda et al., 2016; Wickland and Hanzawa, 2015). Elucidate why these residues are essential for activation or repressive function and establish whether they determine a distinctive FT-partner interaction are two major

challenges in future studies aimed to uncover the molecular mechanism of action of FT proteins.

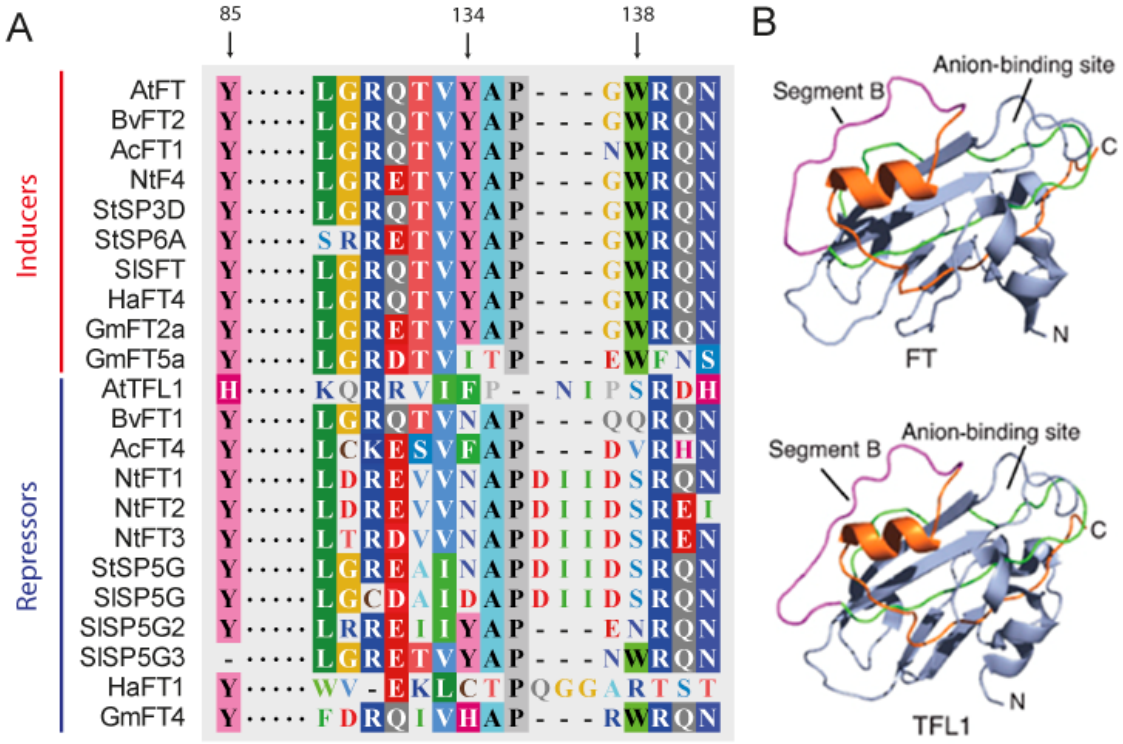

Figure 3. Amino acid sequence comparison of the external P-loop region of FT proteins with antagonistic functions. (A) Amino acid sequence alignment of the conserved segment B of different FT paralogs with inductive and repressive functions. All FT proteins with an inducer function, except *GmFT5a*, contain tyrosine at positions 85 and 134 and tryptophan at position 138. Amino acid positions are based on the *Arabidopsis* FT protein sequence. At (*Arabidopsis thaliana*), Bv (*Beta vulgaris*), Ac (*Allium cepa*), Nt (*Nicotiana tabacum*), St (*Solanum tuberosum)*, Sl (*Solanum lycopersicum*), Ha (*Helianthus annuus*), Gm (*Glycine max*) (adapted from Wickland and Hanzawa, 2015) (B) Cartoon diagrams of the crystal structure of the *Arabidopsis* FT and TFL1 proteins. Segment B (coloured in magenta) is in close proximity to the functionally critical Tyr85/His88 and the residues comprising the potential ligand-binding site of the FT and TFL1 proteins (adapted from Ahn et al., 2006).

5. FT regulation by photoperiod

5.1 FT regulation in *Arabidopsis*, a LDP model

The molecular mechanisms by which plants regulate *FT* expression in response to day-length conditions have been best characterized in *Arabidopsis* (Andres and Coupland, 2012). In this facultative LD plant, the B-box zinc finger CCT (for CO, CO-LIKE and TOC1)-domain CONSTANS (CO) factor has been shown to activate *FT* expression in the leaf vasculature. The CO factor activates *FT* by directly binding two conserved TGTG(N2-3)ATG (CORE) elements in the proximal *FT* promoter region, the CO CCT-domain being shown to

be required for DNA-binding capacity of this protein (Tiwari et al., 2010). CO has been shown to interact with factors of the NUCLEAR FACTOR-Y (NF-Y) family, complex formation with these regulators being proposed to recruit CO to the *FT* promoter by increasing its DNA binding affinity (Ben-Naim et al., 2006; Wenkel et al., 2006). Indeed, various distal NF-Y CCAAT-recognition elements were identified in the *FT* promoter, and at least one of these elements proved to be essential for CO-mediated activation of *FT* (Cao et al., 2014).

CO expression is regulated by the circadian clock, light stabilization of the protein ensuring specific activation of *FT* under floral-inductive LDs. As such, coincidence of increased transcript levels with daytime provides a simple and elegant molecular mechanism to the 'external coincidence' model proposed by E. Bunning in 1936 to explain photoperiodic sensitivity (Bünning E, 1936). Two circadian oscillator-controlled proteins, the ubiquitin ligase FLAVIN-BINDING, KELCH REPEAT, F-box 1 (FKF1) and the plant-specific protein GIGANTEA (GI), were described to control diurnal *CO* expression by modulating stability of CYCLING DOF FACTORs (CDFs), that function to repress *CO* transcription (Sawa et al., 2007). In LDs, peaks of *FKF1* and *GI* expression coincide during late afternoon and blue-light promotes FKF1 and GI interaction, with the FKF1-GI complex shown to mediate ubiquitination of the CDFs and subsequent degradation of these repressors via proteasome, thus leading to up-regulation of *CO*. Timing of *FKF1* and *GI* expression is out of phase in SDs, due to *FKF1* is expressed mainly at night, and rise in *CO* expression during LD afternoon is therefore not observed (Sawa et al., 2007).

Light also controls CO activity by regulating stability of the protein. In the dark, CO is ubiquitinated and marked for degradation by the CONSTITUTIVE PHOTOMORPHOGENIC 1 (COP1)-SUPRESSOR of PHYTOCHROME A (SPA1) E3 ubiquitin ligase complex (Jang et al., 2008; Laubinger et al., 2006). Activity of this complex is inhibited by light, in part due to the action of *CRY1*, *CRY2* and *PHYA* (Lian et al., 2011; Sheerin et al., 2015; Zuo et al., 2011). Besides exerting a control on *CO* transcription, *FKF1* has been reported to interact at the protein level with CO and contribute to its stabilization in blue light (Song et al., 2012). More recently, the PSEUDO RESPONSE REGULATOR (PRRs) CCT-domain factors were also reported to interact with CO and promote accumulation of the protein in LDs (Hayama et al., 2017). Conversely, PHYB negatively regulates CO stability in the morning, probably by promoting degradation of the protein via the ubiquitin ligase HIGH EXPRESSION OF OSMOTICALLY RESPONSE GENE 1 (HOS1) (Lazaro et al., 2012). Notably, this PHYB effect is suppressed in the afternoon by PHYTOCHROME-DEPENDENT LATE-FLOWERING (PHL), which regulates photoperiodic flowering by forming a complex with both PHYB and CO in red light (Endo et al., 2013). Thus, CO specifically activates *FT* during LDs

afternoon, due to the coincidence of light that stabilizes the CO protein, and peak phase of *CO* transcription (Sawa et al., 2007) (Figure 4).

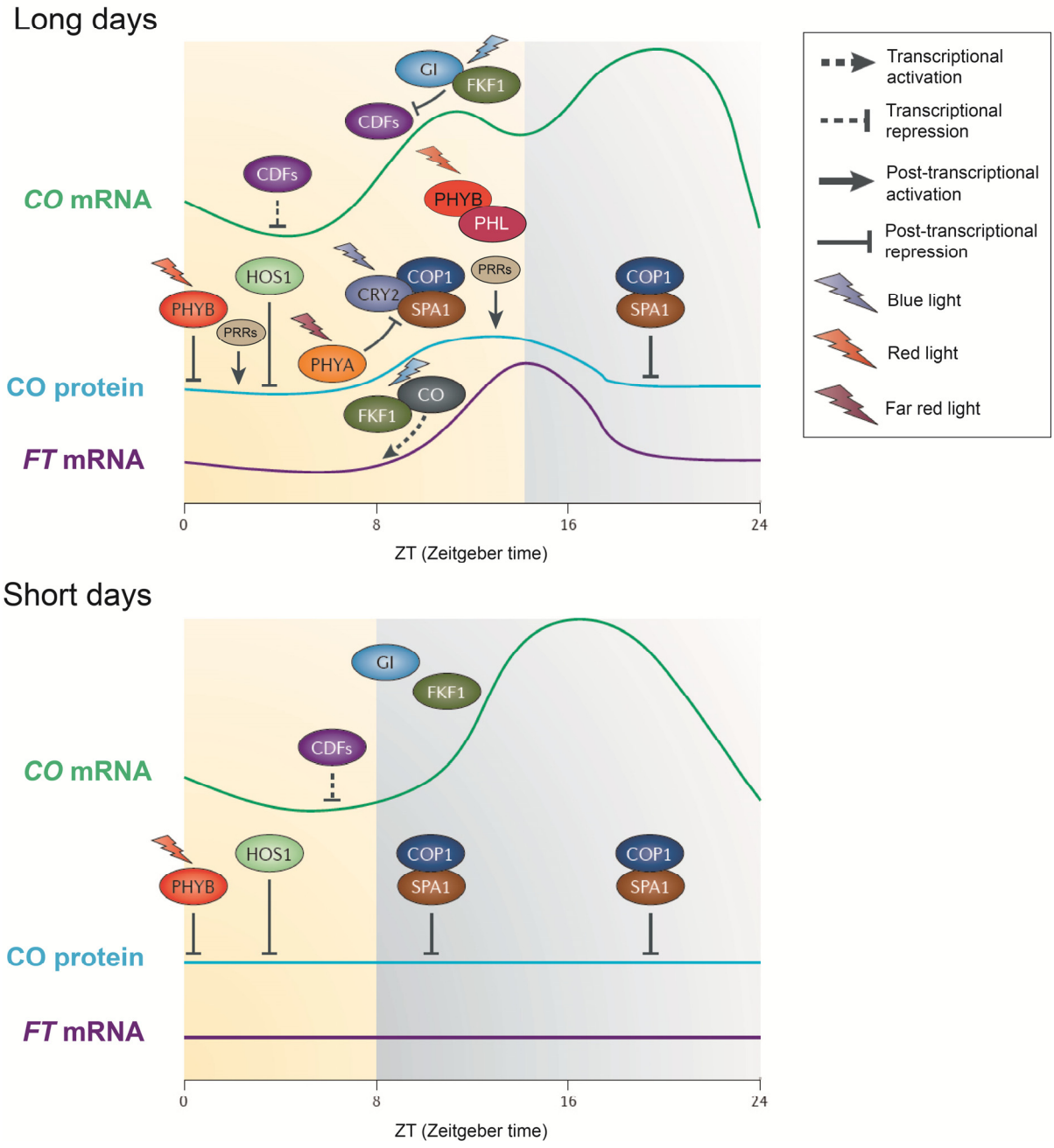

Figure 4. Photoperiodic regulation of *CO* activity in *Arabidopsis*. Transcriptional and post-transcriptional regulation of CO ensures *FT* activation specifically in LDs. *CO* transcription is repressed by the CDFs proteins and this repression is released in the LDs afternoon, due to CDFs degradation by the GI-FKF1 complex formed in response to blue light. CDFs degradation does not occur in SDs, since *FKF1* is mainly expressed during the night. CO protein degradation is triggered by the COP1-SPA complex during the night and by PHYB and HOS1 in the morning. CRY1, CRY2 and PHYA promote CO protein accumulation by inhibiting the COP1-SPA complex. PRRs also mediate CO protein accumulation under LDs. Later in the day, CO protein is stabilized by PHL, which suppresses PHYB-dependent degradation of CO, and by FKF1 (adapted from Andres and Coupland, 2012).

Noteworthy, *GI*, *FKF1*, and *CDF1* were also reported to directly bind the *FT* promoter and regulate *FT* transcription independently of *CO*. Indeed, *FKF1* has been demonstrated to contribute to *FT* activation, by removing the *CDF1* repressor from the *FT* promoter, while *GI* would directly promote *FT* expression by regulating protein stability of other *FT* repressors such as SHORT VEGETATIVE PHASE (SVP) or TEMPRANILLO (TEM) 1 and 2 (Sawa and Kay, 2011; Song et al., 2012).

5.2 FT regulation in rice, a SDP model

The day-length pathway for *FT* activation is remarkably conserved between *Arabidopsis* and rice, despite the different day-length requirements for flowering of these plants (Andres and Coupland, 2012; Tsuji et al., 2013). Rice is a SD plant, and it is somehow surprising that the *CO* homolog HEADING DATE 1 (Hd1) shows a similar expression pattern as At*CO*, hence displaying a peak of expression that coincides in LDs with late afternoon and in SD with the night. Actually, Hd1 induces flowering in SDs by activating the *FT*-like HEADING DATE 3 (Hd3a) “florigen” gene at night. However, unlike *Arabidopsis*, Hd1 acts as well as a flowering repressor and inhibits *Hd3a* expression in LDs (Izawa et al., 2002). The switch in Hd1 activity from an activator to repressor is dependent on PHYB activity and occurs in LDs because of the coincidence of *Hd1* transcription with light.

Overexpression of the *GI*-like *OsGI* gene in transgenic rice plants induces *Hd1* expression independently of day-length conditions, proving that function of GI in the regulation of *CO* expression is conserved in SD-flowering (Hayama et al., 2003). However, novel mechanisms for photoperiodic control of flowering were also recruited during rice domestication, since various genes with no clear ortholog in *Arabidopsis* control expression of *Hd3a* and its paralogue RICE FT-LIKE1 (RFT1) in response to day-length and independently of *Hd1*. One of these genes, the B-type response regulator EARLY HEADING DATE 1 (Ehd1) activates *Hd3a* and *RFT1* expression under SDs and LDs, respectively. Notably, transcription of this gene is controlled by another rice protein with no obvious *Arabidopsis* counterpart, the CCT-domain GRAIN NUMBER, PLANT HEIGHT and HEADING DATE 7 (Ghd7) repressor (Doi et al., 2004; Xue et al., 2008). Ghd7 strongly represses *Ehd1* transcription and expression of this gene responds to red light pulses with a different gating window depending on day-length (Itoh et al., 2010). Peak of *Ghd7* inducibility coincides with dawn in LD, but is shifted to midnight in SD conditions. Hence, morning expression of *Ghd7*, represses *Ehd1* and prevents *Hd3a* activation specifically in LDs (Itoh et al., 2010). Still, transcription of *Ehd1* is modulated by additional upstream regulators, including other repressors like *OsCOL4* and transcriptional activators such as INDETERMINATE 1 (*OsID1*) and *OsMADS50* (Shrestha et al., 2014; Tsuji et al., 2013).

5.3 FT regulation in potato

Activation of the *StSP6A* tuberization signal in potato is also controlled by a CO-like homolog. Actually, three *CO*-like homologues organized in tandem on chr02 have been identified in potato, of which only *StCOL1* and *StCOL2* are expressed to detectable levels. StCOL1 and StCOL2 share highly conserved B-box and CCT-domains but differ in the length of a poly-Q stretch located between these regions. Both of these proteins were shown to bind a consensus TGTGGT element, that is related to the TGTG(N2-3)ATG CORE element recognized by the *Arabidopsis* CO protein (Abelenda et al., 2016; Tiwari et al., 2010). Notably, *StCOL1* and *StCOL2* show different diurnal expression patterns. *StCOL2* peaks at dusk, and therefore its expression resembles that of the rice *Hd1* or *Arabidopsis CO* genes, while *StCOL1* displays a sharp peak of expression at dawn, hence mimicking the diurnal expression patterns of *Arabidopsis COL1* and *COL2* (Abelenda et al., 2016; Simon et al., 2015).

Transgenic *Andigena* plants silenced for *StCOL1* expression were shown to tuberize in LDs and accumulate high levels of the *StSP6A* transcript in leaves, which demonstrates that StCOL1 represses *StSP6A* expression and therefore acts as a tuberization repressor under LDs (Navarro et al., 2011). However, in contrast to Hd1, StCOL1 does not seem to activate *StSP6A* expression in SDs, since levels of *StSP6A* are similar in WT and *StCOL1*i lines under these inductive conditions (Abelenda et al., 2016).

Grafting experiments revealed that, in addition to repress *StSP6A* in the leaves, *StCOL1* also inhibits the autoregulatory loop that drives *StSP6A* expression in underground stolons (Navarro et al., 2011). Furthermore, silencing of *StCOL1* in *Andigena* leads to an early flowering phenotype and activation of the FT-like flowering inducer StSP3D, evidencing that *StCOL1* not only controls potato tuberization but also plays a role in flowering transition (Abelenda et al., 2016; Navarro et al., 2011). Gene expression studies showed that *StCOL1* represses *StSP6A* expression in the leaves by directly activating the FT-like *StSP5G* gene, which is a tuberization repressor (Abelenda et al., 2016). Indeed, StCOL1 directly binds the *StSP5G* promoter and activates expression of this gene in LDs, impaired *StSP5G* expression in *StCOL1*i plants then leading to *StSP6A* activation and to tuber formation under non-inductive conditions (Abelenda et al., 2016).

As seen for *Arabidopsis* CO, accumulation of the potato StCOL1 and StCOL2 proteins is regulated by light, these proteins being degraded in darkness but stabilized by blue light. However, unlike the *Arabidopsis* CO protein, StCOL1 is more stable in red light and is destabilized in far red light, which suggests that this factor is stabilized by phytochromes (Abelenda et al., 2016). Supporting this idea, antisense inhibition of *PHYB* in *Andigena* plants

impairs StCOL1 protein accumulation in the LD morning and reduces *StSP5G* expression. Hence, *StSP5G* activation relies upon the coincidence of the morning peak of *StCOL1* transcription and stabilization of the StCOL1 protein by PHYB. On the contrary, peak of *StCOL1* transcription is shifted in SDs toward the night, which makes the *StCOL1* protein be destabilized in the absence of light. *StSP5G* is then not transcribed, which allows activation of *StSP6A* by a yet unidentified regulator (Abelenda et al., 2016) (Figure 5).

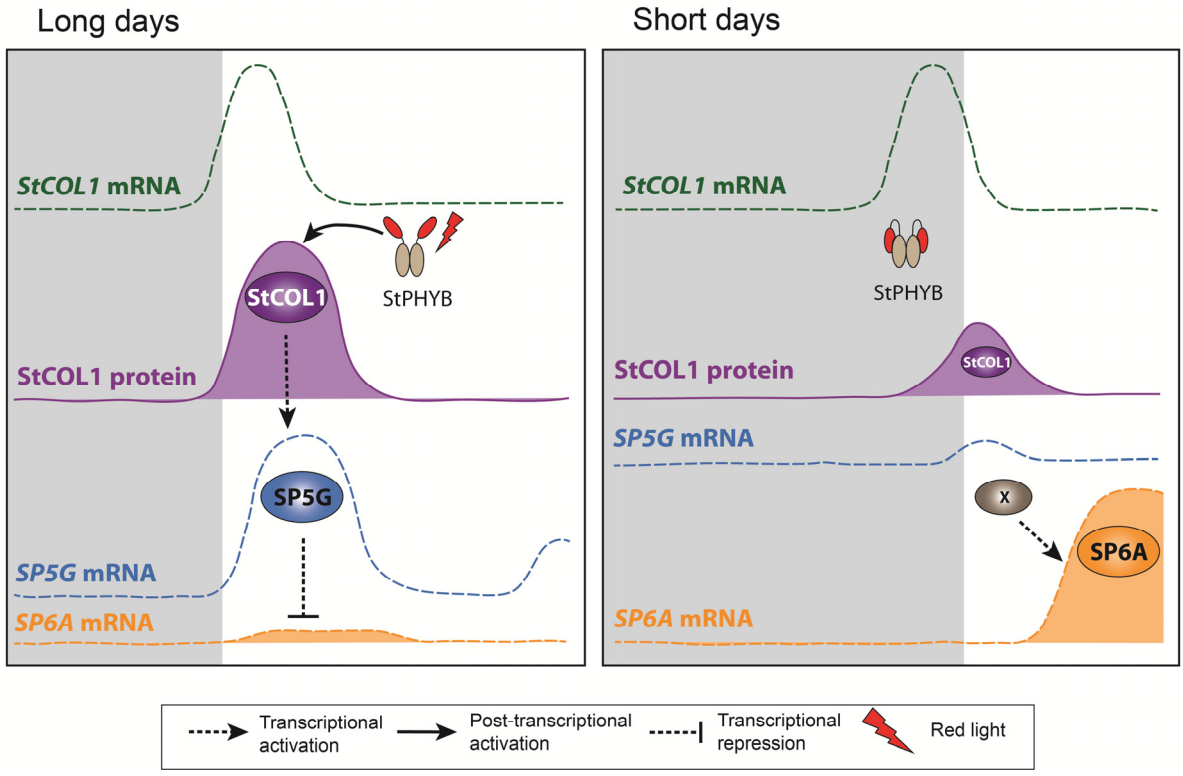

Figure 5. Photoperiodic regulation of St*COL1* in potato. Transcriptional and post-transcriptional regulation of StCOL1 ensures *StSP6A* expression specifically in SDs. *StCOL1* is transcribed at dawn under LDs and at the end of the night under SDs. The StCOL1 protein is degraded in darkness, whereas in the morning is stabilized by PHYB. In LDs, the coincidence of *StCOL1* transcription and the light results in StCOL1 accumulation and the activation of *StSP5G,* that is a repressor of *StSP6A* transcription. In SDs, StCOL1 is degraded during the night and *StSP5G* is not transcribed, allowing the activation of *StSP6A* by an unidentified X regulator (adapted from Abelenda et al., 2016).

A member of the potato CDFs family, *StCDF1*, has been also shown to play a central role in the regulation of *StCOL1* and *StCOL2* transcription. *StCDF1* underlies a major QTL for timing of tuber formation and plant maturity (Kloosterman et al., 2013) and it has been established that shorter life cycle, early tuberizing genotypes carry allelic variants of *StCDF1* which encode for truncated forms of the protein that lack the FKF1 interaction domain. As seen in *Arabidopsis*, the potato orthologs of GI and FKF1 bind StCFD1 and are thought to form a light dependent complex that promotes StCDF1 degradation. The truncated StCDF1

variants therefore escape StFKF1 post-translational regulation and are more stable during the day. As a consequence of this stabilization, expression of *StCOL1* and *StCOL2* is reduced and *StSP5G* is not transcribed in LDs, which allows activation of *StSP6A*. Notably, StCDF1 effects on *StCOL2* are stronger than on *StCOL1*, which suggests that *StCOL2* plays also a relevant role in the photoperiodic control of tuberization (Kloosterman et al., 2013).

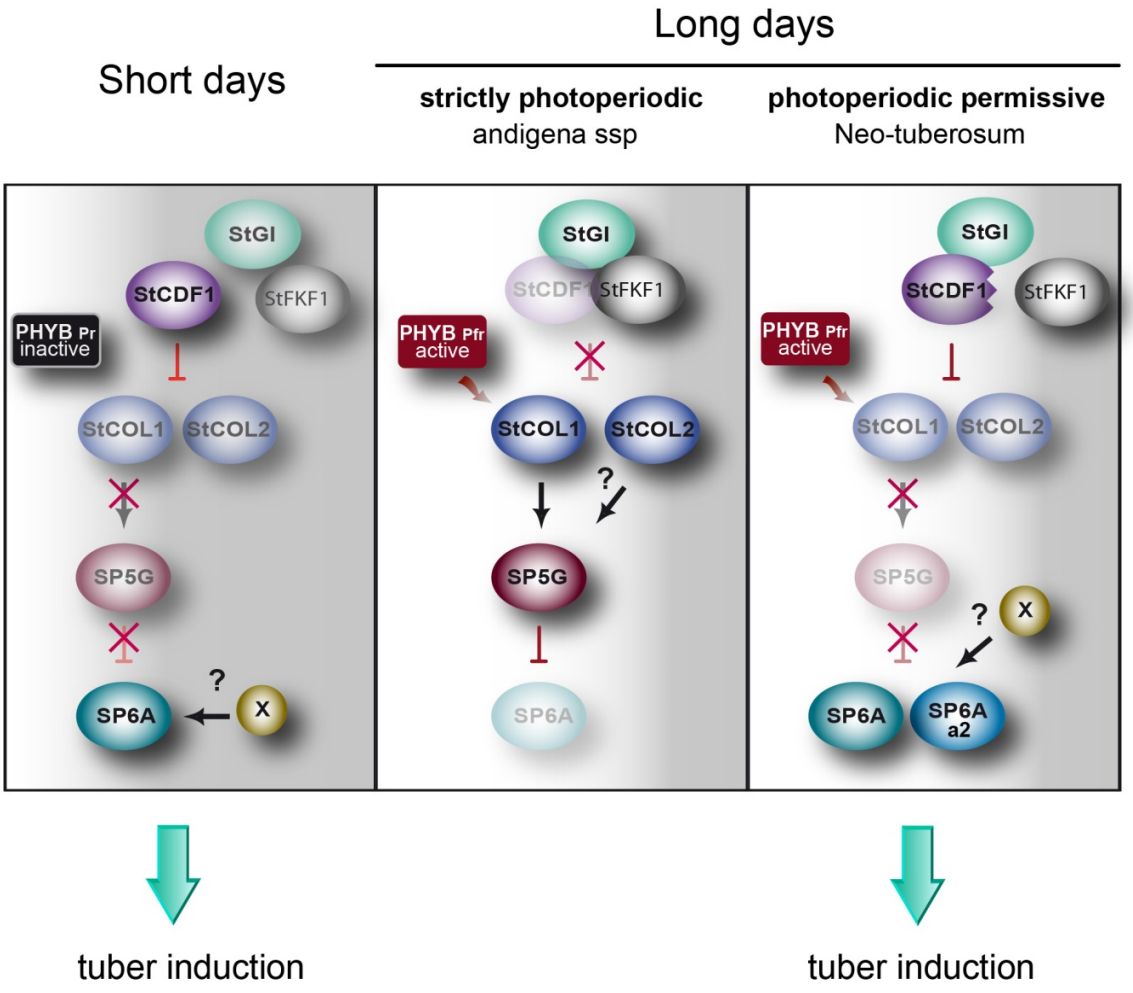

Figure 6. Control of tuber formation in potato genotypes with strict or permissive photoperiodic requirements. *Andigena* genotypes are strictly dependent on SD for tuberization. StCDF1 represses StCOL1 and StCOL2 transcription, which prevents *StSP5G* activation. *StSP6A* is then activated by an unidentified regulator (X) and transported to the stolon to induce tuber formation. StGI and StFKF1 interact with StCDF1 and promote its degradation, which leads to enhanced *StCOL1* and *StCOL2* expression. In LDs, StCOL1 is stabilized by PHYB during the morning and activates *StSP5G*, which acts as a repressor of *StSP6A* transcription. StCOL2 is likely to play also a role controlling *StSP5G* transcription. Neo-tuberosum genotypes tuberize under non-inductive LDs. These genotypes carry truncated StCDF1 alleles that do not interact with StFKF1, and thus evade degradation by the GI-FKF1 complex. Stabilization of StCDF1 leads to inhibition of *StCOL1*, *StCOL2* and *StSP5G*, which allows activation of *StSP6A* in LDs. An additional *StSP6A* allele, *StSP6Aa2*, has been identified in the Neo-tuberosum genotypes and is transcribed in non-inductive LDs. Arrows and blunted lines indicate activation and repression, respectively (adapted from Navarro et al., 2015).

In consonance with the proposed model, overexpression of the *Arabidopsis* LOV KELCH REPEAT PROTEIN 2 (LKP2), a member of the same family of proteins as *FKF1*, was found to enhance the tuber yield of potato plants of the cv.*May Queen* grown under LD conditions (Inui et al., 2010). Also, it is noteworthy that SD-obligate *Andigena* genotypes contain only full-length alleles of the *StCDF1* gene, while *Neo-tuberosum* genotypes contain both full-length and truncated *StCDF1* alleles. Therefore, the dominant character of these natural truncated variants was key during domestication to the adaptation of these genotypes to northern latitudes, characterized by longer summer day-lengths (Morris et al., 2014) (Figure 6).

6. Floral induction in response to FT-like proteins

6.1 The Florigen Activator Complex

Although the mechanism for *FT* activation in leaves has been relatively well characterized in multiple species, the biochemical activity of this protein and its function in the meristem still remains poorly understood. In *Arabidopsis*, FT is produced in the leaf companion cells and transported though the phloem to the shoot apical meristem (Notaguchi et al., 2008). FT export from companion cells to phloem sieve elements is favoured by FT interaction with the endoplasmic reticulum membrane protein FT-INTERACTING PROTEIN 1 (FTIP1), which indicates that FT moves in a regulated manner (Liu et al., 2012). In the SAM, FT interacts with the bZIP transcription factor FD and these proteins induce floral transition by activating expression of floral meristem identity genes (Abe et al., 2005; Andres and Coupland, 2012; Wigge et al., 2005).

In rice, interaction between the *FT*-like protein Hd3a and OsFD has been shown to be mediated by 14-3-3 proteins (Taoka et al., 2011). 14-3-3 are highly conserved eukaryotic proteins that usually act as sensors for phospho-motifs, modulating the activity, stability, localization or partner-interactions of their target proteins (de Boer et al., 2013). The 14-3-3 rice GF14c protein binds to Hd3a in the cytoplasm and contributes to its translocation into the nucleus, where both proteins interact with OsFD to form a ternary "Florigen activation complex" (FAC). GF14c then acts as a scaffold protein to the formation of the FAC complex, which induces transcription of the APETALA1 homolog *OsMADS15* and leads to flowering transition (Taoka et al., 2011). Similar FT-14-3-3-FD interactions have been reported in *Arabidopsis* and tomato, which suggests that FAC formation is probably a conserved mechanism for FT-mediated gene activation across angiosperms (Lifschitz et al., 2006; Pnueli et al., 2001). FT-FD interaction is also dependent on phosphorylation of threonine residue at position 282 of FD, which is promoted by calcium-dependent protein kinases such as *Arabidopsis* CDPK33 (Kawamoto et al., 2015a; Kawamoto et al., 2015b). TFL1 acts as

flowering repressor in the shoot apex, being shown to inhibit most of the genes activated by the FT-FD complex. Notably, TFL1 also interacts with FD and repressive function of the TFL1 protein depends on this interaction, hence suggesting that FT and TFL1 respectively act as coactivator and corepressor proteins modulating FD activity (Hanano and Goto, 2011).

In potato, three FD-like genes, StFD, StFDL1a and StFDL1b, have been identified and StSP6A shown to bind these three factors, in addition to various St14-3-3 proteins. Whereas inhibition of the *StFD* gene does not affect tuber formation of potato plants of the cv.*Sakara*, transgenic lines with reduced levels of expression of *StFDL1a/b* show a significant delay in tuberization. In addition, mutation of the 14-3-3 binding sites in the StSP6A protein strongly impair its tuber promoting activity, which suggests that formation of a FAC-like complex between StSP6A, StFDL1a/b and St14-3-3 is required for induction of stolon-to-tuber transition (Teo et al., 2016) (Figure 7).

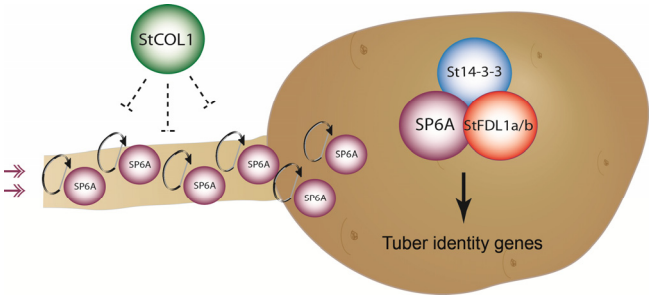

Figure 7. Tuber differentiation in the stolon. StSP6A is produced in the leaves and phloem transported to the stolon to induce tuber formation. During its transport, *StSP6A* expression is amplified by an autorelay mechanism that is negatively regulated by StCOL1. StSP6A forms a complex in the stolon with StFDL1a/b and St14-3-3 proteins which is likely to promote stolon-to-tuber transition by activating expression of tuber identity genes. Arrows and blunted lines indicate activation and repression, respectively (adapted from Abelenda et al., 2014).

6.2 MADS-box proteins as regulators of floral transition

The MADS-box transcription factors play fundamental roles in several developmental processes in eukaryotes (Messenguy and Dubois, 2003). In plants, this family of regulators has extensively diversified, with 45 members of the MIKC-type protein family for instance identified in *Arabidopsis.* Many of these factors function as important regulators of flowering transition, in addition to flower organ specification and fruit development (Dreni and Kater, 2014; Heijmans et al., 2012). Formation of the FAC ternary complex in the *Arabidopsis* shoot apical meristem triggers floral transition by activating the MADS-box *SUPPRESSOR OF OVEREXPRESSION OF CO 1* (*SOC1*), *FRUITFUL* (*FUL* or *AGL8*) and *APETALA 1* (*AP1)*

(Abe et al., 2005; Andres and Coupland, 2012; Jung et al., 2012; Wigge et al., 2005). *SOC1* integrates signals from the different flowering pathways and is essential for FT-mediated flowering transition (Lee and Lee, 2010). In the shoot apex, it interacts with other MADS-box proteins, like AGAMOUS-LIKE 24 (AGL24), which relocates SOC1 into the nucleus to activate together the floral meristem identity gene *LEAFY* (*LFY*) (Lee et al., 2008). Likewise, FUL integrates signals from the photoperiod and age pathways and promotes *LFY* transcription cooperatively with SOC1 (Balanza et al., 2014). FUL has been also proposed to act upstream of *SOC1* by interacting with SHORT VEGETATIVE PHASE (SVP) and counteracting its repressive effects (Balanza et al., 2014). Indeed, SVP and FLOWERING LOCUS C (FLC) are two additional MADS-box integrating signals from the autonomous and vernalization pathways, which function as flowering inhibitors by repressing as a complex *SOC1* and *FT* transcription in the leaves, as well as in the shoot apical meristem (Li et al., 2008; Searle et al., 2006).

Upon activation, *LFY* and *AP1* orchestrate flower development by regulating downstream expression of floral homeotic ABC genes involved in organ specification. Except for *AP2*, all ABC genes correspond to MADS-domain proteins (Irish, 2010). According to the floral quartet model, each floral organ type is specified by tetrameric complexes formed by combinatorial interaction of the MADS-box proteins AP1 (A-function), APETALA 3 and PISTILATA (B-function), AGAMOUS (C-function) and SEPALLATA 3 (E-function), in which SEP-like subunits mediate interaction of the rest ABC proteins by enhancing their binding affinity (Figure 8B) (Krizek and Fletcher, 2005; Sablowski, 2015; Theissen et al., 2016; Wellmer et al., 2014). Expression of these genes is restricted to particular floral organs and multiple regulators control their time- and region-specific activation (Figure 8A) (Kaufmann et al., 2009; Kaufmann et al., 2010; Krizek, 2001; Krogan et al., 2012). An (A)BC model where function (A), contributed by the *AP1*, *SEP* and *AGL6*-like genes, plays a role in controlling floral meristem identity besides specification of the first two floral whorls has also been proposed (Causier et al., 2010), cumulative evidence indicating that Floral quartet-like complexes (FQCs) play an important role far beyond specifying floral organ identity.

Function of the MADS-box factors SOC1, AP1 and FUL in the promotion of floral transition is conserved in several plant species. MACROCALYX (MC) from tomato, PROLIFERATING INFLORESCENCE MERISTEM (PIM) from pea (*Pisum sativum* L.), SQUAMOSA (SQUA) from *Antirrihinum majus* L., and WAP1/VRN1 from wheat are orthologs of *Arabidopsis* AP1 that were identified as important regulators of inflorescence determinacy (Huijser et al., 1992; Murai et al., 2003; Taylor et al., 2002; Vrebalov et al., 2002). In rice, the *SOC1*-like protein OsMADS50 is a major flowering activator and three AP1/FUL-like proteins, in combination with the *SEP*-like protein PANICLE PHYTOMER 2 (P2P), were reported to

promote inflorescence meristem identity downstream of the florigen signal (Kobayashi et al., 2012; Lee et al., 2003). Two maize MADS-box genes, *ZMM4* and *ZmMADS1*, that share strong homology with *FUL* and *SOC1* respectively, were shown to induce floral transition and play a role in inflorescence development in maize (Alter et al., 2016; Danilevskaya et al., 2008). Furthermore, overexpression of the *SOC1*-like protein UNSHAVEN (UNS) in petunia (*Petunia hybrida*) is shown to accelerate flowering (Ferrario et al., 2004).

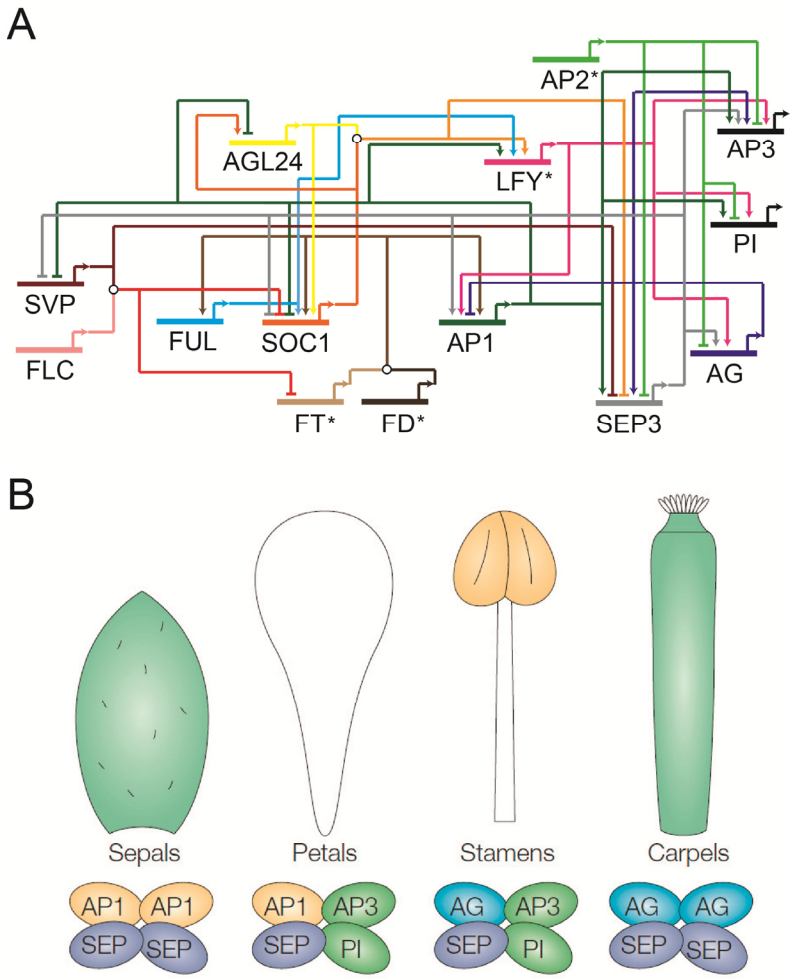

Figure 8. MADS-box regulation during floral transition and organogenesis. (A) Regulatory network of MADS-box transcription factors in *Arabidopsis* flowering development. *SOC1*, *FUL* and *AP1* are activated by the FT-FD complex and promote activation of *LFY*, among other targets. AP1 and LFY orchestrate floral development by activating homeotic genes such as *AP3, PI, AG* and *SEP3* involved in floral organogenesis. The spatial and temporal expression of these homeotic genes is tightly regulated and involves several activation and repression feed-back loops. * denotes non-MADS-box family proteins. Arrows and blunted lines indicate activation and repression, respectively (adapted from Kaufmann et al., 2010). (B) Diagram illustrating the floral quartet model. In each whorl of the floral meristem, tetramers formed through protein-protein interactions between MADS-box proteins promote the formation of sepals (whorl 1, AP1-SEP-AP1-SEP), petals (whorl 2, AP1-SEP-AP3-PI), stamens (whorl 3, AG-SEP-AP3-PI) and carpels (whorl 4, AG-SEP-AG-SEP). A, B, C and E function proteins are coloured in yellow, green, blue and violet respectively (Sablowski, 2005).

In potato, transgenic plants with reduced levels of the *FUL*-like *StAGL8* gene, also called *POTM1*, were shown to exhibit reduced apical dominance and increased cytokinin levels in axillary buds. Moreover, inhibition of *StAGL8* also led to reduced tuber formation, evidencing that *StAGL8* positively regulates tuberization in potato (Rosin et al., 2003). In consonance with these findings, transcriptome analyses of potato leaves revealed that *StAGL8* and *StSP6A* show similar expression profiles in *Andigena* and *Neo-tuberosum* genotypes, suggesting that both genes are co-regulated (Morris et al., 2014).

7. Hormonal control of tuber formation

Tuber formation involves local activation of cell division and cell expansion in a defined region below the stolon tip (Xu et al., 1998b). At the onset of tuberization, stolons stop growing and initiate radial expansion of the subapical region (Cutter, 1978). The signalling mechanisms involved in reprogramming division of these cells on arrival of the StSP6A tuberigen signal have not been yet elucidated, but several plant hormones were established to play an essential role in this process (Figure 9) (Rodriguez-Falcon et al., 2006; Roumeliotis et al., 2012b).

Gibberellins (GAs) have been long considered as inhibitors of tuber formation (Xu et al., 1998a). The *StGA2ox1* catabolic enzyme is strongly induced prior to stolon swelling and promotes the drop of active gibberellins required for tuberization onset (Kloosterman et al., 2007). Notably, the effect of GAs on tuberization has also been studied via functional characterization of two GA biosynthetic genes, *StGA20ox1* and *StGA3ox2*. Overexpression of *StGA20ox1* in *Andigena* plants delays tuberization, confirming an inhibitory effect of GAs on stolon-to-tuber transition (Carrera et al., 2000). However, a slightly earlier tuberization was observed in plants over-expressing *StGA3ox2* in the leaves, which indicated that effect of GAs on tuberization is different in leaves than in the stolon (Bou-Torrent et al., 2011; Roumeliotis et al., 2013).

Because of their important role in the formation and maintenance of meristems and in signalling asymmetrical cell divisions (Vanneste and Friml, 2009), auxins are also likely to be key regulators of tuber development. Many auxin-related PIN-FORMED (PIN) and AUXIN RESPONSE FACTOR (ARF) family genes are transcriptionally regulated during tuber formation (Faivre-Rampant et al., 2004; Kloosterman et al., 2008). Additionally, auxin levels strongly increase in the stolon before tuber initiation and remain relatively high during subsequent tuber growth, suggesting a positive role of auxins in tuberization (Roumeliotis et al., 2012a). Auxins, together with strigolactones (SLs), also regulate stolon architecture by repressing axillary bud outgrotwth, hence exerting a similar control as described for shoot branching (Pasare et al., 2013; Roumeliotis et al., 2012a). Furthermore, silencing of the SL

biosynthetic gene *StCCD8* in the cv.*Desiree* leads to reduced apical dominance, the promotion of secondary tuber growth in underground tubers and reduced dormancy, which evidences that SLs not only inhibit shoot branching but also play an important role in repressing tuber bud outgrowth (Pasare et al., 2013).

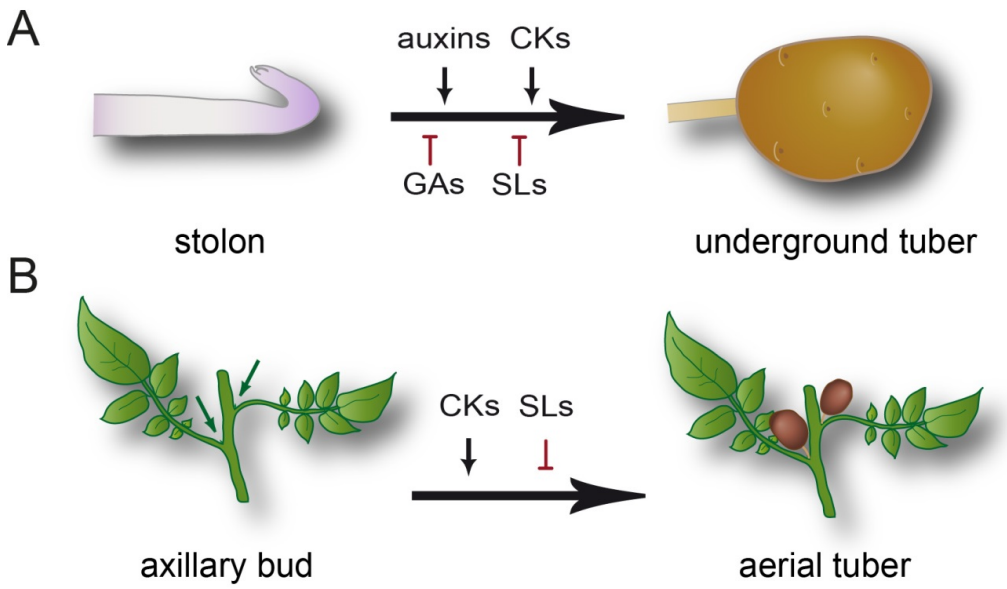

Figure 9. Hormonal regulation of tuber formation. Potato tubers develop from underground stolons, but can also be induced from axillary buds. (A) In stolons, GAs and SLs repress tuber formation, whereas CKs and auxins are tuber inducers. (B) Aerial tubers are formed from axillary meristems in plants with either increased CKs biosynthesis or reduced SLs biosynthesis. Arrows and blunted lines indicate activation and repression, respectively (adapted from Navarro et al., 2015).

Cytokinins (CKs) play as well a prominent role in tuberization by promoting cell division during tuberization onset and by creating a local sink (Abelenda and Prat, 2013). Exogenous application of CKs induces tuber formation *in vitro,* whereas overexpression of the *Arabidopsis* CK catabolic *CKX1* enzyme in the cv. *Solara* was shown to reduce tuber yield (Estrada et al., 1986; Hartmann et al., 2011). Moreover, ectopic expression of the CK-activating *LONELY GUY 1* (*LOG1*) gene, encoding CK riboside 5'-monophosphate phosphoribohydrolase, was recently shown to confer tomato plants the ability to generate aerial minitubers from juvenile axillary meristems (Eviatar-Ribak et al., 2013). Notably, this tuber-forming potential is extended to every node axillary meristem by overexpression of *miR156*, which promotes juvenile development (Bhogale et al., 2014; Chuck et al., 2007; Wu et al., 2009; Zhang et al., 2011). Hence, these findings strongly suggest that CKs act as universal regulators of storage-organ formation in plants, while provide a framework for understanding the hormonal regulatory control of this developmental transition.

8. Temperature control of tuberization

Temperature is one of the most significant factors affecting growth and development of potato plants. Given its Andean origin, potato is a cool climate crop and is very sensitive to high temperatures. The optimal daytime temperature for yield is usually in the 14-22ºC range and temperatures above strongly reduce tuber production in most potato genotypes (Van Dam et al., 1996). Warm temperatures result in taller potato plants, with a thinner stem, longer inter-nodes and smaller leaves; thus resembling the thermomorphogenic effects reported in *Arabidopsis* (Lafta and Lorenzen, 1995; Quint et al., 2016). In potato, temperature has also a great influence on photosynthetic rates, carbon partitioning and dry matter accumulation in the tubers.

It has been long established that heat stress decreases leaf photosynthetic rates in potato largely by impairing photosystem II (PSII) efficiency (Havaux, 1996; Prange et al., 1990). However, continuous exposure to moderated warm temperatures up to 30ºC has a positive or no significant effects on the photosynthetic rate of potato cultivars with different heat tolerances (Dwelle et al., 1981; Hancock et al., 2014; Lafta and Lorenzen, 1995; Singh et al., 2015). Temperatures of 31/29ºC (day/night) were reported to modify carbohydrate partitioning and reduce total plant dry matter (Lafta and Lorenzen, 1995). Furthermore, these temperatures impair net translocation of carbohydrates to the tubers and their incorporation into tuber starch, evidencing that temperature also controls diversion of photosynthates from source leaves and their allocation into sink organs (Wolf et al., 1991). Taken together, these findings suggest that multiple metabolic responses might affect tuber formation in response to heat stress.

Recently, independent transcriptomic analyses have been performed out of leaves and tubers to identify those genes differentially regulated in response to warm temperatures (Hancock et al., 2014; Singh et al., 2015). These studies revealed that *StSP6A* is down-regulated in both leaves and tubers. Moreover, *StSP6A* inhibition is apparently conditioned to the heat tolerance of the cultivar analyzed, since the heat tolerant cultivar *Kufri Surya* exhibits at 24ºC higher levels of expression of *StSP6A* in the leaves than the heat sensitive cultivar *Kufri Chandramukhi* (Singh et al., 2015). These findings therefore indicate that drop in tuber production at warm temperatures is caused to an important extent by inhibition of the FT *StSP6A* inducing signal in the leaves.

Owing to global warming, potato production is expected to fall in the coming decades in most parts of the world, especially in tropics and subtropics zones where shifting planting time or location is less feasible. In fact, global potato yield is expected to decrease between 10-19% by 2010-39 and 18-32% by the 2050s (Hijmans, 2003). Hence, understanding the

molecular mechanisms by which warm temperatures inhibit tuber formation is crucial to improve thermo-tolerance in potato and develop new cultivars capable to overcome future rises in temperature.

Objectives

Over last few years, achievements in our understanding of the photoperiodic control of tuberization have been remarkable. Two members of the *FT* gene family, *StSP6A* and *StSP5G*, were identified as major components of the regulatory network controlling this developmental process in potato. While *StSP6A* promotes tuber formation and is the major component of the mobile "tuberigen" signal, *StSP5G* acts as a tuberization inhibitor and seems to negatively regulate *StSP6A* transcription in the leaf (Abelenda et al., 2016; Navarro et al., 2011). Studies in *Andigena* genotypes revealed that StCOL1 is stabilized in non-inductive LDs conditions and suppresses tuberization by activating *StSP5G* transcription (Abelenda et al., 2016). *StCOL1* and *StCOL2* transcription is repressed by StCDF1, which underlies a QTL for plant maturity and tuber development. Notably, early tuberizing cultivars carry *StCDF1* alleles that lack the C-terminal end and do not bind the clock-controlled StFKF1 protein, which therefore stabilizes these truncated StCDF1 proteins (Kloosterman et al., 2013). Taken together, these findings suggest that the photoperiodic pathway for tuber formation is highly similar to the day-length flowering pathway in *Arabidopsis* (Abelenda et al., 2011; Navarro et al., 2015). However, many aspects regarding the specific regulation of *FT* genes in potato and their molecular functions in both leaves and tubers still remain poorly understood. A main regulatory role of the circadian clock oscillator *GIGANTEA* has been suggested but not yet established. The molecular mechanisms by which *StSP5G* inhibits tuberization and its function in tissues other than leaves also remain so far uncharacterized. Furthermore, determine in which way temperature signals control tuber formation is another fundamental aspect that needs to be clarified. Hence, main objectives of this work are the following:

1. Characterize the role of GIGANTEA in the photoperiodic control of tuber formation.

2. Identify the genes differentially regulated in response to StSP5G and the biological function of this repressor in different plant tissues.

3. Determine the role of StSP6A in reversing inhibitory effects of warm temperatures on tuber formation.

Materials and Methods

1. Plant material and growth conditions

Solanum tuberosum L. ssp. *Andigena* (A7540) and the commercial cultivars *Spunta* and *Sylvana* were used along this work as WT plants. Potato plantlets were vegetatively propagated *in vitro*, by culture of single node stem cuttings in Murashige and Skoog (MS) medium supplemented with 8g L^{-1} Bacto^{TM}agar (BD) and 20g L^{-1} sucrose. Plants were grown at 22ºC under LD conditions (16 h light/ 8h dark) and two weeks later, once they had produced new roots, were transferred to pots containing a 3:1 soil-vermiculite mixture and cultivated in the glasshouse also at 22ºC and under LD photoperiodic conditions.

For day-length and temperature treatments, plants were grown in the glasshouse until they reached a 10-leaf stage, and then transferred to controlled growth chambers. Relative humidity was set to 55% and light was provided by cool white fluorescent tubes (T58W/020) at 100µmol m^{-2} s^{-1} PAR. Plants were grown in LDs (16h light/ 8h dark) or SDs (8h light/ 16h dark) for at least two weeks before sampling. For 24-h time course experiments, leaf samples were collected every 3h over a 24-h period, using a green safe light for seeing in the dark. Warm temperature treatments of 28ºC were applied in LDs, for at least 30 days before sampling. As leaf samples, the third and fourth fully expanded leaves starting from the apex were collected and independent plants were used for each time point. Stolon samples correspond to 5 cm long segments from the stolon tip. Tuber samples were obtained by pooling at least three mature tubers. Tuber sprouts were individually excised from the mother tuber with a razor blade, and tissue collected until approximately 2 mm deep. Samples were immediately frozen in liquid N_2 and grinded to fine powder with a mortar and pestle for subsequent RNA, protein or reducing sugars and starch analyses.

2. Quantification of plant maturity, plant height, tuber yield and tuber dormancy

Plant maturity was assessed by monitoring plant survival in relation to the number of days after planting. Total plant height was measured from the soil surface to the tip of the plant, after plants were grown for 8 weeks at 22ºC or 28ºC. In all experiments, tuber yield was quantified in at least 15 plants and was defined as the tuber fresh weight per plant after 12 weeks of growth under specific photoperiod and temperature conditions. For tuber dormancy measurements, tubers were let at room temperature for 3-4 days and then stored at 4ºC in darkness. Sprout length was periodically measured after the second month of storage.

3. Grafting experiments

For grafting studies, 6-10 week-old plants were used and subsequently grown in LD conditions in the glasshouse to analyse their tuberization response (Jackson et al., 1998). Scions were obtained by cutting the stem diagonally with a razor blade, between the 3rd and 4rd internode from the apex. Stocks were obtained by similarly cutting the stem at about 5 cm above soil, followed by removal of the lower leaves. After cutting, scions were immediately placed in water and a drop of water was applied to the stock to prevent its drying out. The end of the stem was then fit into a 2 cm-long PVC cylindrical tube with the same inner diameter (3-4 mm Portex) and the scion was placed on top of the stock, taking care that both sections were tightly connected. Sections were then held in place by wrapping the edges of the PVC tube with Parafilm M® tape (Bemis), and plants were covered for at least one week with a plastic bag humidified by inside spraying of water. Bags were sprayed with water for the first 2-3 days and removed once the graft had taken.

For expression analyses, stems of the grafted plants were sampled into 4 different parts, the apical and basal regions above the graft junction, the stem of the stock plant below the graft, and the stolons. We referred to these samples as Apical stem, Basal stem, Underground stem and Stolons. The apical and basal stems included the first 3 nodes from the apex and the last 3 nodes above the graft junction respectively, while the underground stem included the whole main stem of the stock. Grafts were grown for at least 12 weeks in the glasshouse, under LD conditions and at 22ºC. Samples were collected 8 weeks after grafting, from at least 3 independent plants. Tuber yield was quantified 12 weeks after grafting, by using at least 15 plants of each graft combination.

4. Cloning procedures

All genes and promoters of interest were amplified by Polymerase Chain Reaction (PCR) using as template genomic DNA or cDNA of *Andigena* plants. PCR reactions were performed with the Expand High Fidelity Taq polymerase (Roche) according to manufacturer's recommendations. Primers (Sigma-Aldrich) used for amplification are shown in Table 1. Amplification products were separated by agarose gel electrophoresis and purified with the QIAquick® gel extraction kit (Qiagen).

The Gateway Cloning System (Invitrogen) was used to generate most of the plasmid constructs. After purification, PCR amplification fragments were inserted into the pENTR™ /D-TOPO® vector and mobilized to the different destination vectors by incubation with the LR clonase™ mix. For particular constructs, PCR products were cloned by conventional positional cloning, using the pGEM®-T Easy plasmid (Promega) as intermediate vector.

Empty destination plasmids were digested with the adequate restriction enzymes, dephosphorylated with Shrimp Alkaline Phosphatase (Roche) and finally ligated with the digested insert by incubation with T4 DNA ligase (Thermo Fisher Scientific).

The sequence of all genes and promoters cloned into pENTR™ /D-TOPO® and pGEM®-T Easy vectors was confirmed by Sanger sequencing (STABvida) and transference to the destination vectors was checked by restriction enzyme digestion (Table 2). Plasmids were purified from *Escherichia coli* either with the QIAGEN®Plasmid Mini or Midi kit (Qiagen) following the manufacturer's recommendations.

5. *E. coli* and *A. tumefaciens* transformation

Escherichia coli cells (strains DH5α and DB3.1) were transformed by the heat-shock method. DNA was added to a 100µL aliquot of competent cells and incubated on ice for 20min. Cells were then incubated at 42ºC for 2min and subsequently placed back on ice for an additional 5min. After that, 250µL of Luria-Bertani [LB] medium (10g L^{-1}tryptone; 5g L^{-1} yeast extract; 10g L^{-1}NaCl; pH 7.5) was added to the tube and cells were incubated at 37ºC for 1h, before being plated on LB media, 8g L^{-1}Bacto™ agar, supplemented with the proper selective antibiotics.

Agrobacterium tumefaciens cells (strain GV3101) were transformed by the freeze-thaw method. DNA was added to a 500µL aliquot of competent cells and the mixture was kept on ice for 5min, put in liquid N_2 for 5min, and finally incubated at 37ºC for an additional 5min. Cells were immediately put back on ice for 5min and 500µL of Yeast Extract Broth [YEB] media (5g L^{-1} beef extract; 1g L^{-1} yeast extract; 5g L^{-1} peptone; 5g L^{-1} sucrose; 2mM $MgSO_4$; pH 7.2) was added to the tube. Cells were incubated at 28ºC for 2h for expression of the antibiotic resistance, before being plated on YEB media, 8g L^{-1}Bacto™ agar, supplemented with rifampicin and the right selective antibiotics.

6. *Solanum tuberosum* transformation

All potato transgenic plants used in this work were generated by *Agrobacterium tumefaciens* transformation of leaf explants, as previously described (Visser et al., 1989) (Table 3). *A. tumefaciens* cells bearing the recombinant T-DNA vector were cultured at 28ºC in 20mL of YEB medium with antibiotics, until reaching an Optical Density (OD_{600nm}) of 0.6-0.8. Bacterial cells were then pelleted by centrifugation at 3500g for 10min and resuspended in 10mL of YEB medium without antibiotics.

For leaf explant infection, healthy fully expanded leaves were collected from 3-4 week-old *in vitro* plantlets. The tip and basal portions were removed with a razor blade and 1-

3 cuts were made along the middle rib to increase the entry surface area. Leaves were placed upside down in MS medium supplemented with 16 g L^{-1} glucose and let floating in the presence of a 1:10^2 dilution of the *A. tumefaciens* suspension. After 48h incubation in darkness at 22ºC, the leaf explants were transferred to Callus Induction Medium CIM (MS medium, 8g L^{-1}Bacto™ agar, supplemented with 16g L^{-1} glucose, 5mg L^{-1} NAA, 0.1mg L^{-1} BAP, 250mg L^{-1}claforan; 50mg L^{-1}kanamycin or 2mg L^{-1}hygromycin). Plates were scratched with the aid of the forceps. Leaves were laid upside-down on the surface, and grown in LDs at 22ºC for 1 week. Then, explants were transferred to Shoot Induction Medium SIM (MS medium, 8g L^{-1}Bacto™ agar, supplemented with 16g L^{-1} glucose, 0.02mg L^{-1} NAA, 2mg L^{-1}zeatin riboside, 0.15mg $L^{-1}GA_3$, 250mg L^{-1}claforan; 50mg L^{-1} kanamycin or 2mg L^{-1}hygromycin) and grown in LDs at 22ºC for at least 6 additional weeks, during which explants were transferred to fresh SIM medium once a week. Once the regenerated shoots reached 2-3 cm long, they were cut at the base with a razor blade and transferred to MS medium, 8g L^{-1}Bacto™ agar supplemented with 16g L^{-1}glucose and 250mg L^{-1}claforan; 50mg L^{-1}kanamycin or 2mg L^{-1}hygromycin for rooting.

7. DNA and RNA extraction

A slightly modified Dellaporta extraction method was used for DNA extraction of potato leaves (Dellaporta et al., 1983). Frozen material was homogenized in Dellaporta buffer (7M Urea; 0.3M NaCl; 50mM Tris-HCl pH 8; 20mM EDTA; 1% Sarcosil), mixed with an equal volume of phenol-chloroform, and centrifuged for 20min at 14000g. The upper aqueous phase was collected into a new tube and DNA was precipitated by adding Ammonium Acetate to a final concentration of 2.5M and 0.6 volumes of Isopropanol. After centrifugation at 10000g for 15min at 4ºC, the pellet was washed twice with 70% ethanol and dissolved in TE solution containing RNAse (10mM Tris-HCl pH 7.5; 1mM EDTA; 0.1mg mL^{-1} RNAse A [QIAGEN]).

For RNA extraction, the frozen material was homogenized in Z6 buffer (8M guanidinium-HCl; 20mM MES pH 7; 20mM EDTA; 50mM β-mercaptoethanol), with the aid of a piston attached to a high power stirrer. An equal volume of phenol-chloroform was added to the homogenized extract, the mix was vigorously vortexed, and centrifuged at 14000g for 30min and 4ºC. The upper aqueous phase was collected into a new tube and mixed with an equal volume of the Lysis/binding buffer provided by the High pure RNA Extraction kit (Roche). The mixture was then loaded into the columns provided by the commercial kit and the RNA purified following the manufacturer's recommendations.

8. cDNA synthesis and qPCR

For cDNA synthesis, 2µg of total RNA were used as template for reverse transcription, with the Transcriptor First strand cDNA synthesis kit (Roche). The synthesis reaction was carried out using random hexamers as primers, according to the manufacturer's recommendations except for the concentration of random hexamers, dNTPs and reverse transcriptase, which were optimized to 30µM, 30µM and 6U respectively.

The obtained cDNA was diluted 1:10 in water for qPCR expression analyses. qPCR reactions were performed in 10µL using 4µL of the 1:10 cDNA dilution, 5µL of Evagreen® dye (Biotium) and a final 0.2µM concentration of the specific primers for the gene of interest (Table 1). A 7500 Real-Time PCR system (Applied Biosystems) was used to run the qPCR reactions (95ºC 10min; [95ºC 15s, 60ºC 1min, 95ºC 15s] x40; melting curve) and three technical replicates run for each biological replicate. Gene expression was calculated either with the -ΔΔCt Pfaffl method (Pfaffl, 2001) using the ACTIN (*StAct*) gene as reference or, in specific cases, quantified in absolute terms respect an external calibration curve, and represented as the ratio between the number of molecules of the gene of interest and the molecules of *StAct*.

qPCR results were represented as the average of at least three independent experiments and error bars correspond to the Standard deviation (s.d.) between samples.

9. CAPS marker for *StSP5G-A*

A Cleaved Amplified Polymorphic Sequence (CAPS) marker for a Single Nucleotide Polymorphism (SNP) detected in *StSP5G-A* was generated to compare the expression profiles of *StSP5G-A* and *StSP5G-B* in different tissues of the *Andigena* potato genotype. The *StSP5G* coding sequence (528bp) was then amplified by RT-PCR from leaves of plants grown in LDs, mature tubers or 2 cm-long tuber sprouts. PCR reactions (95ºC 5min; [95ºC 15s, 55ºC 30s, 72ºC 1min] x35; 72ºC 7min) were performed with the Biotools Taq DNA polymerase (Biotools) according to manufacturer's recommendations. Digestion of the amplified products with the HindII restriction enzyme (Roche) yielded 2 fragments of 372bp and 153bp, corresponding to the *StSP5G-A* transcripts, and an undigested fragment of 525bp that corresponds to transcripts for *StSP5G-B*. The amplified product was in parallel digested with BamHI (Roche) yielding two fragments of 324bp and 201bp, as loading control.

10. Protein extraction and immunodetection

Total protein extracts of potato leaves were obtained by homogenization in a denaturing extraction buffer (6M Urea; 125mM Tris-HCl pH 7.4; 2% SDS; 10% Glycerol; 10mM β-mercaptoethanol; 1mM PMSF). Frozen material homogenized in this buffer, was then boiled at 95ºC for 3 min and cleared by 14000g centrifugation for 10min, at 4ºC. Equal amounts of material (4 leaf discs) were used for extraction, and 20 µl of extract was loaded onto a 8% SDS-PAGE gel. After separation, proteins were transferred to a 0.2µm nitrocellulose membrane (Amersham) using a semi-dry transfer blot system and immunodetected by Western Blot. To this purpose, membranes were saturated with a 10% non-fat milk solution in TBS buffer (50mM Tris-HCl pH 7.4; 150mM NaCl) + 0.1% Tween-20 for 1 hour, washed 3 times with TBS-T and incubated overnight at 4ºC with an anti-HA-HRP antibody (Roche). Incubation with an anti-RPT5 antibody (Enzo Life Sciences), followed by incubation for 1h and 30 min with an anti-rabbit IgG-HRP secondary antibody (GE Healthcare), was used as loading control. For electrochemiluminescent (ECL) detection, blots were washed 3 x 5 min with TBS-T buffer, 3 x 5 min with TBS buffer without Tween-20 and, depending on the intensity of the signal, the Supersignal® West Pico or a dilution of the Supersignal® West Femto Chemiluminiscent substrate (Thermo Fisher Scientific) was used for exposure to a radiography film (CP-BU Agfa).

11. GUS staining

To analyze tissue-specific expression of the *StSP5G-A* gene, histochemical staining of β-glucuronidase (GUS) activity (Jefferson et al., 1987) was performed on *in vitro* plantlets and minitubers of *Andigena* plants bearing the *pStSP5G-A::*GUS construct.

3-4 week-old plantlets and 1 cm-long minitubers grown *in vitro* were fixed on ice for 30 min with a 90% acetone solution. After fixation, samples were washed with water for 5 min and incubated overnight at 37ºC with a GUS staining solution (100mM Tris-HCl pH 7; 50mM NaCl; 0.2% Triton X-100; 1mM potassium ferricyanide; 1mM potassium ferrocyanide; 2 mM 5-bromo-4-chloro-3-indolyl-β-D-glucuronide [Glycosynth]). Before transfer to 37 ºC, vacuum was applied for 30min to all samples to help the staining solution to infiltrate the plant tissues. After staining, plantlets and minitubers were dehydrated by incubation with increasing concentrations of ethanol and kept in 100% ethanol for at least 2 additional days for removal of chlorophyll. Finally, samples were rehydrated, mounted on slides and photographed with the help of a stereomicroscope (Leica M165FC).

To the generation of *in vitro* minitubers, single node stem cuttings were cultivated on MS medium, 8g L^{-1}Bacto™ agar, supplemented with 90g L^{-1} sucrose and 2.5mg BAP, and

kept in darkness for 2-3 weeks. For leaf staining, plantlets were grown in LDs on solid MS medium + 20 g L^{-1} sucrose.

12. Lugol's staining

For starch detection, 2cm-diameter leaf discs were collected out of the third and fourth fully expanded leaves, starting from the apex, from WT Spunta and *StSP6A*ox plants that had been grown for 30 days under 22ºC or 28ºC. Discs were harvested at LD ZT5 and at least 20 discs (4 discs x 5 replicates) were obtained for each genotype. Discs were fixed in 3:1 ethanol/acetic acid solution directly after harvesting and maintained in the fixing solution until total decoloration of the chlorophylls. Samples were then rehydrated by incubation with decreasing concentrations of ethanol and finally stained with Lugol's iodine solution (Riedel-de Haën) for 10 min in darkness. Stained discs were then rinsed in deionised water and pictures of representative stainings were taken.

13. Reducing sugars and starch measurements

To determine both reducing sugars and starch content, 100mg of the frozen powdered tuber samples were shaken in 1ml 80% ethanol for 1h at 80ºC and then centrifuged for 10min at 14000g. The cleared supernatant was transferred to a new tube for subsequent reducing sugars quantification, while the pellet was washed again with 80% ethanol, dried for 10min at 45ºC and resuspended in 1mL of deionised water. The starch present in this insoluble fraction was then solubilized by heat (1h at 130ºC and 1.2atm in the autoclave) and digested to glucose using a commercial enzymatic kit (Starch; R-Biopharm AG). Enzymatic digestions were carried out following manufacturer's recommendations and starch content was finally quantified by measuring absorbance at 340nm.

Reducing sugars content was quantified using a Dinitrosalicylic Acid reagent (Miller, 1959). The cleared supernatant containing the soluble sugars and other low molecular weight molecules was dried with a Speedvac® concentrator and dissolved in 100µL of deionized water. 20µL were mixed with 100µL of the DNS solution (10 g L^{-1} 2-hydroxy-3,5-dinitrobenzoic acid; 300 g L^{-1} potassium sodium tartrate; 0.4N NaOH), heated for 5min at 95ºC and placed on ice. Finally, samples were brought to 1mL with deionized water and reducing sugars content was quantified by measuring absorbance at 530nm. Quantification was done against a calibration curve obtained by serial dilutions of a 100mM glucose solution.

14. Hybridization and analysis of Agilent gene expression microarrays.

The transcriptome of leaves of Spunta WT and *StSP6A*ox plants grown at 22ºC and 28ºC was analysed using an Agilent microarray (ID033033) containing 60mer probes for all predicted potato transcripts from assembly v.3.4 of the DM potato genome (Hancock et al., 2014; Xu et al., 2011). Leaf samples were collected for RNA extraction at LD ZT5, after plants were subjected for 30 days to the different temperature treatments.

For the transcriptomic analyses of *Andigena* WT and *StSP5G*i leaves, mature tubers and sprouts, the same Agilent microarray was used. Leaf samples were also collected at LD ZT5, whereas tuber samples were obtained from plants grown under SDs for 60 days. Sprouts were 2 cm-long sprouts, with a shoot or tuber semblance, harvested from tubers that had been stored for 2-3 months at 4ºC.

Three independent biological replicates were used per genotype, tissue or treatment, and hybridized in triplicate. Total RNA was extracted from these samples as indicated above, and integrity of the purified RNA verified by using a 2100 BioAnalyzer (Agilent technologies). RNA labelling and subsequent microarray processing was carried out in collaboration with Dr. Sonnewald's group at the University of Erlangen (Germany) using the One-Color Microarray-Based Gene expression Analysis protocol (v6.6; Agilent technologies). Briefly, double stranded cDNA was synthetized from 200ng of total RNA using the one-color RNA spike-in kit (Agilent technologies) with T7 promoter oligo-dT primers. The obtained cDNA was used as template for *in vitro* transcription with a T7 RNA polymerase, in the presence of Cyanine 3-CTP (Cy3). The labelled cRNA was then purified with RNeasy columns (Quiagen) and 600ng were fragmented at 60ºC for 30 min and used for hybridization of the Array slides, for 17h at 65ºC. After washing, slides were scanned with a DNA microarray Scanner (Agilent technologies) with an extended dynamic range at high resolution and data sets were extracted with the Feature Extraction (FE) Software (Agilent technologies).

FE datasets were analysed using the GeneSpringGX software (Agilent technologies). Raw intensity values less than 1 were adjusted to 1, and data flagged as compromised by the FE software was discarded. Signal values were log transformed and normalized to the 75th percentile. Differentially expressed genes (DEGs) were identified using analysis of variance (ANOVA; $p<0.05$) with the Student Newman-Keuls (SNK) post-hoc test and Benjamini Hochberg FDR multiple testing corrections. Hierarchical clustering of the expression profiles was carried out also with GeneSpring GX software and using Pearson's correlation coefficient as distance metrics and average linkage method.

15. RNA sequencing

The leaf transcriptome of *Andigena* WT and *StGl*i plants was analyzed by RNA sequencing (RNA-seq) in collaboration with the Spanish National Center for Genome Analysis (CNAG-CRG; Barcelona).

Leaves were collected at LD ZT8 and total RNA was extracted from 3 independent WT and *StGl*i samples for triplicate studies. RNA was purified as indicated above, quantified using Qubit® RNA BR Assay kit (Thermo Fisher Scientific) and its integrity assessed by RNA 6000 Nano Assay on a 2100 BioAnalyzer (Agilent). RNA-seq libraries were prepared using the KAPA Stranded mRNA-Seq Kit Illumina® Platforms (Kapa Biosystems), with minor modifications. Briefly, 500ng of total RNA was mRNA-enriched with oligo-dT magnetic beads and fragmented to 80-250bp-size fragments. The second strand cDNA synthesis was performed in the presence of dUTP instead of dTTP, to achieve the strand specificity. The blunt-ended double stranded cDNA was 3´adenylated and Illumina indexed adapters (Illumina) were ligated. The ligation product was enriched with 15 PCR cycles and the final library was validated on an Agilent 2100 Bioanalyzer, using the DNA 7500 assay (Agilent technologies). Each library was sequenced using the TruSeq SBS Kit v4-HS, in paired-end mode, with a read length of 2x76bp. 60 million paired-end reads were generated on average for each sample, as a fraction of a sequencing lane on HiSeq2000 (Illumina). Image analysis, base calling and quality scoring of the run were obtained by using the manufacturer's Real Time Analysis (RTA 1.18.66.3) software, followed by generation of FASTQ sequence files with CASAVA.

The RNA-seq data was aligned to the potato reference genome (SolTub_3.0) using STAR (version 2.5.1b) and ENCODE parameters for long RNA (Dobin et al., 2013). The *Solanum tuberosum* gene annotation file was downloaded from ensembl release 32. Transcript abundance was quantified using RSEM (version 1.2.28) and the default parameters (Li and Dewey, 2011). Normalization and differential expression analysis was performed with the DESeq2 R package (version 1.10.1) (Love et al., 2014). DEGs were considered to be statistical significant if they had a Wald test p-value less than 0.05 when compared with WT leaves.

16. Comparison and functional enrichment analysis of DEGs

The gene expression data obtained from the microarray and RNA-seq experiments was visualized with the Mapman software and using the Stub_PGSC_DM_v3.4 mapping file available at http://mapman.gabipd.org/ (Usadel et al., 2005). DEGs were classified based on the first level of Mapman Bin classification and enrichment on each category of genes was

tested based on the one-sided Fisher's exact test ($p<0.05$). The percentage of DEGs for each category was calculated from the total number of genes assigned to at least one functional category and unassigned genes were not taken into account. Input data is shown in Supplementary file 1 sheets 1-2, for Figure 19; Supplementary file 1 sheets 6-7, for Figure 32; and Supplementary file 1 sheets 17-18 for Figure 38.

Venn diagrams comparing different sets of DEGs were generated using the BioVenn web tool (http://www.biovenn.nl/). Input data is shown in Supplementary file 1 sheets 3-6 for Figure 27C and in Supplementary file 1 sheets 11-16 for Figure 37B.

17. Sequence alignment

DNA and protein sequence alignments were carried out using the Multalin web tool with default parameters (http://multalin.toulouse.inra.fr/multalin/).

The genomic region encompassing the *SP5G* locus in potato and tomato was compared using nBLAST and represented with the Easyfig software (Altschul et al., 1990; Sullivan et al., 2011). Potato (v4.03; chr05:49292800..49357300) and tomato (vSL2.50; chr05:63885150..63911650) sequences were annotated according to NCBI database and missing genes were annotated manually (http://www.ncbi.nlm.nih.gov). Unknown N1 and N2 regions were amplified from *Andigena*, sequenced, and added to the genome sequence before nBLAST analysis.

Table 1. Primers used in this work.

Primer name	Sequence (5' to 3')	Target	Amplicon	Usage
***StGI* RNAi for**	CACCATCTTGGGCTCC GGATG	*StGI* (chr12:54737061..54723121)	705bp	RNAi cloning
***StGI* RNAi rev**	TTCTGCCACAGCAAGAT TTTT	*StGI* (chr12:54737061..54723121)	705bp	RNAi cloning
p*StCDF1* for	CTCCAATCCCTAGCGTG AAA	*StCDF1* promoter	2455bp	promoter cloning
p*StCDF1* rev	TTTCTTGAATTCCTCTTC TCAATTC	*StCDF1* promoter	2455bp	promoter cloning
HA-StCDF1 for	CACCATGTATCCCTATG ACGTCCCGGACTATGC AGGATCCTATCCATATG ACGTTCCAGATTACGCT GCTCAGTGCAGCATGT CTGAAGTTAGAGATCCT GC	*StCDF1* (PGSC0003DMG400018408)	1408bp	gene cloning
***StCDF1* rev**	TCATTGTGTGCTCTCGC GGAAATG	*StCDF1* (PGSC0003DMG400018408)	1408bp	gene cloning
***StGI* for**	CACCATGGCTTCTTCAA GCACAAGGTG	*StGI* (chr12:54737061..54723121)	3517bp	gene cloning
***StGI* rev**	GACTGATATAGTACAGC CTAATT	*StGI* (chr12:54737061..54723121)	3517bp	gene cloning
p*StSP5G* for	CACCCCTTACCATAAGG TGGCT	*StSP5G-A* promoter	2461bp	promoter cloning
p*StSP5G* rev	TCTCAATTATAATAAGCT CAATT	*StSP5G-A* promoter	2461bp	promoter cloning
***StSP5G* for**	ATGCCTAGAGATCCTCT AAT	*StSP5G-A* (chr05:49298571..49301691) *StSP5G-B* (chr05:49318369..49321451)	525bp	CAPS marker
***StSP5G* rev**	TAGGCGACGACCACCG GTAC	*StSP5G-A* (chr05:49298571..49301691) *StSP5G-B* (chr05:49318369..49321451)	525bp	CAPS marker
q-Actin for	GGAAAAGCTTGCCTATG TGG	*StAct* (PGSC0003DMG400003985)	59bp	qPCR
q-Actin rev	CTGCTCCTGGCAGTTTC AA	*StAct* (PGSC0003DMG400003985)	59bp	qPCR
q-*StGI* for	ACAAAGGACAGGCATTT TGG	*StGI* (chr12:54737061..54723121)	107bp	qPCR
q-*StGI* rev	TGCCAGAGCAATGAGA CAAC	*StGI* (chr12:54737061..54723121)	107bp	qPCR
q-*StGI-like1* for	ACCTGTAGGTGAAGATC CTCACCAT	*StGI-like1* (chr04:61226774..61193170)	85bp	qPCR
q-*StGI-like1* rev	GGGATTTTTTTCTTTCT GCTTTCCAC	*StGI-like1* (chr04:61226774..61193170)	85bp	qPCR
q-*StCOL1* for	GTAGCAACAATTGGGCA AGGG	*StCOL1* (PGSC0003DMG402010056)	64bp	qPCR
q-*StCOL1* rev	AGTAAACGGTACATGTT GCGGA	*StCOL1* (PGSC0003DMG402010056)	64bp	qPCR
q-*StCOL2* for	GATGGCAGCAGCAATTA CTGG	*StCOL2* (PGSC0003DMG401010056)	61bp	qPCR
q-*StCOL2* rev	TGGTACAGGTAACTAAA CGGCA	*StCOL2* (PGSC0003DMG401010056)	61bp	qPCR
q-*StSP5G* for	GGTGTGTAGACTTTGGT GTGGTTT	*StSP5G-A* (chr05:49298571..49301691) *StSP5G-B* (chr05:49318369..49321451)	64bp	qPCR

Table 1. Primers used in this work.

Primer name	Sequence (5' to 3')	Target	Amplicon	Usage
q-StSP5G rev	GGCCTCAAGGCACATC CAT	*StSP5G-A* (chr05:49298571..49301691) *StSP5G-B* (chr05:49318369..49321451)	64bp	qPCR
q-*StSP6A* for	GACGATCTTCGCAACTT TTACA	*StSP6A* (PGSC0003DMG400023365)	74bp	qPCR
q-*StSP6A* rev	CCTCAAGTTAGGGTCG CTTG	*StSP6A* (PGSC0003DMG400023365)	74bp	qPCR
q-*StSP6A* cv for	AATCTTGGATTGCCTGT TGC	cultivar *StSP6A* (PGSC0003DMG400023365)	60bp	qPCR
q-*StSP6A* cv rev	TCCAGTGCCACTCTCCC TAT	cultivar *StSP6A* (PGSC0003DMG400023365)	60bp	qPCR
q-*StCDF1* for	TGCAGACTCGTCGATTG AAC	*StCDF1* (PGSC0003DMG400018408)	130bp	qPCR
q-*StCDF1* rev	GAGTGCCTTTTCCTCAC TCG	*StCDF1* (PGSC0003DMG400018408)	130bp	qPCR
q-*StFKF1* for	ACGACGATGACGATGAT GAA	*StFKF1* (PGSC0003DMG400019971)	91bp	qPCR
q-*StFKF1* rev	GGCGTCGTTGAAGGAT AGAA	*StFKF1* (PGSC0003DMG400019971)	91bp	qPCR
q-*StAGL8* for	AGCAAAACAACCAGCTT TCCAA	*StAGL8* (PGSC0003DMG400004081)	73bp	qPCR
q-*StAGL8* rev	TGATCCCACTGATTTTG CTGTG	*StAGL8* (PGSC0003DMG400004081)	73bp	qPCR
q-*StGA2ox1* for	AGGCACAGAGTGATCG CAGAT	*StGA2ox1* (PGSC0003DMG400021095)	65bp	qPCR
q-*StGA2ox1* rev	TGGTGGCCCTCCAAAG TAAA	*StGA2ox1* (PGSC0003DMG400021095)	65bp	qPCR
q-*StIAA19* for	ACTGGATGCTTGTGGGT GAC	*StIAA19* (PGSC0003DMG400016512)	100bp	qPCR
q-*StIAA19* rev	CGAAGCCCTATCACTTT TGC	*StIAA19* (PGSC0003DMG400016512)	100bp	qPCR
q-*StXTH9* for	GATGAGACCCCTGTTC GTGT	*StXTH9* (PGSC0003DMG400026189)	120bp	qPCR
q-*StXTH9* rev	GCCTTGTGTAGCCCAAT CAT	*StXTH9* (PGSC0003DMG400026189)	120bp	qPCR
q-*StSAUR76* for	TGCCGTAGCAACTCATC ATC	*StSAUR76* (PGSC0003DMG400013549)	63bp	qPCR
q-*StSAUR76* rev	CGATTTTCATCGGAAAA GGA	*StSAUR76* (PGSC0003DMG400013549)	63bp	qPCR
q-*StSBPase* for	GATACACCGGAGGAAT GGTG	*StSBPase* (PGSC0003DMG400027125)	93bp	qPCR
q-*StSBPase* rev	TCGCCTTAGCTGTTGGA GAT	*StSBPase* (PGSC0003DMG400027125)	93bp	qPCR
q-*StMEX1* for	CGATTGTGCCCTTGTAT CCT	*StMEX1* (PGSC0003DMG400024812)	109bp	qPCR
q-*StMEX1* rev	TCGAGCTTCAACATGCA TTC	*StMEX1* (PGSC0003DMG400024812)	109bp	qPCR
q-*StBAM3-like1* for	GCACGTATGTTCGTGAA ACG	*StBAM3-like1* (PGSC0003DMG402020509)	66bp	qPCR
q-*StBAM3-like1* rev	CTCTCCATCCCTCATTT CCA	*StBAM3-like1* (PGSC0003DMG402020509)	66bp	qPCR
q-*StBAM6-like1* for	ATGCTAAGTCTGGCCCT CAA	*StBAM6-like1* (PGSC0003DMG400026166)	93bp	qPCR
q-*StBAM6-like1* rev	TTGCAAGTGCATTCTCA CCT	*StBAM6-like1* (PGSC0003DMG400026166)	93bp	qPCR

Table 1. Primers used in this work.

Primer name	Sequence (5' to 3')	Target	Amplicon	Usage
q-*StSUS2* for	CACCGTTGGACAGTATG AGAG	*StSUS2* (PGSC0003DMG400013546)	91bp	qPCR
q-*StSUS2* rev	GAATTTGGGATCGAACA CATC	*StSUS2* (PGSC0003DMG400013546)	91bp	qPCR
q-*StSUS4* for	TGGGAATACATCCGTGT GAA	*StSUS4* (PGSC0003DMG400002895)	95bp	qPCR
q-*StSUS4* rev	GCTCCGTCGACAAGTTC TTC	*StSUS4* (PGSC0003DMG400002895)	95bp	qPCR
q-*StLHY* for	ATGTGGACCGCAGTTA GACC	*StLHY* (chr10:147555..171501)	66bp	qPCR
q-*StLHY* rev	TCCATTGTTTGGTGACT GGA	*StLHY* (chr10:147555..171501)	66bp	qPCR
q-*StTOC1* for	CAAAGCCCAACCTCTAT CCA	*StTOC1* (PGSC0003DMG400033048)	80bp	qPCR
q-*StTOC1* rev	TGTTCATGTCCTCCCAA TGA	*StTOC1* (PGSC0003DMG400033048)	80bp	qPCR
q-*StPRR5* for	CCCGTGGTCCGATTACT AGA	*StPRR5* (PGSC0003DMG400000584)	71bp	qPCR
q-*StPRR5* rev	CATTTCAGCTGGTCCTG GTT	*StPRR5* (PGSC0003DMG400000584)	71bp	qPCR

Table 2. Constructs used in this work.

Construct name	Plasmid	Insert	Method of Cloning	Reference
TOPO RNAi *StGI*	pENTR™ /D-TOPO®	*StGI* RNAi	PCR product (*StGI* RNAi for + *StGI* RNAi rev)	
pBIN19 RNAi *StGI*	pBIN19 RNAi	*StGI* RNAi	LR reaction from TOPO RNAi *StGI*	
pGEMT p*StCDF1*	pGEM®-T Easy	p*StCDF1*	PCR product (p*StCDF1* for + p*StCDF1* rev)	
TOPO HA-StCDF1	pENTR™ /D-TOPO®	HA-StCDF1	PCR product (HA-StCDF1 for + *StCDF1* rev)	
TOPO p*StCDF1*::HA-StCDF1	pENTR™ /D-TOPO®	p*StCDF1*::HA-StCDF1	p*StCDF1* cloned into NotI site of pENTR™ /D-TOPO®	
pGWB13 *pStCDF1*::HA-StCDF1	pGWB13	p*StCDF1*::HA-StCDF1	LR reaction from TOPO p*StCDF1*::HA-StCDF1	
TOPO *StGI*	pENTR™ /D-TOPO®	*StGI*	PCR product (*StGI* for + *StGI* rev)	
pGWB14 *StGI*	pGWB14	*StGI*	LR reaction from TOPO *StGI*	
TOPO p*StSP5G*	pENTR™ /D-TOPO®	p*StSP5G*	PCR product (p*StSP5G* for + p*StSP5G* rev)	
pGWB3 p*StSP5G*	pGWB3	p*StSP5G*	LR reaction from TOPO p*StSP5G*	
pBINAR *StSP5G*	pBINAR	*StSP5G*	*StSP5G* ORF cloned into SmaI site of pBINAR	Navarro et al., unpublished
pBINAR *StSP6A*	pBINAR	*StSP6A*	*StSP6A* ORF cloned into SmaI site of pBINAR	Navarro et al., 2011

Table 3. Transgenic plants used in this work.

Transgenic line name	Background	Construct	Selection	Reference
***StGI*i**	*Andigena* 7540	pBIN19 RNAi *StGI*	Kan+	
35S::StCDF1.2	*Andigena* 7540	pk7WG2 StCDF1.2	Kan+	Kloosterman et al., 2013
p*StCDF1*::HA-StCDF1	*Andigena* 7540	pGWB13 p*StCDF1*::HA-StCDF1	Kan+/Hyg+	
***StGI*i p*StCDF1*::HA-StCDF1**	*Andigena* 7540	pBIN19 RNAi *StGI* pGWB13 p*StCDF1*::HA-StCDF1	Kan+/Hyg+	
35S::StGI-HA	*Andigena* 7540	pGWB14 *StGI*	Kan+/Hyg+	
p*StSP5G*::GUS	*Andigena* 7540	pGWB3 p*StSP5G*	Kan+/Hyg+	
***StSP5G*i**	*Andigena* 7540	pBIN19 RNAi *StSP5G*	Kan+	Abelenda et al., 2016
***StSP5G*ox**	*Andigena* 7540	pBINAR *StSP5G*	Kan+	
***StSP6A*ox**	*Spunta*	pBINAR *StSP6A*	Kan+	
***StSP6A*ox**	*Sylvana*	pBINAR *StSP6A*	Kan+	

Results: Chapter 1

Role of StGIGANTEA in SD-dependent tuberization of *Andigena* plants

GIGANTEA is a plant specific protein whose function has been associated with multiple physiological processes including flowering time, the circadian oscillator, hypocotyl elongation, carbohydrate metabolism, salt tolerance and chlorophyll accumulation, among others (Mishra and Panigrahi, 2015). It was first isolated in *Arabidopsis*, by identification of the genetic lesions in a mutant which showed delayed flowering in LDs but that flowered normally in SD, hence suggesting a role for the encoded protein in the day-length flowering pathway (Fowler et al., 1999). Expression of *GI* is regulated by the circadian clock and peaks with the light period, its oscillation phase being slightly changed in LD or SDs. *GI* encodes a nuclear localized protein of 1173 amino acids which shares no significant homology to other proteins of known function. Overexpression of the GI protein in the *lhy cca1* mutant showed that this protein has distinct roles in promoting flowering and in the regulation of circadian clock function (Mizoguchi et al., 2005). Indeed, expression of *CO* and *FT*, but not other clock regulated genes, is activated in *35S::GI* lines, with loss of function *co-2* and *ft-1* mutations being shown to delay early flowering of *35S::GI* plants (Mizoguchi et al., 2005). GI has been reported to interact with two homologous proteins, i.e. FLAVIN-BINDING, KELCH REPEAT, F-BOX1 (FKF1) and ZEITLUPE (ZTL), with antagonistic functions in the control of CO protein stability (Song et al., 2014; Song et al., 2012). In particular, GI stabilizes the ZTL and FKF1 proteins and indirectly contributes to CO protein destabilization in the morning and accumulation in the late afternoon. GI-FKF1 interaction also mediates ubiquitin-dependent degradation of the CYCLING DOF FACTOR (CDF) proteins, which repress *CO* transcription during LD late afternoon (Kim et al., 2007; Sawa et al., 2007). Likewise, GI has been proposed to directly activate *FT* transcription, and shown to bind the *FT* repressors SHORT VEGETATIVE PHASE (SVP), and TEMPRANILLO 1 (TEM1) and TEM2 in the nucleus (Sawa and Kay, 2011). Moreover, it indirectly activates *FT* transcription by positively regulating miR172 expression, a small RNA that targets the *FT* repressors TARGET OF EAT 1 (TOE1) and TOE2. (Jung et al., 2007). Notably, although molecular function of GI had remained elusive since its discovery two decades ago, GI has been shown in a recent study to act as a co-chaperone that associates with HSP90 to facilitate ZTL maturation (Cha et al., 2017). It has been proposed that the protein GI controls maturation of a wide range of HSP90 client proteins in plants, hence explaining the large diversity of phenotypes observed in the *Arabidopsis gi* mutants (Mishra and Panigrahi, 2015).

GI is highly conserved among vascular plants, but its function in *Solanaceae* has not been extensively studied. Therefore, in a first set of studies, we focused to analyse whether function of this protein in the control of *CO* and *FT* expression is conserved in potato.

1. GIGANTEA represses tuber formation and controls plant maturity in potato

We identified two potato homologs of the *GIGANTEA* gene, *StGI* and *StGI-like1*, on chromosomes 12 and 4 respectively. *StGI* and *StGI-like1* encode two highly conserved proteins that share more than 70% identity at the amino acid level with the *Arabidopsis* GI protein (Figure S1).

To assess the role of these two *GI*-like genes in the photoperiodic control of tuberization we first analysed their diurnal oscillation pattern in leaves of *Andigena* plants grown under LD and SD conditions. RT-qPCR amplification showed that *StGI* is more abundantly expressed than *StGI-like1* and that both *GI*-like transcripts rise during early morning to reach a peak of expression between ZT8 and ZT11 in LDs (Figure 11A). In SDs, this peak is shifted towards ZT5 to ZT8, thus coinciding with daytime (Figure 11A). Overall, both of these genes show an analogous expression pattern as *Arabidopsis GI* (Fowler et al., 1999), hence suggesting that they exert redundant functions in potato leaves.

StGI was identified as a phyB-dependent day-length regulated gene in comparative analyses of leaves of *Andigena* plants grown in LD and SD (Rutitzky et al., 2009). Also, in Bimolecular Fluorescence Complementation (BiFC) assays, we could show that the StGI protein interacts with StFKF1 and StCDF1 (Kloosterman et al., 2013), pointing to a conserved function of potato StGI in the regulation of *CO* and *FT* expression, and therefore in the day-length tuberization pathway. To confirm this hypothesis, we generated transgenic *Andigena* RNAi (*StGIi*) lines, in which *StGI* expression was silenced (Figure 10D). These plants tuberized in LDs, proving that GIGANTEA acts as a repressor of tuberization in potato (Figure 10C). Interestingly, *StGI* inhibition leads also to smaller plants that show accelerated signs of senescence (Figure 10A; Figure 10B). On average, these plants reach to maturity much earlier than the WT and this effect is even more notorious in LDs, in which WT plants are unable to tuberize and remain green while *StGIi* plants tuberize and soon after complete their life cycle (Figure 10E).

Given that *StGI* and *StGI*-like1 share highly conserved nucleotide sequences, we tested *StGI-like1* expression in the *StGIi* lines. Notably, only a small reduction in *StGI-like1* expression levels was observed in these plants (Figure 11B), demonstrating that their phenotype is principally caused by specific inhibition of the *StGI* gene.

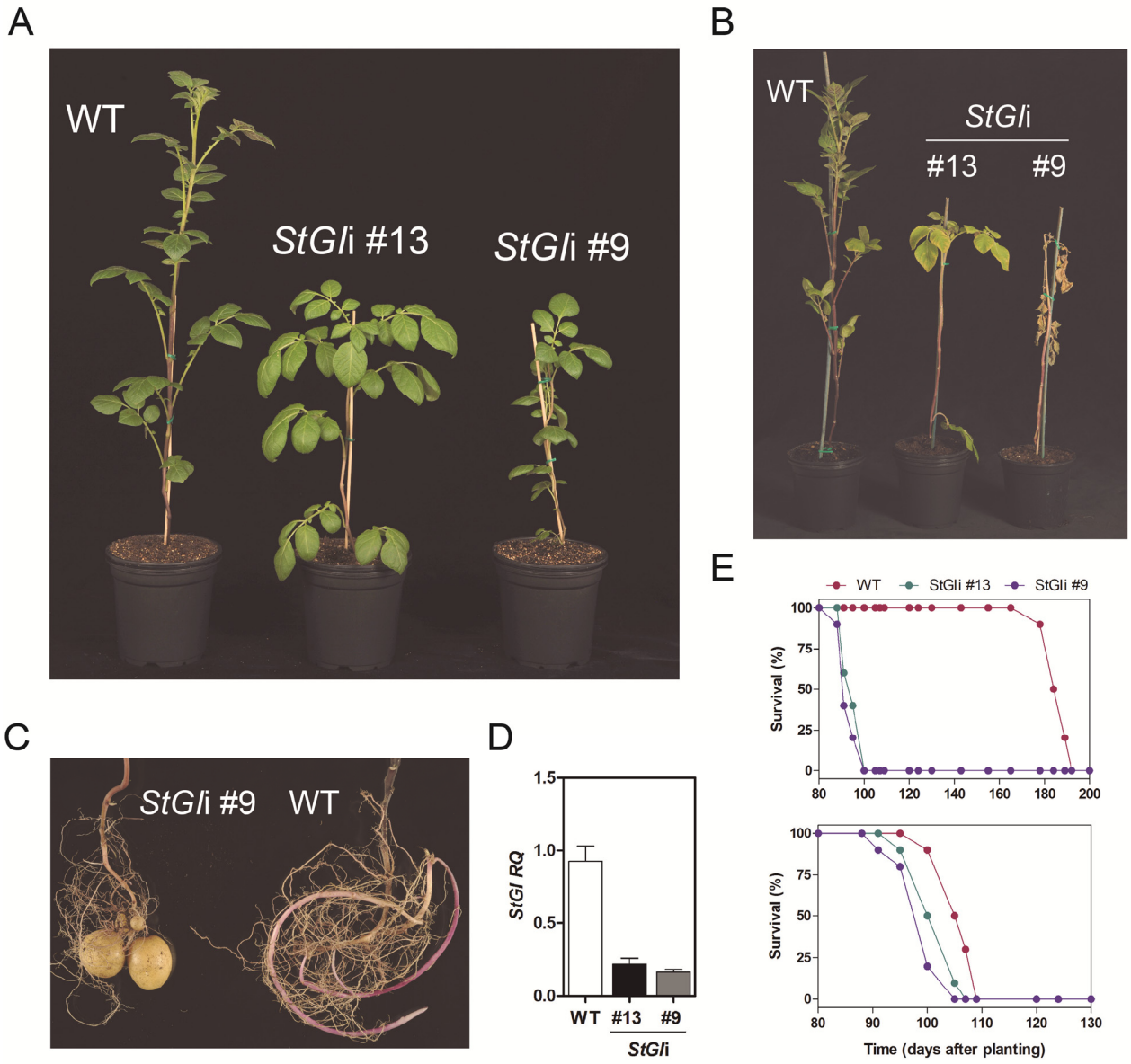

Figure 10. *StGl* inhibition promotes tuberization in LDs and accelerates plant senescence. (A) 5 weeks-old *Andigena* WT and *StGl*i plants grown in LDs. *StGl*i lines are smaller and show paler leaves. (B) *Andigena* WT and *StGl*i plants grown under LDs for 14 weeks. *StGl*i plants show accelerated signs of senescence whereas WT plants remain green. (C) Tuberization phenotype of *Andigena StGl*i plants under LDs. (D) qPCR analysis of *StGl* expression in two independent *StGl*i lines. Leaves of LD grown plants were harvested at ZT8 for analyses. (E) Percentage of plant survival in function of the plant age (days after planting) as determined in WT and *StGl*i plants grown under LD (upper graph) or SD conditions (lower graph).

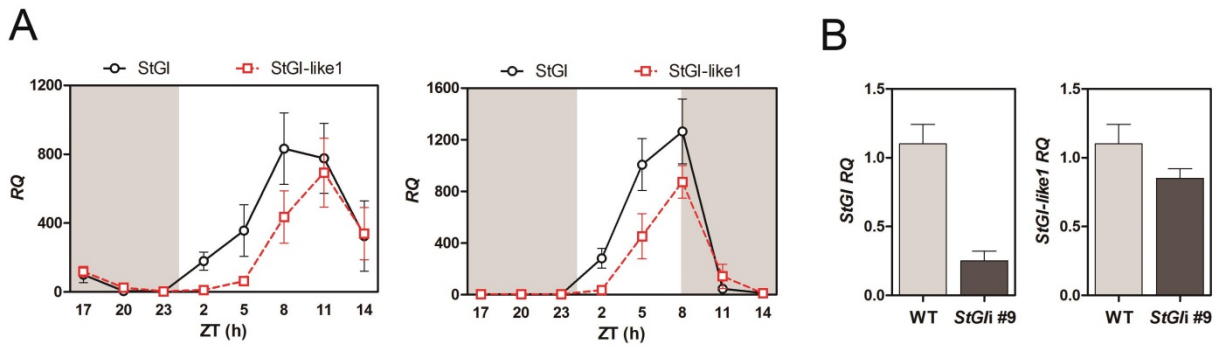

Figure 11. Diurnal pattern of oscillation of the *StGI* and *StGI-like1* genes and specificity of the *StGI*-RNAi construct. (A) qPCR analysis of *StGI* and *StGI-like1* expression levels in leaves of *Andigena* plants grown under LD (left) or SD conditions (right). (B) qPCR analysis of *StGI* and *StGI-like1* transcript levels in *StGI*i line #9. Plants were grown in LD conditions and leaves were harvested at ZT8 for analyses. Error bars represent ±s.d. of three biological replicates.

2. *StGI* inhibition mimics the effects of *StCFD1.2* overexpression

Mutations in *GIGANTEA* increase *Arabidopsis* CDFs abundance and lead to late flowering in LDs, due to suppressed activation of *CONSTANS* and *FT* (Sawa et al., 2007). In potato, alleles of *StCDF1* coding for a truncated form of the protein unable to interact with *StFKF1,* confer the early tuberization and maturation traits of genotypes adapted to northern latitudes and they have been strongly selected during breeding because of their dominant character (Kloosterman et al., 2013).

Notably, the tuberization and early maturation phenotype of *StGI*i plants phenocopies the effects of overexpression of the truncated *StCDF1.2* allele (Figure 12A), suggesting that StGI plays a role in modulating StCDF1 stability (Kloosterman et al., 2013). To further assess that these phenotypes are related at the functional level, we analysed tuber yield and levels of expression of the tuberization pathway genes in WT, *StGI*i and *35S::StCDF1.2* plants grown under LD and SDs. These studies confirmed that both *StGI*i and *35S::StCDF1.2* plants tuberize under non-inductive LDs, while yield in tubers was slightly lower in *35S::StCDF1.2* plants than in *StGI*i (Figure 12B). Moreover, both lines showed in SDs a similar reduction in tuber yield with respect to the WT (Figure 12B), probably because they tuberize with a smaller number of leaves and senesce earlier.

RT-qPCR analyses of diurnal expression patterns of the *StCOL1* and *StCOL2* genes, and the FT homologs *StSP5G* and *StSP6A*, revealed that expression of *StCOL1*, *StCOL2* and *StSP5G* was similarly reduced in *StGI*i and *StCDF1.2*ox leaves independently of day-length conditions (Figure 13). Repressive effects of *StGI* inhibition or *StCDF1.2* overexpression were also stronger on *StCOL2* than on *StCOL1* (Figure 13). Moreover, in

consonance with the reduction in *StCOL1, StCOL2* and *StSP5G* transcript levels, *StSP6A* was strongly up-regulated in these plants under non-inductive LDs (Figure 13). Taken together, these findings suggest that lack of StGI leads to StCDF1 stabilization and to enhanced repression of the *StCOL1* and *StCOL2* genes, hence supporting a critical function of StGI in modulating potato StCDF1 protein stability. Suppressed *StCOL1* and *StCOL2* expression leads, in turn, to impaired *StSP5G* expression, *StSP6A* activation and induction of tuber formation in LDs (Figure 13). Also, as *StSP5G* expression is repressed in the WT in SDs, effects on *StSP6A* activation are less evident than in LDs. Still, constitutively elevated levels of *StSP6A* expression at night are observed in *StGI*i and *35S::StCDF1.2* leaves under SDs (Figure 13). Hence, altogether these results showed that overexpression of *StCDF1.2* or silencing of the *StGI* gene result in identical tuberization and gene expression effects, thus demonstrating that StGI regulation of StCDF1 protein levels plays a critical role in day-length tuberization control.

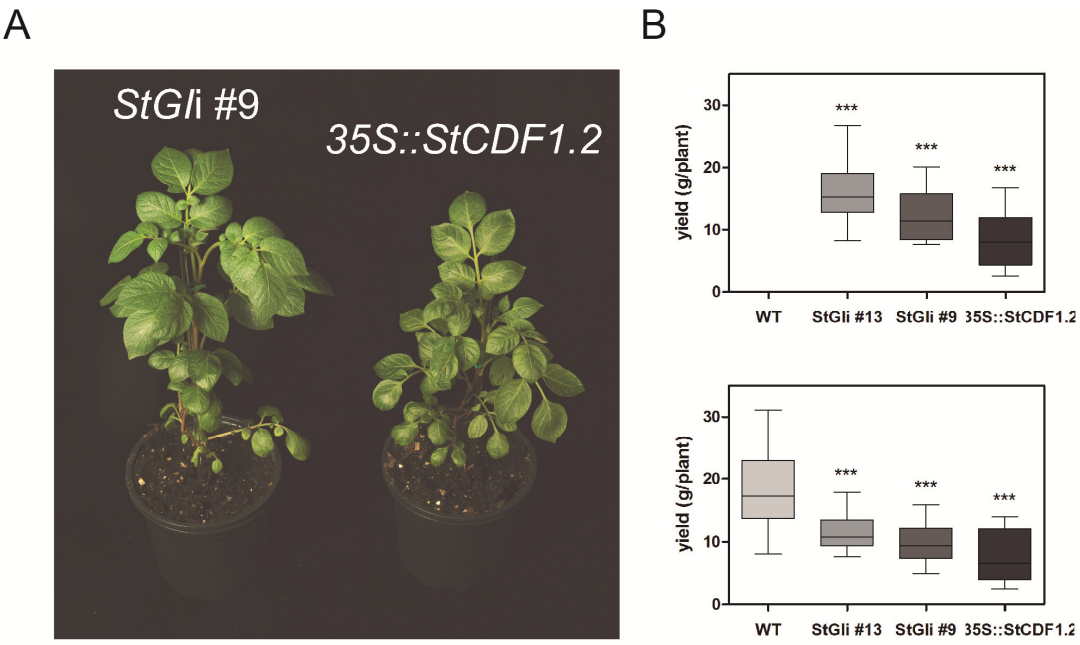

Figure 12. *StGI* inhibition phenocopies the effects of *StCDF1.2* overexpression. (A) *StGI*i and *35S::StCDF1.2* plants grown under LDs for 5 weeks. (B) Tuber yield of WT, *StGI*i and *35S::StCDF1.2* plants grown under LDs (top) and SD conditions (bottom). *** denotes statistical significance ($p<0.001$) respect to WT plants.

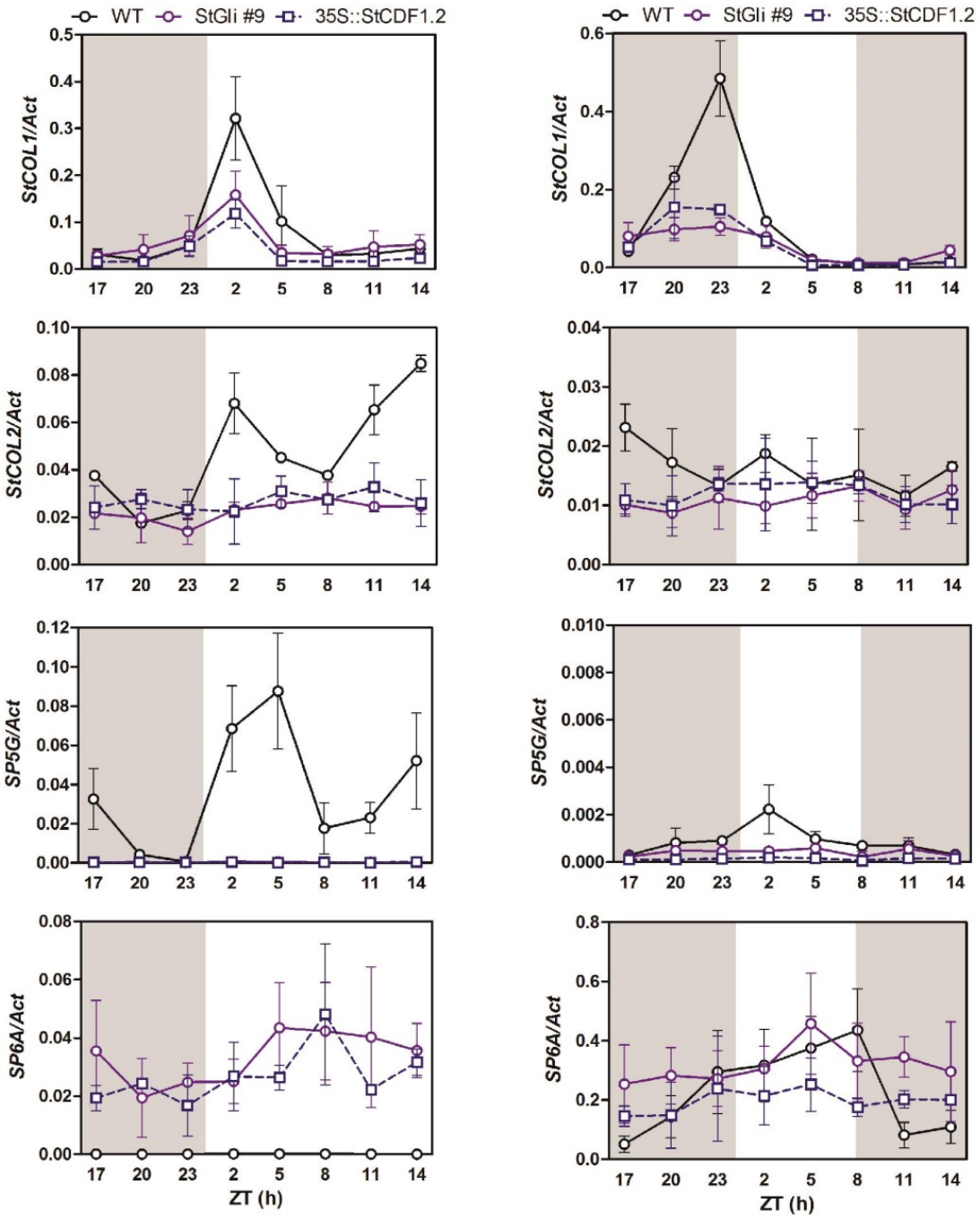

Figure 13. Diurnal oscillation of the day-length pathway tuberization genes in *StGIi* and *35S::StCDF1.2* plants. qPCR amplification of the *StCOL1*, *StCOL2*, *StSP5G* and *StSP6A* genes in WT, *StGIi* and *35S::StCDF1.2* plants grown under LDs (left column) and SDs (right column). Error bars represent ±s.d. of three biological replicates.

3. StGI mediates StCDF1 degradation during late afternoon

In *Arabidopsis*, blue light promotes FKF1 and GIGANTEA interaction and mediates proteasomal degradation of the CDF factors, leading to up-regulated expression of *CONSTANS* during LD late afternoon. Coincidence of *CO* expression with light allows stabilization of the CO protein and promotes the specific activation of *FT* in LDs (Imaizumi et al., 2005; Sawa et al., 2007).

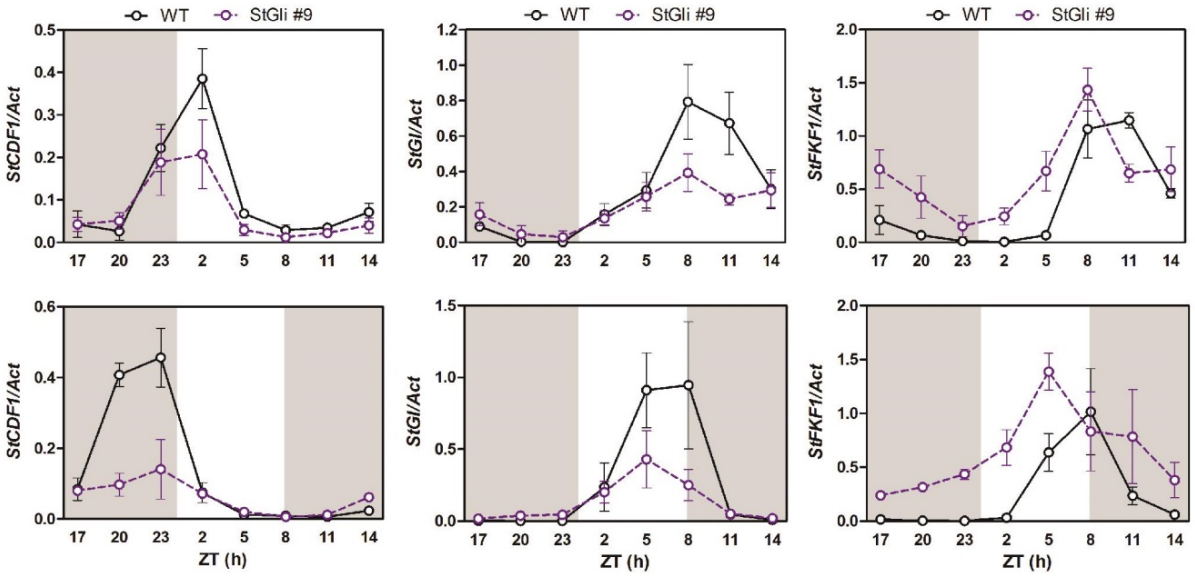

Figure 14. Diurnal oscillation of the *StCDF1*, *StGI* and *StFKF1* genes in *StGI*i plants. qPCR amplification of *StCDF1*, *StGI* and *StFKF1* transcript levels in WT and *StGI*i plants grown in LDs (upper row) and SD conditions (lower row). Error bars represent ±s.d. of three biological replicates.

The finding that *StGI*i and *35S::StCDF1.2* lines share almost identical phenotypes, strongly suggests a conserved function of potato StGI in promoting StCDF1 protein degradation. To gain further insight into the mechanisms underlying this regulation, we first analysed the diurnal rhythm of expression of the *StCDF1*, *StGI* and *StFKF1* genes in WT and *StGI*i plants. In WT plants, *StCDF1* transcription peaks during early morning in LDs, while in SDs this peak is shifted by few hours and coincides with late night (Figure 14). By opposite, *StFKF1* and *StGI* transcription is activated during the afternoon and in LDs they reach a peak of expression between ZT8 and ZT11, while peak of these genes is shifted to ZT8 in SDs, coinciding with dusk (Figure 14). Hence, *StCDF1*, *StGI* and *StFKF1* display analogous oscillation patterns as their *Arabidopsis* homologs (Imaizumi et al., 2005; Sawa et al., 2007). More remarkably, expression of *StCDF1* is reduced in *StGI*i plants (Figure 14) and this suppression is stronger in SD, in agreement with a previous report showing that *CDF2*

expression is reduced in the *Arabidopsis gi* mutants (Fornara et al., 2009). However, unlike *Arabidopsis* (Mizoguchi et al., 2005), we observed *StFKF1* to be induced in potato *StGI*i plants (Figure 14). Peak of *StFKF1* expression is also shifted to an earlier time in the day, with *StFKF1* transcript levels found to rise in these plants already at dawn (Figure 14). Thus, it is tempting to speculate that, in LDs, co-expression of StFKF1 and StCOL1 during early morning modulates the stability of StCOL1 protein, as seen in *Arabidopsis* (Song et al., 2012).

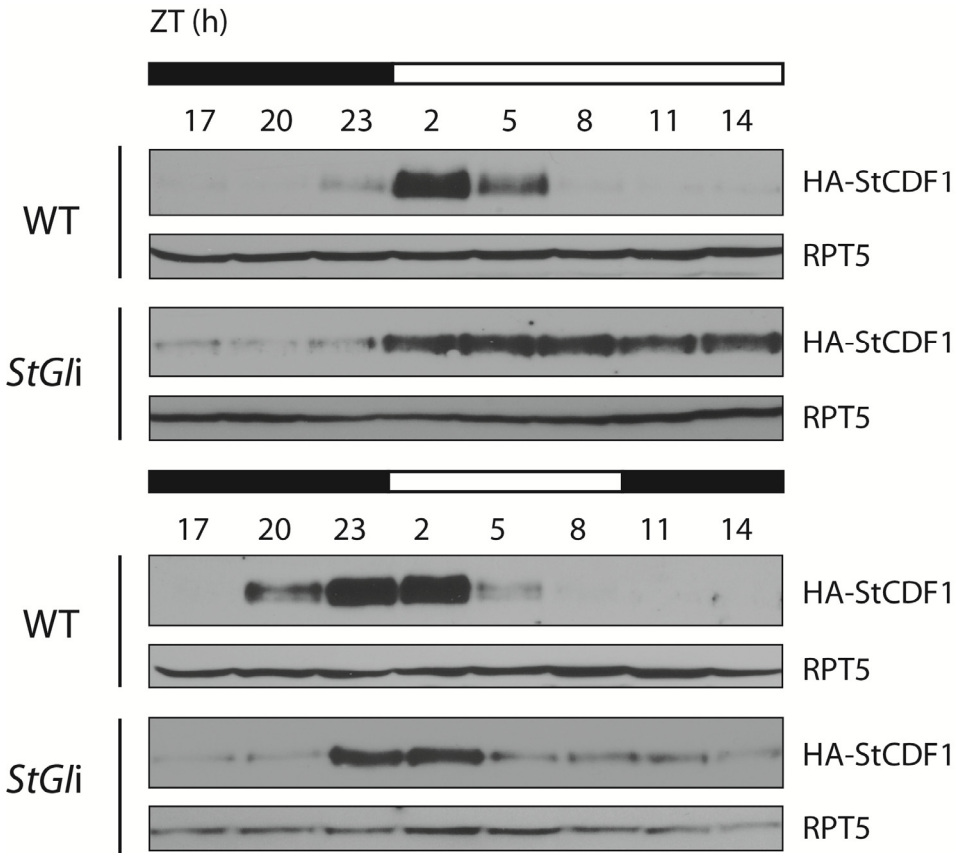

Figure 15. Diurnal accumulation of StCDF1 protein in WT and *StGI*i plants. Western blot detection of HA-StCDF1 protein in p*StCDF1*::HA-StCDF1 and *StGI*i p*StCDF1*::HA-StCDF1 plants grown under LDs (upper blots) and under SDs (lower blots) . RPT5 detection was used as loading control.

To study the effects of StGI on StCDF1 protein stability, we expressed the HA-StCDF1 fusion under control of its native promoter in *Andigena* WT and *StGI*i transgenic plants. Western blot analyses of leaf protein extracts showed that in WT plants, HA-StCDF1 accumulates in LDs in the morning, coinciding with transcription of the gene, and is destabilized after ZT5 (Figure 15). In SDs, HA-StCDF1 accumulates late at night, and is detected until ZT2, which again corresponds to the transcription profile of the gene (Figure 15). However, inhibition of *StGI* causes a notable stabilization of the protein. Indeed, in *StGI*i

lines, HA-StCDF1 was found to accumulate in LDs all day long, while the protein is detected to background levels at night (Figure 15). In SDs, HA-StCDF1 protein levels are elevated at ZT23 and ZT2, and basal levels of the protein are detected the rest of the time (Figure 15).

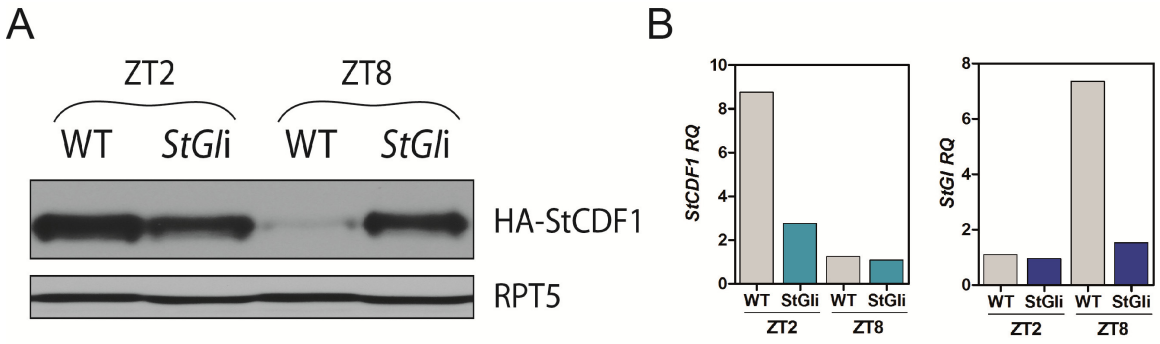

Figure 16. StGI regulates StCDF1 protein accumulation at the post-transcriptional level. (A) Western blot detection of the HA-StCDF1 protein in samples of WT and *StGIi* plants transformed with the p*StCDF1*::HA-StCDF1 construct. Samples corresponding to LD ZT2 and ZT8 were run on the same gel. RPT5 detection was used as loading control. (B) qPCR analyses comparing *StCDF1* (left graph) and *StGI* (right graph) expression in these samples.

Together, these findings indicate that inhibition of StGI stabilizes the StCDF1 protein, and leads to the low levels of HA-StCDF1 protein accumulation detected during night time. However, this effect is obscured by the additional control on *StCDF1* transcription (Figure 14). Actually, when WT and *StGI*i samples are run on the same gel, we observe that HA-StCDF1 protein levels are slightly lower at ZT2 in the *StGIi* background, due to inhibition of *StCDF1* transcription (Figure 16A; Figure 16B). However, at ZT8, levels of the protein are higher in *StGIi* than in the WT (Figure 16A; Figure 16B), thus supporting an important function of StGI in the post-transcriptional control of StCDF1 protein levels.

4. StGI is destabilized at night

To gain further insight into *StGI* function in the photoperiod control of tuberization, we generated *Andigena* transgenic plants that overexpressed the StGI protein fused to the HA tag (*35S*::StGI-HA) (Figure 17A). In *Arabidopsis*, GIGANTEA is post-translationally regulated by the COP1-ELF3 complex, which promotes its ubiquitination and degradation via proteasome at night (Yu et al., 2008). To test whether stability of the StGI protein is also regulated by light, we analysed diurnal StGI-HA levels in *35S::*StGI-HA plants. As seen in Figure 17C, StGI-HA was found to be more stable during daytime and first hours after dusk, levels of the protein being reduced at night both in LD and SD conditions. Notably, this pattern reminds that reported for the *Arabidopsis* GI protein (David et al., 2006), suggesting that potato StGI is also regulated at the post-translational level.

Since overexpression of *GIGANTEA* leads to activation of *FT* and an early *Arabidopsis* flowering phenotype, we analysed tuber yield and diurnal oscillation of the day-length pathway genes in *35S::*StGI-HA lines. To our surprise, we did not observe that *35S::*StGI-HA lines had any tuberization phenotype. These plants did not tuberize in LDs, and their tuber yields in SD were equivalent to the WT (Figure 17B). In consonance with this, expression profiles of the *StCOL1*, *StCOL2*, *StSP5G* and *StSP6A* genes were identical to the WT (Figure 18). Also, although a mild activation of *StCOL2* was observed in SDs (Figure 18), this was not sufficient to affect *StSP6A* expression or tuberization. Therefore, these results suggest either that StGI overexpression is not sufficient for repressing tuberization under SDs because it requires a limiting co-factor, or that fusion of the HA epitope to the C-terminal end of StGI largely inactivates the protein.

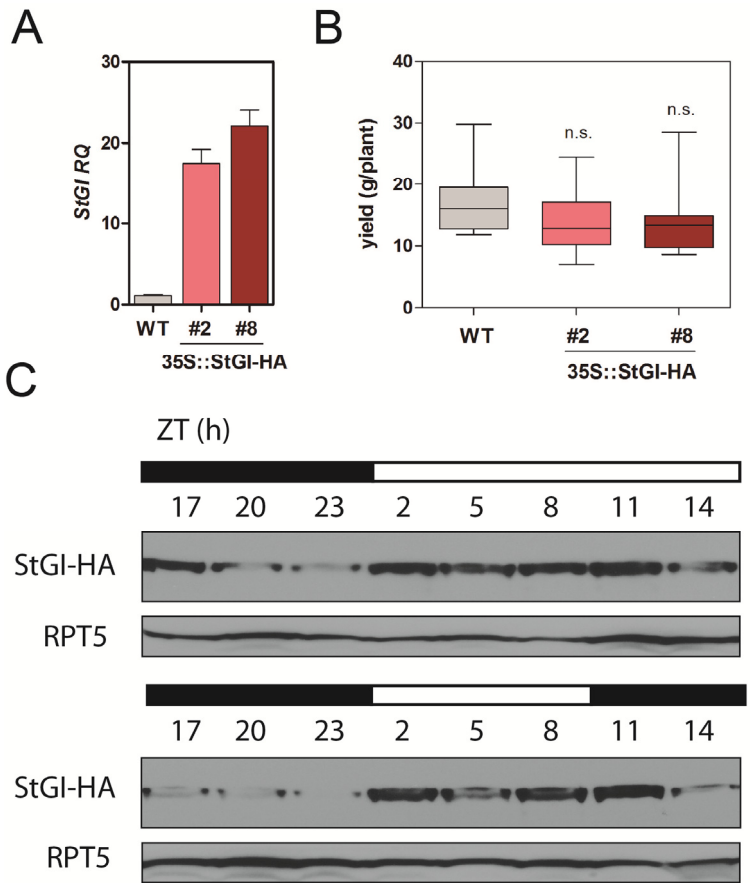

Figure 17. Tuberization phenotype and protein accumulation levels of 35S::StGI-HA plants. (A) qPCR analyses of *StGI* expression in two independent 35S::StGI-HA lines. Leaves were collected at LD ZT23. (B) Tuber yield of WT and *35S::*StGI-HA plants grown in SDs. n.s denotes a not significant difference respect to WT plants. (C) Western blot detection of StGI-HA protein levels in *35S::*StGI-HA plants grown in LDs (upper blots) and SDs (lower blots). RPT5 detection was used as loading control.

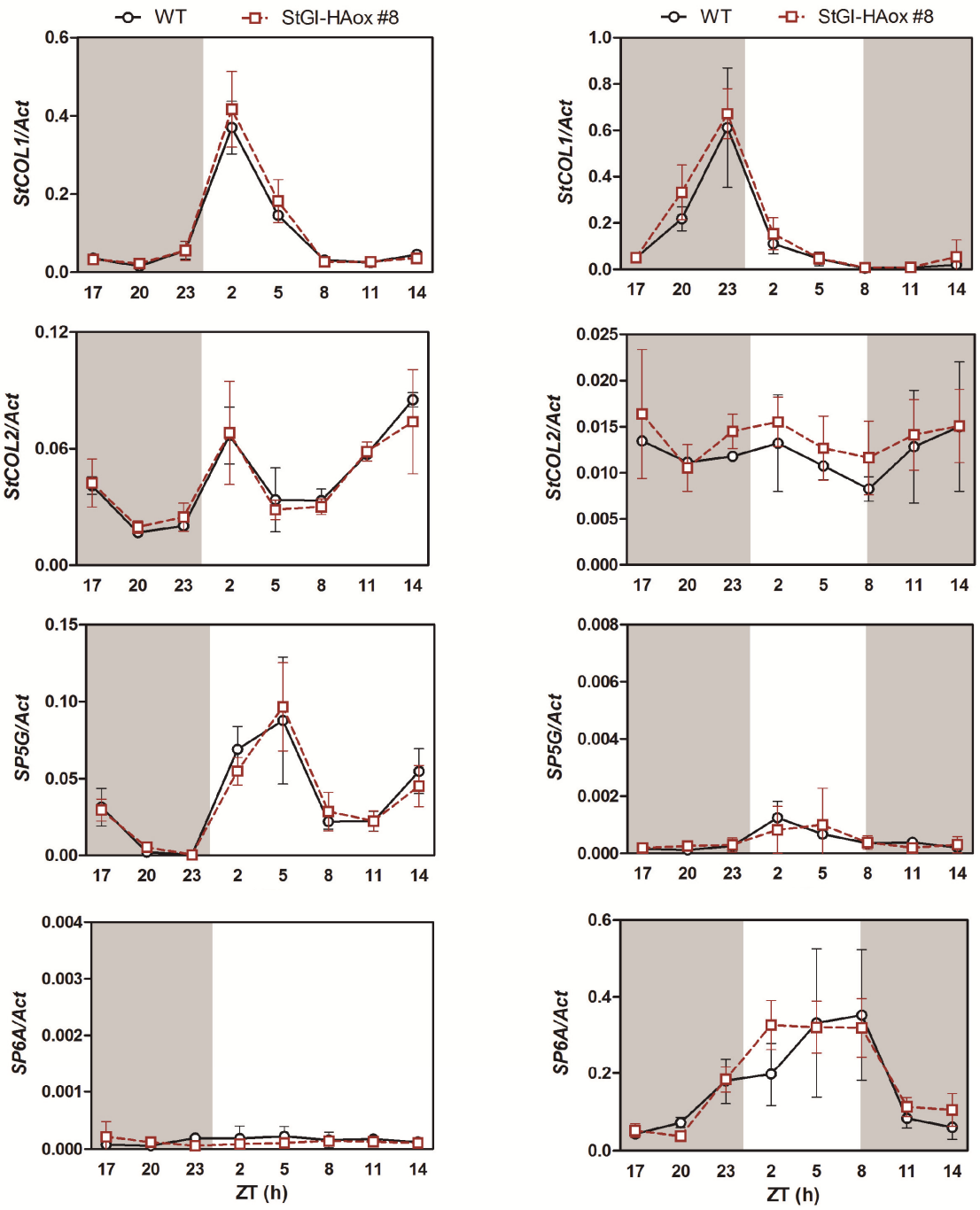

Figure 18. Diurnal oscillation of core tuberization genes in 35S::StGI-HA plants. qPCR analyses of *StCOL1*, *StCOL2*, *StSP5G* and *StSP6A* expression pattern in WT and 35S::StGI-HA plants grown under LDs (left column) and under SDs (right column). Error bars represent ±s.d. of three biological replicates.

5. *StGI* inhibition leads to activation of several MADS-box and senescence-related genes

Besides its function in the control of flowering time, GIGANTEA has been associated in *Arabidopsis* with light signalling, circadian clock regulation, sugar metabolism and stress tolerance, among other responses (Mishra and Panigrahi, 2015). Moreover, while *Arabidopsis gi* mutants senesce later than WT, a hastened senescence was observed in potato *StGIi* plants. Hence, to gain insight into the regulatory pathways activated downstream of *StGI* in potato, we performed high-throughput RNA sequencing (RNA-seq) of leaves from WT and *StGI*i plants grown under LD conditions. After application of the computational pipeline and statistical filtering described in Materials and Methods, we identified 991 genes that were up-regulated and 1057 genes that were down-regulated in *StGI*i lines as compared to WT plants ($p<0.05$; $Log_2FC \leq -0.7$ or ≥ 0.7). Gene ontology analyses of these DEGs revealed that genes up-regulated are over-represented in genes involved in carbohydrate metabolism, secondary metabolism, hormonal regulation, stress, transport, and sulfur assimilation, among others; whereas those down-regulated are significantly enriched in functional categories related with photosynthesis, DNA modification, hormonal regulation and secondary metabolism, among others (Figure 19A; Figure 19B).

Interestingly, silencing of *StGI* promotes activation of multiple MADS-box family genes, including the homologs of the *Arabidopsis* floral regulators *FUL*, *AP1* and *SEP4* (Figure 20). In *Arabidopsis*, *FUL* and *AP1* are direct down-stream targets of the FT-FD complex, and have been reported to control floral meristem transition (Andres and Coupland, 2012). The potato *FUL* homolog*, StAGL8,* was identified in microarray studies as a gene that is strongly co-regulated with *StSP6A* (Morris et al., 2014). Transgenic lines in which expression of this gene is down-regulated were also reported to be impaired in tuber formation in a stem-node *in vitro* system (Rosin et al., 2003). Hence, these data suggest that StGI suppresses expression of these MADS-box genes through the control of *StSP5G* and *StSP6A* expression.

These studies also revealed that silencing of *StGI* leads to activation of a large group of heat shock proteins (HSPs), in addition to three Heat shock transcription factors (HSFs) (Figure 20). HSPs constitute a large family of molecular chaperones that protect eukaryotic cells from different kinds of stresses (Park and Seo, 2015). HSFs bind to Heat Shock Elements (HSE) in the promoter of stress responsive genes, such as those encoding HSPs, and regulate their transcription (Guo et al., 2016). Notably, various HSFs are up-regulated in *Arabidopsis* during leaf senescence, *hsf1b* loss of function being also shown to cause accelerated leaf senescence and lead to plants with reduced tolerance to drought stress

(Breeze et al., 2008; Buchanan-Wollaston et al., 2005). This has led to propose that HSFs and HSPs exert a protective role during leaf senescence and contribute to maintain plant viability during this developmental process. According to this hypothesis, activation of these genes reflects premature senescence of *StGl*i leaves.

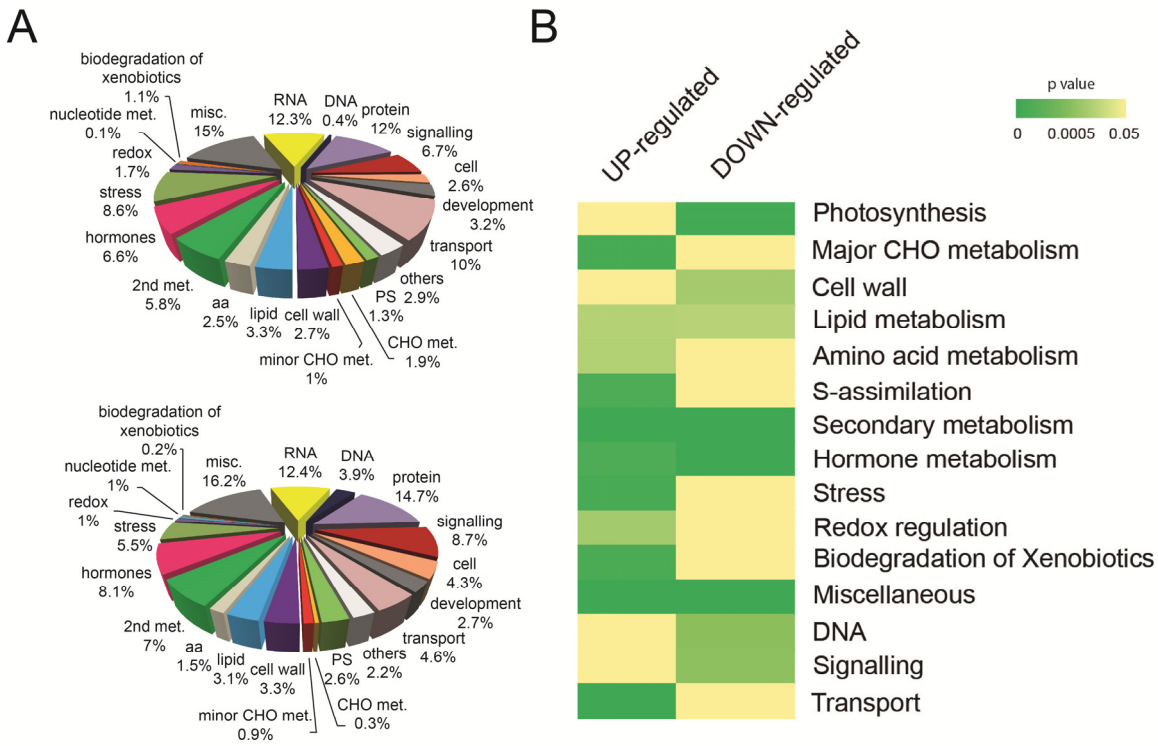

Figure 19. Gene onthology analysis of DEGs in *StGl*i leaves. (A) Functional annotation of the up-regulated (top) and down-regulated genes (bottom) in *StGl*i leaves performed according to the Mapman bin classification. Percentages of genes were calculated from the total of genes assigned to at least one of the 34 functional categories. PS, photosynthesis; CHO met, major carbohydrate metabolism; min CHO met., minor carbohydrate metabolism; aa, amino acid metabolism; 2nd met, secondary metabolism; misc, miscellaneous. (B) Heatmap showing the p values of the functional categories significantly enriched ($p<0.05$) in up- or down-regulated DEGs in *StGl*i leaves. P values were calculated by one-side Fisher's exact test.

Consistent with this, two homologs of SENESCENCE RELATED GENE 1 (SRG1) are also up-regulated in *StGl*i leaves, while a big set of light-harvesting clorohpyll a/b binding proteins are suppressed in these plants (Figure 20). Light-harvesting chlorophyll a/b-binding proteins are apoproteins of the light-harvesting complex of photosystem II (Jansson, 1994). Expression of these antenna proteins is tightly regulated in response to environmental cues, such as light conditions, in addition to be output targets of the circadian clock (Millar and Kay, 1996). Accumulation of these proteins was also shown to be strongly inhibited during leaf senescence (Bate et al., 1991; Miller et al., 1999). In addition, we observed that transcript levels for two STAYGREEN proteins, which regulate the first step in chlorophyll dismantling

from the chlorophyll binding proteins, were reduced in *StGl*i leaves, the same as several ethylene signalling and biosynthesis genes (Figure 20). Interestingly, both groups of genes are generally associated to senescence, hence evidencing that *StGI* inhibition accelerates this process in potato without the activation of these well-known senescence inducers (Kusaba et al., 2013; Oh et al., 1997).

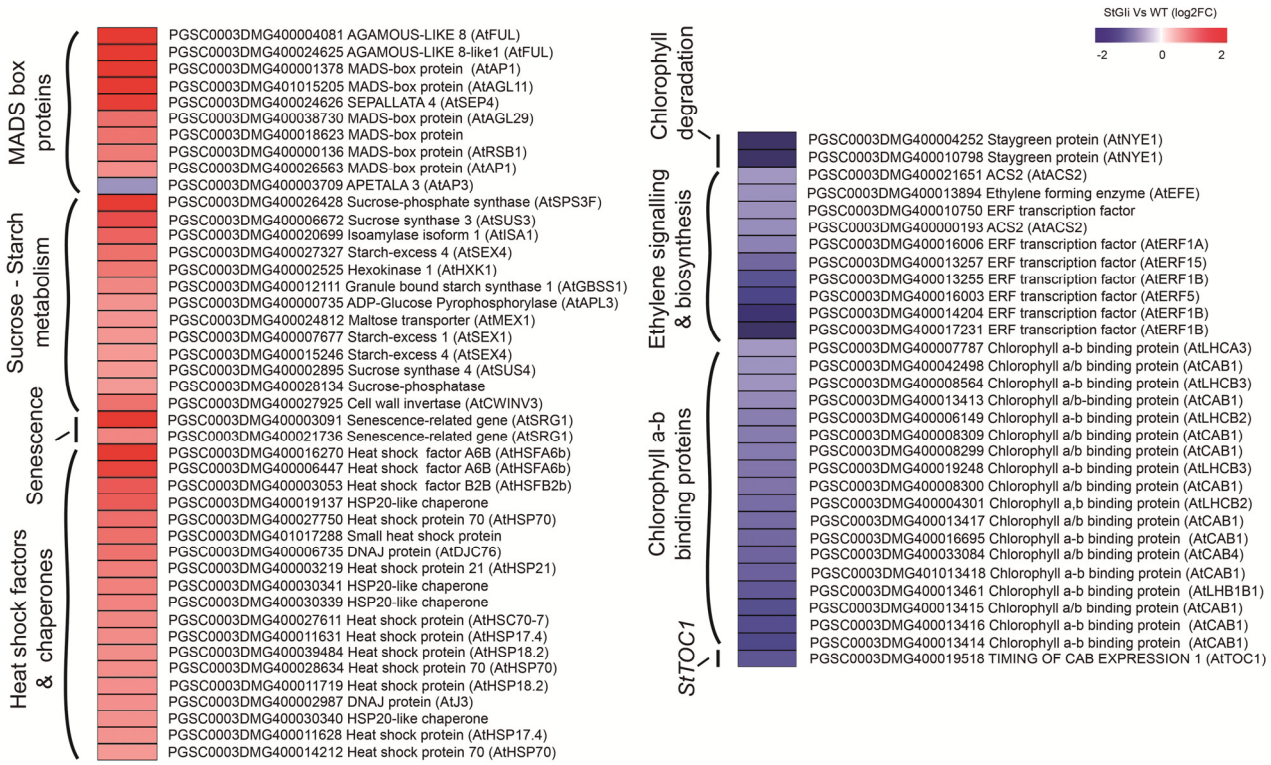

Figure 20. Representative DEGs in *StGl*i leaves. Heatmap showing relative expression levels of a number of representative DEGs in *StGl*i leaves. Genes are represented with their ID number and their closest *Arabidopsis* homolog is shown in parentheses.

Moreover, expression of several transporters and enzymes involved in sucrose-mobilization is also found to be induced in *StGl*i leaves. These included genes involved in starch degradation, like homologs of the *Arabidopsis* Starch-excess (SEX) genes, the MEX1 maltose transporter, and the sucrose phosphate synthase (SPS) gene; in addition to genes involved sucrose catabolism and starch biosynthesis such as *StSUS3*, *StSUS4*, *ADP-glucose pyrophosphorylase* (*StAPL3*) and *Granule Bound Starch Synthase 1* (*GBSS1*) (Figure 20). Consistent with these changes in gene expression, up-regulated levels of expression of *HEXOKINASE 1* (*HXK1*) are also observed in these plants, this enzyme being proposed to be involved in sensing endogenous sugar levels in photosynthetic tissues and to play a role in regulation of photosynthesis and growth. *Arabidopsis* plants over-expressing

HXK1 in photosynthetic tissues were indeed shown to display reduced photosynthetic rates and undergo rapid senescence (Dai et al., 1999; Moore et al., 2003), and thus its up-regulation might participate in mediating the early senescing phenotype of *StGIi* plants.

6. *StGIi* plants are altered in clock function

GIGANTEA also functions as a main component of the circadian clock that operates in several repressor loops with other clock components to maintain circadian clock rhythmicity and period length (Nohales and Kay, 2016). *Arabidopsis gi* mutants were reported to exhibit altered period lengths and reduced transcript levels of the *CCA1* and *LHY* morning clock genes (Fowler et al., 1999; Martin-Tryon et al., 2007). Consistent with this, they also exhibit an altered pattern of oscillation of the chlorophyll a/b-binding protein 2 (CAB2), frequently used as an output marker for circadian clock function (Park et al., 1999). Noteworthy, our RNA-seq studies disclosed that *StTOC1*, encoding one of the core components of the central oscillator, is down-regulated in *StGIi* leaves (Figure 20), hence suggesting that these plants might show a similar impaired clock function as reported for the *Arabidopsis* mutants. To assess this possibility, we analysed the oscillation patterns of the core clock genes *StTOC1*, *StLHY* and *StPRR5*, in leaves of WT and *StGIi* plants. RT-qPCR amplification studies showed that, in the WT, *StLHY* peaks with a sharp peak of expression that coincides in LDs with ZT2. *StPRR5* and *StTOC1* oscillate with evening peaks of expression that coincide in LDs with ZT8 and ZT11 respectively (Figure 21). These oscillation patterns were slightly modified in SDs, with *StLHY* found to peak earlier and display a broader peak from ZT20 to ZT2. Slightly earlier peaks of expression than in LDs were also observed for both *StTOC1* and *StPRR5* (Figure 21). Thus, rhythmic expression of these genes strongly resembles the patterns reported for their *Arabidopsis* homologs (http://diurnal.mocklerlab.org). Quite remarkably, *StTOC1* and *StLHY* expression is strongly repressed in *StGIi* leaves (Figure 21). By contrast, *StPRR5* expression is up-regulated in these plants in LDs, whereas a shift towards early morning in the *StPRR5* oscillation phase is observed both in LD and SD (Figure 21). Interestingly, this earlier peak of expression reminds that we previously observed for *StFKF1*, indicating that *StGI* silencing alters rhythmic expression of several genes. A similar repression of *LHY* and a reduction in *TOC1* expression levels has been reported in *Arabidopsis gi-2* and *gi-201* mutants, hence indicating that StGI acts as well as a core component of the circadian clock in potato (Kawamura et al., 2008; Martin-Tryon et al., 2007).

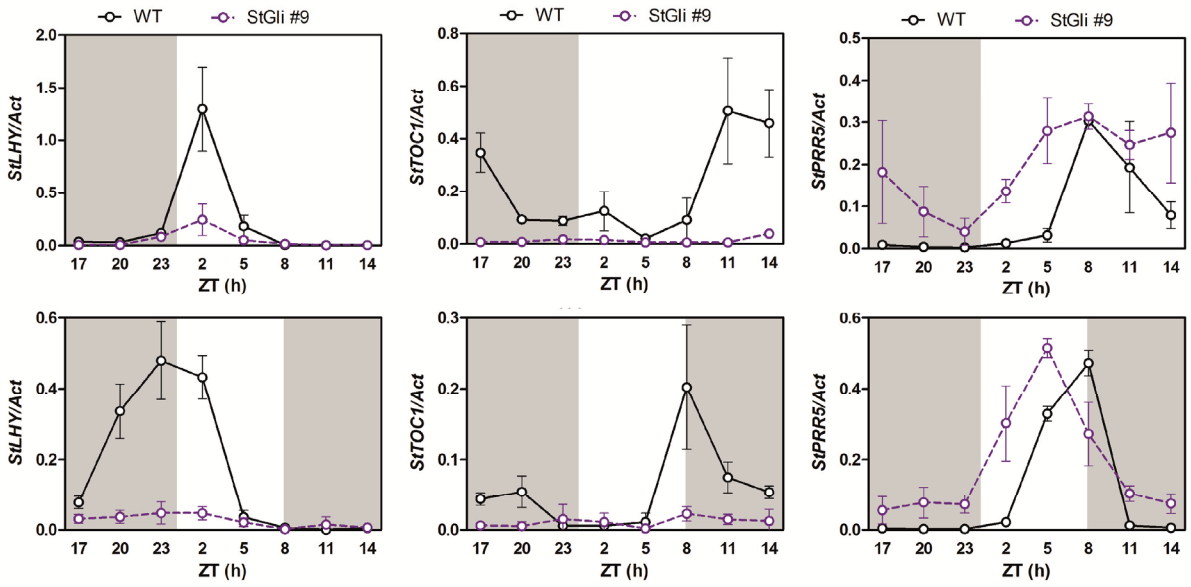

Figure 21. Diurnal oscillation of the *SLHY*, *StTOC1* and *StPRR5* genes in *StGl*i plants. qPCR amplification of the *StLHY*, *StTOC1* and *StPRR5* transcripts in WT and *StGl*i plants grown under LDs (upper row) and SDs (lower row). Error bars represent ±s.d. of three biological replicates.

Results: Chapter 2

StSP5G regulatory network in strict photoperiodic *Andigena* plants

StSP5G encodes a FT-like protein recently proposed to function as a tuberization repressor (Abelenda et al., 2016). In photoperiodic *Andigena* species, *StSP5G* is expressed under LDs in the leaves and shows a biphasic pattern of expression, characterised by a rise in transcript levels at ZT5 and a second peak before dusk (Abelenda et al., 2016). Transgenic plants silenced in expression of this gene (*StSP5G*i lines) tuberize under non-inductive LDs conditions and exhibit a slight activation of *StSP6A* expression in the leaves (Abelenda et al., 2016). Notably, the StCOL1 factor was shown to bind in LDs a conserved *cis*-element in the *StSP5G* promoter and activate its expression during the morning (Abelenda et al., 2016).

In tomato, *cis*-regulatory variation in the *SlSP5G* locus has been shown to be responsible for the loss of day-length sensitivity for flowering in modern domesticated tomatoes (Soyk et al., 2017), this recent study also showing that *SlSP5G* represses flowering through the suppression of *SFT* expression in tomato leaves (Soyk et al., 2017).

Therefore, all evidences obtained so far indicate that SP5G acts as a repressor of tuberization in potato and flowering in tomato by mediating transcriptional repression of other *FT*-family genes. However, the molecular mechanism by which this FT-like protein controls *StSP6A* or *StSFT* transcription remain poorly understood as none of these proteins has DNA-binding activity. Moreover, SP5G might exert different functions in leaves and tubers, as studies performed in our laboratory revealed that *StSP5G* is also expressed in mature tubers. Therefore, to further define the leaf and tuber-specific function of this FT-like repressor, we performed a second set of studies focused to identify the gene regulatory network controlled by *StSP5G* in these organs.

1. Potato StSP5G is encoded by two tandem repeated genes with different expression patterns

StSP5G is encoded in potato by two genes, *StSP5G-A* and *StSP5G-B*, organised in tandem on chromosome 5 (Figure 22). Comparison of this genomic region with the corresponding tomato locus showed that such a tandem arrangement is specific of potato, with the tomato genome encoding a single *SlSP5G* gene. BLAST alignment between these two genomic regions showed that, besides the *SP5G* gene, part of the coding sequence for an organic/carnitine transporter and a tRNA-Lys is as well duplicated in potato (Figure 22). In addition, we observed that this genomic region includes segments with high homology to a retrotransposon gag protein in tomato and to a transposase-derived nuclease in potato (Figure 22). Overall, these findings suggest that a recent genomic rearrangement occurred on this chromosome 5 region in potato, leading to duplication of the *StSP5G* gene and surrounding sequences.

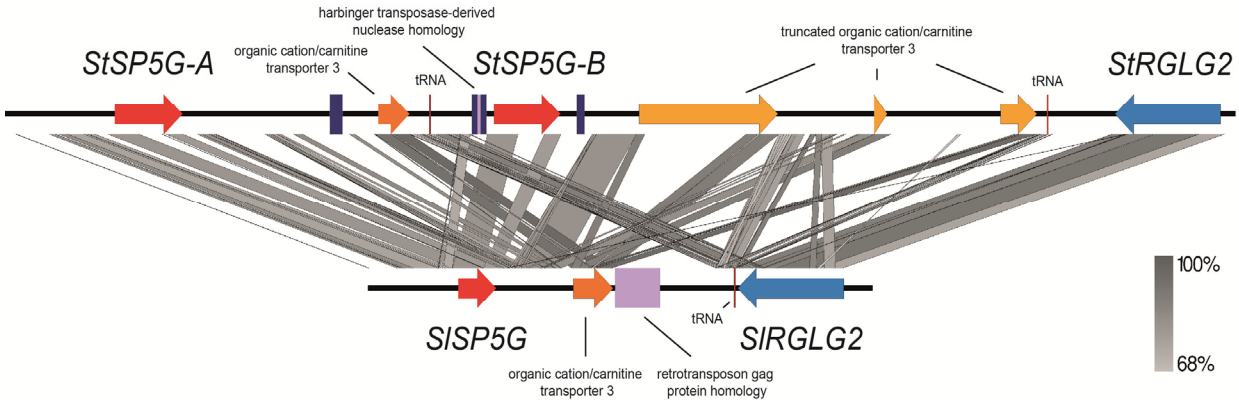

Figure 22. Rearrangement of the *SP5G* locus in potato. BLAST comparison of the genomic regions encompassing the duplicated *SP5G* gene in potato (top) and single copy in tomato (bottom). Arrows indicate predicted genes whereas magenta boxes indicate regions that share homology to transposon-related repeated sequences. Three regions unassigned in the potato genome (n regions) are shown as dark blue boxes. N1 and N2 were amplified from *Andigena* and their nucleotide sequence included in the analysis. Easyfig software was used to draw homologous regions between potato and tomato sequences.

StSP5G-A and *StSP5G-B* genes exhibit more than 98% homology in their coding sequences (Figure S2A). However, their promoter regions are significantly different and share only two conserved regions of approximately 400 bp at -381 bp and -1689 bp from the start codon, hence indicating that during duplication an additional nucleotide segment was inserted in one of the genes (Figure S2B). In previous studies we showed that *StSP5G* is specifically expressed in potato leaves under LDs, with transcripts for this gene being also detected in mature tubers (Abelenda et al., 2016; Navarro et al., 2011). To determine

whether this organ specific expression relies on a different expression pattern of these gene copies, we analysed relative abundance of the *StSP5G-A* and *StSP5G-B* transcripts in leaves, mature tubers and tuber sprouts. To this aim, we took advantage of a single nucleotide substitution creating a *HindII* cleavage site in the *StSP5G-A* gene to generate a *StSP5G* CAPS marker discriminating between these two almost identical transcripts (Figure S2A). RT-PCR amplification using primers on this region amplified both *StSP5G-A* and *StSP5G-B* transcripts, which were later differentiated by *HindII* digestion. Results from these analyses showed that *StSP5G-A* is not only expressed in leaves in LDs, but also in mature tubers and tuber sprouts (Figure 23). By contrast, *StSP5G-B* is barely expressed in leaves or tuber sprouts, whereas is expressed to high levels in mature tubers (Figure 23). Hence, these data demonstrates that even though *StSP5G-A* and *StSP5G-B* share almost identical coding regions, they display different expression patterns in potato. Moreover, the fact that *StSP5G-B* is only expressed in tubers indicates that this gene lacks the regulatory elements for LD activation by StCOL1 and may have acquired a specific role in the tuber. Generation of CRISPR-Cas mutations in this gene copy will help to define whether its function is different or just redundant to that of *StSP5G-A*.

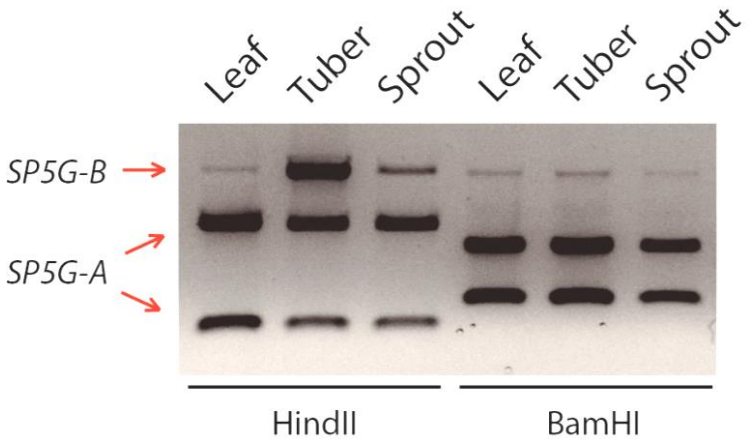

Figure 23. *StSP5G-B* is specifically expressed in tubers. CAPS detection of *StSP5G-A* and *StSP5G-B* relative abundance in leaves (LD), mature tubers and tuber sprouts of *Andigena* plants. cDNA was generated from total RNA extracted from these tissues and used as template for PCR amplification. *HindII* digestion shows that the uncut *StSP5G-B* product is abundantly expressed in tubers. *BamHI* cleavage was used as loading control.

Due to the impossibility to discriminate by RT-qPCR between *StSP5G-A* and *StSP5G-B* gene expression, from now on we will refer to *StSP5G* expression as the sum of expression levels of both genes.

2. *StSP5G* is expressed in vascular bundles and shows an inverse expression pattern to *StSP6A* in leaves, whereas is co-expressed with this gene during tuber development

StSP5G was shown in *Andigena* plants to be specifically activated in the leaves under LDs by the transcription factor StCOL1, and inhibit tuberization through the repression of *StSP6A* transcription (Abelenda et al., 2016). Moreover, *StSP5G* is expressed in stolons during tuber development, but its function in tubers is little understood (Navarro et al., 2011).

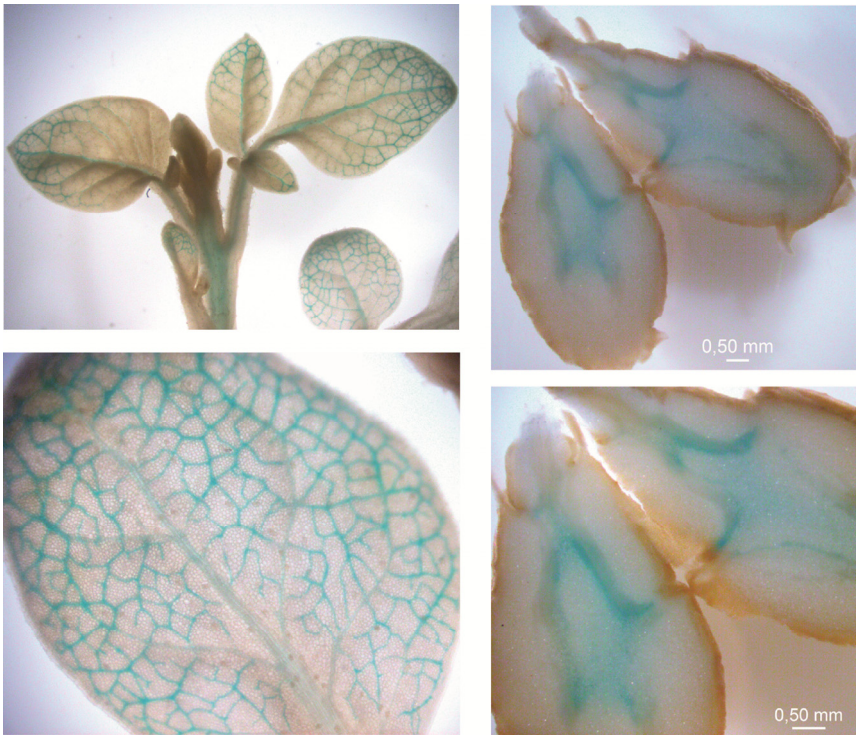

Figure 24. *StSP5G-A* expression is confined to vascular tissues. GUS staining of p*StSP5G-A*::GUS *in vitro* plantlets grown under LDs and minitubers. *StSP5G-A* is expressed to high levels in minor veins of the leaves and in the shoot vasculature. A vascular pattern is also observed after prolonged staining of minitubers, indicative of a lower level of expression.

To confirm that *StSP5G-A* corresponds to the active gene copy in leaves, we generated *Andigena* transgenic lines expressing the *GUS* reporter gene under the control of the *StSP5G-A* upstream promoter region. GUS staining of these plants revealed that *StSP5G-A* is expressed in the leaf vasculature under LDs, and in tubers (Figure 24). These data thus confirms that as described for *Arabidopsis FT*, *TSF*, *CO* and *CDF1* (An et al., 2004; Imaizumi et al., 2005; Takada and Goto, 2003; Yamaguchi et al., 2005), expression of the *StSP5G-A* gene is confined to the vascular tissue.

To further corroborate an inverse correlation between the *StSP5G* and *StSP6A* transcripts, indicative of a negative regulatory function of StSP5G on *StSP6A* transcription, we analysed by RT-qPCR the expression pattern of these genes in the leaves of plants grown under LDs and SDs; and in the stolons of plants transferred to SD for induction of tuber development. These studies confirmed that *StSP5G* and *StSP6A* show inverse expression patterns in *Andigena* leaves, *StSP5G* being expressed only under LDs, whereas *StSP6A* is induced in leaves under SDs (Figure 25A). However, upon tuberization transition, both genes are up-regulated in the stolon, *StSP5G* and *StSP6A* thus showing an analogous expression pattern during this developmental process (Figure 25B). Taken together, these results are consistent with previous data indicating that *StSP5G* represses *StSP6A* in the leaves, but show that this repression is not seen in swelling stolons.

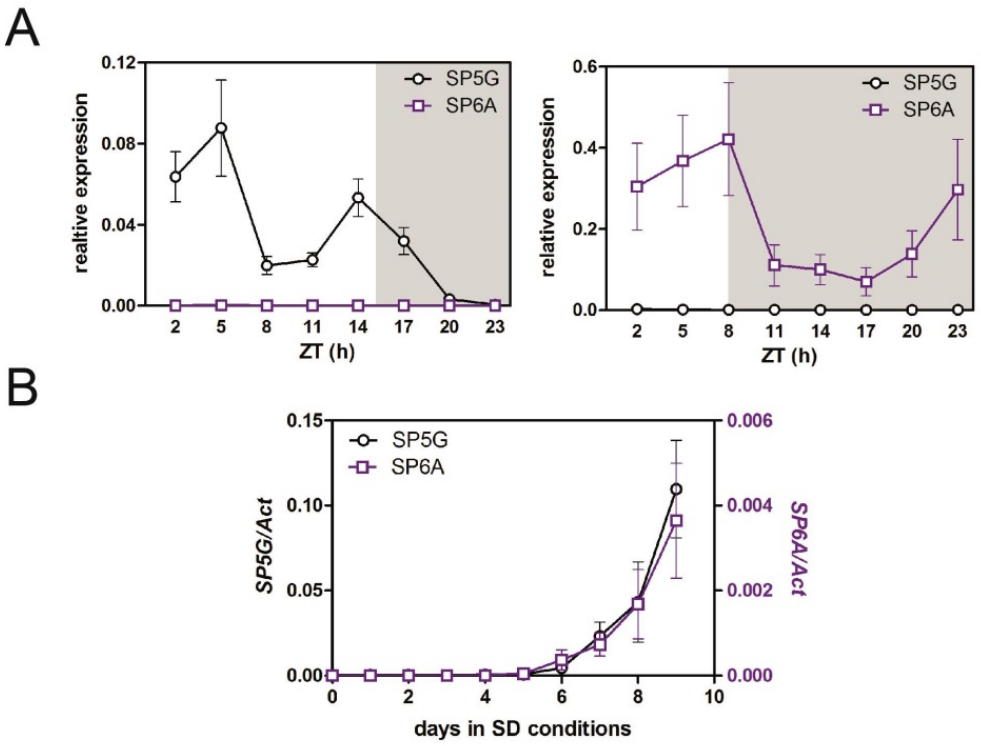

Figure 25. *StSP5G* and *StSP6A* expression in the leaves and stolons of *Andigena* plants grown under LD or SD conditions. (A) qPCR analyses of the diurnal oscillation patterns of the *StSP5G* and *StSP6A* genes in leaves of *Andigena* plants grown under LD (left) or SDs (right). (B) qPCR analysis of *StSP5G* and *StSP6A* expression levels in stolons of plants transferred to SD conditions to induce tuber development. Relative expression levels are represented in function of the number of days since plants were transferred to SDs. First swelling of stolons was observed at day 8. Error bars represents ± s.d. of 3 biological replicates.

3. StSP5G represses tuberization in the leaves and has a systemic long distance effect on *StSP6A* expression

*StSP5G*i lines tuberize under non-inductive LDs and show slightly increased levels of the *StSP6A* transcript in the leaves compared to WT plants (Abelenda et al., 2016). However, activation this gene was much weaker than in *StCOL1*i leaves or in leaves of plants grown in SDs (Abelenda et al., 2016). To determine whether this reduced activation levels in leaves were sufficient to trigger tuberization or, on the contrary, *StSP5G* suppression is having a major effect in underground tissues, we performed grafting experiments by using different scion to stock combinations of *Andigena* WT, *StSP5G*i and *StSP5G*ox lines (Figure 26B). Plants were covered with a plastic bag until resumption of vascular connections and kept in the greenhouse under LDs, to analyse tuber production. Notably, all grafts in which *StSP5Gi* plants were used as donor scions tuberized in LDs, independently of levels of *StSP5G* expression in the rootstock (Figure 26A; Figure 26C). That is, graft combinations bearing aerial *StSP5G*i scions tuberized in LDs and tuber production was not reduced even when grafted on *StSP5Gox* rootstocks (Figure 26A; Figure 26C). On the other hand, WT scions grafted onto *StSP5G*i rootstocks did not tuberize, evidencing that StSP5G suppression in the rootstock is not sufficient to trigger tuberization in LDs. These results thus demonstrate that *StSP5G* activity as a negative regulator of tuberization is exerted in the aerial part of the plant (Figure 26A; Figure 26C).

StSP6A is the potato mobile signal that induces tuberization and is regulated by an autorelay mechanism that involves *StCOL1* and sustains its own synthesis in stolons (Navarro et al., 2011). To assess whether *StSP5G* has a long range effect on *StSP6A* autoactivation in the stolons, *StSP6A* expression levels were analysed by RT-qPCR amplification of samples corresponding to the above graft and below graft tissues of all grafted plants. These were the apical stem, which includes the first three nodes below the shoot apical meristem; the basal stem, which includes the last three nodes above the graft junction; the underground stem, which is the main stem below the graft junction and is mostly located underground; and the stolons.

Results from these studies showed that *StSP6A* was barely expressed in the apical and basal stems in any of the graft combinations, neither in those that used the *StSP5G*i lines as scion (Figure 26D). By opposite, strong up-regulated expression of the *StSP6A* gene was observed in the underground stems and stolons of grafts bearing *StSP5G*i as donor scions, in strong correlation with ability of these plants to tuberize under LDs (Figure 26C, Figure 26D).

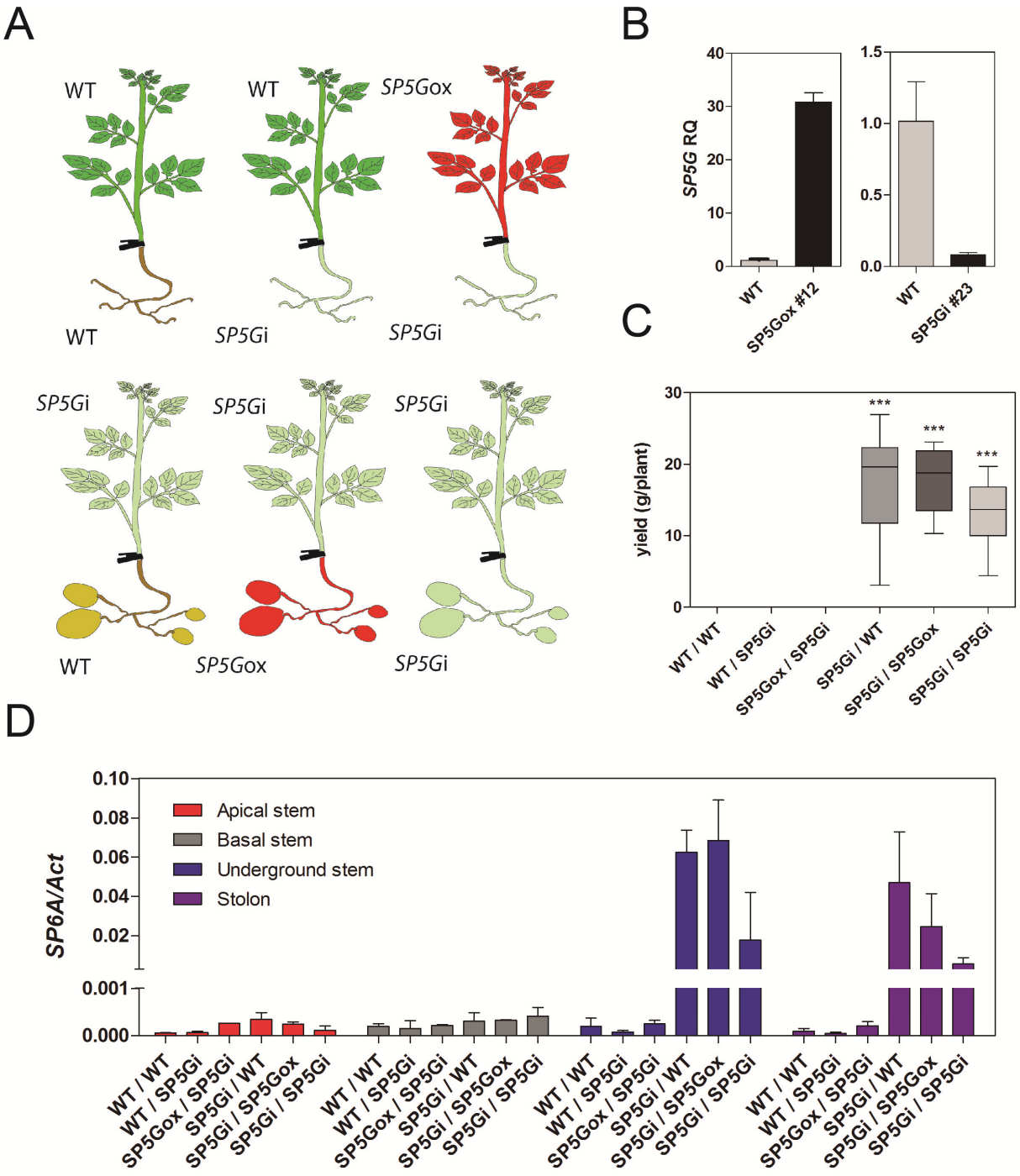

Figure 26. *StSP5G* grafting experiments. (A) Schematic representation of the LD tuberization phenotype of graft combinations of WT, *StSP5G*i and *StSP5G*ox plants. (B) qPCR analysis of *StSP5G* expression levels in *StSP5G*ox line #12 under SDs and in *StSP5G*i line #23 under LDs. (C) Tuber yield under LDs of the grafted plants. Only graft combinations bearing *StSP5G*i as the donor scion tuberized in LDs. *** denotes statistical significance ($p<0.001$) in comparison to WT/WT grafts. (D) qPCR analysis of *StSP6A* expression in stem sections above and below graft junction, and in stolons of plants grown in LDs. Samples corresponding to all graft combinations were collected at ZT5.

Overall, this is a crucial finding as it demonstrates that even though silencing of *StSP5G* has a rather mild effect on *StSP6A* expression levels in leaves and stem, it has a dramatic long distance effect on *StSP6A* expression in the underground stem and stolons. Moreover, this long range effect is not impaired by *StSP5G* overexpression in the underground stem, which indicates that StSP5G exerts a negative effect on *StSP6A* activation in the leaves, but does not affect its auto-relay regulation in underground tissues.

4. StSP5G induces different transcriptomic changes in tubers and leaves.

Remarkably, tubers of LD *StSP5Gi* plants show a knobby and irregular shape, and are more elongated than tubers of WT plants after transfer to SD (Figure 27B). As *StSP5G* is expressed to high levels during tuber development, and over-expression of this gene in underground organs does not to repress *StSP6A* expression and tuber initiation, it seemed reasonable to assume that besides negative regulation of *StSP6A* in leaves, StSP5G might have an additional biological function in tubers. To test this hypothesis and identify the genes regulated by *StSP5G* in each of these tissues, we hybridized an Agilent 60-mer microarray that contains probes for all 39031 protein coding regions predicted from the potato genome sequence (Xu et al., 2011), with probes corresponding to the RNA extracted out of leaf and tuber tissues from WT and *StSP5G*i lines. After application of the statistical filtering described in Materials and Methods, we identified 1687 DEGs in *StSP5G*i leaves and 4391 in tubers ($p<0.05$; FC≤ -2 or ≥ 2). Comparison of these two datasets disclosed that only a 19% of the total genes up-regulated in *StSP5G*i tubers are also up-regulated in leaves, being this percentage even lower (9%) for the down-regulated genes (Figure 27C). Hierarchical clustering of the DEGs, confirmed that *StSP5G* silencing leads to a significantly stronger transcriptional reprogramming in tubers than in leaves (Figure 27A). Still, functional analyses of these genes revealed that members of the MADS-box protein family are over-represented among the up-regulated genes in leaves and tubers, while an enrichment in NF-Y family genes is also observed among the down-regulated genes in both organs. In particular, homologs of the *Arabidopsis FUL*, *AP1*, *SOC1*, and *SEPALLATA* genes were found to be induced in leaves and tubers of *StSP5G*i lines, while homologs of the floral repressors *SVP* and *AGL15* are down-regulated (Figure 28A; Figure 28B). Remarkably, these MADS-box proteins play in *Arabidopsis* a crucial role in floral development and meristem determinacy, being shown to work in concert with other non-MADS regulators in the control of flowering time transition and the shift from vegetative to inflorescence meristem identity (Pose et al., 2012; Smaczniak et al., 2012). Thus, the finding that these MADS-box genes are

downstream targets of StSP5G, suggests that function of these proteins as integrators of the day-length pathway, together with FT, is conserved in potato (Pose et al., 2012).

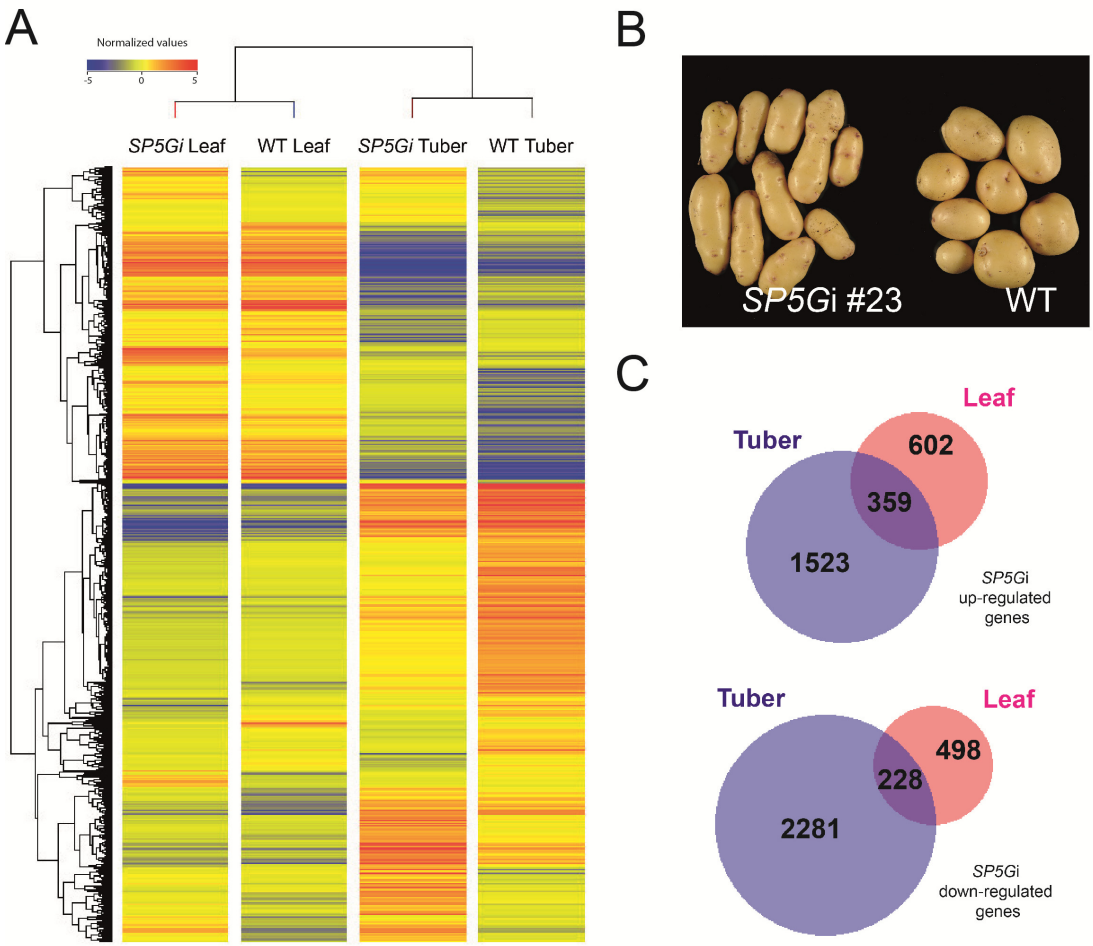

Figure 27. Transcriptome analysis of *StSP5G*i lines and morphology of *StSP5G*i tubers. (A) Heatmap of the hierarchical clustering analysis of DEGs in *StSP5G*i leaves and tubers. *StSP5G* silencing causes stronger gene expression changes in tubers than in leaves. (B) Tubers of WT and *StSP5G*i plants grown in SDs. *StSP5G*i tubers are more elongated than the WT and show an irregular tuber shape. (C) Venn diagrams showing overlap between up-regulated (upper diagram) and down-regulated (lower diagram) genes in *StSP5G*i tubers and leaves.

On the other hand, NF-Y/ HAP regulators were shown to physically interact with CO (Ben-Naim et al., 2006; Wenkel et al., 2006), and cooperatively act with this regulator to activate *FT* expression. NF-Y factors bind to DNA as a complex consisting of the NF-YA, NF-YB and NF-YC subunits, assembly of NF-YB and NF-YC in the cytosol being shown to induce their translocation into the nucleus, where they interact with NF-YA and form an active trimeric complex. In *Arabidopsis* there are 30 predicted NF-Y members, whose function has been associated to the regulation of several plant developmental and stress-

induced responses (Petroni et al., 2012). Notably, our transcriptomic analyses evidenced that inhibition of *StSP5G* leads to suppression of various potato NF-Y genes in the leaves and tubers (Figure 28A; Figure 28B). These include members of all NF-YA, NF-YB and NF-YC subfamilies. Interestingly, an homolog of *NF-YC4*, which in *Arabidopsis* was described to be required for CO-mediated activation of *FT* (Cao et al., 2014; Kumimoto et al., 2010), is found to be specifically down-regulated in leaves (Figure 28A).

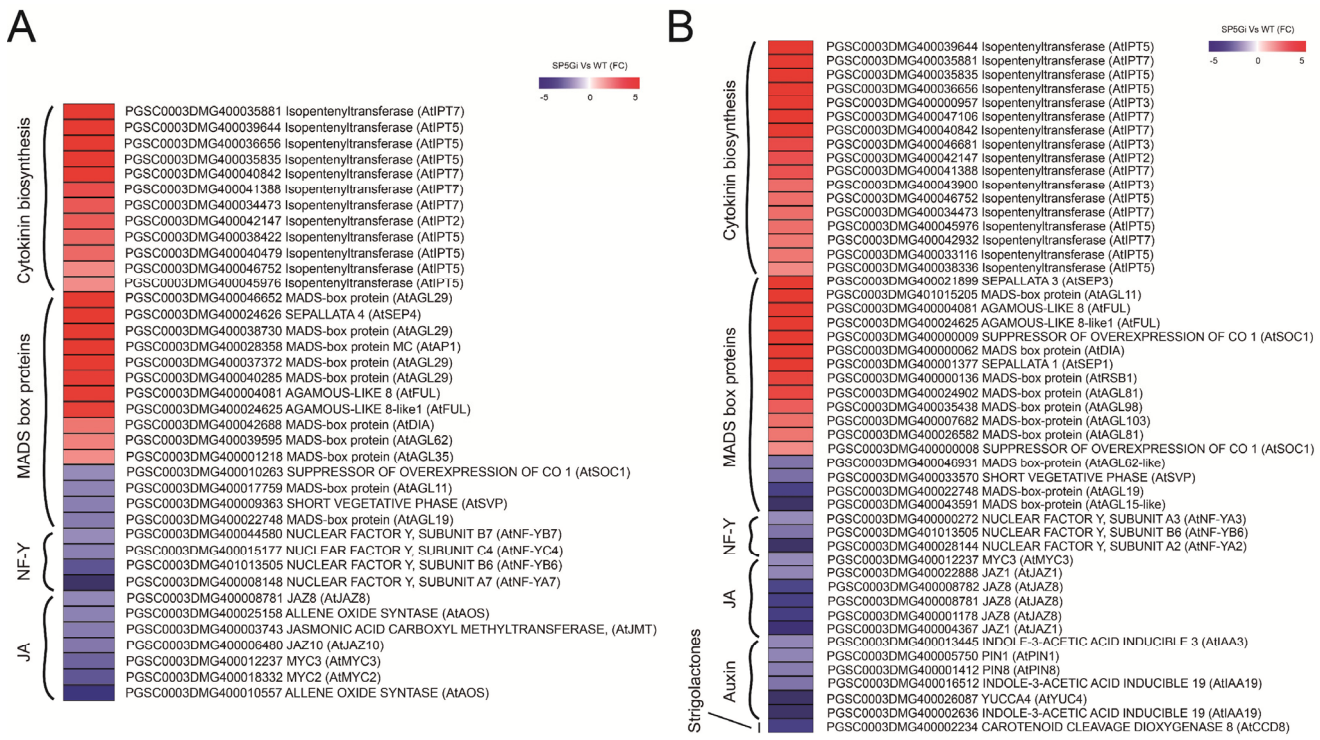

Figure 28. Most representative DEGs in *StSP5G*i leaves and tubers. (A) Heatmap showing the transcriptional changes of the selected subset of DEGs in *StSP5G*i leaves. (B) Heatmap showing the transcriptional changes of the selected subset of DEGs in *StSP5G*i tubers. Genes are represented with their ID number and their closest *Arabidopsis* homolog in shown in parentheses.

Taken together, these findings suggest that *StSP5G* has a major role in the transcriptional regulation of several MADS-box and NF-Y family genes in both leaves and tubers.

5. StSP5G regulates several hormone-related genes.

Cytokinins have been long proposed as positive regulators of tuberization, by promoting cell division during the initial steps of tuber formation and create a local sink (Guivarc'h et al., 2002). Auxins and strigolactones, known to play opposite roles to cytokinins in the control of axillary bud outgrowth (El-Showk et al., 2013), are also described to regulate

tuber formation and development in potato. Multiple auxin-related genes are up-regulated during stolon-to-tuber transition, auxin levels being described to increase during initial steps of tuber formation (Roumeliotis et al., 2012b). In addition, silencing of the *StCCD8* strigolactone biosynthetic gene was found to promote tuber formation in juvenile axillary buds and critically affect tuber morphology, hence evidencing a repressive role of this hormone on potato tuberization (Pasare et al., 2013).

Notably, besides the MADS-box and *NF-Y* family genes reported above, we identified a large set of hormone-related genes that were differentially expressed in *StSP5G*i lines. Various cytokinin biosynthetic enzymes belonging to the isopentenyltransferase (IPT) gene family are for instance strongly up-regulated in both *StSP5G*i leaves and tubers (Figure 28A; Figure 28B). In contrast, multiple Jasmonic acid-related genes, including homologs of *Arabidopsis JAZ* and *MYC* genes, are down-regulated in both *StSP5G*i tissues (Figure 28A; Figure 28B). Consistent with an antagonic function of CK and auxin/strigolactones, reduced expression levels of the *StCCD8* strigolactone biosynthetic gene, and various auxin-related genes were also observed in *StSP5G*i tubers, including two *PIN* carriers and the potato homologs of *YUCCA4* and *IAA19* (Figure 28B).

Overall, these findings suggest that inhibition of *StSP5G* disrupts the hormonal balance of potato leaves and tubers by promoting CK biosynthesis, which leads to a reduced auxin response in the tuber and indirectly to suppression of JA signalling in both tissues. Moreover, down-regulated expression of auxin and strigolactone-related genes likely is responsible for the altered shape and development of *StSP5G*i tubers.

6. Activation of *StAGL8/FUL* mediates the long range tuberization effects of *StSP5G*i plants

MADS-box genes play important roles in the control of flower and fruit development across flowering plants (Heijmans et al., 2012; Smaczniak et al., 2012). Results reported so far show that MADS-box genes are downstream targets of *StSP5G* regulation in both leaves and tubers (Figure 28A; Figure 28B). In the *Arabidopsis* shoot apical meristem, FT has been reported to interact with the bZIP factor FD and with 14-3-3 proteins, forming a Flowering activator complex (FAC) that activates *AP1*, *FUL* and *SOC1*, to trigger floral meristem transition (Andres and Coupland, 2012; Lee and Lee, 2010). *AP1* and *SOC1*, in turn, promote the activation of *LFY* and that of other MADS-box genes expressed in the meristem, which play a role in floral development according to the ABC model (Wellmer et al., 2014). In opposite to these activators, the MADS-box genes *FLC* and *SVP* act as flowering inhibitors

by repressing *FT* and *SOC1* transcription both in the leaf and apical meristem (Li et al., 2008; Searle et al., 2006).

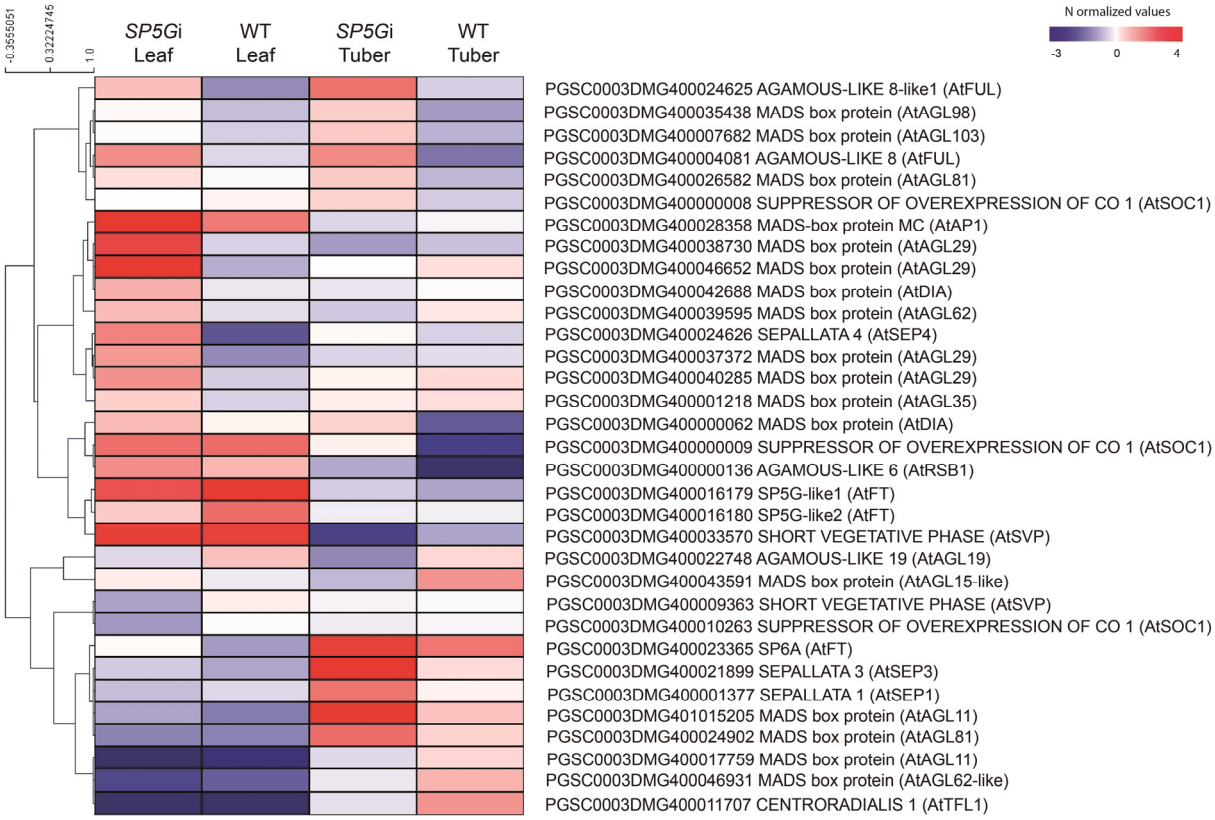

Figure 29. Genes of the MADS box and CETS families differentially expressed in *StSP5G*i lines. Heatmap showing the normalised expression levels of all MADS-box and CETS genes that are differentially expressed in *StSP5G*i leaves or tubers. Genes are represented with their ID number and their closest *Arabidopsis* homolog is shown in parentheses.

To further analyse if potato MADS-box genes exert a role in photoperiodic control of tuberization in potato, we grouped by hierarchical clustering all MADS and CETS family genes differentially expressed in *StSP5G*i leaves or tubers according to their expression profile. This analysis allowed us to identify which are the genes co-regulated or with an antagonic expression profile to *StSP5G* in one or in both of these tissues (Figure 29). Regarding the CETS family, *StSP6A* was found to be induced in both leaves and tubers of *StSP5Gi* plants, thus confirming an antagonic profile of these genes, as previously reported. By opposite, two *StSP5G*-like genes on chr11, *StSP5G-like1* and *StSP5G-like2*, and the *TFL1*-like *StCEN1* gene, were respectively down-regulated in *StSP5Gi* leaves and tubers, and thus show a co-regulated pattern of expression with *StSP5G* in these organs (Figure 29). Clustering analyses also revealed that *StSP6A* expression is strongly co-regulated with two *SEPALLATA* genes, *StSEP1* and *StSEP3*, normally expressed at higher levels in tubers

than in leaves, and which are strongly induced in *StSP5Gi* tubers (Figure 29). Regarding MADS-box genes, members of the *SOC1*-like and *SVP*-like families tended to be coordinately regulated in response to *StSP5G* inhibition. Actually, two of the three *SOC1*-like genes are strongly induced in *StSP5Gi* tubers (Figure 29), whereas each of the *SVP*-like genes is found to be suppressed by *StSP5G* inhibition. However, while one of these SVP-like genes is specifically suppressed in tubers, the other is down-regulated in leaves (Figure 29). Overall, these data suggest that StSP5G not only acts at negative regulation of *StSP6A* in leaves but also plays a role in repressing *SOC1*-like gene expression in the tuber, at the same time that contributes to *SVP*-like gene activation both in tubers and leaves.

To gain insight into the hierarchical function of these MADS-box proteins downstream of StSP5G, we first focused on members that are misexpressed in both *StSP5G*i tubers and leaves, as we reasoned that these are the best candidates to be directly regulated in response to StSP5G. Notably, two *FRUITFUL* (*FUL)* homologs, *StAGL8* and *StAGL8*-like1, showed up-regulated expression in both *StSP5G*i leaves and tubers and thus behave in this way (Figure 29). Indeed, *StAGL8* has been recently described to be co-regulated with *StSP6A*, as it displays an identical day-length regulated response in potato leaves as this gene (Morris et al., 2014). Also, antisense inhibition of the *StAGL8/POTM1* had been reported to lead to smaller plants, with decreased apical dominance, and which are unable to tuberize in a stem node cutting system (Rosin et al., 2003). In consonance with these findings, *FUL* has been recently described as a modulator of *Arabidopsis SOC1* and *SVP* activity, with sequential formation of the FUL-SVP and FUL-SOC1 heterodimers being proposed to mediate the vegetative and inflorescence meristem identity transitions by counteracting the repressive effect of SVP (Balanza et al., 2014).

Therefore, we first verified that *StAGL8* and *StSP6A* are co-regulated by doing timecourse analyses of leaves of both WT and *StSP5G*i plants grown under LDs and SDs. RT-qPCR amplification of these samples showed that *StAGL8* is expressed in WT plants to higher levels under SDs than in LDs, and its transcripts oscillate with a peak of expression between ZT5 and ZT8 (Figure 30A). *StAGL8* transcript levels were also higher in *StSP5G*i leaves than in the WT, and were not reduced in LDs. Therefore, fold induction in *StSP5G*i leaves was significantly increased in LDs, consistent with our transcriptomic results (Figure 30A). *StAGL8* expression was also higher in mature *StSP5Gi* tubers (Figure 30D), levels of this transcript being found to increase in the stolons upon stolon-to-tuber transition (Figure 30C). More remarkably, RT-qPCR amplification of the graft combinations used to *StSP6A* expression showed that *StAGL8* is strongly activated in grafts bearing *StSP5G*i as the donor scion, in a similar way as observed for the *StSP6A* gene. However, unlike for *StSP6A*, we also detected an up-regulated expression of *StAGL8* in the upper stem of these plants

(Figure 30B). Taken together, these findings demonstrate that *StAGL8* expression strongly correlates with *StSP6A* expression in WT leaves and stolons (Navarro et al., 2011), confirming a co-regulated pattern of expression of both genes. However, silencing of *StSP5G* has a different effect on both genes, as it activates *StAGL8* expression in leaves, but has only a minor effect on *StSP6A* expression levels in this organ. Hence, these data would suggest that *StAGL8* is a direct downstream target of StSP5G, while *StSP6A* may be activated in underground organs in response to StAGL8 up-regulation. Further studies will be required to establish whether *StSP6A* is in fact a regulatory target of the StAGL8/FRUITFUL homolog, and to understand why this MADS-box factor is unable to induce *StSP6A* expression in leaves.

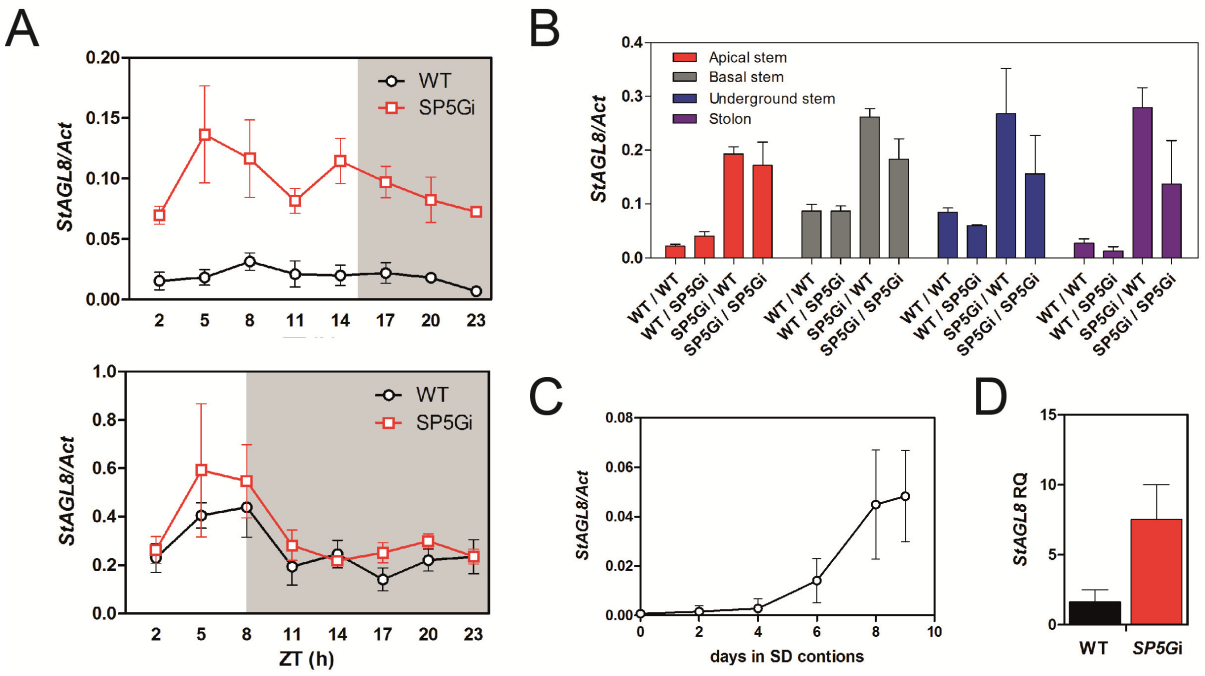

Figure 30. *StAGL8* expression profile in *Andigena*. (A) qPCR analysis of the pattern of expression of the *StAGL8* gene in leaves of WT and *StSP5G*i plants grown under LDs (top) or SDs (bottom). (B) qPCR amplification of the *StAGL8* gene in stem sections above and below the graft junction, and in the stolons of WT and *StSP5G*i graft combinations. Plants were grown in LDs (C) qPCR analysis of *StAGL8* expression in WT stolons during tuber development. Stolon-to-tuber transition is represented as the number of days after plants were transferred to SD conditions. Macroscopic swelling of stolons is observed at day 8. (D) qPCR analysis of *StAGL8* expression in WT and *StSP5G*i mature tubers harvested from plants grown under SDs. Error bars represents ± s.d. of 3 biological replicates.

7. StSP5G maintains shoot identity of tuber sprouts.

Potato tubers undergo a period of dormancy after formation, in which visible bud outgrowth is inhibited even if tubers are placed into favourable conditions. After this period, cell division is re-activated in the bud meristems, which grow and differentiate into a new shoot in a process known as tuber sprouting (Sonnewald and Sonnewald, 2014). Notably, several plant hormones, including ABA, Ethylene, GAs and CKs, have been described as important regulators of potato tuber dormancy, bud outbreak and sprout elongation (Sonnewald and Sonnewald, 2014). Results reported so far clearly show that inhibition of *StSP5G* has a tremendous effect on the expression levels of many hormone-related genes in the tuber (Figure 28B). To assess whether these transcriptional changes have any significant effects on tuber sprouting, we characterized the dormancy time and sprout growth of mature WT and *StSP5G*i tubers stored at 4ºC. Periodic examination of these tubers revealed that inhibition of *StSP5G* was of no effect on the dormancy time of tubers. However, after meristem re-activation, *StSP5G*i tubers were found to form secondary tubers instead of proper shoots or sprouts (Figure 31A). To further confirm tuber-identity of these organs, we analysed *StSP6A*, *StGA2ox* and *StSUS4* expression levels in both WT and *StSP5Gi* sprouts. *StGA2ox1* and *StSUS4* are specifically expressed in tubers and are respectively involved in gibberellin inactivation and sucrose breakdown, hence mediating symplastic sucrose import and sink strength (Kloosterman et al., 2007; Zrenner et al., 1995).

Notably, RT-qPCR amplification showed that *StGA2ox1* and *StSUS4* are strongly induced in *StSP5G*i secondary tubers, whereas *StSP6A* is expressed to similar levels as in WT sprouts (Figure 31B). Altogether, these findings demonstrate that *StSP5G* plays an important role in signalling shoot identity of tuber sprouts, in addition to its role in suppressing *StSP6A* activation in LDs. On the other hand, our finding that *StSP6A* is not induced in these secondary tubers, suggests that *StSP5G* inhibition promotes tuber fate identity of axillary buds independently of *StSP6A* function.

To gain insight into the molecular events underlying *StSP5G*-dependent change in sprout cell identity to a tuber fate, we analysed the transcriptomes of WT sprouts and *StSP5G*i secondary tuber by hybridising an Agilent 60-mer microarray that contains probes for all protein coding sequences predicted from the potato genome sequence (Xu et al., 2011). After application of the statistical filtering described in Material and Methods, we identified 5327 genes that were differentially expressed in *StSP5G*i secondary-tubers ($p<0.05$; FC≤ -2 or ≥ 2).

Functional enrichment analyses of these DEGs revealed that genes with up-regulated expression are significantly enriched in functional categories like carbohydrate metabolism,

secondary metabolism, hormonal regulation and stress among others (Figure 32A; Figure 32B), while down-regulated genes are over-represented in genes involved in photosynthesis, cell wall, and lipid metabolism, in addition to the secondary metabolism and hormonal regulation functions (Figure 32A; Figure 32B).

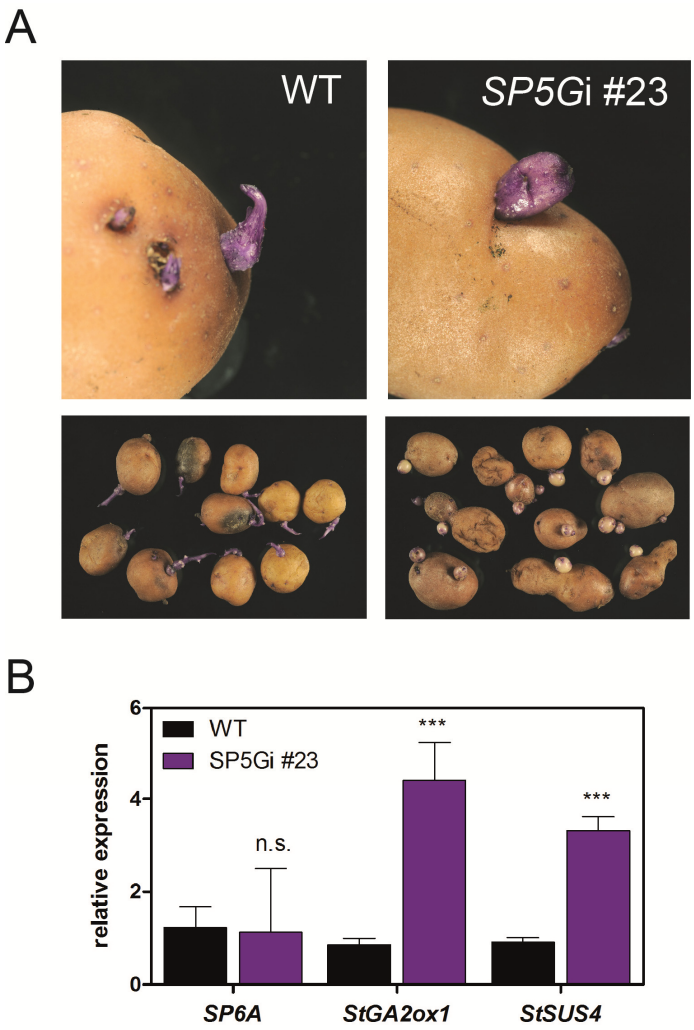

Figure 31. *StSP5G* is required to specify shoot identity of tuber sprouts. (A) WT and *StSP5G*i tubers after dormancy release. In *StSP5G*i tubers bud break leads to secondary tuber formation instead of shoots. (B) qPCR analysis of *StSP6A*, *StGA2ox1* and *StSUS4* expression in WT sprouts and in *StSP5G*i secondary tubers. Expression of the tuber-specific *StGA2ox1* and *StSUS4* genes is induced in *StSP5G*i secondary tubers. Error bars represent ± s.d. of three biological replicates. *** denotes a statistical significant difference ($p<0.001$) in comparison to WT sprouts.

Interestingly, several MADS-box family genes, including homologues of the *Arabidopsis FUL*, *AP3*, *AG*, *SEP* and *SVP* genes, were again found to be misregulated in *StSP5G*i secondary tubers (Figure 33), in support of our previous findings indicating that *StSP5G* functions as a central modulator of several MADS-box genes in potato. Moreover,

this observation would suggest that proteins of the MADS-box family play an important role in specifying shoot or tuber fate identity in growing sprouts.

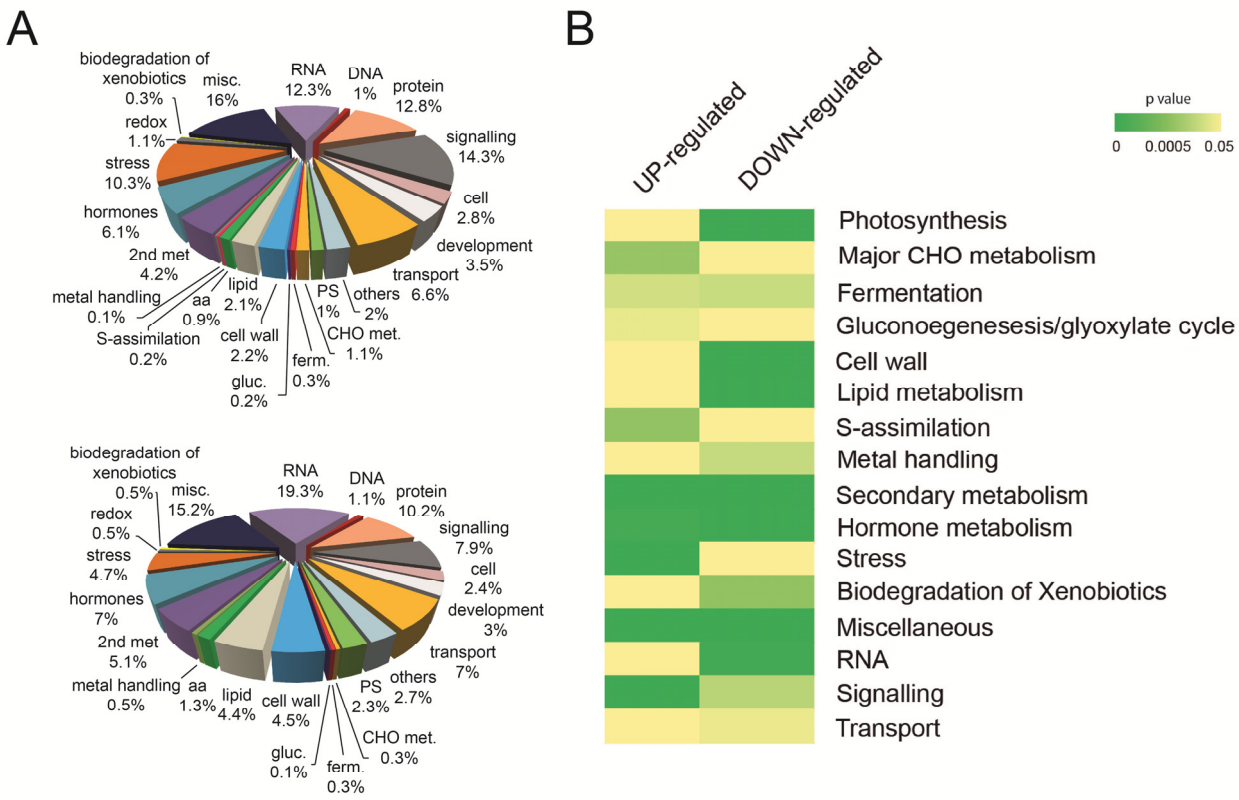

Figure 32. Gene onthology analysis of the DEGs in *StSP5G*i secondary tubers. (A) Functional annotation of the up-regulated (top) and down-regulated genes (bottom) in *StSP5G*i secondary tubers performed according to the Mapman bin classification. Percentage of genes in each category was calculated according to the total of genes assigned to at least one of the 34 functional categories. PS, photosynthesis; CHO met, major carbohydrate metabolism; ferm, fermentation; gluc, gluconeogenesis and glyoxylate cycle; aa, amino acid metabolism; 2nd met, secondary metabolism; misc, miscellaneous. (B) Heatmap showing p values of the functional categories significantly enriched ($p<0.05$) in up- or down-regulated DEGs in *StSP5G*i secondary tubers. P values were calculated by one-side Fisher's exact test.

On the other hand, these transcriptomic studies also revealed that *StSP5Gi* secondary tubers show up-regulated levels of expression of multiple genes that are normally expressed in tubers, like patatin-like storage glycoproteins, or several starch biosynthetic enzymes like starch synthases, ADP-glucose pyrophosphorylases and isoamylases (Figure 33). By opposite, expression of three invertase enzymes, which catalyse irreversible hydrolysis of sucrose and negatively correlate with starch accumulation, is reduced in these organs (Figure 33). Overall, these results indicate the same pathways that promote starch and storage protein accumulation during stolon-to-tuber transition (Kloosterman et al., 2005; Visser et al., 1994), are also induced in *StSP5Gi* buds during sprouting. Furthermore, as for

primary tubers (Figure 28), up-regulated expression of several isopentenyltransferases (IPT), and reduced expression of various auxin signalling and transport genes, including homologs of the *Arabidopsis* auxin carriers *PIN1, PIN2, PIN3, PIN6* and *LAX3,* is observed in *StSP5Gi* chain tubers (Figure 33). Therefore, all evidences indicate that secondary tubers growing from *StSP5G*i tubers after dormancy end have all characteristics of a soil tuber.

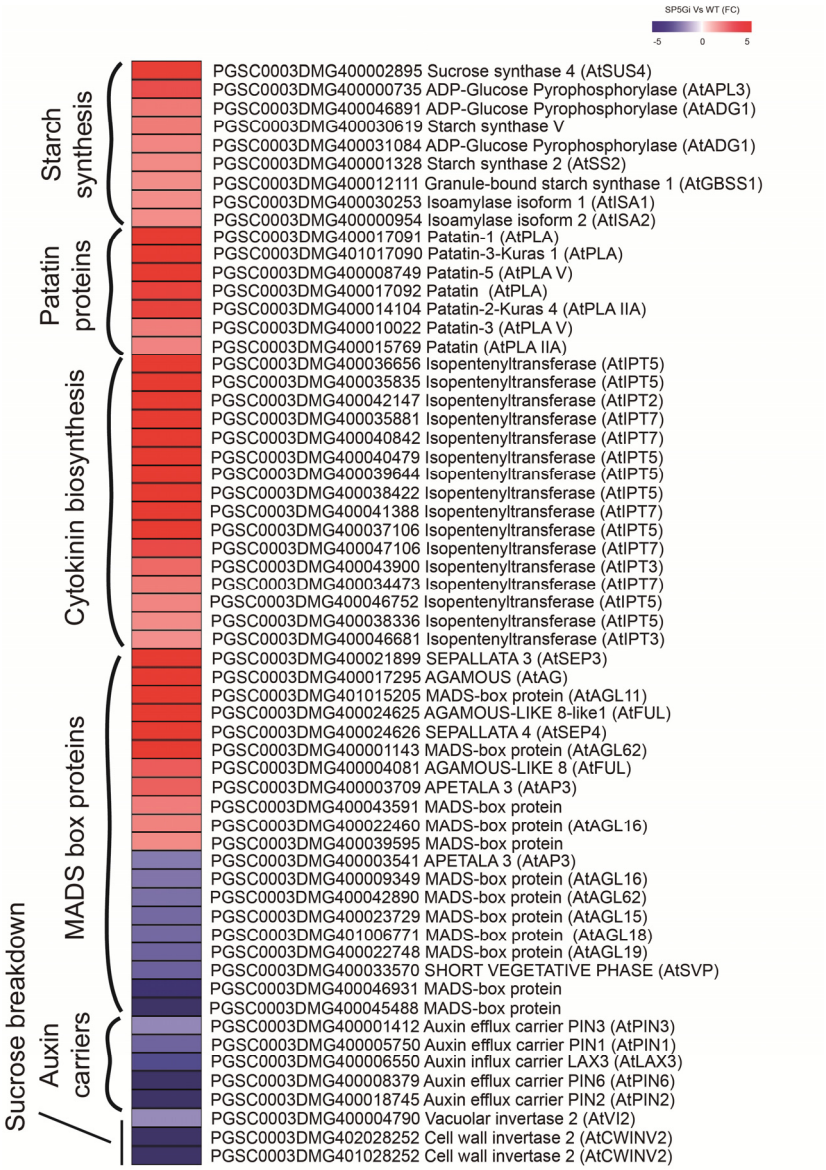

Figure 33. Representative DEGs in *StSP5G*i secondary tubers. Heatmap showing differential expression levels of these genes with respect to WT sprouts. Genes are represented with their ID number and their closest *Arabidopsis* homolog is shown in parentheses.

Results: Chapter 3

Analysis of StSP6A function in the response of commercial potato cultivars to warm temperatures

Besides photoperiod, temperature is one of the most important environmental factors controlling tuber formation in potato. Despite it has been long stablished that warm temperatures repress tuberization (Van Dam et al., 1996), the molecular mechanisms by which tuber formation is inhibited by heat remain poorly understood. Previous studies performed in our laboratory had demonstrated that the *FT* family *StSP6A* gene encodes the mobile signal that promotes tuber formation in potato (Navarro et al., 2011). More recently, it has been shown that day-length regulation of *StSP6A* is dependent on the transcription factor StCOL1, which indirectly inhibits *StSP6A* transcription by activating expression of the *FT* family *StSP5G* repressor (Abelenda et al., 2016). However, to date, little is known about the effects of temperature on this photoperiodic tuberization pathway. Recent studies showed that warm temperatures suppress *StSP6A* expression (Hancock et al., 2014; Singh et al., 2015), although the mechanism underlying this inhibition and its consequences on tuber formation and temperature stress adaptation remain to be established. Therefore, in our last set of studies we focused on analysing the role *StSP6A* in modulating the response to warm temperatures in potato.

1. Warm temperatures inhibit tuberization through the transcriptional repression of *StSP6A*

Temperatures above 22ºC are reported to reduce tuber production in most potato genotypes (Van Dam et al., 1996). To assess whether this inhibition depends on a direct effect of warm temperatures on the photoperiodic tuberization pathway, we first determined the relative heat tolerance of two potato cultivars: Spunta and Sylvana. The analysis of tuber yields of plants grown at 22ºC and 28ºC revealed that warm temperatures inhibit tuber formation in both cultivars, but this reduction is more pronounced in Spunta than in Sylvana (Figure 34C). To better understand the nature of this inhibitory effect, we analysed by RT-qPCR the diurnal expression patterns of the photoperiodic pathway genes *StCOL1*, *StCOL2*, *StSP5G* and *StSP6A*, in plants cultivated under both control and restrictive temperatures. Results from these analyses showed that *StSP6A* expression is strongly suppressed in leaves of both Spunta and Sylvana plants after 30 days at 28ºC. Inhibition of this gene is also stronger in Spunta, consistent with the more severe effects of temperature in suppressing tuber formation in this genetic background (Figure 34A). By opposite, warm temperatures had only a minor effect on *StCOL1*, *StCOL2* and *StSP5G* expression levels in both cultivars, these genes being observed to maintain normal diurnal oscillation at 28ºC and a similar expression level as in plants grown at 22ºC (Figure 34A). Overall, these findings indicate that moderate temperatures suppress *StSP6A* transcription in the leaves, and suggest that this suppression is mediated independently of the upstream day-length *StSP6A* regulators *StCOL1*, *StCOL2* and *StSP5G*.

To verify that inhibition of *StSP6A* transcription is one of the main factors determining reduced tuber production at warmer temperatures, we generated Spunta and Sylvana lines that overexpressed the *StSP6A* gene (*StSP6Aox*) and analysed tuber yields of these plants at 22ºC and 28ºC (Figure 34B). Notably, *StSP6A* overexpression was able to overcome the negative effects of temperature on tuber production, higher tuber yields being observed at 28ºC in both cultivars (Figure 34C; Figure 46A). Moreover, although *StSP6A* is expressed to lower levels in Sylvana and is less affected by temperature than in the more heat-sensitive Spunta cultivar, its overexpression leads also to increased tuber production at 28ºC. Thus, a *StSP6A*-dependent heat response is shared by both cultivars, independently of *StSP6A* be slightly different regulated in Sylvana. Altogether, these findings point to transcriptional repression of *StSP6A* as the main factor leading to reduced tuber yields under warm temperatures.

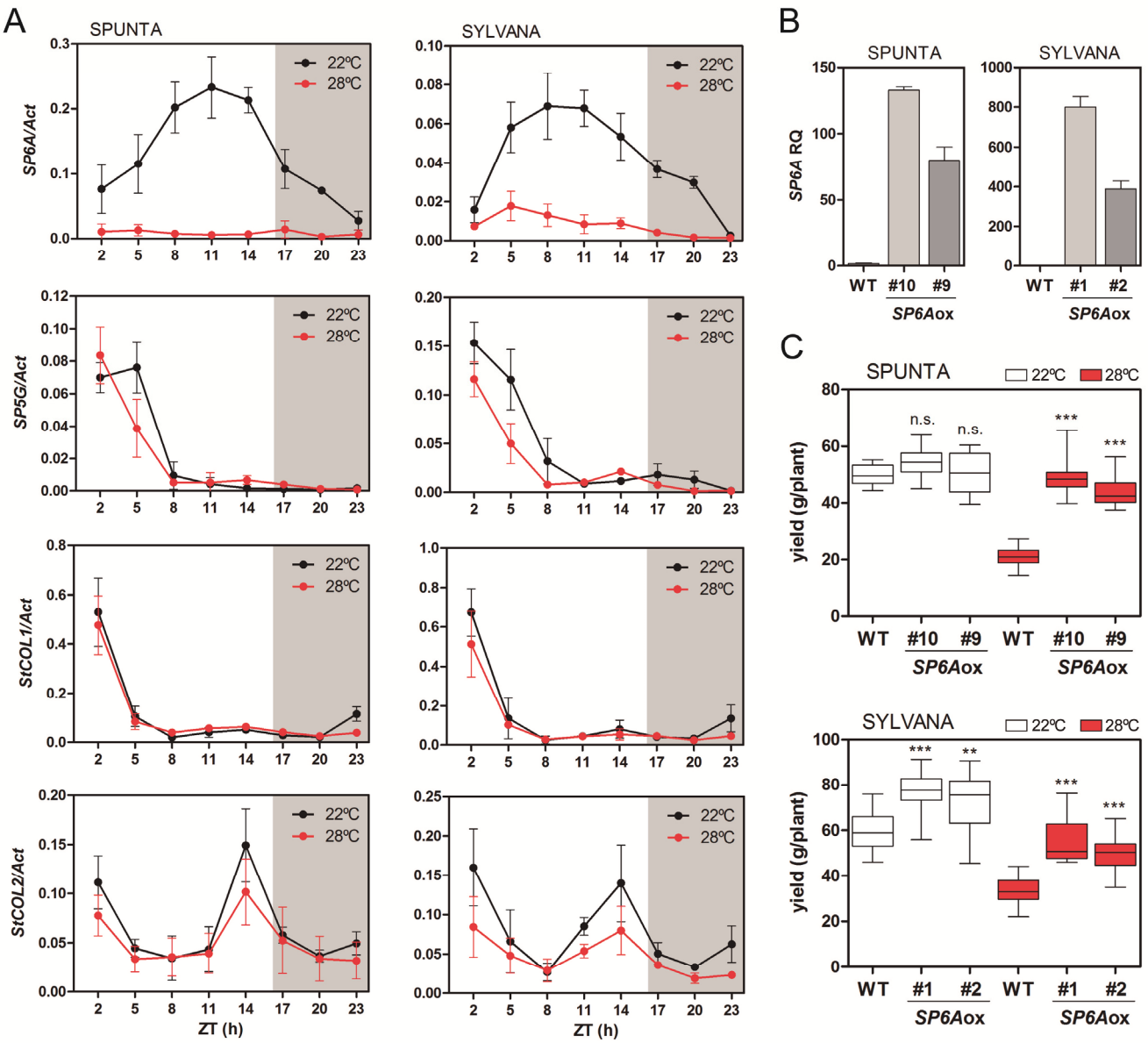

Figure 34. *StSP6A* repression by warm temperatures leads to reduced tuber production. (A) qPCR analyses of *StCOL1*, *StCOL2*, *StSP5G* and *StSP6A* expression patterns at 22ºC and 28ºC in Spunta (left column) and Sylvana (right column) plants (B) qPCR analysis of *StSP6A* expression in two independent Spunta (left graph) and Sylvana (right graph) *StSP6Aox* lines. (C) Tuber yield of Spunta (upper graph) and Sylvana (lower graph) WT and *StSP6A*ox plants grown at 22ºC and 28ºC. Error bars denote standard deviation. ***, ** and * denote statistical significance ($p<0.001$; $p<0.01$; $p<0.05$) compared to WT plants.

2. StSP6A modulates the thermomorphogenic response induced by warm temperatures

Effects of warm temperatures on plant morphology have been well characterized in *Arabidopsis* and involve increased hypocotyl and petiole elongation, hyponastic growth and reduced area of the leaves, among others (Quint et al., 2016). Consistent with this, elevated temperatures were reported to induce in potato a taller growth of the stem and smaller leaf size (Lafta and Lorenzen, 1995). To verify that a similar thermomorphogenic response is shared by the Spunta and Sylvana cultivars, and assess its possible connection with tuber production, we measured the height of WT and *StSP6A*ox lines grown at 22ºC and 28ºC.

Figure 35. *StSP6A* modulates the thermomorphogenic response of potato plants. 7 weeks-old Spunta (top) and Sylvana (bottom) WT and *StSP6A*ox plants grown at 22ºC or 28ºC.

These studies confirmed that warm temperatures trigger stem elongation and a reduction of leaf size in both Spunta and Sylvana cultivars, with this response found to be more severe in the heat-sensitive Spunta genetic background (Figure 35; Figure 36A, Figure 36B). Moreover, Spunta and Sylvana *StSP6Aox* lines were shorter and displayed larger leaves at 28ºC than the corresponding WT, hence indicating that in addition to its role in tuber formation, *StSP6A* modulates the potato thermomorphogenic response (Figure 35, Figure 36A, Figure 36B). As seen for tuber yield, effects of *StSP6A* overexpression on plant height differed slightly between both cultivars. Sylvana *StSP6A*ox lines were significantly shorter at 22ºC than WT plants (Figure 36B). Spunta plants, however, showed a more pronounced thermomorphogenic response than the Sylvana genotype, and this growth response was largely suppressed by StSP6A.

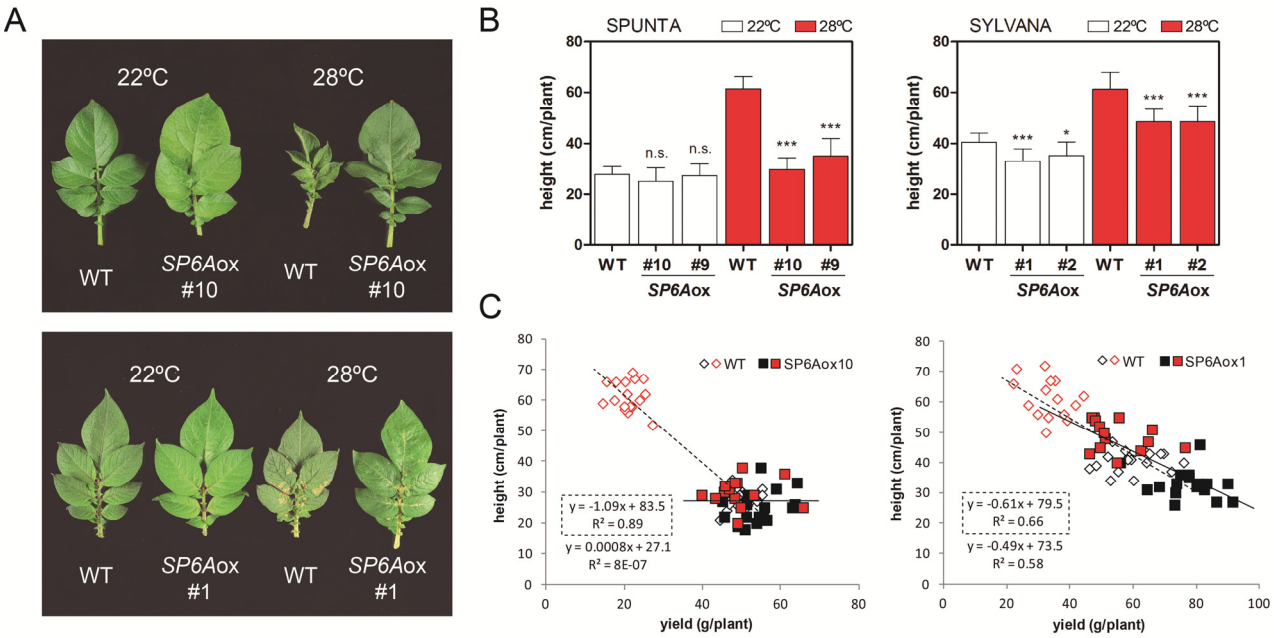

Figure 36. *StSP6A*ox palliates both stem elongation and tuberization inhibition effects of warm temperatures. (A) Third fully expanded leaf from the apex of 7 weeks-old Spunta (top) and Sylvana (bottom) WT and *StSP6A*ox plants grown at 22ºC or 28ºC. (B) Plant height of 11 weeks-old Spunta (left) and Sylvana (right) WT and *StSP6A*ox plants grown at 22ºC and 28ºC. Error bars denote standard deviation. ***, ** and * denote statistical significance ($p<0.001$; $p<0.01$; $p<0.05$) compared to WT plants. (C) Linear regression analyses comparing plant height and tuber yield of Spunta (left) and Sylvana (right) WT and *StSP6A*ox plants grown at 22ºC (black) and 28ºC (red). Regression equations are represented with a dotted line for WT plants and a solid line for *StSP6A*ox lines.

These findings point to a function of *StSP6A* in reversing both reduced tuber yield and the internode elongation response induced by warm temperatures, suggesting that these two processes are part of the same response and likely keep a linear relationship. Regression

analyses of the plant height and tuber yields of WT and *StSP6A*ox lines actually showed that there is a strong inverse correlation among these two variables in Spunta plants grown at 22ºC and 28ºC (Figure 36D). Also, while *StSP6A* overexpression strongly suppresses the growth elongation and reduced tuber yield effects of temperature in Spunta plants, in Sylvana these heat responses are only partially attenuated (Figure 36D).

Taken together, these results demonstrate that Spunta is more sensitive to warm temperatures than the Sylvana cultivar and that its stronger heat response is mostly dependent on *StSP6A* repression. In addition, although Sylvana exhibits an important *StSP6A*-dependent response to temperature, behaviour of these plants suggests that during breeding they were selected for a heat tolerant tuberization response that is partially independent of *StSP6A* expression levels. This phenotype likely relies on other pathways converging on tuberization control and therefore we selected the genotype Spunta for further studies.

3. The leaf transcriptomic changes induced by warm temperatures are attenuated in *StSP6A*ox lines

To bring some light into the molecular events mediating *StSP6A*-dependent increased tolerance to heat, we analysed the leaf transcriptome of Spunta WT and *StSP6A*ox plants grown at 22ºC and 28ºC. To this purpose, an Agilent 60-mer microarray including probes for all 39031 predicted coding regions from the potato genome sequence (Xu et al., 2011) was probed with the RNA extracted from leaves of plants grown for 30 days under LD conditions (16h light/ 8h dark), and constant 22ºC or 28ºC. After application of the statistical cut-off described in Material and Methods we identified 4417 genes that were differentially expressed (DEGs) in WT plants at 28ºC and 4364 in *StSP6A*ox lines ($p<0.05$; FC≤ -2 or ≥ 2). Comparison of these two datasets showed that *StSP6A* overexpression prevents activation at warm temperatures of 27% of the total up-regulated genes in WT leaves, and also suppresses inhibition of 11% of the total down-regulated genes (Figure 37B). Through hierarchical clustering we grouped these DEGs according to their pattern of expression in response to elevated temperatures and *StSP6A* overexpression. Examination of the generated heatmap confirmed that StSP6A modulates an important part of the heat response in Spunta leaves by preventing temperature-dependent down-regulation or activation of a significant number of genes (Figure 37A).

To further identify the signalling events underlying the heat tolerant phenotype of *StSP6A*ox lines, we focused on two clusters of DEGs. The first of these clusters corresponds to *StSP6A* co-regulated genes and includes DEGs with a similar expression profile as

StSP6A. Expression of these genes is reduced in WT plants at 28ºC, but up-regulated in *StSP6A*ox lines (Figure 37A). The second cluster, designated as UP-regulated genes Supressed by *StSP6A* (UPS-SP6A), includes DEGs that are induced by heat in WT plants, but their activation is inhibited in *StSP6A*ox lines.

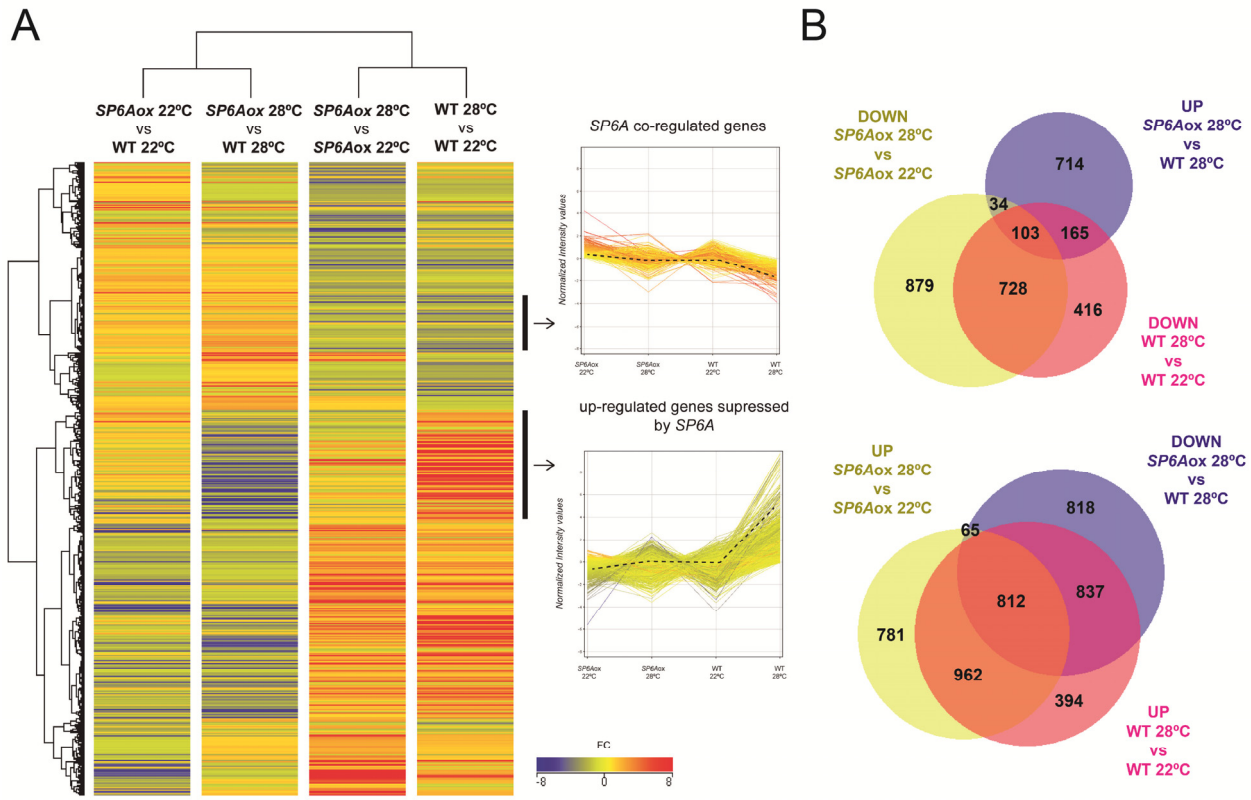

Figure 37. Transcriptomic changes induced by *StSP6A* overexpression and warm temperatures in potato leaves. (A) Heatmap of the hierarchical clustering analysis of all DEGs in Spunta WT and *StSP6A*ox leaves of plants grown at 22ºC and 28ºC. The normalized expression values of genes grouped into the UPS-SP6A and SP6A co-regulated clusters are represented in two independent graphs on the right (B) Venn diagrams showing the overlap of genes up- or down-regulated at 28ºC in WT and *StSP6A*ox plants, and those exhibiting an inverse expression pattern in *StSP6A*ox plants.

Functional enrichment analyses of these two clusters revealed that UPS-SP6A is over-represented in genes associated with cell wall, lipid metabolism, secondary metabolism and stress-related genes, among others (Figure 38A; Figure 38B). By contrast, the SP6A co-regulated cluster shows enrichment in genes involved in photosynthesis, carbohydrate metabolism, redox regulation and transport (Figure 38A; Figure 38B).

Notably, the *FUL* homolog *StAGL8-like1* and a *SOC1*-like gene were found to be co-regulated with *StSP6A* (Figure 39), indicating that this protein promotes activation of these MADS-box as reported in *Arabidopsis* for *FT* (Andres and Coupland, 2012). Moreover,

homologs of *AGL11* and *BEL1*, shown in *Arabidopsis* to control ovule development (Brambilla et al., 2007), also exhibit a similar expression profile than that of *StSP6A* (Figure 39). An homolog of *BEL1*, i.e. *BEL5*, was recently reported to activate *StSP6A* expression (Sharma et al., 2016) and therefore it will be worth analysing whether this family of transcription factors is involved in positive feedback regulation of the StSP6A tuberization signal. Furthermore, the SP6A co-regulated cluster includes additional flowering regulators such as *AP2a, BFT*, *COL9* and *CDF2*, in addition to the circadian regulators *StPRR5* and *StCIR*, and the DELLA-protein *StRGL2* (Figure 39). Whether differential expression of these genes plays a role in tuberization control will be analysed in future studies.

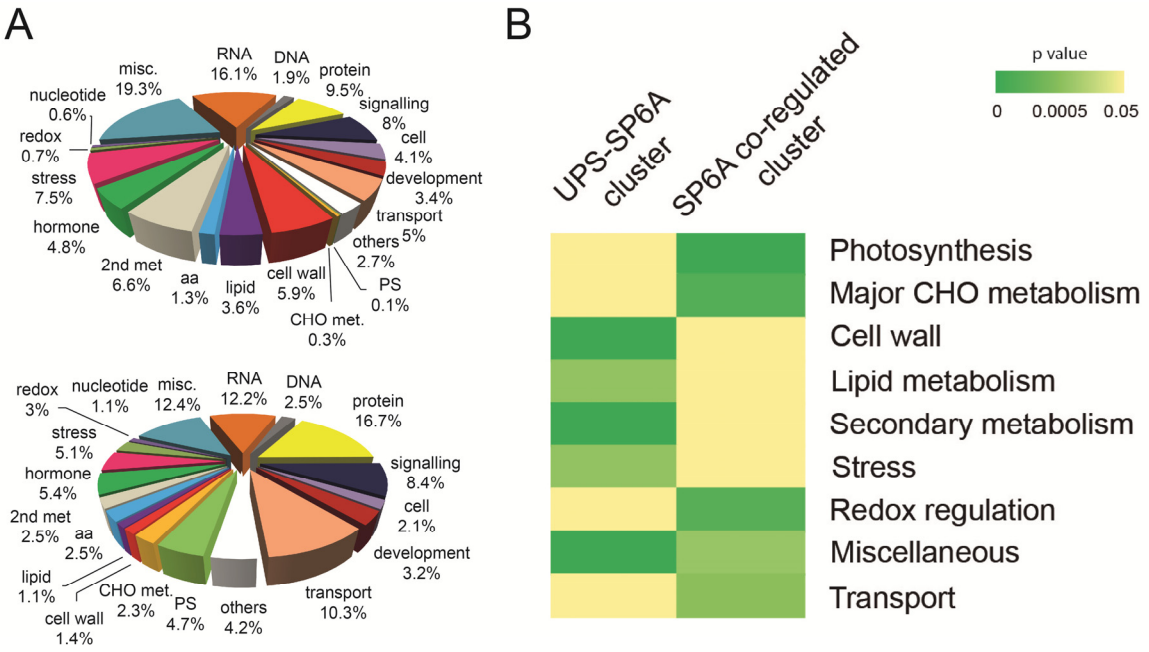

Figure 38. Functional annotation of the UPS-SP6A and SP6A co-regulated cluster genes. (A) Functional annotation of all DEGs included into the UPS-SP6A (top) and SP6A co-regulated (bottom) clusters performed according to the Mapman bin classification. Percentages were calculated according to the total number of genes assigned to at least one of the 34 functional categories. PS, photosynthesis; CHO met, major carbohydrate metabolism; aa, amino acid metabolism; 2nd met, secondary metabolism; misc, miscellaneous. (B) Heatmap showing the p value of the functional categories significantly enriched ($p<0.05$) in UPS-SP6A or SP6A co-regulated clusters. p values were calculated by one-sided Fisher's exact test.

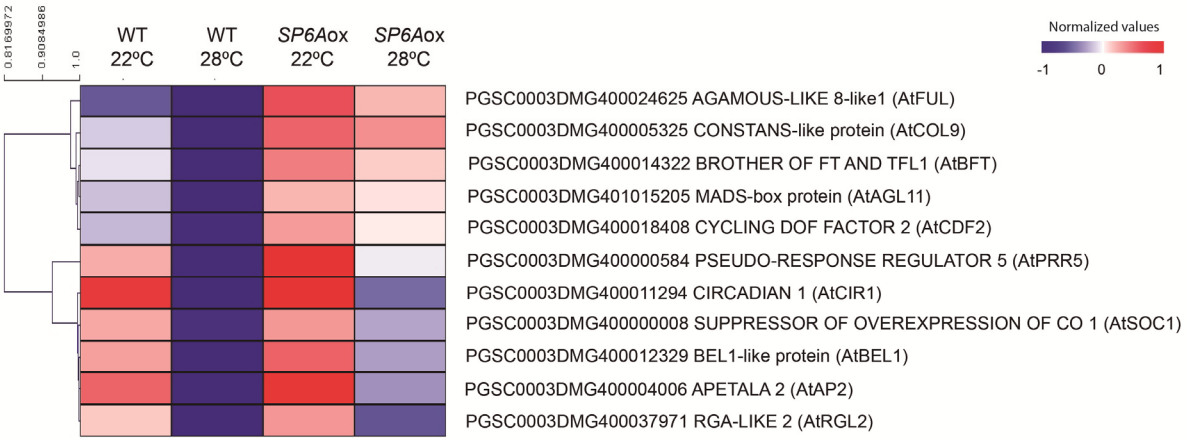

Figure 39. Functionally relevant genes co-regulated with *StSP6A*. Heatmap showing the normalised expression levels of a selection of interesting *StSP6A* co-regulated genes including those reported in *Arabidopsis* to act upstream or downstream of *FT* in the flowering pathway. Genes are represented with their ID number and their closest *Arabidopsis* homolog is shown in parentheses.

4. StSP6A suppresses activation of auxin- and cell wall-related genes involved in thermomorphogenic growth

Small increases in temperature induce a thermomorphogenic response that in *Arabidopsis* is characterized by an elongation of the hypocotyl and leaf petioles, and reduced expansion of the cotyledons and leaves. Leaves also acquire an upwards position, away from the heated soil, which favours evaporative cooling and promotes plant survival, by preventing the photooxidative damage of photosynthetic leaves. Notably, these morphological changes remind in several aspects those of plants grown in the shade, and the bHLH light-signalling factor PHYTOCHROME INTERACTING FACTOR 4 (PIF4) was established in *Arabidopsis* to control this response (Koini et al., 2009). Warm temperatures induce a faster dark reversion of the light receptor PHYTOCHROME B (phyB) (Legris et al., 2016), which leads to increased stabilization of the PIF4 protein. This factor triggers hypocotyl and petiole elongation through the regulation of auxin biosynthetic and signalling genes. As observed during shade-avoidance, genes like *YUC8*, *AUX/IAA*s and *SAUR*s were shown to be transcriptionally activated in response to warm temperatures (Franklin et al., 2011; Gray et al., 1998). Consistent with these observations, several auxin-related genes were induced in the leaves of potato plants grown at 28ºC, and grouped into the UPS-SP6A cluster. In particular, homologs of the *Arabidopsis IAA19*, *IAA29* genes and several *SAUR*s are up-regulated at 28ºC in WT plants, and activation of these genes is strongly suppressed in the *StSP6A*ox transgenic lines, in agreement with their smaller thermomorphogenic response (Figure 40).

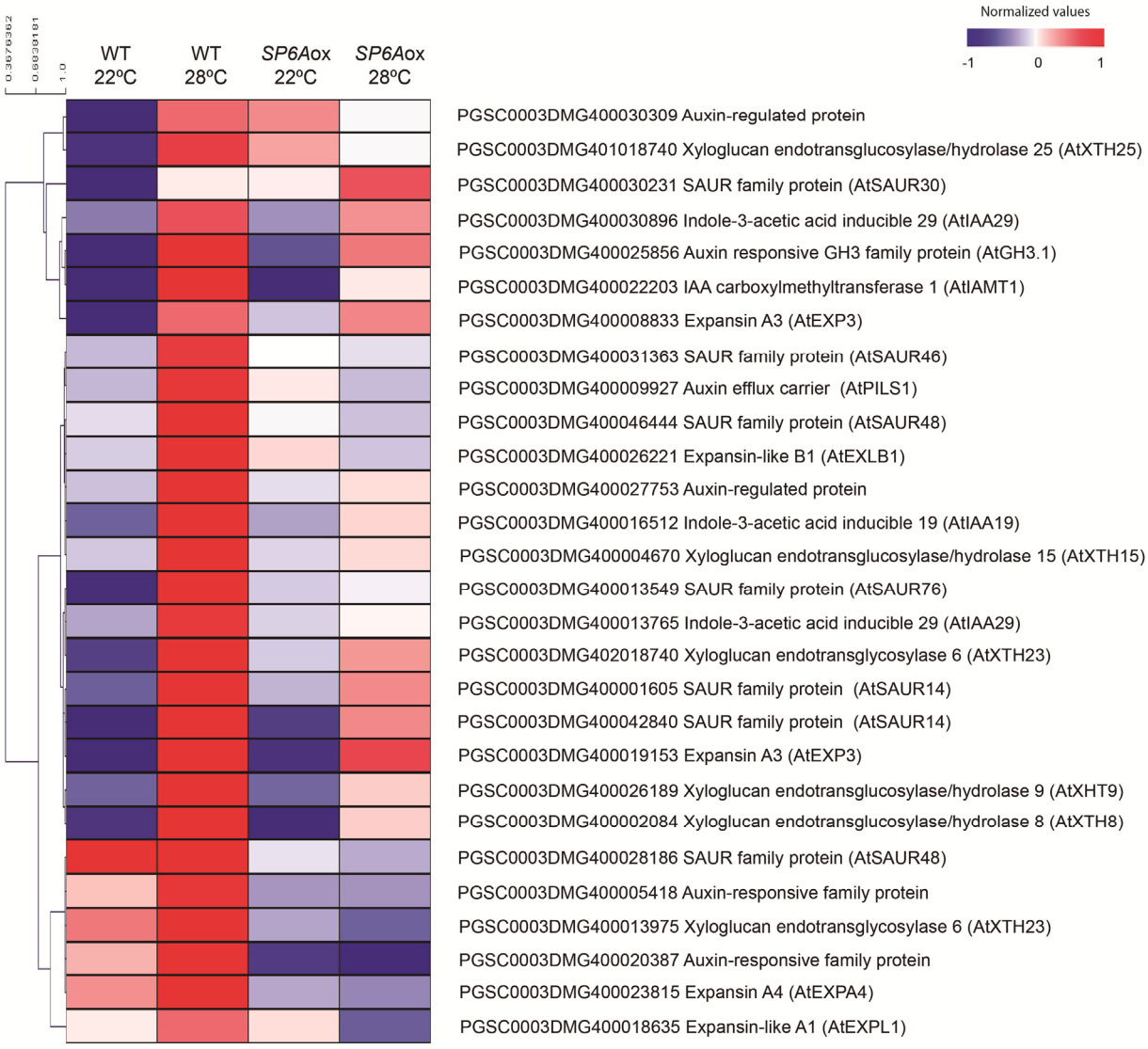

Figure 40. Regulation of auxin-related and expansin and XTHs family genes grouped into the UPS-SP6A cluster. Heatmap showing the normalized expression levels of auxin-related, expansin and XTHs family genes in the UPS-SP6A cluster. *StSP6A* suppresses activation of these genes at 28ºC. Genes are represented with their ID number and their closest *Arabidopsis* homolog is shown in parentheses.

In addition to auxins, plant cell elongation requires the activation of cell wall remodelling enzymes that loosen the rigid wall layer around cells, to enable cell expansion. Two main families of cell wall modifying proteins, i.e. expansins and xyloglucan endotransglucosylase/hydrolases (XTHs), were reported to be activated by shade and warm temperatures in *Arabidopsis*, and play a role in cell wall loosening and growth elongation (Bai et al., 2012; Sasidharan and Pierik, 2010). Previous reports suggested that these genes are as well direct activation targets of PIF4, which recognizes conserved G-box elements in their promoters (Hornitschek et al., 2012; Zhang et al., 2013). In consonance with this regulation,

we identified a big set of expansin and XTH family genes in the UPS-SP6A cluster (Figure 40), indicating that *StSP6A* somehow inhibits activation of these PIF4 target genes.

To further validate these results, we carried out RT-qPCR analyses of three representative genes, *StIAA19*, *StXTH9* and *StSAUR76*, in RNA samples extracted from an independent set of plants. Amplification results were consistent with the microarray data and showed that these genes are induced at 28ºC in WT leaves, but their activation is notably reduced in the *StSP6A*ox lines (Figure 41). Taken together, these results would demonstrate that *StSP6A* suppresses the thermomorphogenic response of potato plants by preventing activation of multiple auxin signalling and cell wall modifying genes. These genes are direct activation targets of PIFs, hence suggesting that StSP6A activates a signalling pathway that negatively regulates transcriptional activity of these factors. Since neither UPS-SP6A nor SP6A co-regulated clusters included any *PIF*-like gene, our findings suggest that StSP6A modulates its function at the post-transcriptional level likely by activating a negative regulator that binds these factors.

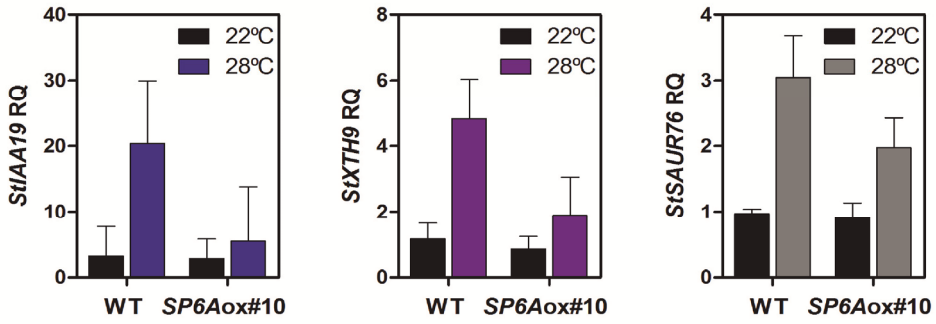

Figure 41. Experimental validation of the expression profile of UPS-SP6A cluster genes. qPCR analyses of *StIAA19*, *StXTH9* and *StSAUR76* expression in WT and *StSP6A*ox #10 lines grown at 22ºC and 28ºC. Error bars represent ± s.d. of three biological replicates.

5. StSP6A regulates genes involved in photosynthesis and starch metabolism and promotes transitory starch accumulation

Although heat stress strongly decreases the photosynthetic rate of potato leaves by impairing photosystem II (PSII) activity (Havaux et al., 1996; Quinn and Williams, 1985), it was reported that exposure of potato plants to moderately warm temperatures up to 30ºC, would not affect or even slightly increase photosynthetic efficiency per unit of leaf area (Hancock et al., 2014; Lafta and Lorenzen, 1995; Singh et al., 2015). Still, moderate heat has a remarkable impact on carbon metabolism, as lower starch and increased sucrose levels were measured in mature leaves of potato plants subjected to a 31/29ºC heat treatment after

tuber initiation (Lafta and Lorenzen, 1995). This response coincided with increased sucrose phosphate synthase (SPS) activity in the leaves, although such changes did not correlate with susceptibility to heat of the analysed cultivars. Carbon translocation to the tubers and its incorporation into tuber starch is also reported to be compromised in potato plants grown at 32ºC (Wolf et al., 1991), hence suggesting that warm temperatures impair source-sink assimilate partitioning.

During the day, a considerable part of the photosynthates provided by the Calvin cycle is stored in the chloroplast as starch, whereas the rest is used for sucrose synthesis and exported to other organs to support metabolism and plant growth. This transitory starch is remobilized during the following night and degraded into maltose and glucose, that are exported to the cytosol and provide a carbohydrate supply for continued growth and metabolism in the absence of light (Streb and Zeeman, 2012). Rate of starch synthesis is tightly regulated by the balance between photosynthetic carbon assimilation and the synthesis of sucrose in the cytosol. Sucrose is synthesized from triose phosphate exported from the chloroplast, in successive reactions involving Fructose 1,6-bisphosphatase (FBPase) and sucrose phosphate synthase (SPS) activities. A fall in sucrose synthesis in response to feedback inhibition on account of decreased utilization by sink organs, decreases available Pi required for triose phosphate export and leads to its retention in the chloroplast, where is used for starch synthesis. Conversely, a fall in photosynthetic carbon assimilation caused by shading or stomatal closure, reduces the concentration of triose phosphate in the chloroplast and starch synthesis is decreased. Besides this short-term control, starch synthesis is also regulated by day-length. The shorter the day the greater the proportion of photosynthates allocated to starch, and thus available for metabolism at night (Sulpice et al., 2014). Starch degradation in the night is also slower under short days, hence ensuring a continued provision of carbohydrates to the plant, until the next light period. As such, expression of many of the genes involved in starch metabolism is under circadian or diurnal regulation (Smith et al., 2004), but the mechanisms adjusting starch accumulation to day-length remain poorly understood (Mugford et al., 2014).

Remarkably, the *StSP6A* co-regulated cluster included a significant number of genes involved in photosynthesis and starch metabolism (Figure 42). In particular, transcripts encoding PSII antenna complex proteins, glycolytic and Calvin cycle enzymes, and a notable number of genes of the photorespiratory pathway were up-regulated in *StSP6A*ox lines, while heat caused a strong repression of these genes in WT plants (Figure 42). The core Calvin cycle SBPase enzyme was found to be included among these DEGs, overexpression of this gene in *N. tabacum* being shown to result in increased starch and sucrose accumulation in the leaves (Lefebvre et al., 2005). Surprisingly, several genes involved in starch-mobilization

such as various β-amylases and the plastid envelope maltose transporter MEX1 (MALTOSE EXCESS 1), could also be identified in the *StSP6A* co-regulated cluster (Figure 42). Maltose is the major product of starch degradation at night, *Arabidopsis mex1* mutants being shown to display stunted growth and accumulate high levels of maltose and starch in the leaves (Niittyla et al., 2004). Once in the cytosol, maltose is metabolized by the DPE2 glucosyltransferase, released glucosyl units being transformed into sucrose in two successive reactions, catalysed by sucrose phosphate synthase (SPS) and sucrose-6P-phosphatase (SPP). Notably, these two genes were found to be co-regulated with *StSP6A*, suggesting that transgenic leaves behave as stronger source organs. In fact, sucrose is the main photoassimilate transported from source to sink organs, silencing of the *NtSPSC* leaf isoform in tobacco, being shown to cause a massive increase in starch content in the leaves (Chen et al., 2005). In *Arabidopsis*, *AtSPSA1* and *AtSPSC* are the major SPS isoforms expressed in leaves, and double *spsa1 spsc* mutants are severely impaired in growth and accumulate high levels of starch in leaves (Volkert et al., 2014). In these plants, sucrose concentration in phloem exudates is considerably reduced, indicating that SPS activity is limiting for sucrose synthesis and export from source leaves. Moreover, starch accumulation appears to be due to the reduced rate of starch mobilization during the night, as no alterations in photosynthetic carbon partitioning were observed in these plants (Volkert et al., 2014). In consonance with these findings, three invertase genes were also identified in the UPS-*SP6A* cluster. These are up-regulated at warm temperatures in the WT, but do not respond in *StSP6A*ox plants (Figure 42). Cell wall invertase (CWI) gene expression is induced in response to different plant pathogens and has been shown to interfere with sucrose export in source leaves, due to catalyse the cleavage of sucrose into glucose and fructose, which are not transported in the phloem (Kocal et al., 2008). Apoplastic accumulation of these sugar hexoses is also linked to photosynthetic inhibition, thus further decreasing sucrose export ability. By opposite, high invertase activity in sink organs correlates with increased sucrose import and enhanced fruit and seed set under heat stress conditions (Li et al., 2012).

Overall, these data suggests that *StSP6A* overexpression confers heat stress resistance in potato by positively regulating genes involved in photosynthesis and carbon fixation, and the expression of genes involved in transitory starch breakdown and sucrose export. Therefore, we assessed if leaves of these plants accumulate less starch, by staining with Lugol solution leaf disks from WT and *StSP6A*ox plants grown at 22ºC and 28ºC. To our surprise, *StSP6A*ox leaves showed a darker staining indicative of higher starch content than WT, although expression of beta-amylase genes was up-regulated (Figure 43). A darker staining than the WT was also observed at 28ºC, although for leaves of plants grown at this

temperature staining was much weaker than in plants grown at 22ºC, hence indicating that warm temperatures suppress starch accumulation in both WT and *StSP6A*ox plants (Figure 43).

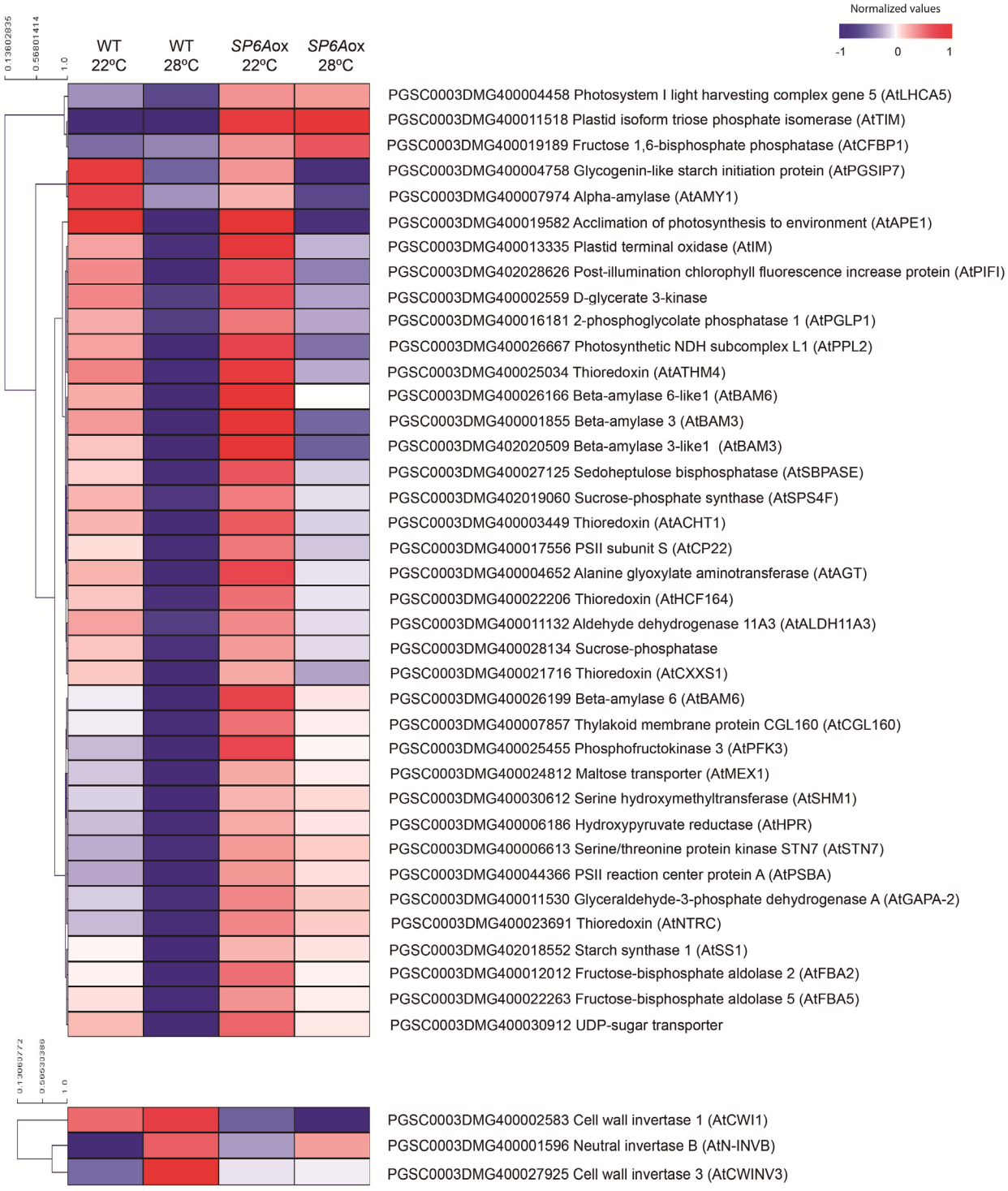

Figure 42. Photosynthesis and starch-related genes in the SP6A co-regulated and UPS-SP6A clusters. Heatmap showing the normalised expression levels of photosynthesis and starch-related genes belonging to the SP6A co-regulated (top) and UPS-SP6A clusters (bottom). Genes are represented with their ID number and the closest *Arabidopsis* homolog is shown in parentheses.

Relative expression of starch metabolism genes was further validated by quantitative real-time PCR amplification of samples obtained in an independent experiment. Amplification of the *StSBPase*, *StMEX1*, *StBAM3* and *StBAM6* genes led to consistent results with those obtained by microarray hybridization and proved that all these genes are up-regulated in *StSP6Aox* leaves. Furthermore, warm temperatures induced a comparable reduction in expression levels of these genes in WT and *StSP6A*ox plants. Therefore, at 28ºC, their expression was higher in *StSP6A*ox leaves than in the WT, although transcript levels were reduced with respect to those of WT leaves at 22ºC (Figure 44A; Figure 44B). Given that *BAM* and *MEX1* genes show circadian oscillation in *Arabidopsis*, in a similar way as other starch biosynthesis and breakdown genes (Lu et al., 2005; Smith et al., 2004), we wondered whether warm temperatures would affect the diurnal expression profile of these genes. To this aim, we analysed *StMEX1* expression in leaves of WT plants grown under LDs at 22ºC and 28ºC, harvested every three hours for the overall interval of one day. RT-qPCR amplification of these samples showed that potato *StMEX1* is as well diurnally regulated and in plants grown at 22ºC peaks in the middle of the day (Figure 44B). At 28C, *StMEX1* transcript levels are however reduced, and its expression peak is slightly shifted toward the night, hence indicating that warm temperatures not only exert a repressor effect on starch breakdown genes, but change their maximal expression levels towards dusk (Figure 44B).

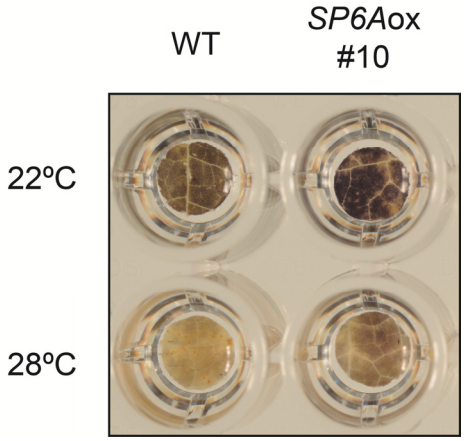

Figure 43. *StSP6A* overexpression increases transitory starch accumulation in the leaves. Lugol staining of leaf disks of WT and *StSP6A*ox plants grown under LDs at 22ºC or 28ºC. Discs were harvested at ZT5.

Taken together, these results point to a role of *StSP6A* in enhancing photosynthesis and photorespiration, at the same time that promotes the breakdown of starch and subsequent synthesis of sucrose in the cytosol. Notably, all these metabolic changes are associated with increased carbon assimilation during the day and higher starch mobilization at night, indicating that *StSP6A*ox leaves are able to export more sucrose, and thus have higher source capacity than WT leaves.

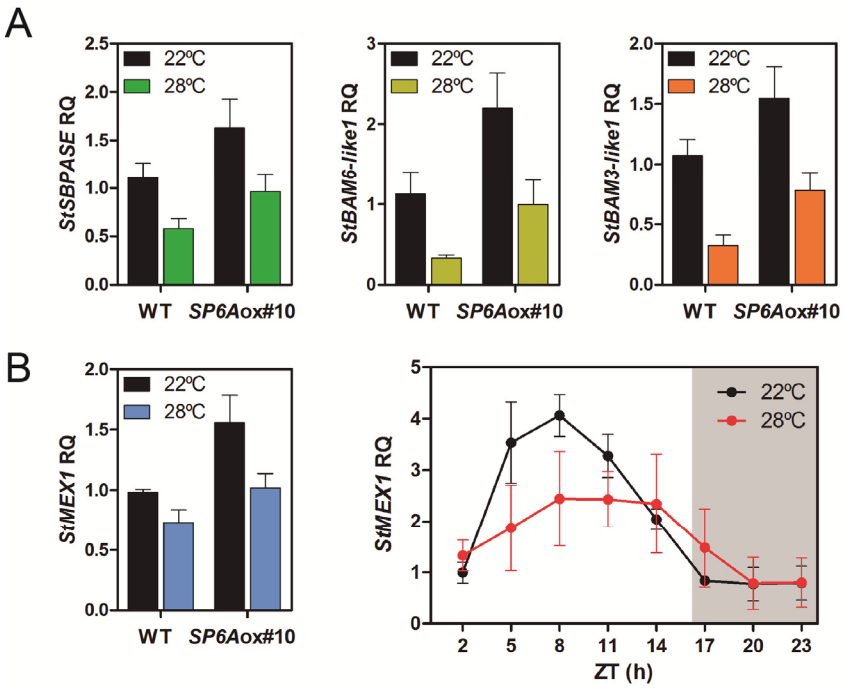

Figure 44. Experimental validation of the expression profile of starch metabolism genes co-regulated with *StSP6A*. (A) qPCR analyses of *StSBPase*, *StBAM6-like1* and *StBAM3-like1* gene expression in WT and *StSP6A*ox #10 plants grown at 22ºC and 28ºC. (B) *StMEX1* expression levels in WT and *StSP6A*ox #10 plants (left) and circadian oscillation of this transcript in WT plants grown at 22ºC and 28ºC (right). Error bars represent ± s.d. of three biological replicates.

6. *StSP6A* overexpression improves tuber processing quality

Two important traits to potato fresh market and processing industry are a high dry matter and long dormancy of tubers. A high starch content and reduced levels of reducing sugars is essential to prevent black coloration during frying, whereas delayed sprouting favours long-term tuber storage and prolongs their shelf life (Kadam et al., 1991; Knowles et al., 2009; Mehta and Ezekiel, 2006). Heat exerts a negative effect on these physiological traits as tubers from plants grown at elevated temperatures accumulate higher levels of reducing sugars, show decreased starch content and a reduced period of dormancy (Burton, 1989; Krauss and Marschner, 1984; Lafta and Lorenzen, 1995).

To determine whether the heat tolerance response conferred by *StSP6A* overexpression palliates as well these deleterious effects on tuber processing quality, we analysed the dry matter, starch and reducing sugars content of tubers harvested from WT and *StSP6A*ox plants grown at 22ºC or 28ºC. Notably, *StSP6A*ox tubers showed a higher dry matter content, higher starch levels and lower levels of reducing sugars than WT tubers (Figure 45A). Moreover, although elevated temperatures caused a similar decrease in starch accumulation in both genotypes, tubers of *StSP6A*ox plants grown at 28ºC showed almost

the same dry matter and starch content as WT tubers grown under cooler temperatures, due to initially accumulate higher levels of starch (Figure 45A). In addition, rise in reducing sugars at 28ºC was much smaller in these tubers, thus showing similar levels of reducing sugars as the WT at 22ºC (Figure 45A).

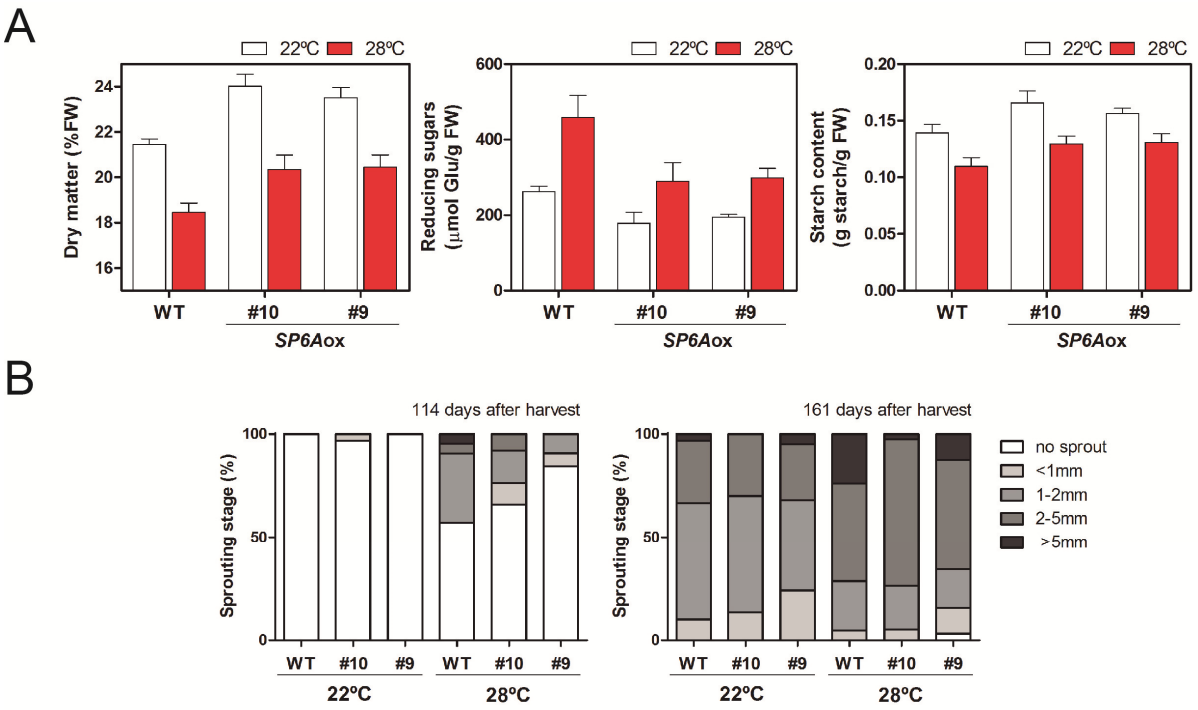

Figure 45. Tuber processing quality of *StSP6A*ox tubers. (A) Dry matter, reducing sugar and starch content of WT and *StSP6A*ox tubers harvested from plants grown at 22ºC and 28ºC. Measurements were done on freshly harvested tubers. Error bars denote standard deviation. (B) Percentage of WT and *StSP6A*ox tubers with emerging sprouts and length of the sprouts after 114 (left) and 161 days (right) of storage at 4ºC.

Sprouting negatively affects tubers processing quality, as it triggers hydrolysis of the stored starch, to sustain developing shoots outgrowth. At harvest, tuber buds are in an endodormant state, and do not sprout even if placed in suitable environmental conditions. However, span of this dormancy state largely depends on the cultivar and growth conditions. Warm temperatures shorten dormancy time and lead to secondary growth of tubers (Suttle, 2004). To assess whether StSP6A reverses these temperature effects, we further analysed dormancy length of tubers from *StSP6A*ox and WT plants grown at 22ºC and 28ºC. To this end, tubers were hold for 3-4 days at room temperature for full maturation and subsequently stored for several month at 4ºC. Percentage of tubers with emerging sprouts and sprout length was then measured after 4 and 5½ month of storage. As shown in Figure 45B, tubers of plants grown at 28ºC displayed a shortened dormancy period and started sprouting after 4

month at 4ºC, while those from plants grown at 22ºC were still dormant. Percentage of tubers with sprouts and length of the sprouts was however reduced in *StSP6A*ox plants, a delayed sprouting of tubers being particularly evident in tubers of line #9, that show clearly smaller sprouts than the WT even after storage for 5½ month (Figure 45B).

Sucrose synthases control the flux of incoming sucrose into starch and thus are considered to be the main determinants of tuber sink strength (Herbers and Sonnewald, 1998). In agreement with this function, overexpression of *StSUS4* in potato tubers strongly increases their starch content and dry weight (Baroja-Fernandez et al., 2009). As such, we set to determine whether increased starch content of *StSP6A*ox tubers is mediated through transcriptional regulation of these genes. Interestingly, RT-qPCR analyses of *StSUS4* and *StSUS2* expression revealed that transcript levels for these genes are not significantly affected either by warm temperatures or *StSP6A* overexpression (Figure 46B). Hence, these findings suggest that improved processing quality of *StSP6A*ox tubers is not caused by specific gene expression changes in tubers leading to enhanced sink strength, but rather derives from an elevated photosynthetic efficiency and increased export of sucrose in source leaves.

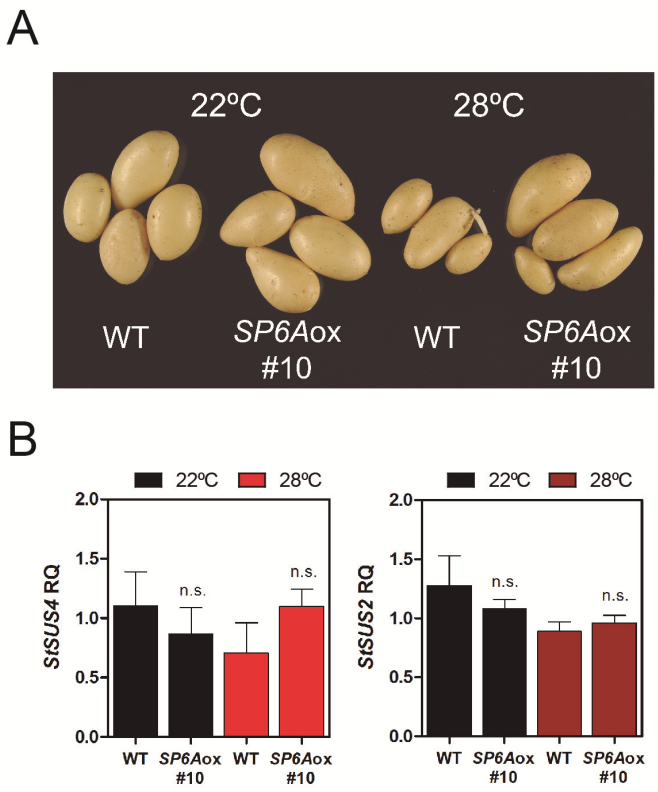

Figure 46. Tuber yield and expression levels of Sucrose Synthase genes in tubers of WT and *StSP6A*ox plants. (A) Picture showing the representative yield in tubers and dormancy phenotype of tubers harvested from WT and *StSP6A*ox plants grown at 22ºC and 28ºC. (B) qPCR analyses of *StSUS4* (left) and *StSUS2* (right) expression levels in tubers from WT and *StSP6A*ox #10 plants grown at 22ºC and 28ºC. Error bars represent ± s.d. of three biological replicates. n.s. denotes a non-significant difference with respect to WT tubers.

7. StSP6A negatively regulates JA signalling

The results obtained so far strongly suggest that *StSP6A* plays a critical role in regulating thermomorphogenesis and carbohydrate metabolism. To gain insight into the molecular mechanism by which *StSP6A* controls these processes, we further examined the UPS-SP6A and SP6A co-regulated clusters for transcriptional regulators showing a differential regulation in *StSP6A*ox leaves. Noteworthy, whereas most of the transcription factors co-regulated with *StSP6A* are associated with flowering or circadian regulation (Figure 39), the UPS-SP6A cluster included a large set of transcription factors involved in different developmental processes.

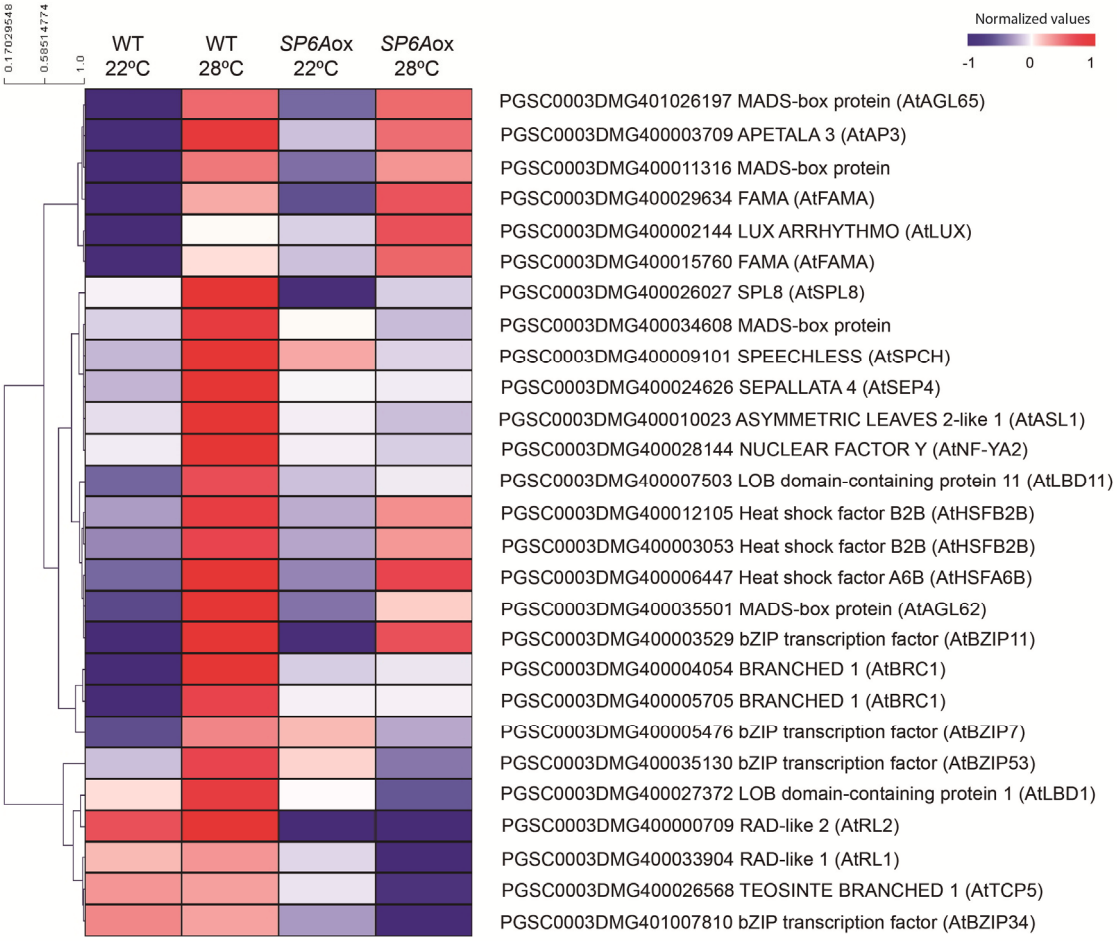

Figure 47. Functionally relevant transcription factors grouped into the UPS-SP6A cluster. Heatmap showing the normalised expression levels of a selection of interesting transcription factors grouped into the UPS-SP6A cluster. Genes are represented with their ID number and their closest *Arabidopsis* homolog is shown in parentheses.

Among them, several MADS-box genes, HSFs, bZIP transcription factors, in addition to a NF-Y factor, and an SQUAMOSA Promoter-Binding Protein-Like were found to be suppressed by StSP6A. *StLUX*, which is part of the evening complex repressing *PIF4* transcription in *Arabidopsis* (Nusinow et al., 2011) was also included in this group of UP-regulated genes Supressed by *StSP6A* (Figure 47). Another interesting group of genes in this cluster are those encoding LOB-domain and RAD-like proteins, which in *Arabidopsis* are implicated in adaxial cell fate specification of lateral organs and in the control of floral asymmetry (Baxter et al., 2007; Xu et al., 2016), or the *FAMA* and *SPEECHLESS* genes implicated in specification of the stomatal cell lineage (Lampard and Bergmann, 2007). Notably, two independent *BRANCHED 1* (*BRC1*) genes, in addition to *TEOSYNTE BRANCHED 1* were also included in this cluster and up-regulated at 28º in WT but not *StSP6A*ox lines (Figure 47). In *Arabidopsis*, BRC1 was shown to suppress branching in response to shade, and its expression be negatively regulated by PHYB (Gonzalez-Grandio et al., 2013). Consistent with this regulation, we observed that warm temperatures induce potato *BRC1* expression, likely by mimicking a shade response, while *StSP6A* impairs this activation. Remarkably, FT and BRC1 were shown to interact at the protein level, *Arabidopsis* BRC1 being shown to repress activation of *FT* down-stream targets and delay floral transition in axillary buds (Niwa et al., 2013). Our finding that *StSP6A* suppresses temperature-mediated activation of the *BRC1* gene adds a further layer of regulation in the transcriptional control of this gene, and underscores a critical function of BRC1-FT protein interaction in modulating FT signalling activity.

In addition to these TFs, a striking number of JA and ET signalling genes were also found to be downregulated by StSP6A. Indeed, multiple DEGs coding for JAZ and MYC regulators could be identified in the UPS-SP6A cluster (Figure 48). In consonance with this, two of the potato gene copies for ALLENE OXIDE SYNTHASE/DELAYED DEHISCENCE2 (AOS/DDE2) encoding CYP74, a chloroplast cytochrome P450 involved in JA biosynthesis, and a large number of protease inhibitors genes, described in potato to be induced in response to wounding and Methyl Jasmonate (Hildmann et al., 1992), were also grouped into this cluster (Figure 48 and Supplemental File 1). Notably, Jasmonic Acid (JA) plays a key role in multiple physiological processes including plant development and defence responses against biotic and abiotic stresses (Wasternack and Hause, 2013). The JASMONATE ZIM-domain proteins (JAZ) play a central role as negative regulators of the JA pathway. These proteins were shown in *Arabidopsis* to interact with the MYC2 transcription factor to block downstream activation of JA-regulated genes (Chini et al., 2007; Fernandez-Calvo et al., 2011; Pauwels et al., 2010). JA is perceived by the receptor COI protein which works as a subunit of the SCF^{COI1} E3 ubiquitin ligase complex responsible to degrade JAZs.

Destabilization of these repressors in the presence of bioactive JA releases the MYC factors from inhibition, and allows activation of JA-regulated responses. Remarkably, our finding that potato JA-responsive genes are highly enriched in the UPS-SP6A cluster strongly suggests that warm temperatures and StSP6A regulate JA signalling in opposite ways. Indeed, endogenous JA levels were reported to increase during heat stress in *Arabidopsis* (Clarke et al., 2009), and other reports showed that *MYC2* and *AOS* are activated in roots of tobacco plants subjected to 32ºC, hence suggesting that JA signalling is activated by heat also in *Solanaceae* (Yang et al., 2016). The genes encoding JA-biosynthetic enzymes, MYC and the JAZ repressors have been shown in *Arabidopsis* to correspond to primary response targets of the JA signalling pathway (Chung et al., 2008). Hence, down-regulated expression of these genes in *StSP6A*ox lines indicates that StSP6A suppresses JA levels, what is expected to promote JAZs stabilization. Interestingly, JAZs positively regulate *FT* by interacting with AP2 (Zhai et al., 2015), which suggests that StSP6A might modulate stability of these proteins to promote its own activation. However, a large number of JAZ genes were suppressed in *StSP6A*ox lines (Figure 48), and in consequence we cannot rule out that these plants behave as JAZ mutants. In this regard, JAZ9 was shown in *Arabidopsis* to inhibit interaction of the RGA repressor with the PIF3 transcription factor, and release PIF3 from RGA inhibition, which promotes plant growth (Yang et al., 2012). This raises the possibility that suppression of *JAZ*s expression by StSP6A increases the growth-inhibiting activity of DELLAs and therefore contributes to inhibit PIFs function, which would explain reduced thermomorphogenesis and suppressed expression of auxin- and cell wall- related genes in *StSP6A*ox plants.

Although further studies will be required to assign a role of these different TFs in the differential gene regulation response observed in *StSP6A*ox plants and to link them to StSP6A activity, our results show that StSP6A critically functions at modulation of distinct metabolic, hormonal, and stress signaling pathways, thus providing a novel strategy to overcome temperature-induced limitations to potato yield.

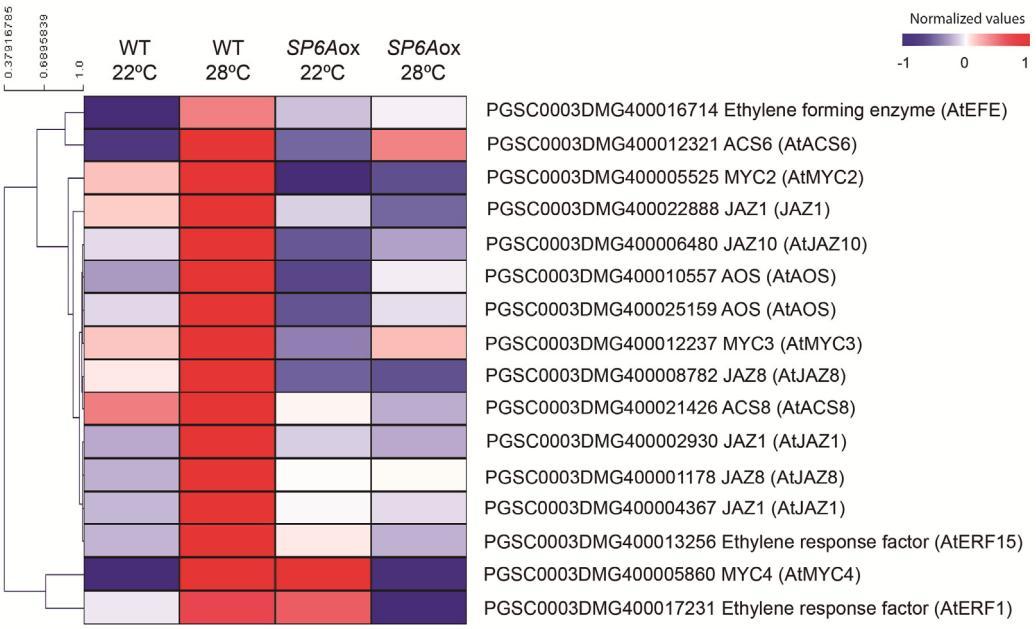

Figure 48. Jasmonate (JA) and ethylene (ET) related genes grouped into the UPS-SP6A cluster. Heatmap showing the normalised expression levels of JA- and ET- related genes grouped into the UPS-SP6A cluster. Genes are represented with their ID number and their closest *Arabidopsis* homolog is shown in parentheses.

Discussion

Potato tubers are an important contribution to human dietary needs in many regions worldwide, due to their easy propagation and high carbohydrate content. Demand for potatoes as fresh or processed chips is globally growing, especially in developing countries. However, potato cultivation area is limited, meaning that tuber yields will have to be significantly increased to meet demands of a continuously growing world population. Critical to this goal is to decipher the molecular mechanism underlying tuber development. Photoperiod and temperature are the two most important environmental factors controlling tuber formation in potato (Rodriguez-Falcon et al., 2006; Van Dam et al., 1996). In this work, we have investigated critical aspects regarding induction of tuber formation in response to day-length and temperature. In particular, we focused on the contribution of *StGI*, *StSP5G* and *StSP6A* to the day-length and temperature control of tuberization. Furthermore, we have characterized downstream gene expression of these 3 core tuberization regulators and analysed their roles in other important physiological processes such as carbohydrate metabolism, the circadian rhythm, plant senescence or tuber sprouting.

1. StGIGANTEA represses tuberization by promoting StCDF1 protein degradation

We identified two *GIGANTEA* homologs, *StGI* and *StGI-like1*, whose pattern of expression is analogous to that of *GI* in *Arabidopsis* (Figure 11A) (Fowler et al., 1999). *StGI* inhibition promotes tuber formation in non-inductive LDs by reducing *StCOL1*, *StCOL2* and *StSP5G* expression levels, which allows *StSP6A* activation in leaves (Figure 10C; Figure 13). Thus, as seen in *Arabidopsis* and rice (Hayama et al., 2003; Sawa et al., 2007), *GIGANTEA* is a positive regulator of the *StCOL1* and *StCOL2* CONSTANS genes in potato. *StGI* is expressed in leaves to higher levels than *StGI-like1,* our finding that *StGI-like1* expression is not reduced *StGI*-RNAi lines (Figure 11A; Figure 11B) pointing to a major role of StGI in *StCOL1* and *StCOL2* regulation. Yet, as both gene copies share a high percentage similarity and analogous oscillation patterns (Figure 11A; Figure S1), a partially redundant role of both genes in tuberization or in the control of other physiological processes cannot be ruled out.

Surprisingly, *35S*::StGI-HA lines were not affected in *StCOL1*, *StCOL2*, *StSP5G* and *StSP6A* expression and did not show any tuberization phenotype (Figure 17B; Figure 18). This would indicate that *StGI* is necessary, but not sufficient, for StCDF1 degradation and StCOL1/2 up-regulation. Indeed, GIGANTEA was recently proposed to act as a co-chaperone, and regulate many physiological processes in *Arabidopsis* by controlling the maturation of a big set of plant proteins (Cha et al., 2017). All evidences obtained so far suggest that *StGI* requires of other limiting co-factors, probably StFKF1, for StCDF1 destabilization and promotion of *StCOL1* and *StCOL2* transcription in potato. However, our

findings are in apparent contradiction with other studies in *Arabidopsis* and rice, showing an opposite effect in flowering time of *GI*ox plants and *gi* mutants (Fowler et al., 1999; Hayama et al., 2003; Izawa et al., 2011; Park et al., 1999). Therefore, further studies will be needed to confirm that fusion to the HA tag in the *35S::*StGI-HA construct does not impair function of the StGI protein.

In *Arabidopsis*, GI controls *CO* expression by interacting with FKF1 and promoting degradation of the CDF repressors during LD afternoon (Imaizumi et al., 2005; Sawa et al., 2007). Accordingly, *Arabidopsis gi-100* mutants accumulate higher levels of the CDF2 protein, mutations in *FKF1* being shown to stabilize CDF1 in the afternoon, both in LDs and SDs (Fornara et al., 2009; Imaizumi et al., 2005). Here, we demonstrate that *StGI* likewise contributes to StCDF1 degradation in potato. In particular, we showed that inhibition of *StGI* stabilizes the StCDF1 protein both in LDs and SDs (Figure 15; Figure 16A). Consistent with an effect on StCDF1 stability, we observed that silencing of *StGI* mimics the plant morphology and tuberization effects of plants overexpressing a truncated *StCDF1* allele, unable to interact with StFKF1 (Figure 12A; Figure 12B) (Kloosterman et al., 2013). Indeed, the pattern of *StCOL1*, *StCOL2*, *StSP5G* and *StSP6A* expression is equivalent in *StGI*i and *35S*::*StCDF1.2* lines, which strongly supports a function of StGI in *StCOL1* and *StCOL2* expression by promoting the degradation of StCDF1 (Figure 13). In addition, we observed that *StCDF1* expression is reduced in *StGI*i plants, which points to a further role of StGI in the transcriptional control of *StCDF1* (Figure 14; Figure 16B).

The GI-FKF1 complex promotes *Arabidopsis* CDFs degradation during LD afternoon, which makes *CO* expression levels increase before dusk. Then, coincidence of *CO* expression with light allows CO protein stabilization, and leads to *FT* activation and flowering in LDs (Sawa et al., 2007). However, unlike the *Arabidopsis* gene, potato *StCOL1* peaks during early morning, and its expression profile overlaps with *StCDF1* expression and protein levels (Figure 13; Figure 14; Figure 15). Thus, based on the model proposed in *Arabidopsis*, only the *StCOL2* late afternoon peak would be regulated by *StGI* (Figure 13; Figure 14). Despite this, we observed that expression of both *StCOL1* and *StCOL2* is reduced in *StGI*i and *35S::StCDF1.2* plants, regardless these genes be expressed at different times in the day (Figure 13). In consonance with these findings, *Arabidopsis gi-100* mutants and *35S::CDF1* lines also display reduced *CO* expression levels all day long (Fornara et al., 2009; Imaizumi et al., 2005), suggesting that in the absence of GI, CDF1 exerts a continued repression on *CO* expression (Figure 13). Given that GIGANTEA controls stability of different CDFs (Fornara et al., 2009; Sawa et al., 2007), one possibility is that *StGI* stabilizes additional StCDFs with a redundant function in repressing *StCOL1* and *StCOL2* transcription. However, even under this scenario, our time course studies showed that, in the WT, morning

accumulation of StCDF1 does not impair *StCOL1* transcription and *StSP5G* activation in LDs (Figure 13; Figure 15). Hence, further studies will be required to understand why stabilization of StCDF1 late in the day leads to a reduction in *StCOL1* expression levels, when expression of this gene peaks in the morning.

2. StGIGANTEA delays plant maturity by repressing several MADS-box family genes.

We also show that potato *StGI* controls plant maturity onset, since *StGI*i lines show accelerated signs of senescence and a shortened life cycle (Figure 10B; Figure 10E). As for tuber formation, an analogous early senescing phenotype was observed in *35S::StCDF1.2* plants (Kloosterman et al., 2013), indicating that this response depends on StCDF1 protein stability. Consistent with their accelerated senescence, increased transcript levels for two senescence-related genes and reduced expression a big set of chlorophyll binding proteins was observed in *StGI*i leaves (Figure 20). *StGI* inhibition also leads to activation of multiple *HSFs* and *HSPs*, which probably exert a protective role to maintain plant viability after senescence onset (Breeze et al., 2008; Buchanan-Wollaston et al., 2005). In *Arabidopsis*, both ethylene-signalling and Staygreen proteins (SGRs) were described as positive regulators of plant senescence (Kusaba et al., 2013; Oh et al., 1997), but we observed that these genes are down-regulated in *StGIi* plants (Figure 20). Ethylene-induced senescence is normally triggered once leaves have reached a defined age (Jing et al., 2005), and therefore it is possible that in *StGIi* leaves early maturation effects obey to a different signalling mechanism. Then, it is likely that *SGRs* and ethylene-related genes are down-regulated as part of a negative feed-back loop mechanism (Wang et al., 2002), to compensate for accelerated senescence.

Notably, effects on plant maturity of potato *StGI* inhibition are completely opposite to those observed in *Arabidopsis gi-3* mutants. Mutations in *Arabidopsis GI* were indeed shown to extend plant longevity and increase chlorophyll accumulation in response to oxidative stress (Kurepa et al., 1998). Given that GI controls as well tuberization and flowering time in opposite ways in potato and *Arabidopsis*, all evidences suggest that onset of plant maturity is somehow associated with tuberization and floral transitions and that GI regulates a common component of both developmental processes. Consistent with this theory, a positive correlation between rosette senescence and flowering is observed in different *Arabidopsis* accessions, confirming a link between floral transition and plant longevity (Levey and Wingler, 2005). Interestingly, our data shows that *StGI* inhibition results in the activation of several MADS-box family genes in potato leaves including various homologs of *Arabidopsis FUL* and *AP1* (Figure 20). These genes were shown to be direct downstream targets of the

floral activator FT-FD complex and function in the apical meristem to promote flowering transition (Andres and Coupland, 2012), our findings suggesting that *StGI* represses their expression through the activation of *StCOL1* and *StSP5G* (Abelenda et al., 2016). Noteworthy, in addition to flowering time control, *FUL* and *SOC1* were reported to affect determinacy of all meristems, these MADS-box factors mediating an annual growth habit by preventing longevity and secondary growth of shoots (Melzer et al., 2008). Therefore, *StGI* inhibition is likely to promote both tuberization and plant senescence through the inhibition of *StCOL1* and subsequent activation of these MADS-box genes.

Sugar signalling plays a pivotal role in ageing and senescence regulation (Wingler et al., 2009). Indeed, senescing leaves accumulate hexoses and senescence onset is accelerated by a high glucose and low nitrogen supply, that activate autophagy and negatively regulate SnRK1 pathway (Baena-Gonzalez et al., 2007; Pourtau et al., 2006; Pourtau et al., 2004). *GIGANTEA* is long reported to modulate sugar signalling in *Arabidopsis* since *gi* mutants exhibit higher starch contents in leaves (Eimert et al., 1995). Consistent with this, several genes involved in sucrose and starch metabolism were observed to be differentially expressed in *StGI*i leaves (Figure 20). Among them, we identified both starch synthesis and degradation enzymes, a cell wall invertase and HEXOKINASE 1, whose mutation in *Arabidopsis* delays senescence (Moore et al., 2003). Noteworthy, mutations in *Arabidopsis* hexokinase 1 also result in a late flowering phenotype (Pourtau et al., 2006), hence suggesting a link between sugar signalling, flowering and plant senescence. Overall, these results suggest that *StGI* positively regulates hexose accumulation in potato leaves, and this probably causes the premature senescence onset. However, further experiments will be required to assess whether *GIGANTEA* regulates transitory starch content in opposite ways in potato and *Arabidopsis*, as seen for senescence and tuberization/flowering time regulation.

3. StSP5G suppresses *StSP6A* expression in leaves and has a role in tubers by controlling tuber morphology

We showed that *StSP5G* is encoded in potato by two gene copies, *StSP5G-A* and *StSP5G-B*, which are arranged in tandem on chromosome 5 (Figure 22) and show different expression patterns. Comparison of the tomato and potato loci suggests that *StSP5G-B* originated from a genomic duplication in potato, likely mediated by excision of a transposable element (Figure 22). Although *StSP5G-A* and *StSP5G-B* share almost identical coding regions, these genes differ in their upstream regulatory regions (Figure S2B). This indicates that after gene duplication, reorganization of one of the gene copies led to the different patterns of expression observed for these genes. In particular, we observed that *StSP5G-A*

is expressed in leaves, tubers and tuber sprouts, whereas *StSP5G-B* is abundantly expressed in tubers (Figure 23). Therefore, a logical assumption is that StSP5G-A and StSP5G-B play redundant roles in the tuber, although we cannot exclude that they also fulfil different functions, by being expressed in different cell types.

StSP5G has been proposed to repress tuber formation in LDs by inhibiting *StSP6A* expression in the leaves (Abelenda et al., 2016). Notably, the *StSP5G* and *StSP6A* genes show an antagonistic pattern of expression in the leaves, but we showed that both genes are up-regulated in the stolon during stolon-to-tuber transition (Figure 25). By grafting studies we have demonstrated that *StSP5G* represses tuberization in the leaves, but over-expression of this protein in underground tissues lack any inhibitory effect (Figure 26A; Figure 26C). Additionally, we observed that *StSP5G*-silencing results in an altered tuber morphology (Figure 27B), indicating that *StSP5G* probably has an additional role in the stolon controlling tuber development. We showed that *StSP6A* is strongly up-regulated in *StSP5G*i tubers (Figure 29), which suggests that a function of *StSP5G* in tuber development is to modulate, among others, *StSP6A* expression. Thus, it is presumable that activation of *StSP5G* in the stolon is part of a negative feed-back loop to prevent excessive *StSP6A* levels in the tuber and allow proper tuber development and sprouting. Moreover, since StCOL1 and StCOL2 are destabilized in darkness (Abelenda et al., 2016), all evidences suggest that these factors do not play a role in *StSP5G* activation during tuberization transition.

4. StSP5G activates CK biosynthesis and modulates expression of genes of the MADS-box and NF-Y families

Our gene expression studies showed that silencing of *StSP5G* leads to activation of several isopentenyltransferase (IPT*)* cytokinin biosynthetic genes in either leaves, tubers and tuber sprouts (Figure 28A; Figure 28B; Figure 33). Notably, expression of *LONELY GUY* (*LOG1*), encoding a CK-activating riboside hydrolase, has been recently shown to induce differentiation of tuber-like organs out of juvenile tomato axillary buds, hence pointing to a general function of CKs as universal regulators of storage-organ fate in plants (Eviatar-Ribak et al., 2013). As such, our findings suggest that *StSP5G* negatively regulates tuber-fate by controlling CK biosynthesis in leaves, tubers and tuber sprouts. Furthermore, *StSP5G* inhibition results in the down-regulation of the strigolactone biosynthetic *StCCD8* gene and multiple auxin-related genes in the tuber, probably due to enhanced CK signalling in these organs (Figure 28B). Overall, these findings suggest that *StSP5G* suppresses tuberization by negatively regulating *StSP6A* expression and by inhibiting CK biosynthesis, but expression of the *StSP5G* gene is required after stolon-to-tuber transition to maintain adequate hormonal balance of growing tubers and to proper tuber development.

In addition to these hormonal changes, *StSP5G* also modulates expression of various *NF-Y*s genes. In particular, we observed that genes belonging to all NF-YA, NF-YB and NF-YC subfamilies are down-regulated in leaves or tubers of *StSP5G*i lines (Figure 28A; Figure 28B). Since NF-Ys were described to interact with CO to mediate activation of *FT* in *Arabidopsis* (Cao et al., 2014; Kumimoto et al., 2010; Wenkel et al., 2006), one possible explanation for this regulation is that *StSP5G* contributes to the activation of *NF-Y*s genes as part of a positive feedback loop that enhances its own activation by StCOL1 in the leaves. However, it is well known that *NF-Y*s control a big set of physiological processes in plants (Petroni et al., 2012). As such, activation of these genes might also be part of the *StSP5G* downstream pathway, involved in *StSP6A* repression.

As observed for *StGI*, silencing of *StSP5G* leads to changes in levels of expression of several MADS-box family genes. Remarkably, members reported to promote floral transition and floral organ differentiation in *Arabidopsis*, as *AP1*, *FUL*, *SOC1*, *SVP* and various *SEP*s, were differentially expressed in *StSP5G*i leaves, tubers or tuber sprouts (Figure 28A; Figure 28B; Figure 33). Among these, two *FUL* homologs, *StAGL8* and *StAGL8-like1*, were up-regulated in all *StSP5G*i tissues analysed, evidencing a direct link between *StSP5G* repression and activation of these genes (Figure 29; Figure 33). Indeed, both *FUL* homologs are co-regulated with *StSP6A* in potato leaves (Morris et al., 2014), and are also up-regulated in *StGI*i lines (Figure 20), hence suggesting that these factors either control *StSP6A* expression or are immediate downstream targets of StSP6A. In support of a role downstream of StSP6A, Spunta plants overexpressing the *StSP6A* gene showed an activated expression of both *StAGL8* and *StAGL8-like1* in the leaves (Supplemental file 1).

5. Silencing *of StSP5G* has different effects on gene expression in tubers and leaves.

Interestingly, whereas *StAGL8* and *StAGL8-like*1 are induced to relatively high levels in leaves of *StSP5G*i lines, *StSP6A* expression is not (Figure 29), which points to a possible role of the potato AGL8/FUL factors upstream of *StSP6A*. Furthermore, unlike *StAGL8* and *StAGL8-like1*, homologs of *AP1*, *SOC1*, *SVP* and *SEP*s are differentially expressed either in *StSP5G*i leaves, tubers or tuber sprouts, which indicates that these genes are indirectly regulated by *StSP5G* in a tissue-dependent manner (Figure 28A; Figure 28B; Figure 33). Altogether, these findings suggest that the signalling mechanisms triggering potato tuberization are to a large extent analogous to the current model for *Arabidopsis* floral transition, where FT forms a floral activator complex (FAC) with FD and 14-3-3 proteins that activates the MADS-box genes *FUL, AP1* and *SOC1*, up-regulation of these genes triggering the activation of additional MADS-box genes and *LFY* to orchestrate floral development

(Andres and Coupland, 2012; Lee and Lee, 2010; Wellmer et al., 2014). According to this, we propose a model for tuber transition in which *StSP6A* activates *StAGL8* and *StAGL8-like1* in both leaves and tubers and subsequent tissue-specific activation of additional MADS-box genes promotes plant maturity in the leaf and tuber development in the stolon (Figure 49).

Noteworthy, *StAGL8* is activated to comparable levels in aerial and underground sections of *StSP5G*i stems, whereas high expression levels of *StSP6A* are only observed in underground stems. This would imply that *StSP6A* expression is repressed in leaves independently of *StSP5G*, or that *StAGL8* activation in these organs does not require of high levels of StSP6A. Given that in *StCOL1*i lines *StSP6A* is strongly activated in leaves (Abelenda et al., 2016), StCOL1 is the most likely candidate to exert this negative control on *StSP6A* transcription in the leaf. Consistent with this, *StGI*i and *35S::StCDF1.2* transgenic lines, which show a constitutive repression of *StCOL1* and *StCOL2* expression, they also display up-regulated levels of expression of *StSP6A* in the leaves under LDs (Figure 13).

Moreover, we showed that both StCOL1 and StCOL2 proteins are destabilized in darkness (Abelenda et al., 2016), and this is possibly the reason why *StSP6A* is strongly up-regulated in underground tissues of *StSP5G*i lines, but not in leaves or aerial stems (Figure 26D). On the other hand, an activation of *StAGL8* independent of the *StSP6A* gene is also observed in the tuber sprouts of *StSP5G*i lines, hence indicating that co-regulation of these genes is largely tissue dependent. Hence, further studies will be needed to elucidate whether StAGL8 regulates *StSP6A* expression downstream of StCOL1 and StSP5G or, on the contrary, StCOL1 plays a role in direct repression of *StSP6A* transcription independently of StSP5G.

6. StSP5G is required to maintain a vegetative fate of tuber axillary meristems.

Remarkably, inhibition of *StSP5G* leads to formation of secondary tubers instead of regular sprouts after tuber dormancy break (Figure 31). These secondary tubers show activated expression of the CK biosynthetic *IPT* genes and misregulated expression of several MADS-box family genes, including *StAGL8* and *StAGL8-like1* (Figure 33). Moreover, these organs show reduced expression of several auxin *PIN* carriers, indicative of decreased apical dominance, whereas starch biosynthethic and patatin-like storage glycoproteins were found to be strongly induced. Thus, all evidences suggest that *StSP5G* maintains tuber axillary meristems in a vegetative stage, likely by suppressing expression of the same genes induced in the stolon during stolon-to-tuber transition (Kloosterman et al., 2005; Visser et al., 1994).

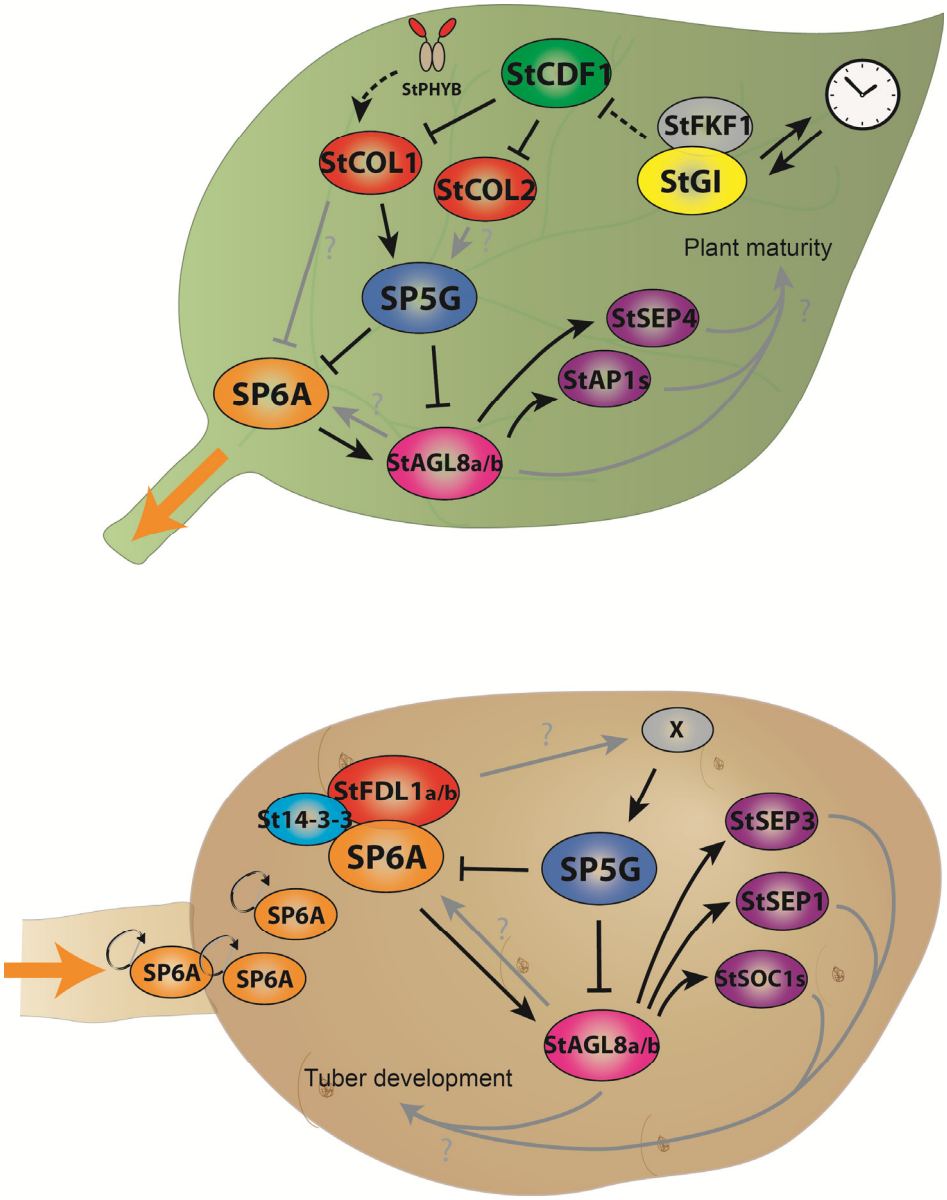

Figure 49. Proposed model for control of tuberization by StGI and StSP5G. In the leaf, StGI works in a feedback loop with components of the circadian clock and together with StFKF1 promotes StCDF1 degradation. StCDF1 represses *StCOL1* and *StCOL2* expression and prevents activation of StSP5G, which acts as a repressor of *StALG8* and *StAGL8-like1* (StAGL8a/b) and *StSP6A*. These MADS-box factors may form a positive regulatory loop with StSP6A, and mutually regulate their expression. Activation of *StAGL8a/b* in the leaf activates other *StAG-like* genes, as *StSEP4* and several *StAP1s* which, together with *StAGL8a/b*, are likely to be involved in the control of plant maturity. StSP6A is transported from the leaf to the stolon where it interacts with StFDL1a/b and 14-3-3 proteins to promote *StAGL8a/b* activation. *StSP5G* is activated in this tissue by mechanism independent of StCOL1 and down-regulates *StAGL8a/b* and *StSP6A* transcription. Expression of *StAGL8a/b* in the stolon triggers activation of additional *StAG-like* genes, as *StSEP1*, *StSEP3* and several *StSOC1*s which, together with *StAGL8a/b*, are involved in the control of tuber development. Arrows and blunted lines indicate activation and repression, respectively. Solid and dotted lines represent transcriptional and post-transcriptional regulation.

7. StSP6A integrates inhibitory effects of warm temperatures in tuber formation.

Strict short day-requirement of *Andigena* species for tuberization is reduced when plants are grown at lower temperatures (Van Dam et al., 1996), which had led to propose that day-length and temperature responses converge at certain point (Rodriguez-Falcon et al., 2006). Here, we showed that warm temperatures suppress tuberization by inhibiting *StSP6A* transcription in the leaves (Figure 34A), and demonstrated that overexpression of *StSP6A* palliates the negative effects of warm temperatures on tuber yield and quality (Figure 34C). In addition, we observed that temperature represses *StSP6A* without affecting transcription of its upstream regulators *StSP5G, StCOL1* and *StCOL2* (Figure 34A). These results indicate that potato *StSP6A* functions as an integrator of both the temperature and day-length pathways, and that warm temperatures directly control transcription of the *StSP6A* gene through repression of an uncharacterized upstream activator. However, it is noteworthy that *StSP5G* is shown by other authors to be slightly up-regulated in leaves of Desiree plants grown at 30ºC/20ºC (day/night) (Hancock et al., 2014). In this work, we analysed the heat response of leaves after 30 days of growth at 28ºC and, at this stage, *StSP5G* expression is already reduced due to the age pathway (Figure 34A). Therefore, it cannot be ruled out that in younger plants part of the response to warm temperatures involves as well an up-regulation of *StSP5G*. Nevertheless, even under this scenario, our findings demonstrate that a main effect of warm temperatures is the direct repression of *StSP6A* transcription.

8. StSP6A reverses thermomorphogenesis and effects of warm temperatures on carbohydrate metabolism.

Besides suppressing potato tuberization, temperature affects a big set of physiological processes including photosynthesis, plant growth and carbohydrate metabolism, among others (Havaux et al., 1996; Lafta and Lorenzen, 1995; Wolf et al., 1991). In this work, we have shown that some of the effects of warm temperatures on these important processes are attenuated by *StSP6A* overexpression. In particular, we observed that at warm temperatures *StSP6A*ox lines are shorter and show bigger leaves than WT plants, hence evidencing that *StSP6A* counterbalances the thermomorphogenic response. In *Arabidopsis*, the transcription factor PIF4 promotes hypocotyl elongation and additional thermomorphogenic responses by regulating auxin biosynthesis (Quint et al., 2016). Indeed, various *AUX*/*IAAs* and *SAUR* genes are induced under warm temperatures in a PIF4-dependent manner (Franklin et al., 2011; Koini et al., 2009). Moreover, it is well-known that auxins promote the activation of cell

wall loosening enzymes to induce cell elongation or expansion by increasing cell wall extensibility (Kotake et al., 2000; Swarup et al., 2008). Consistent with this, we observed that *StSP6A* overexpression prevents 28ºC activation of several auxin-related genes, including *AUX/IAAs* and *SAUR*, and cell wall modification enzymes belonging to the expansin and XTH families (Figure 41; Figure 42). In *Arabidopsis*, *PIF4* transcription is repressed early at night by the clock EVENING COMPLEX (EC), which is composed of the proteins ELF3, ELF4 and LUX (Nusinow et al., 2011). The EC complex recognises through the LUX factor conserved LBS elements in the *PIF4*, *PRR9, LUX* and *GI* promoters (Helfer et al., 2011; Mizuno et al., 2014) and as such, *LUX* negatively regulates its own transcription. Interestingly, we found *StLUX* to be induced under warm temperatures and repressed in *StSP6A*ox lines (Figure 47). This indicates that warm temperatures impair potato EC complex function and de-repress *StLUX* expression, as reported in *Arabidopsis*, although this response is attenuated in *StSP6A*ox lines. However, as we could not identify any *PIF*-like gene in the UPS-SP6A cluster, further experiment will be needed to confirm up-regulated expression of PIF homologs during late night, and function of these factors in triggering the potato thermomorphogenic response. Besides, it cannot be dismissed that *StSP6A* can inhibit thermomorphogenesis independently of the EC complex. Consistent with this, the DELLA protein *StRGL2* was found to be co-regulated with StSP6A (Figure 39). DELLAs have been shown in *Arabidopsis* to interact with PIFs and block their transcriptional activity (de Lucas et al., 2008), and therefore it is feasible that *StSP6A* regulates PIFs at post-transcriptional level by promoting expression of *StRGL2*.

Transitory starch functions as an over-flow product synthetized when CO_2 fixation exceeds sucrose synthesis, in addition to provide a continuous supply of carbon at night, when CO_2 cannot be fixed by photosynthesis (Weise et al., 2011). In potato, warm temperatures reduce total dry weight and starch content of tubers, and have been reported to impair translocation of photoassimilates from leaves to the tubers (Lafta and Lorenzen, 1995; Wolf et al., 1991). Here, we have demonstrated that *StSP6A* and warm temperatures regulate in opposite ways several genes involved in photosynthesis and carbohydrate metabolism in the leaves. In particular, we observed that *StSP6A* overexpression leads to increased expression of antenna components of the photosystem II and enzymes of the Calvin cycle such as *StSBPase,* that are down-regulated in response to warm temperatures (Figure 44). Actually, warm temperatures inhibit photosynthesis mainly by decreasing PSII activity and *SBPase* overexpression was reported in tobacco to lead to enhanced photosynthetic efficiency and starch content in the leaves (Havaux et al., 1996; Lefebvre et al., 2005), our data therefore indicating that overexpression of *StSP6A* increases the rate of photosynthesis and carbon fixation at 28ºC. Furthermore, in *StSP6A*ox lines, three invertase

enzymes involved in hydrolytic cleavage of sucrose were down-regulated at 28ºC, while a sucrose phosphatase, a sucrose phosphate synthase, and several genes involved in chloroplast and mitochondrial photorespiration were induced (Figure 42; Figure 44A; Figure 44B). Likewise, expression of various β-amylases and the maltose transporter *StMEX1* is up-regulated, demonstrating that *StSP6A* overexpression promotes starch break-down and sucrose synthesis in favour of sugar export to sink organs. Surprisingly, *StSP6A* overexpression also increases starch content of leaves (Figure 43), indicating that besides export more sugars, *StSP6A* leaves have also a higher photosynthetic efficiency. We showed that warm temperatures affect diurnal oscillation of *StMEX1* in leaves by reducing its amplitude and shifting its peak expression towards the night (Figure 44B), hence evidencing that warm temperatures have a notable effect on the circadian regulation of starch synthesis and breakdown enzymes. Therefore, further studies will be required to assess whether StSP6A is able to compensate effects of warm temperatures on starch metabolism, especially during the night where sucrose export is critical to support growth and night-time metabolism (Streb and Zeeman, 2012; Weise et al., 2011).

Based on these findings, we propose a model by which *StSP6A* confers an increased tolerance to temperature in potato by positively regulating photosynthesis in the leaf and promoting sucrose export to sink organs, due to increase sucrose synthesis and starch-breakdown (Figure 50). In consonance with this mechanism of action, the heat tolerant cultivar *Kufri Surya* was recently reported to exhibit increased photosynthesis, up-regulated expression of multiple photosynthesis-associated genes and higher expression levels of *StSP6A* at 24ºC, than the heat sensitive *Chandramukhi* cultivar (Singh et al., 2015). However, effects of temperature on photosynthetic efficiency seem to be largely dependent on light intensity and growth conditions, given that a number of reports describe that moderate temperatures up to 30ºC do not reduce photosynthetic rates of potato leaves (Hancock et al., 2014; Lafta and Lorenzen, 1995; Singh et al., 2015). Not only that, but Hancock et al. recently reported that multiple photosynthesis-related genes, such as PSII polypeptides and Calvin cycle enzymes, were up-regulated in the leaves of Desiree plants grown under 30ºC/20ºC (day/night) conditions. A possible explanation to these contradictory results is that we used constant temperatures of 28ºC, instead of cooler temperatures at night. However, it is also possible that differences in photosynthetic rates depend on plant age and on the timing of temperature treatments, as both factors also have an influence on tuber yield reduction. Indeed, it has long been established that photosynthesis and sink utilization of carbohydrates are highly coordinated (Osorio et al., 2014; Paul and Foyer, 2001). In potato, removal of tubers leads to reduced net photosynthesis as a result of the imbalance between source and sink-activity (Sberger and Humphries, 1965). Furthermore,

assimilate translocation to tubers is likely to be regulated by sucrose metabolism in these organs (Wolf et al., 1991) and in line with this regulatory mechanism, we observed that *StSP6Aox* tubers had a higher starch content and reduced levels of reducing sugars than WT tubers (Figure 45A). In light of these findings, it cannot be dismissed that *StSP6A* effects on photosynthetic and starch metabolism in leaves can be a direct consequence of the increased sink demand of *StSP6Aox* tubers. Under this scenario, our data indicate that *StSP6A* controls sink strength independently of *StSUS4* and *StSUS3* activity, as *StSP6A*ox tubers do not show a significant increase on expression levels of these genes (Figure 46B).

9. StSP6A reduces the JA signalling in potato leaves

Finally, we showed that *StSP6A* overexpression leads to inhibition of a big a set of genes associated with Jasmonic acid signalling, which in WT plants are up-regulated at 28ºC. Among them, we identified two allene oxide synthase (AOS) enzymes and several JAZ and MYC transcription factors (Figure 48). In *Arabidopsis*, the bHLH MYC transcription factors have been shown to regulate JA-responsive gene expression, and their transcriptional activity be repressed by direct interaction with the JAZ proteins (Chini et al., 2007; Fernandez-Calvo et al., 2011; Pauwels et al., 2010). In the presence of bioactive JA, JAZs are degraded by the SCF^{COI1} E3 ubiquitin ligase complex, allowing accumulation of the MYC factors in their free active form and activation of JA signalling.

JA regulates plant responses to biotic and abiotic stresses, in addition to control plant growth and development (Wasternack and Hause, 2013). Activation of JA signalling increases thermotolerance of *Arabidopsis* seedlings*,* heat also being reported to up-regulate *AOS* and *MYC* gene expression in tomato roots (Clarke et al., 2009; Yang et al., 2016). Actually, *AOS* concurrently with the JAZs and *MYC* factors are central to JA signalling, in addition to be primary activation targets of the JA pathway (Chung et al., 2008). Therefore, our data strongly suggest that warm temperatures activate JA signalling and *StSP6A* negatively regulates this response. In support of this observation, we also identified a large set of genes coding for proteinase inhibitor proteins in the UPS-SP6A cluster (Supplemental file 1), which in potato were shown to be up-regulated in response to wounding and MeJA (Hildmann et al., 1992). Furthermore, various *AOS*, *JAZ* and *MYC* genes, together with a large set of proteinase inhibitors, were also found to be downregulated in the leaves of *StSP5G*i plants (Figure 28A; Supplemental file 1), hence indicating that both *StSP6A* overexpression and *StSP5G* inhibition repress JA signalling in potato.

Noteworthy, JAZs were shown to regulate *FT* transcription by interacting with the *Arabidopsis* AP2 factors TARGET OF EAT1 (TOE1) and TOE2 (Zhai et al., 2015). Hence, all evidences so far suggest that *FT* might be negatively regulating JA signalling as part of a

negative feedback loop that promotes its own activation. However, decreased JA signalling is somehow controversial with the reduced internode elongation of *StSP6A*ox lines at 28ºC. JA has been shown to repress plant growth by promoting JAZs degradation, which releases RGA from JAZs-inhibition and allows the RGA repressor to associate and block transcriptional activity of the PIF3 and PIF4 factors (Yang et al., 2012). Hence, additional studies will be required to confirm that JA signalling is suppressed by StSP6A, and to elucidate how JA inhibition is compatible with a repression of the thermomorphogenic response in *StSP6A*ox plants.

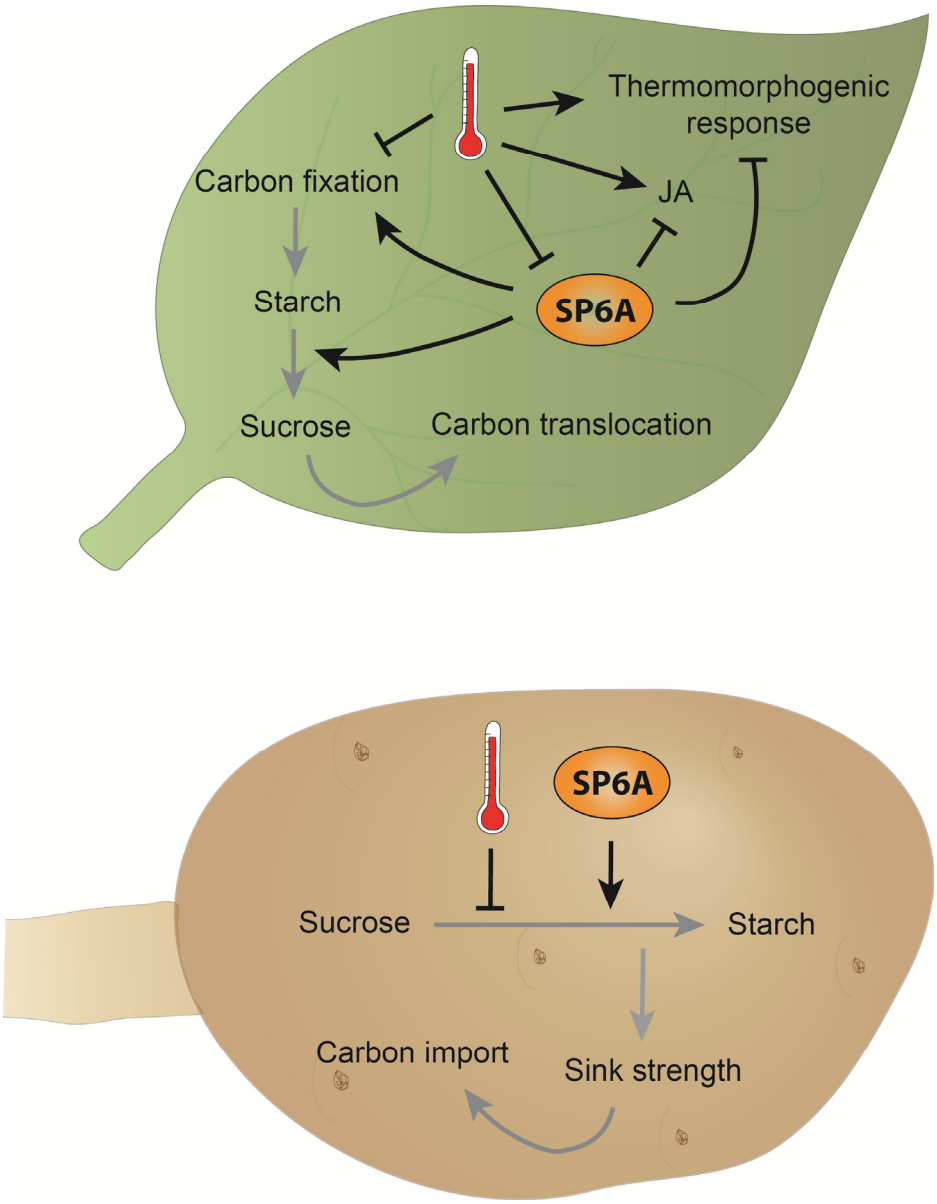

Figure 50. Proposed model for StSP6A-mediated thermotolerance. Warm temperatures induce thermomorphogenesis and inhibit tuber formation by repressing *StSP6A* transcription in the leaves. Increased temperatures also reduce carbon fixation and starch synthesis in the leaf, less carbon being translocated to tubers. *StSP6A* prevents activation of auxin signalling and cell wall modification enzymes that mediate the thermomorphogenic response and positively regulates photosynthesis associated genes. In addition, *StSP6A* contributes to activate expression of genes involved in starch-breakdown and sugar transport, enhancing carbon translocation to sink organs. Whereas warm temperatures reduce tuber starch content, *StSP6A* promotes starch synthesis and increases sink-strength, favouring carbon import to the tubers. Furthermore, StSP6A negatively regulates multiple genes involved in JA biosynthesis and signalling that are up-regulated by warm temperatures in the leaf. Arrows and blunted lines indicate activation and repression, respectively. Grey lines represent a linkage or association between physiological processes or molecules.

Conclusions

1. GIGANTEA inhibits tuber formation and delays plant maturity by mediating degradation of the StCDF1 factor, which leads to up-regulation of *StCOL1*, *StCOL2* and *StSP5G* in LDs.

2. Silencing of the *StGI* gene in the *Andigena* genotype leads to activation of *StSP6A* and up-regulated expression of *AP1* and *FUL* MADS-box genes.

3. *StGI* silencing is correlated with inhibition of multiple *CAB* genes and with an activation of heat-shock proteins, senescence-related and starch metabolism genes in leaves, indicative of a premature maturation of these organs.

4. StSP5G is expressed in tubers where it controls tuber development and preserves shoot identity of tuber sprouts.

5. *StSP5G* regulates multiple NF-Y and MADS-box genes, including *FUL*, *SVP* and *SOC1* factors, and suppresses CK biosynthesis by modulating multiple *isopentenyltransferase* (*IPT*) genes in leaves, tubers and tuber sprouts.

6. The *FUL* homologs *StAGL8* and *StAGL8-like1* are activated by *StSP6A* and repressed by *StSP5G*, hence suggesting an important function of these factors in tuberization induction.

7. Warm temperatures reduce tuber formation by repressing *StSP6A* expression in the leaves, although they do not affect *StCOL1* or *StSP5G* expression.

8. *StSP6A* inhibits the potato thermomorphogenic response by suppressing expression of auxin-related and cell wall modification genes.

9. *StSP6A* activates in leaves the expression of multiple genes associated with photosynthesis and starch breakdown that are negatively regulated by warm temperatures, and increases source capacity of leaves.

10. Warm temperatures activate multiple genes of the Jasmonate pathway whose expression is reduced in *StSP6A*ox lines.

1. GIGANTEA inhibe la formación de tubérculos y retrasa la madurez de la planta mediando en la degradación del factor StCDF1 y promoviendo la activación de *StCOL1*, *StCOL2* y *StSP5G* en días largos.

2. El silenciamiento del gen *StGI* en el genotipo *Andigena* promueve la activación de *StSP6A* y de factores MADS-box AP1 y FUL.

3. El silenciamiento del gen *StGI* se correlaciona con la inhibición de múltiples genes *CAB* y con la activación de proteínas “heat-shock” y de genes relacionados con senescencia y metabolismo del almidón en la hojas, lo cual es indicativo de una maduración prematura de estos órganos.

4. StSP5G se expresa en el tubérculo donde controla desarrollo del tubérculo y preserva la identidad de tallo de los brotes del tubérculo.

5. StSP5G regula múltiples genes NF-Y y MADS-box, entre los que se encuentran factores *FUL*, SVP y SOC1, y suprime la síntesis de CKs modulando la expresión de múltiples isopentenil transferasas (IPT) en las hojas, tubérculos y brotes del tubérculo.

6. Los homólogos de *FUL StAGL8* y *StAGL8-like1* son activados por *StSP6A* y reprimidos por *StSP5G*, lo cual sugiere que estos dos factores ejercen funciones importantes para la tuberización.

7. Las temperaturas cálidas reducen la formación de tubérculos mediante la represión de *StSP6A* en las hojas sin afectar la expresión de *StCOL1* o *StSP5G*.

8. StSP6A inhibe la respuesta termomorfogénica de patata mediante la inhibición de genes relacionados con auxinas y modificación de la pared celular.

9. StSP6A promueve la activación en las hojas de múltiples genes asociados a fotosíntesis y degradación de almidón, los cuales son reprimidos a altas temperaturas, incrementando así la capacidad de las hojas como fuente de carbono.

10. Las temperaturas cálidas activan múltiples genes de la vía del Jasmonato cuya expresión se ve reducida en las líneas *StSP6A*ox.

Bibliography

Abe, M., Kobayashi, Y., Yamamoto, S., Daimon, Y., Yamaguchi, A., Ikeda, Y., Ichinoki, H., Notaguchi, M., Goto, K., and Araki, T. (2005). FD, a bZIP protein mediating signals from the floral pathway integrator FT at the shoot apex. Science *309*, 1052-1056.

Abelenda, J.A., Cruz-Oro, E., Franco-Zorrilla, J.M., and Prat, S. (2016). Potato StCONSTANS-like1 Suppresses Storage Organ Formation by Directly Activating the FT-like StSP5G Repressor. Curr Biol *26*, 872-881.

Abelenda, J.A., Navarro, C., and Prat, S. (2011). From the model to the crop: genes controlling tuber formation in potato. Curr Opin Biotechnol *22*, 287-292.

Abelenda, J.A., Navarro, C., and Prat, S. (2014). Flowering and tuberization: a tale of two nightshades. Trends Plant Sci *19*, 115-122.

Abelenda, J.A., and Prat, S. (2013). Cytokinins: determinants of sink storage ability. Curr Biol *23*, R561-563.

Ahn, J.H., Miller, D., Winter, V.J., Banfield, M.J., Lee, J.H., Yoo, S.Y., Henz, S.R., Brady, R.L., and Weigel, D. (2006). A divergent external loop confers antagonistic activity on floral regulators FT and TFL1. Embo J *25*, 605-614.

Alter, P., Bircheneder, S., Zhou, L.Z., Schluter, U., Gahrtz, M., Sonnewald, U., and Dresselhaus, T. (2016). Flowering Time-Regulated Genes in Maize Include the Transcription Factor ZmMADS1. Plant Physiol *172*, 389-404.

Altschul, S.F., Gish, W., Miller, W., Myers, E.W., and Lipman, D.J. (1990). Basic local alignment search tool. J Mol Biol *215*, 403-410.

An, H., Roussot, C., Suarez-Lopez, P., Corbesier, L., Vincent, C., Pineiro, M., Hepworth, S., Mouradov, A., Justin, S., Turnbull, C*., et al.* (2004). CONSTANS acts in the phloem to regulate a systemic signal that induces photoperiodic flowering of Arabidopsis. Development *131*, 3615-3626.

Andres, F., and Coupland, G. (2012). The genetic basis of flowering responses to seasonal cues. Nat Rev Genet *13*, 627-639.

Appeldoorn, N.J., Sergeeva, L., Vreugdenhil, D., Van Der Plas, L.H., and Visser, R.G. (2002). In situ analysis of enzymes involved in sucrose to hexose-phosphate conversion during stolon-to-tuber transition of potato. Physiol Plant *115*, 303-310.

Asiedu, S.K., Astatkie, T., and Yiridoe, E.K. (2003). The Effect of Seed-Tuber Physiological Age and Cultivar on Early Potato Production. Journal of Agronomy and Crop Science *189*, 176-184.

Baena-Gonzalez, E., Rolland, F., Thevelein, J.M., and Sheen, J. (2007). A central integrator of transcription networks in plant stress and energy signalling. Nature *448*, 938-942.

Bai, M.Y., Fan, M., Oh, E., and Wang, Z.Y. (2012). A triple helix-loop-helix/basic helix-loop-helix cascade controls cell elongation downstream of multiple hormonal and environmental signaling pathways in Arabidopsis. Plant Cell *24*, 4917-4929.

Balanza, V., Martinez-Fernandez, I., and Ferrandiz, C. (2014). Sequential action of FRUITFULL as a modulator of the activity of the floral regulators SVP and SOC1. J Exp Bot *65*, 1193-1203.

Baroja-Fernandez, E., Munoz, F.J., Montero, M., Etxeberria, E., Sesma, M.T., Ovecka, M., Bahaji, A., Ezquer, I., Li, J., Prat, S.*, et al.* (2009). Enhancing sucrose synthase activity in transgenic potato (Solanum tuberosum L.) tubers results in increased levels of starch, ADPglucose and UDPglucose and total yield. Plant Cell Physiol *50*, 1651-1662.

Bate, N.J., Rothstein, S.J., and Thompson, J.E. (1991). Expression of Nuclear and Chloroplast Photosynthesis-Specific Genes During Leaf Senescence. J Exp Bot *42*, 801-811.

Batutis, E.J., and Ewing, E.E. (1982). Far-Red Reversal of Red Light Effect during Long-Night Induction of Potato (Solanum tuberosum L.) Tuberization. Plant Physiol *69*, 672-674.

Baxter, C.E., Costa, M.M., and Coen, E.S. (2007). Diversification and co-option of RAD-like genes in the evolution of floral asymmetry. Plant J *52*, 105-113.

Ben-Naim, O., Eshed, R., Parnis, A., Teper-Bamnolker, P., Shalit, A., Coupland, G., Samach, A., and Lifschitz, E. (2006). The CCAAT binding factor can mediate interactions between CONSTANS-like proteins and DNA. Plant J *46*, 462-476.

Bhogale, S., Mahajan, A.S., Natarajan, B., Rajabhoj, M., Thulasiram, H.V., and Banerjee, A.K. (2014). MicroRNA156: a potential graft-transmissible microRNA that modulates plant architecture and tuberization in Solanum tuberosum ssp. andigena. Plant Physiol *164*, 1011-1027.

Birch, P.R.J., Bryan, G., Fenton, B., Gilroy, E.M., Hein, I., Jones, J.T., Prashar, A., Taylor, M.A., Torrance, L., and Toth, I.K. (2012). Crops that feed the world 8: Potato: are the trends of increased global production sustainable? Food Security *4*, 477-508.

Blackman, B.K., Strasburg, J.L., Raduski, A.R., Michaels, S.D., and Rieseberg, L.H. (2010). The role of recently derived FT paralogs in sunflower domestication. Curr biol *20*, 629-635.

Bohs, L. (2007). Phylogeny of the Cyphomandra Clade of the Genus Solanum (Solanaceae) Based on ITS Sequence Data. Taxon *56*, 1012-1026.

Bou-Torrent, J., Martinez-Garcia, J.F., Garcia-Martinez, J.L., and Prat, S. (2011). Gibberellin A1 metabolism contributes to the control of photoperiod-mediated tuberization in potato. PLoS One *6*, e24458.

Brambilla, V., Battaglia, R., Colombo, M., Masiero, S., Bencivenga, S., Kater, M.M., and Colombo, L. (2007). Genetic and molecular interactions between BELL1 and MADS box factors support ovule development in Arabidopsis. Plant Cell *19*, 2544-2556.

Breeze, E., Harrison, E., Page, T., Warner, N., Shen, C., Zhang, C., and Buchanan-Wollaston, V. (2008). Transcriptional regulation of plant senescence: from functional genomics to systems biology. Plant Biol (Stuttg) *10 Suppl 1*, 99-109.

Buchanan-Wollaston, V., Page, T., Harrison, E., Breeze, E., Lim, P.O., Nam, H.G., Lin, J.F., Wu, S.H., Swidzinski, J., Ishizaki, K.*, et al.* (2005). Comparative transcriptome analysis reveals significant differences in gene expression and signalling pathways between developmental and dark/starvation-induced senescence in Arabidopsis. Plant J *42*, 567-585.

Bünning E (1936). Die endogene tagersrhythmik als grundlage der photoperiodischen reaktion. Ber Dtsch Bot Ges *54*, 590-607.

Burton, W.G. (1989). The Potato (Longman Scientific & Technical).

Campbell, M., Segear, E., Beers, L., Knauber, D., and Suttle, J. (2008). Dormancy in potato tuber meristems: chemically induced cessation in dormancy matches the natural process based on transcript profiles. Functional & integrative genomics *8*, 317-328.

Cao, K., Cui, L., Zhou, X., Ye, L., Zou, Z., and Deng, S. (2015). Four Tomato FLOWERING LOCUS T-Like Proteins Act Antagonistically to Regulate Floral Initiation. Front Plant Sci *6*, 1213.

Cao, S., Kumimoto, R.W., Gnesutta, N., Calogero, A.M., Mantovani, R., and Holt, B.F., 3rd (2014). A distal CCAAT/NUCLEAR FACTOR Y complex promotes chromatin looping at the FLOWERING LOCUS T promoter and regulates the timing of flowering in Arabidopsis. Plant Cell *26*, 1009-1017.

Carrera, E., Bou, J., Garcia-Martinez, J.L., and Prat, S. (2000). Changes in GA 20-oxidase gene expression strongly affect stem length, tuber induction and tuber yield of potato plants. Plant J *22*, 247-256.

Causier, B., Schwarz-Sommer, Z., and Davies, B. (2010). Floral organ identity: 20 years of ABCs. Semin Cell Dev Biol *21*, 73-79.

Clarke, S.M., Cristescu, S.M., Miersch, O., Harren, F.J., Wasternack, C., and Mur, L.A. (2009). Jasmonates act with salicylic acid to confer basal thermotolerance in Arabidopsis thaliana. New Phytol *182*, 175-187.

Cha, J.Y., Kim, J., Kim, T.S., Zeng, Q., Wang, L., Lee, S.Y., Kim, W.Y., and Somers, D.E. (2017). GIGANTEA is a co-chaperone which facilitates maturation of ZEITLUPE in the Arabidopsis circadian clock. Nat Commun *8*, 3.

Chailakhyan, M., Yanina, L., Devedzhyan, A., and Lotova, G. (1981). Photoperiodism and tuber formation in grafting of tobacco onto potato. Dokl Akad Nauk SSSR *257*, 1276-1280.

Chapman, H.W. (1958). Tuberization in the Potato Plant. Physiologia Plantarum *11*, 215-224.

Chautard, H., Jacquet, M., Schoentgen, F., Bureaud, N., and Bénédetti, H. (2004). Tfs1p, a Member of the PEBP Family, Inhibits the Ira2p but Not the Ira1p Ras GTPase-Activating Protein in Saccharomyces cerevisiae. Eukaryotic Cell *3*, 459-470.

Chen, S., Hajirezaei, M., and Bornke, F. (2005). Differential expression of sucrose-phosphate synthase isoenzymes in tobacco reflects their functional specialization during dark-governed starch mobilization in source leaves. Plant Physiol *139*, 1163-1174.

Chini, A., Fonseca, S., Fernandez, G., Adie, B., Chico, J.M., Lorenzo, O., Garcia-Casado, G., Lopez-Vidriero, I., Lozano, F.M., Ponce, M.R*., et al.* (2007). The JAZ family of repressors is the missing link in jasmonate signalling. Nature *448*, 666-671.

Chuck, G., Cigan, A.M., Saeteurn, K., and Hake, S. (2007). The heterochronic maize mutant Corngrass1 results from overexpression of a tandem microRNA. Nat Genet *39*, 544-549.

Chung, H.S., Koo, A.J., Gao, X., Jayanty, S., Thines, B., Jones, A.D., and Howe, G.A. (2008). Regulation and function of Arabidopsis JASMONATE ZIM-domain genes in response to wounding and herbivory. Plant Physiol *146*, 952-964.

Cutter, E.G. (1978). Structure and development of the potato plant. In The Potato Crop: The scientific basis for improvement, P.M. Harris, ed. (Boston, MA, Springer US), 70-152.

Dai, N., Schaffer, A., Petreikov, M., Shahak, Y., Giller, Y., Ratner, K., Levine, A., and Granot, D. (1999). Overexpression of Arabidopsis hexokinase in tomato plants inhibits growth, reduces photosynthesis, and induces rapid senescence. Plant Cell *11*, 1253-1266.

Danilevskaya, O.N., Meng, X., Selinger, D.A., Deschamps, S., Hermon, P., Vansant, G., Gupta, R., Ananiev, E.V., and Muszynski, M.G. (2008). Involvement of the MADS-box gene ZMM4 in floral induction and inflorescence development in maize. Plant Physiol *147*, 2054-2069.

David, K.M., Armbruster, U., Tama, N., and Putterill, J. (2006). Arabidopsis GIGANTEA protein is post-transcriptionally regulated by light and dark. FEBS Lett *580*, 1193-1197.

de Boer, A.H., van Kleeff, P.J., and Gao, J. (2013). Plant 14-3-3 proteins as spiders in a web of phosphorylation. Protoplasma *250*, 425-440.

de Lucas, M., Daviere, J.M., Rodriguez-Falcon, M., Pontin, M., Iglesias-Pedraz, J.M., Lorrain, S., Fankhauser, C., Blazquez, M.A., Titarenko, E., and Prat, S. (2008). A molecular framework for light and gibberellin control of cell elongation. Nature *451*, 480-484.

Dellaporta, S.L., Wood, J., and Hicks, J.B. (1983). A plant DNA minipreparation: Version II. Plant Molecular Biology Reporter *1*, 19-21.

Dobin, A., Davis, C.A., Schlesinger, F., Drenkow, J., Zaleski, C., Jha, S., Batut, P., Chaisson, M., and Gingeras, T.R. (2013). STAR: ultrafast universal RNA-seq aligner. Bioinformatics *29*, 15-21.

Doi, K., Izawa, T., Fuse, T., Yamanouchi, U., Kubo, T., Shimatani, Z., Yano, M., and Yoshimura, A. (2004). Ehd1, a B-type response regulator in rice, confers short-day promotion of flowering and controls FT-like gene expression independently of Hd1. Genes Dev *18*, 926-936.

Dreni, L., and Kater, M.M. (2014). MADS reloaded: evolution of the AGAMOUS subfamily genes. New Phytol *201*, 717-732.

Dwelle, R.B., Kleinkopf, G.E., and Pavek, J.J. (1981). Stomatal conductance and gross photosynthesis of potato (Solanum tuberosum L.) as influenced by irradiance, temperature, and growth stage. Potato Research *24*, 49-59.

Eimert, K., Wang, S.M., Lue, W.I., and Chen, J. (1995). Monogenic Recessive Mutations Causing Both Late Floral Initiation and Excess Starch Accumulation in Arabidopsis. Plant Cell *7*, 1703-1712.

El-Showk, S., Ruonala, R., and Helariutta, Y. (2013). Crossing paths: cytokinin signalling and crosstalk. Development *140*, 1373-1383.

Endo, M., Tanigawa, Y., Murakami, T., Araki, T., and Nagatani, A. (2013). PHYTOCHROME-DEPENDENT LATE-FLOWERING accelerates flowering through physical interactions with phytochrome B and CONSTANS. Proc Natl Acad of Sci U S A *110*, 18017-18022.

Estrada, R., Tovar, P., and Dodds, J.H. (1986). Induction of in vitro tubers in a broad range of potato genotypes. Plant Cell, Tissue and Organ Culture *7*, 3-10.

Eviatar-Ribak, T., Shalit-Kaneh, A., Chappell-Maor, L., Amsellem, Z., Eshed, Y., and Lifschitz, E. (2013). A cytokinin-activating enzyme promotes tuber formation in tomato. Curr Biol *23*, 1057-1064.

Faivre-Rampant, O., Cardle, L., Marshall, D., Viola, R., and Taylor, M.A. (2004). Changes in gene expression during meristem activation processes in Solanum tuberosum with a focus on the regulation of an auxin response factor gene. J Exp Bot *55*, 613-622.

Fernandez-Calvo, P., Chini, A., Fernandez-Barbero, G., Chico, J.M., Gimenez-Ibanez, S., Geerinck, J., Eeckhout, D., Schweizer, F., Godoy, M., Franco-Zorrilla, J.M.*, et al.* (2011). The Arabidopsis bHLH transcription factors MYC3 and MYC4 are targets of JAZ repressors and act additively with MYC2 in the activation of jasmonate responses. Plant Cell *23*, 701-715.

Ferrario, S., Busscher, J., Franken, J., Gerats, T., Vandenbussche, M., Angenent, G.C., and Immink, R.G. (2004). Ectopic expression of the petunia MADS box gene UNSHAVEN accelerates flowering and confers leaf-like characteristics to floral organs in a dominant-negative manner. Plant Cell *16*, 1490-1505.

Fornara, F., Panigrahi, K.C., Gissot, L., Sauerbrunn, N., Ruhl, M., Jarillo, J.A., and Coupland, G. (2009). Arabidopsis DOF transcription factors act redundantly to reduce CONSTANS expression and are essential for a photoperiodic flowering response. Dev Cell *17*, 75-86.

Fowler, S., Lee, K., Onouchi, H., Samach, A., Richardson, K., Morris, B., Coupland, G., and Putterill, J. (1999). GIGANTEA: a circadian clock-controlled gene that regulates photoperiodic flowering in Arabidopsis and encodes a protein with several possible membrane-spanning domains. Embo J *18*, 4679-4688.

Franklin, K.A., Lee, S.H., Patel, D., Kumar, S.V., Spartz, A.K., Gu, C., Ye, S., Yu, P., Breen, G., Cohen, J.D.*, et al.* (2011). Phytochrome-interacting factor 4 (PIF4) regulates auxin biosynthesis at high temperature. Proc Natl Acad Sci U S A *108*, 20231-20235.

Ghislain, M., Nunez, J., Herrera Mdel, R., and Spooner, D.M. (2009). The single Andigenum origin of Neo-Tuberosum potato materials is not supported by microsatellite and plastid marker analyses. TAG Theoretical and applied genetics Theoretische und angewandte Genetik *118*, 963-969.

Gonzalez-Grandio, E., Poza-Carrion, C., Sorzano, C.O., and Cubas, P. (2013). BRANCHED1 promotes axillary bud dormancy in response to shade in Arabidopsis. Plant Cell *25*, 834-850.

Gray, W.M., Ostin, A., Sandberg, G., Romano, C.P., and Estelle, M. (1998). High temperature promotes auxin-mediated hypocotyl elongation in Arabidopsis. Proc Natl Acad Sci U S A *95*, 7197-7202.

Guivarc'h, A., Rembur, J., Goetz, M., Roitsch, T., Noin, M., Schmulling, T., and Chriqui, D. (2002). Local expression of the ipt gene in transgenic tobacco (Nicotiana tabacum L. cv. SR1) axillary buds establishes a role for cytokinins in tuberization and sink formation. J Exp Bot *53*, 621-629.

Guo, M., Liu, J.H., Ma, X., Luo, D.X., Gong, Z.H., and Lu, M.H. (2016). The Plant Heat Stress Transcription Factors (HSFs): Structure, Regulation, and Function in Response to Abiotic Stresses. Front Plant Sci *7*, 114.

Hanano, S., and Goto, K. (2011). Arabidopsis TERMINAL FLOWER1 is involved in the regulation of flowering time and inflorescence development through transcriptional repression. Plant Cell *23*, 3172-3184.

Hancock, R.D., Morris, W.L., Ducreux, L.J., Morris, J.A., Usman, M., Verrall, S.R., Fuller, J., Simpson, C.G., Zhang, R., Hedley, P.E.*, et al.* (2014). Physiological, biochemical and molecular responses of the potato (Solanum tuberosum L.) plant to moderately elevated temperature. Plant Cell Environ *37*, 439-450.

Hanzawa, Y., Money, T., and Bradley, D. (2005). A single amino acid converts a repressor to an activator of flowering. Proc Natl Acad Sci U S A *102*, 7748-7753.

Harig, L., Beinecke, F.A., Oltmanns, J., Muth, J., Muller, O., Ruping, B., Twyman, R.M., Fischer, R., Prufer, D., and Noll, G.A. (2012). Proteins from the FLOWERING LOCUS T-like subclade of the PEBP family act antagonistically to regulate floral initiation in tobacco. Plant J *72*, 908-921.

Hartmann, A., Senning, M., Hedden, P., Sonnewald, U., and Sonnewald, S. (2011). Reactivation of meristem activity and sprout growth in potato tubers require both cytokinin and gibberellin. Plant Physiol *155*, 776-796.

Havaux, M. (1996). Short-term responses of Photosystem I to heat stress : Induction of a PS II-independent electron transport through PS I fed by stromal components. Photosynth Res *47*, 85-97.

Havaux, M., Tardy, F., Ravenel, J., Chanu, D., and Parot, P. (1996). Thylakoid membrane stability to heat stress studied by flash spectroscopic measurements of the electrochromic shift in intact potato leaves: influence of the xanthophyll content. Plant Cell Environ *19*, 1359-1368.

Hayama, R., Sarid-Krebs, L., Richter, R., Fernandez, V., Jang, S., and Coupland, G. (2017). PSEUDO RESPONSE REGULATORs stabilize CONSTANS protein to promote flowering in response to day length. Embo J *36*, 904-918.

Hayama, R., Yokoi, S., Tamaki, S., Yano, M., and Shimamoto, K. (2003). Adaptation of photoperiodic control pathways produces short-day flowering in rice. Nature *422*, 719-722.

Heijmans, K., Morel, P., and Vandenbussche, M. (2012). MADS-box genes and floral development: the dark side. J Exp Bot *63*, 5397-5404.

Helfer, A., Nusinow, D.A., Chow, B.Y., Gehrke, A.R., Bulyk, M.L., and Kay, S.A. (2011). LUX ARRHYTHMO encodes a nighttime repressor of circadian gene expression in the Arabidopsis core clock. Curr Biol *21*, 126-133.

Herbers, K., and Sonnewald, U. (1998). Molecular determinants of sink strength. Curr Opin Plant Biol *1*, 207-216.

Hijmans, R.J. (2003). The effect of climate change on global potato production. American Journal of Potato Research *80*, 271-279.

Hildmann, T., Ebneth, M., Pena-Cortes, H., Sanchez-Serrano, J.J., Willmitzer, L., and Prat, S. (1992). General roles of abscisic and jasmonic acids in gene activation as a result of mechanical wounding. Plant Cell *4*, 1157-1170.

Hornitschek, P., Kohnen, M.V., Lorrain, S., Rougemont, J., Ljung, K., Lopez-Vidriero, I., Franco-Zorrilla, J.M., Solano, R., Trevisan, M., Pradervand, S.*, et al.* (2012). Phytochrome interacting factors 4 and 5 control seedling growth in changing light conditions by directly controlling auxin signaling. Plant J *71*, 699-711.

Huijser, P., Klein, J., Lonnig, W.E., Meijer, H., Saedler, H., and Sommer, H. (1992). Bracteomania, an inflorescence anomaly, is caused by the loss of function of the MADS-box gene squamosa in Antirrhinum majus. Embo J *11*, 1239-1249.

Imaizumi, T., Schultz, T.F., Harmon, F.G., Ho, L.A., and Kay, S.A. (2005). FKF1 F-box protein mediates cyclic degradation of a repressor of CONSTANS in Arabidopsis. Science *309*, 293-297.

Inui, H., Ogura, Y., and Kiyosue, T. (2010). Overexpression of Arabidopsis thaliana LOV KELCH REPEAT PROTEIN 2 promotes tuberization in potato (Solanum tuberosum cv. May Queen). FEBS letters *584*, 2393-2396.

Irish, V.F. (2010). The flowering of Arabidopsis flower development. Plant J *61*, 1014-1028.

Itoh, H., Nonoue, Y., Yano, M., and Izawa, T. (2010). A pair of floral regulators sets critical day length for Hd3a florigen expression in rice. Nat Genet *42*, 635-638.

Izawa, T., Mihara, M., Suzuki, Y., Gupta, M., Itoh, H., Nagano, A.J., Motoyama, R., Sawada, Y., Yano, M., Hirai, M.Y.*, et al.* (2011). Os-GIGANTEA confers robust diurnal rhythms on the global transcriptome of rice in the field. Plant Cell *23*, 1741-1755.

Izawa, T., Oikawa, T., Sugiyama, N., Tanisaka, T., Yano, M., and Shimamoto, K. (2002). Phytochrome mediates the external light signal to repress FT orthologs in photoperiodic flowering of rice. Genes Dev *16*, 2006-2020.

Jackson, S.D. (2009). Plant responses to photoperiod. New Phytol *181*, 517-531.

Jackson, S.D., Heyer, A., Dietze, J., and Prat, S. (1996). Phytochrome B mediates the photoperiodic control of tuber formation in potato. Plant J *9*, 159-166.

Jackson, S.D., James, P., Prat, S., and Thomas, B. (1998). Phytochrome B affects the levels of a graft-transmissible signal involved in tuberization. Plant Physiol *117*, 29-32.

Jang, S., Marchal, V., Panigrahi, K.C., Wenkel, S., Soppe, W., Deng, X.W., Valverde, F., and Coupland, G. (2008). Arabidopsis COP1 shapes the temporal pattern of CO accumulation conferring a photoperiodic flowering response. Embo J *27*, 1277-1288.

Jansson, S. (1994). The light-harvesting chlorophyll a/b-binding proteins. Biochim Biophys Acta *1184*, 1-19.

Jefferson, R.A., Kavanagh, T.A., and Bevan, M.W. (1987). GUS fusions: beta-glucuronidase as a sensitive and versatile gene fusion marker in higher plants. Embo J *6*, 3901-3907.

Jing, H.C., Schippers, J.H., Hille, J., and Dijkwel, P.P. (2005). Ethylene-induced leaf senescence depends on age-related changes and OLD genes in Arabidopsis. J Exp Bot *56*, 2915-2923.

Jung, J.H., Ju, Y., Seo, P.J., Lee, J.H., and Park, C.M. (2012). The SOC1-SPL module integrates photoperiod and gibberellic acid signals to control flowering time in Arabidopsis. Plant J *69*, 577-588.

Jung, J.H., Seo, Y.H., Seo, P.J., Reyes, J.L., Yun, J., Chua, N.H., and Park, C.M. (2007). The GIGANTEA-regulated microRNA172 mediates photoperiodic flowering independent of CONSTANS in Arabidopsis. Plant Cell *19*, 2736-2748.

Kadam, S., Dhumal, S., and Jambhale, N. (1991). Structure, nutritional composition, and quality. In Potato production, processing and products, D. Salunkhe, S. Kadam, and S. Jadhav, eds. (Boca Raton, CRC Press).

Karlgren, A., Gyllenstrand, N., Kallman, T., Sundstrom, J.F., Moore, D., Lascoux, M., and Lagercrantz, U. (2011). Evolution of the PEBP gene family in plants: functional diversification in seed plant evolution. Plant Physiol *156*, 1967-1977.

Kaufmann, K., Muino, J.M., Jauregui, R., Airoldi, C.A., Smaczniak, C., Krajewski, P., and Angenent, G.C. (2009). Target genes of the MADS transcription factor SEPALLATA3: integration of developmental and hormonal pathways in the Arabidopsis flower. PLoS Biol *7*, e1000090.

Kaufmann, K., Pajoro, A., and Angenent, G.C. (2010). Regulation of transcription in plants: mechanisms controlling developmental switches. Nat Rev Genet *11*, 830-842.

Kawamoto, N., Endo, M., and Araki, T. (2015a). Expression of a kinase-dead form of CPK33 involved in florigen complex formation causes delayed flowering. Plant Signal Behav *10*, e1086856.

Kawamoto, N., Sasabe, M., Endo, M., Machida, Y., and Araki, T. (2015b). Calcium-dependent protein kinases responsible for the phosphorylation of a bZIP transcription factor FD crucial for the florigen complex formation. Sci Rep *5*, 8341.

Kawamura, H., Ito, S., Yamashino, T., Niwa, Y., Nakamichi, N., and Mizuno, T. (2008). Characterization of genetic links between two clock-associated genes, GI and PRR5 in the current clock model of Arabidopsis thaliana. Biosci Biotechnol Biochem *72*, 2770-2774.

Kim, W.Y., Fujiwara, S., Suh, S.S., Kim, J., Kim, Y., Han, L., David, K., Putterill, J., Nam, H.G., and Somers, D.E. (2007). ZEITLUPE is a circadian photoreceptor stabilized by GIGANTEA in blue light. Nature *449*, 356-360.

Kloosterman, B., Abelenda, J.A., Gomez Mdel, M., Oortwijn, M., de Boer, J.M., Kowitwanich, K., Horvath, B.M., van Eck, H.J., Smaczniak, C., Prat, S.*, et al.* (2013). Naturally occurring allele diversity allows potato cultivation in northern latitudes. Nature *495*, 246-250.

Kloosterman, B., De Koeyer, D., Griffiths, R., Flinn, B., Steuernagel, B., Scholz, U., Sonnewald, S., Sonnewald, U., Bryan, G.J., Prat, S.*, et al.* (2008). Genes driving potato tuber initiation and growth: identification based on transcriptional changes using the POCI array. Funct Integr Genomics *8*, 329-340.

Kloosterman, B., Navarro, C., Bijsterbosch, G., Lange, T., Prat, S., Visser, R.G., and Bachem, C.W. (2007). StGA2ox1 is induced prior to stolon swelling and controls GA levels during potato tuber development. Plant J *52*, 362-373.

Kloosterman, B., Vorst, O., Hall, R.D., Visser, R.G., and Bachem, C.W. (2005). Tuber on a chip: differential gene expression during potato tuber development. Plant Biotechnol J *3*, 505-519.

Knowles, N.R., Driskill Jr, E.P., and Knowles, L.O. (2009). Sweetening responses of potato tubers of different maturity to conventional and non-conventional storage temperature regimes. Postharvest Biology and Technology *52*, 49-61.

Kobayashi, K., Yasuno, N., Sato, Y., Yoda, M., Yamazaki, R., Kimizu, M., Yoshida, H., Nagamura, Y., and Kyozuka, J. (2012). Inflorescence meristem identity in rice is specified by overlapping functions of three AP1/FUL-like MADS box genes and PAP2, a SEPALLATA MADS box gene. Plant Cell *24*, 1848-1859.

Kobayashi, Y., Kaya, H., Goto, K., Iwabuchi, M., and Araki, T. (1999). A pair of related genes with antagonistic roles in mediating flowering signals. Science *286*, 1960-1962.

Kocal, N., Sonnewald, U., and Sonnewald, S. (2008). Cell wall-bound invertase limits sucrose export and is involved in symptom development and inhibition of photosynthesis during compatible interaction between tomato and Xanthomonas campestris pv vesicatoria. Plant Physiol *148*, 1523-1536.

Koini, M.A., Alvey, L., Allen, T., Tilley, C.A., Harberd, N.P., Whitelam, G.C., and Franklin, K.A. (2009). High temperature-mediated adaptations in plant architecture require the bHLH transcription factor PIF4. Curr Biol *19*, 408-413.

Kotake, T., Nakagawa, N., Takeda, K., and Sakurai, N. (2000). Auxin-induced elongation growth and expressions of cell wall-bound exo- and endo-beta-glucanases in barley coleoptiles. Plant Cell Physiol *41*, 1272-1278.

Krauss, A., and Marschner, H. (1984). Growth rate and carbohydrate metabolism of potato tubers exposed to high temperatures. Potato Research *27*, 297-303.

Krizek, B.A. (2001). Arabidopsis: Flower Development and Patterning. In eLS (John Wiley & Sons, Ltd).

Krizek, B.A., and Fletcher, J.C. (2005). Molecular mechanisms of flower development: an armchair guide. Nat Rev Genet *6*, 688-698.

Krogan, N.T., Hogan, K., and Long, J.A. (2012). APETALA2 negatively regulates multiple floral organ identity genes in Arabidopsis by recruiting the co-repressor TOPLESS and the histone deacetylase HDA19. Development *139*, 4180-4190.

Kumimoto, R.W., Zhang, Y., Siefers, N., and Holt, B.F., 3rd (2010). NF-YC3, NF-YC4 and NF-YC9 are required for CONSTANS-mediated, photoperiod-dependent flowering in Arabidopsis thaliana. Plant J *63*, 379-391.

Kurepa, J., Smalle, J., Van Montagu, M., and Inze, D. (1998). Oxidative stress tolerance and longevity in Arabidopsis: the late-flowering mutant gigantea is tolerant to paraquat. Plant J *14*, 759-764.

Kusaba, M., Tanaka, A., and Tanaka, R. (2013). Stay-green plants: what do they tell us about the molecular mechanism of leaf senescence. Photosynth Res *117*, 221-234.

Lafta, A.M., and Lorenzen, J.H. (1995). Effect of High Temperature on Plant Growth and Carbohydrate Metabolism in Potato. Plant Physiol *109*, 637-643.

Lampard, G.R., and Bergmann, D.C. (2007). A Shout-Out to Stomatal Development: How the bHLH Proteins SPEECHLESS, MUTE and FAMA Regulate Cell Division and Cell Fate. Plant Signal Behav *2*, 290-292.

Laubinger, S., Marchal, V., Le Gourrierec, J., Wenkel, S., Adrian, J., Jang, S., Kulajta, C., Braun, H., Coupland, G., and Hoecker, U. (2006). Arabidopsis SPA proteins regulate photoperiodic flowering and interact with the floral inducer CONSTANS to regulate its stability. Development *133*, 3213-3222.

Lazaro, A., Valverde, F., Pineiro, M., and Jarillo, J.A. (2012). The Arabidopsis E3 ubiquitin ligase HOS1 negatively regulates CONSTANS abundance in the photoperiodic control of flowering. Plant Cell *24*, 982-999.

Lee, J., and Lee, I. (2010). Regulation and function of SOC1, a flowering pathway integrator. J Exp Bot *61*, 2247-2254.

Lee, J., Oh, M., Park, H., and Lee, I. (2008). SOC1 translocated to the nucleus by interaction with AGL24 directly regulates leafy. Plant J *55*, 832-843.

Lee, R., Baldwin, S., Kenel, F., McCallum, J., and Macknight, R. (2013). FLOWERING LOCUS T genes control onion bulb formation and flowering. Nat Commun *4*, 2884.

Lee, S., Kim, J., Son, J.S., Nam, J., Jeong, D.H., Lee, K., Jang, S., Yoo, J., Lee, J., Lee, D.Y.*, et al.* (2003). Systematic reverse genetic screening of T-DNA tagged genes in rice for functional genomic analyses: MADS-box genes as a test case. Plant Cell Physiol *44*, 1403-1411.

Lefebvre, S., Lawson, T., Zakhleniuk, O.V., Lloyd, J.C., Raines, C.A., and Fryer, M. (2005). Increased sedoheptulose-1,7-bisphosphatase activity in transgenic tobacco plants stimulates photosynthesis and growth from an early stage in development. Plant Physiol *138*, 451-460.

Legris, M., Klose, C., Burgie, E.S., Rojas, C.C., Neme, M., Hiltbrunner, A., Wigge, P.A., Schafer, E., Vierstra, R.D., and Casal, J.J. (2016). Phytochrome B integrates light and temperature signals in Arabidopsis. Science *354*, 897-900.

Levey, S., and Wingler, A. (2005). Natural variation in the regulation of leaf senescence and relation to other traits in Arabidopsis. Plant Cell Environ *28*, 223-231.

Li, B., and Dewey, C.N. (2011). RSEM: accurate transcript quantification from RNA-Seq data with or without a reference genome. BMC Bioinformatics *12*, 323.

Li, D., Liu, C., Shen, L., Wu, Y., Chen, H., Robertson, M., Helliwell, C.A., Ito, T., Meyerowitz, E., and Yu, H. (2008). A repressor complex governs the integration of flowering signals in Arabidopsis. Dev Cell *15*, 110-120.

Li, J., Li, G., Wang, H., and Wang Deng, X. (2011). Phytochrome Signaling Mechanisms. The Arabidopsis Book / American Society of Plant Biologists *9*, e0148.

Li, Z., Palmer, W.M., Martin, A.P., Wang, R., Rainsford, F., Jin, Y., Patrick, J.W., Yang, Y., and Ruan, Y.L. (2012). High invertase activity in tomato reproductive organs correlates with enhanced sucrose import into, and heat tolerance of, young fruit. J Exp Bot *63*, 1155-1166.

Lian, H.L., He, S.B., Zhang, Y.C., Zhu, D.M., Zhang, J.Y., Jia, K.P., Sun, S.X., Li, L., and Yang, H.Q. (2011). Blue-light-dependent interaction of cryptochrome 1 with SPA1 defines a dynamic signaling mechanism. Genes Dev *25*, 1023-1028.

Lifschitz, E., and Eshed, Y. (2006). Universal florigenic signals triggered by FT homologues regulate growth and flowering cycles in perennial day-neutral tomato. J Exp Bot *57*, 3405-3414.

Lifschitz, E., Eviatar, T., Rozman, A., Shalit, A., Goldshmidt, A., Amsellem, Z., Alvarez, J.P., and Eshed, Y. (2006). The tomato FT ortholog triggers systemic signals that regulate growth and flowering and substitute for diverse environmental stimuli. Proc Natl Acad Sci U S A *103*, 6398-6403.

Liu, L., Liu, C., Hou, X., Xi, W., Shen, L., Tao, Z., Wang, Y., and Yu, H. (2012). FTIP1 is an essential regulator required for florigen transport. PLoS Biol *10*, e1001313.

Love, M.I., Huber, W., and Anders, S. (2014). Moderated estimation of fold change and dispersion for RNA-seq data with DESeq2. Genome Biol *15*, 550.

Lu, Y., Gehan, J.P., and Sharkey, T.D. (2005). Daylength and circadian effects on starch degradation and maltose metabolism. Plant Physiol *138*, 2280-2291.

Martin-Tryon, E.L., Kreps, J.A., and Harmer, S.L. (2007). GIGANTEA acts in blue light signaling and has biochemically separable roles in circadian clock and flowering time regulation. Plant Physiol *143*, 473-486.

Mehta, A., and Ezekiel, R. (2006). Potato storage: Need, present scenario, emerging technologies and future strategies: A critical appraisal. Journal of food science and technology-mysore *43*, 453-466.

Melzer, S., Lens, F., Gennen, J., Vanneste, S., Rohde, A., and Beeckman, T. (2008). Flowering-time genes modulate meristem determinacy and growth form in Arabidopsis thaliana. Nat Genet *40*, 1489-1492.

Messenguy, F., and Dubois, E. (2003). Role of MADS box proteins and their cofactors in combinatorial control of gene expression and cell development. Gene *316*, 1-21.

Millar, A.J., and Kay, S.A. (1996). Integration of circadian and phototransduction pathways in the network controlling CAB gene transcription in Arabidopsis. Proc Natl Acad Sci U S A *93*, 15491-15496.

Miller, G.L. (1959). Use of Dinitrosalicylic Acid Reagent for Determination of Reducing Sugar. Anal Chem *31*, 426-428.

Miller, J.D., Arteca, R.N., and Pell, E.J. (1999). Senescence-associated gene expression during ozone-induced leaf senescence in Arabidopsis. Plant Physiol *120*, 1015-1024.

Mishra, P., and Panigrahi, K.C. (2015). GIGANTEA - an emerging story. Front Plant Sci *6*, 8.

Mizoguchi, T., Wright, L., Fujiwara, S., Cremer, F., Lee, K., Onouchi, H., Mouradov, A., Fowler, S., Kamada, H., Putterill, J.*, et al.* (2005). Distinct roles of GIGANTEA in promoting flowering and regulating circadian rhythms in Arabidopsis. Plant Cell *17*, 2255-2270.

Mizuno, T., Nomoto, Y., Oka, H., Kitayama, M., Takeuchi, A., Tsubouchi, M., and Yamashino, T. (2014). Ambient temperature signal feeds into the circadian clock transcriptional circuitry through the EC night-time repressor in Arabidopsis thaliana. Plant Cell Physiol *55*, 958-976.

Molinero-Rosales, N., Latorre, A., Jamilena, M., and Lozano, R. (2004). SINGLE FLOWER TRUSS regulates the transition and maintenance of flowering in tomato. Planta *218*, 427-434.

Moore, B., Zhou, L., Rolland, F., Hall, Q., Cheng, W.H., Liu, Y.X., Hwang, I., Jones, T., and Sheen, J. (2003). Role of the Arabidopsis glucose sensor HXK1 in nutrient, light, and hormonal signaling. Science *300*, 332-336.

Morris, W.L., Hancock, R.D., Ducreux, L.J., Morris, J.A., Usman, M., Verrall, S.R., Sharma, S.K., Bryan, G., McNicol, J.W., Hedley, P.E.*, et al.* (2014). Day length dependent restructuring of the leaf transcriptome and metabolome in potato genotypes with contrasting tuberization phenotypes. Plant Cell Environ *37*, 1351-1363.

Mugford, S.T., Fernandez, O., Brinton, J., Flis, A., Krohn, N., Encke, B., Feil, R., Sulpice, R., Lunn, J.E., Stitt, M.*, et al.* (2014). Regulatory properties of ADP glucose pyrophosphorylase are required for adjustment of leaf starch synthesis in different photoperiods. Plant Physiol *166*, 1733-1747.

Murai, K., Miyamae, M., Kato, H., Takumi, S., and Ogihara, Y. (2003). WAP1, a wheat APETALA1 homolog, plays a central role in the phase transition from vegetative to reproductive growth. Plant Cell Physiol *44*, 1255-1265.

Navarro, C., Abelenda, J.A., Cruz-Oro, E., Cuellar, C.A., Tamaki, S., Silva, J., Shimamoto, K., and Prat, S. (2011). Control of flowering and storage organ formation in potato by FLOWERING LOCUS T. Nature *478*, 119-122.

Navarro, C., Cruz-Oro, E., and Prat, S. (2015). Conserved function of FLOWERING LOCUS T (FT) homologues as signals for storage organ differentiation. Curr Opin Plant Biol *23*, 45-53.

Niittyla, T., Messerli, G., Trevisan, M., Chen, J., Smith, A.M., and Zeeman, S.C. (2004). A previously unknown maltose transporter essential for starch degradation in leaves. Science *303*, 87-89.

Niwa, M., Daimon, Y., Kurotani, K., Higo, A., Pruneda-Paz, J.L., Breton, G., Mitsuda, N., Kay, S.A., Ohme-Takagi, M., Endo, M.*, et al.* (2013). BRANCHED1 interacts with FLOWERING LOCUS T to repress the floral transition of the axillary meristems in Arabidopsis. Plant Cell *25*, 1228-1242.

Nohales, M.A., and Kay, S.A. (2016). Molecular mechanisms at the core of the plant circadian oscillator. Nat Struct Mol Biol *23*, 1061-1069.

Notaguchi, M., Abe, M., Kimura, T., Daimon, Y., Kobayashi, T., Yamaguchi, A., Tomita, Y., Dohi, K., Mori, M., and Araki, T. (2008). Long-distance, graft-transmissible action of Arabidopsis FLOWERING LOCUS T protein to promote flowering. Plant Cell Physiol *49*, 1645-1658.

Nusinow, D.A., Helfer, A., Hamilton, E.E., King, J.J., Imaizumi, T., Schultz, T.F., Farre, E.M., and Kay, S.A. (2011). The ELF4-ELF3-LUX complex links the circadian clock to diurnal control of hypocotyl growth. Nature *475*, 398-402.

Oh, S.A., Park, J.H., Lee, G.I., Paek, K.H., Park, S.K., and Nam, H.G. (1997). Identification of three genetic loci controlling leaf senescence in Arabidopsis thaliana. Plant J *12*, 527-535.

Osorio, S., Ruan, Y.L., and Fernie, A.R. (2014). An update on source-to-sink carbon partitioning in tomato. Front Plant Sci *5*, 516.

Park, C.J., and Seo, Y.S. (2015). Heat Shock Proteins: A Review of the Molecular Chaperones for Plant Immunity. Plant Pathol J *31*, 323-333.

Park, D.H., Somers, D.E., Kim, Y.S., Choy, Y.H., Lim, H.K., Soh, M.S., Kim, H.J., Kay, S.A., and Nam, H.G. (1999). Control of circadian rhythms and photoperiodic flowering by the Arabidopsis GIGANTEA gene. Science *285*, 1579-1582.

Pasare, S.A., Ducreux, L.J., Morris, W.L., Campbell, R., Sharma, S.K., Roumeliotis, E., Kohlen, W., van der Krol, S., Bramley, P.M., Roberts, A.G.*, et al.* (2013). The role of the potato (Solanum tuberosum) CCD8 gene in stolon and tuber development. New Phytol *198*, 1108-1120.

Paul, M.J., and Foyer, C.H. (2001). Sink regulation of photosynthesis. J Exp Bot *52*, 1383-1400.

Pauwels, L., Barbero, G.F., Geerinck, J., Tilleman, S., Grunewald, W., Perez, A.C., Chico, J.M., Bossche, R.V., Sewell, J., Gil, E.*, et al.* (2010). NINJA connects the co-repressor TOPLESS to jasmonate signalling. Nature *464*, 788-791.

Petroni, K., Kumimoto, R.W., Gnesutta, N., Calvenzani, V., Fornari, M., Tonelli, C., Holt, B.F., 3rd, and Mantovani, R. (2012). The promiscuous life of plant NUCLEAR FACTOR Y transcription factors. Plant Cell *24*, 4777-4792.

Pfaffl, M.W. (2001). A new mathematical model for relative quantification in real-time RT-PCR. Nucleic acids research *29*, e45.

Pin, P.A., Benlloch, R., Bonnet, D., Wremerth-Weich, E., Kraft, T., Gielen, J.J., and Nilsson, O. (2010). An antagonistic pair of FT homologs mediates the control of flowering time in sugar beet. Science *330*, 1397-1400.

Pnueli, L., Carmel-Goren, L., Hareven, D., Gutfinger, T., Alvarez, J., Ganal, M., Zamir, D., and Lifschitz, E. (1998). The SELF-PRUNING gene of tomato regulates vegetative to reproductive switching of sympodial meristems and is the ortholog of CEN and TFL1. Development *125*, 1979-1989.

Pnueli, L., Gutfinger, T., Hareven, D., Ben-Naim, O., Ron, N., Adir, N., and Lifschitz, E. (2001). Tomato SP-interacting proteins define a conserved signaling system that regulates shoot architecture and flowering. Plant Cell *13*, 2687-2702.

Pose, D., Yant, L., and Schmid, M. (2012). The end of innocence: flowering networks explode in complexity. Curr Opin Plant Biol *15*, 45-50.

Pourtau, N., Jennings, R., Pelzer, E., Pallas, J., and Wingler, A. (2006). Effect of sugar-induced senescence on gene expression and implications for the regulation of senescence in Arabidopsis. Planta *224*, 556-568.

Pourtau, N., Mares, M., Purdy, S., Quentin, N., Ruel, A., and Wingler, A. (2004). Interactions of abscisic acid and sugar signalling in the regulation of leaf senescence. Planta *219*, 765-772.

Prange, R.K., McRae, K.B., Midmore, D.J., and Deng, R. (1990). Reduction in potato growth at high temperature: role of photosynthesis and dark respiration. American Potato Journal *67*, 357.

Prat, S., Frommer, W.B., Hofgen, R., Keil, M., Kossmann, J., Koster-Topfer, M., Liu, X.J., Muller, B., Pena-Cortes, H., Rocha-Sosa, M.*, et al.* (1990). Gene expression during tuber development in potato plants. FEBS Lett *268*, 334-338.

Quinn, P., and Williams, W. (1985). Environmentally induced changes in chloroplast membranes and their effects on photosynthetic function. In Photosynthetic Mechanisms and the Environment, J. Barber, and N. Baker, eds. (Amsterdam, Elsevier), 1–47.

Quint, M., Delker, C., Franklin, K.A., Wigge, P.A., Halliday, K.J., and van Zanten, M. (2016). Molecular and genetic control of plant thermomorphogenesis. Nat Plants *2*, 15190.

Rodriguez-Falcon, M., Bou, J., and Prat, S. (2006). Seasonal control of tuberization in potato: conserved elements with the flowering response. Annu Rev Plant Biol *57*, 151-180.

Rosin, F.M., Hart, J.K., Van Onckelen, H., and Hannapel, D.J. (2003). Suppression of a vegetative MADS box gene of potato activates axillary meristem development. Plant Physiol *131*, 1613-1622.

Roumeliotis, E., Kloosterman, B., Oortwijn, M., Kohlen, W., Bouwmeester, H.J., Visser, R.G., and Bachem, C.W. (2012a). The effects of auxin and strigolactones on tuber initiation and stolon architecture in potato. J Exp Bot *63*, 4539-4547.

Roumeliotis, E., Kloosterman, B., Oortwijn, M., Lange, T., Visser, R.G., and Bachem, C.W. (2013). Down regulation of StGA3ox genes in potato results in altered GA content and affect plant and tuber growth characteristics. J Plant Physiol *170*, 1228-1234.

Roumeliotis, E., Visser, R.G., and Bachem, C.W. (2012b). A crosstalk of auxin and GA during tuber development. Plant Signal Behav *7*, 1360-1363.

Rutitzky, M., Ghiglione, H.O., Cura, J.A., Casal, J.J., and Yanovsky, M.J. (2009). Comparative genomic analysis of light-regulated transcripts in the Solanaceae. BMC Genomics *10*, 60.

Sablowski, R. (2015). Control of patterning, growth, and differentiation by floral organ identity genes. J Exp Bot *66*, 1065-1073.

Sasidharan, R., and Pierik, R. (2010). Cell wall modification involving XTHs controls phytochrome-mediated petiole elongation in Arabidopsis thaliana. Plant Signal Behav *5*, 1491-1492.

Sawa, M., and Kay, S.A. (2011). GIGANTEA directly activates Flowering Locus T in Arabidopsis thaliana. Proc Natl Acad Sci U S A *108*, 11698-11703.

Sawa, M., Nusinow, D.A., Kay, S.A., and Imaizumi, T. (2007). FKF1 and GIGANTEA complex formation is required for day-length measurement in Arabidopsis. Science *318*, 261-265.

Sberger, J., and Humphries, E.C. (1965). The Influence of Removing Tubers on Dry-matter Production and Net Assimilation Rate of Potato Plants. Annals of Botany *29*, 579-588.

Searle, I., He, Y., Turck, F., Vincent, C., Fornara, F., Krober, S., Amasino, R.A., and Coupland, G. (2006). The transcription factor FLC confers a flowering response to vernalization by repressing meristem competence and systemic signaling in Arabidopsis. Genes Dev *20*, 898-912.

Sharma, P., Lin, T., and Hannapel, D.J. (2016). Targets of the StBEL5 Transcription Factor Include the FT Ortholog StSP6A. Plant Physiol *170*, 310-324.

Sheerin, D.J., Menon, C., zur Oven-Krockhaus, S., Enderle, B., Zhu, L., Johnen, P., Schleifenbaum, F., Stierhof, Y.D., Huq, E., and Hiltbrunner, A. (2015). Light-activated phytochrome A and B interact with members of the SPA family to promote photomorphogenesis in Arabidopsis by reorganizing the COP1/SPA complex. Plant Cell *27*, 189-201.

Shrestha, R., Gomez-Ariza, J., Brambilla, V., and Fornara, F. (2014). Molecular control of seasonal flowering in rice, arabidopsis and temperate cereals. Annals of botany *114*, 1445-1458.

Simon, S., Ruhl, M., de Montaigu, A., Wotzel, S., and Coupland, G. (2015). Evolution of CONSTANS Regulation and Function after Gene Duplication Produced a Photoperiodic Flowering Switch in the Brassicaceae. Mol Biol Evol *32*, 2284-2301.

Singh, A., Siddappa, S., Bhardwaj, V., Singh, B., Kumar, D., and Singh, B.P. (2015). Expression profiling of potato cultivars with contrasting tuberization at elevated temperature using microarray analysis. Plant Physiol Biochem *97*, 108-116.

Smaczniak, C., Immink, R.G., Angenent, G.C., and Kaufmann, K. (2012). Developmental and evolutionary diversity of plant MADS-domain factors: insights from recent studies. Development *139*, 3081-3098.

Smith, S.M., Fulton, D.C., Chia, T., Thorneycroft, D., Chapple, A., Dunstan, H., Hylton, C., Zeeman, S.C., and Smith, A.M. (2004). Diurnal changes in the transcriptome encoding enzymes of starch metabolism provide evidence for both transcriptional and posttranscriptional regulation of starch metabolism in Arabidopsis leaves. Plant Physiol *136*, 2687-2699.

Song, Y.H., Estrada, D.A., Johnson, R.S., Kim, S.K., Lee, S.Y., MacCoss, M.J., and Imaizumi, T. (2014). Distinct roles of FKF1, Gigantea, and Zeitlupe proteins in the regulation of Constans stability in Arabidopsis photoperiodic flowering. Proc Natl Acad Sci U S A *111*, 17672-17677.

Song, Y.H., Smith, R.W., To, B.J., Millar, A.J., and Imaizumi, T. (2012). FKF1 conveys timing information for CONSTANS stabilization in photoperiodic flowering. Science *336*, 1045-1049.

Sonnewald, S., and Sonnewald, U. (2014). Regulation of potato tuber sprouting. Planta *239*, 27-38.

Soyk, S., Muller, N.A., Park, S.J., Schmalenbach, I., Jiang, K., Hayama, R., Zhang, L., Van Eck, J., Jimenez-Gomez, J.M., and Lippman, Z.B. (2017). Variation in the flowering gene SELF PRUNING 5G promotes day-neutrality and early yield in tomato. Nat Genet *49*, 162-168.

Spooner, D.M., McLean, K., Ramsay, G., Waugh, R., and Bryan, G.J. (2005). A single domestication for potato based on multilocus amplified fragment length polymorphism genotyping. Proc Natl Acad Sci U S A *102*, 14694-14699.

Streb, S., and Zeeman, S.C. (2012). Starch Metabolism in Arabidopsis. The Arabidopsis Book / American Society of Plant Biologists *10*, e0160.

Sulpice, R., Flis, A., Ivakov, A.A., Apelt, F., Krohn, N., Encke, B., Abel, C., Feil, R., Lunn, J.E., and Stitt, M. (2014). Arabidopsis coordinates the diurnal regulation of carbon allocation and growth across a wide range of photoperiods. Mol Plant *7*, 137-155.

Sullivan, M.J., Petty, N.K., and Beatson, S.A. (2011). Easyfig: a genome comparison visualizer. Bioinformatics *27*, 1009-1010.

Suttle, J.C. (2004). Physiological regulation of potato tuber dormancy. American Journal of Potato Research *81*, 253-262.

Swarup, K., Benkova, E., Swarup, R., Casimiro, I., Peret, B., Yang, Y., Parry, G., Nielsen, E., De Smet, I., Vanneste, S.*, et al.* (2008). The auxin influx carrier LAX3 promotes lateral root emergence. Nat Cell Biol *10*, 946-954.

Takada, S., and Goto, K. (2003). Terminal flower2, an Arabidopsis homolog of heterochromatin protein1, counteracts the activation of flowering locus T by constans in the vascular tissues of leaves to regulate flowering time. Plant Cell *15*, 2856-2865.

Taoka, K., Ohki, I., Tsuji, H., Furuita, K., Hayashi, K., Yanase, T., Yamaguchi, M., Nakashima, C., Purwestri, Y.A., Tamaki, S.*, et al.* (2011). 14-3-3 proteins act as intracellular receptors for rice Hd3a florigen. Nature *476*, 332-335.

Taylor, S.A., Hofer, J.M., Murfet, I.C., Sollinger, J.D., Singer, S.R., Knox, M.R., and Ellis, T.H. (2002). PROLIFERATING INFLORESCENCE MERISTEM, a MADS-box gene that regulates floral meristem identity in pea. Plant Physiol *129*, 1150-1159.

Teo, C.J., Takahashi, K., Shimizu, K., Shimamoto, K., and Taoka, K.I. (2016). Potato Tuber Induction is Regulated by Interactions Between Components of a Tuberigen Complex. Plant Cell Physiol *58,* 365-374

Theissen, G., Melzer, R., and Rumpler, F. (2016). MADS-domain transcription factors and the floral quartet model of flower development: linking plant development and evolution. Development *143*, 3259-3271.

Tiwari, S.B., Shen, Y., Chang, H.C., Hou, Y., Harris, A., Ma, S.F., McPartland, M., Hymus, G.J., Adam, L., Marion, C.*, et al.* (2010). The flowering time regulator CONSTANS is recruited to the FLOWERING LOCUS T promoter via a unique cis-element. New Phytol *187*, 57-66.

Tsuji, H., Taoka, K., and Shimamoto, K. (2013). Florigen in rice: complex gene network for florigen transcription, florigen activation complex, and multiple functions. Curr Opin Plant Biol *16*, 228-235.

Turck, F., Fornara, F., and Coupland, G. (2008). Regulation and identity of florigen: FLOWERING LOCUS T moves center stage. Annu Rev Plant Biol *59*, 573-594.

Usadel, B., Nagel, A., Thimm, O., Redestig, H., Blaesing, O.E., Palacios-Rojas, N., Selbig, J., Hannemann, J., Piques, M.C., Steinhauser, D.*, et al.* (2005). Extension of the visualization tool MapMan to allow statistical analysis of arrays, display of corresponding genes, and comparison with known responses. Plant Physiol *138*, 1195-1204.

Van Dam, J., Kooman, P.L., and Struik, P.C. (1996). Effects of temperature and photoperiod on early growth and final number of tubers in potato (Solanum tuberosum L.). Potato Research *39*, 51-62.

Vanneste, S., and Friml, J. (2009). Auxin: a trigger for change in plant development. Cell *136*, 1005-1016.

Viczian, A., Klose, C., Ádám, É., and Nagy, F. (2016). New insights of red light-induced development. Plant Cell Environ

Viola, R., Pelloux, J., van der Ploeg, A., Gillespie, T., Marquis, N., Roberts, A.G., and Hancock, R.D. (2007). Symplastic connection is required for bud outgrowth following dormancy in potato (Solanum tuberosum L.) tubers. Plant Cell Environ *30*, 973-983.

Viola, R., Roberts, A.G., Haupt, S., Gazzani, S., Hancock, R.D., Marmiroli, N., Machray, G.C., and Oparka, K.J. (2001). Tuberization in potato involves a switch from apoplastic to symplastic phloem unloading. Plant Cell *13*, 385-398.

Visser, R.G., Jacobsen, E., Hesseling-Meinders, A., Schans, M.J., Witholt, B., and Feenstra, W.J. (1989). Transformation of homozygous diploid potato with an Agrobacterium tumefaciens binary vector system by adventitious shoot regeneration on leaf and stem segments. Plant molecular biology *12*, 329-337.

Visser, R.G.F., Vreugdenhil, D., Hendriks, T., and Jacobsen, E. (1994). Gene expression and carbohydrate content during stolon to tuber transition in potatoes (Solanum tuberosum). Physiologia Plantarum *90*, 285-292.

Volkert, K., Debast, S., Voll, L.M., Voll, H., Schiessl, I., Hofmann, J., Schneider, S., and Bornke, F. (2014). Loss of the two major leaf isoforms of sucrose-phosphate synthase in Arabidopsis thaliana limits sucrose synthesis and nocturnal starch degradation but does not alter carbon partitioning during photosynthesis. J Exp Bot *65*, 5217-5229.

Vrebalov, J., Ruezinsky, D., Padmanabhan, V., White, R., Medrano, D., Drake, R., Schuch, W., and Giovannoni, J. (2002). A MADS-box gene necessary for fruit ripening at the tomato ripening-inhibitor (rin) locus. Science *296*, 343-346.

Wang, K.L., Li, H., and Ecker, J.R. (2002). Ethylene biosynthesis and signaling networks. Plant Cell *14 Suppl*, S131-151.

Wasternack, C., and Hause, B. (2013). Jasmonates: biosynthesis, perception, signal transduction and action in plant stress response, growth and development. An update to the 2007 review in Annals of Botany. Annals of Botany *111*, 1021-1058.

Weise, S.E., van Wijk, K.J., and Sharkey, T.D. (2011). The role of transitory starch in C(3), CAM, and C(4) metabolism and opportunities for engineering leaf starch accumulation. J Exp Bot *62*, 3109-3118.

Wellmer, F., Graciet, E., and Riechmann, J.L. (2014). Specification of floral organs in Arabidopsis. J Exp Bot *65*, 1-9.

Wenkel, S., Turck, F., Singer, K., Gissot, L., Le Gourrierec, J., Samach, A., and Coupland, G. (2006). CONSTANS and the CCAAT box binding complex share a functionally important domain and interact to regulate flowering of Arabidopsis. Plant Cell *18*, 2971-2984.

Wickland, D.P., and Hanzawa, Y. (2015). The FLOWERING LOCUS T/TERMINAL FLOWER 1 Gene Family: Functional Evolution and Molecular Mechanisms. Mol Plant *8*, 983-997.

Wigge, P.A., Kim, M.C., Jaeger, K.E., Busch, W., Schmid, M., Lohmann, J.U., and Weigel, D. (2005). Integration of spatial and temporal information during floral induction in Arabidopsis. Science *309*, 1056-1059.

Wingler, A., Masclaux-Daubresse, C., and Fischer, A.M. (2009). Sugars, senescence, and ageing in plants and heterotrophic organisms. J Exp Bot *60*, 1063-1066.

Wolf, S., Marani, A., and Rudich, J. (1991). Effect of Temperature on Carbohydrate Metabolism in Potato Plants. J Exp Bot *42*, 619-625.

Wu, G., Park, M.Y., Conway, S.R., Wang, J.W., Weigel, D., and Poethig, R.S. (2009). The sequential action of miR156 and miR172 regulates developmental timing in Arabidopsis. Cell *138*, 750-759.

Xu, C., Luo, F., and Hochholdinger, F. (2016). LOB Domain Proteins: Beyond Lateral Organ Boundaries. Trends Plant Sci *21*, 159-167.

Xu, X., Pan, S., Cheng, S., Zhang, B., Mu, D., Ni, P., Zhang, G., Yang, S., Li, R., Wang, J.*, et al.* (2011). Genome sequence and analysis of the tuber crop potato. Nature *475*, 189-195.

Xu, X., van Lammeren, A.A., Vermeer, E., and Vreugdenhil, D. (1998a). The role of gibberellin, abscisic acid, and sucrose in the regulation of potato tuber formation in vitro. Plant Physiol *117*, 575-584.

Xu, X., Vreugdenhil, D., and Lammeren, A.A.M.v. (1998b). Cell division and cell enlargement during potato tuber formation. J Exp Bot *49*, 573-582.

Xue, W., Xing, Y., Weng, X., Zhao, Y., Tang, W., Wang, L., Zhou, H., Yu, S., Xu, C., Li, X.*, et al.* (2008). Natural variation in Ghd7 is an important regulator of heading date and yield potential in rice. Nat Genet *40*, 761-767.

Yamaguchi, A., Kobayashi, Y., Goto, K., Abe, M., and Araki, T. (2005). TWIN SISTER OF FT (TSF) acts as a floral pathway integrator redundantly with FT. Plant Cell Physiol *46*, 1175-1189.

Yang, D.L., Yao, J., Mei, C.S., Tong, X.H., Zeng, L.J., Li, Q., Xiao, L.T., Sun, T.P., Li, J., Deng, X.W.*, et al.* (2012). Plant hormone jasmonate prioritizes defense over growth by interfering with gibberellin signaling cascade. Proc Natl Acad Sci U S A *109*, E1192-1200.

Yang, L., Li, J., Ji, J., Li, P., Yu, L., Abd Allah, E.F., Luo, Y., Hu, L., and Hu, X. (2016). High Temperature Induces Expression of Tobacco Transcription Factor NtMYC2a to Regulate Nicotine and JA Biosynthesis. Front Physiol *7*, 465.

Yanovsky, M.J., Izaguirre, M., Wagmaister, J.A., Gatz, C., Jackson, S.D., Thomas, B., and Casal, J.J. (2000). Phytochrome A resets the circadian clock and delays tuber formation under long days in potato. Plant J *23*, 223-232.

Yeung, K., Seitz, T., Li, S., Janosch, P., McFerran, B., Kaiser, C., Fee, F., Katsanakis, K.D., Rose, D.W., Mischak, H.*, et al.* (1999). Suppression of Raf-1 kinase activity and MAP kinase signalling by RKIP. Nature *401*, 173-177.

Yu, J.W., Rubio, V., Lee, N.Y., Bai, S., Lee, S.Y., Kim, S.S., Liu, L., Zhang, Y., Irigoyen, M.L., Sullivan, J.A.*, et al.* (2008). COP1 and ELF3 control circadian function and photoperiodic flowering by regulating GI stability. Molecular cell *32*, 617-630.

Zhai, H., Lu, S., Liang, S., Wu, H., Zhang, X., Liu, B., Kong, F., Yuan, X., Li, J., and Xia, Z. (2014). GmFT4, a homolog of FLOWERING LOCUS T, is positively regulated by E1 and functions as a flowering repressor in soybean. PLoS One *9*, e89030.

Zhai, Q., Zhang, X., Wu, F., Feng, H., Deng, L., Xu, L., Zhang, M., Wang, Q., and Li, C. (2015). Transcriptional Mechanism of Jasmonate Receptor COI1-Mediated Delay of Flowering Time in Arabidopsis. Plant Cell *27*, 2814-2828.

Zhang, X., Zou, Z., Zhang, J., Zhang, Y., Han, Q., Hu, T., Xu, X., Liu, H., Li, H., and Ye, Z. (2011). Over-expression of sly-miR156a in tomato results in multiple vegetative and reproductive trait alterations and partial phenocopy of the sft mutant. FEBS letters *585*, 435-439.

Zhang, Y., Mayba, O., Pfeiffer, A., Shi, H., Tepperman, J.M., Speed, T.P., and Quail, P.H. (2013). A quartet of PIF bHLH factors provides a transcriptionally centered signaling hub that regulates seedling morphogenesis through differential expression-patterning of shared target genes in Arabidopsis. PLoS Genet *9*, e1003244.

Zrenner, R., Salanoubat, M., Willmitzer, L., and Sonnewald, U. (1995). Evidence of the crucial role of sucrose synthase for sink strength using transgenic potato plants (Solanum tuberosum L.). Plant J *7*, 97-107.

Zuo, Z., Liu, H., Liu, B., Liu, X., and Lin, C. (2011). Blue light-dependent interaction of CRY2 with SPA1 regulates COP1 activity and floral initiation in Arabidopsis. Curr Biol *21*, 841-847.

Annex 1: Supplemental Data

Supplemental file 1. Supplemental file 1 is a Microsoft Excel file included on the CD-ROM attached to this thesis containing all lists of DEGs used for functional enrichment, clustering and Venn diagram analysis.

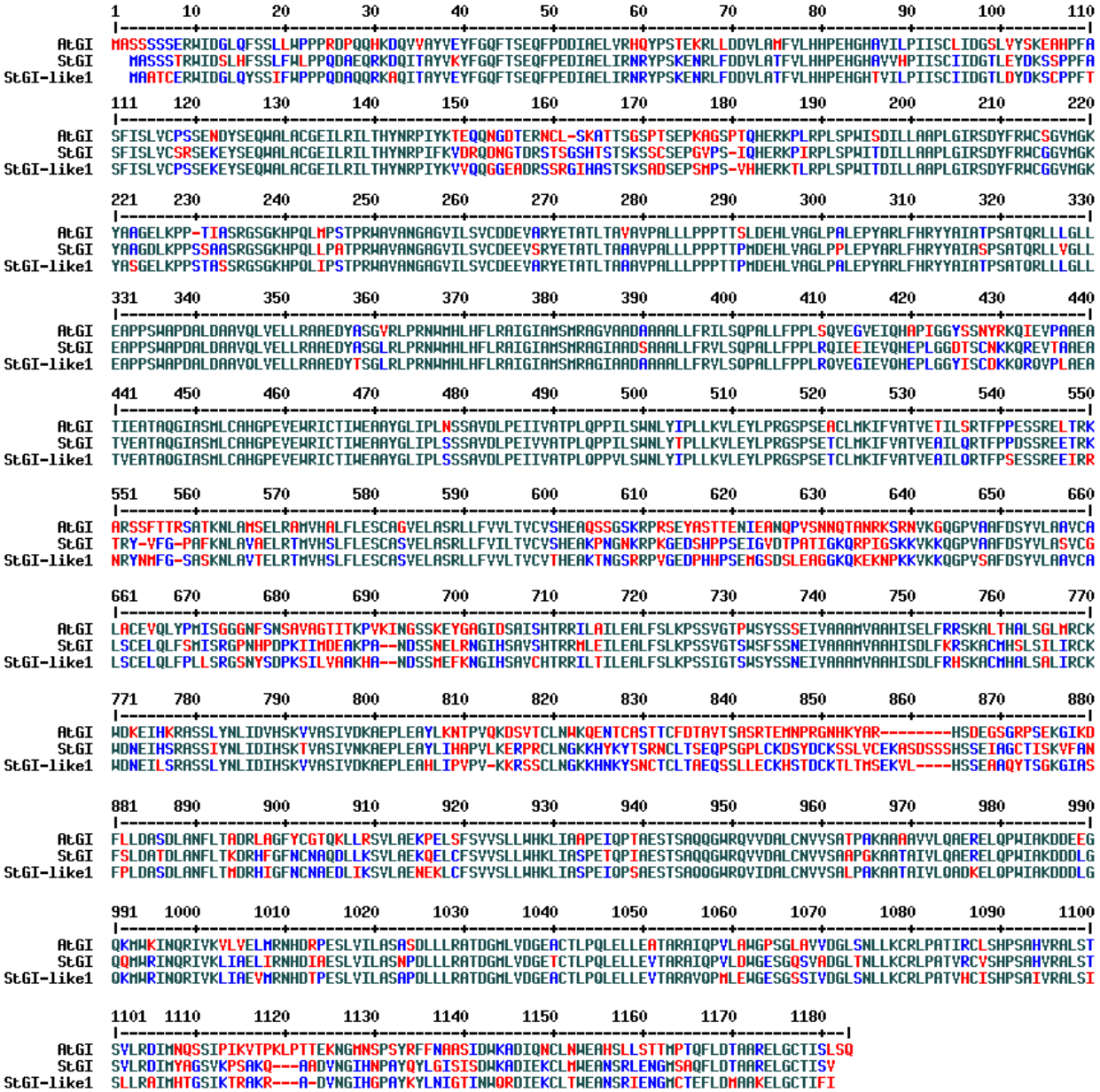

Figure S1. AtGI, StGI and StGI-like1 sequence comparison. (A) Amino acid sequence alignment of AtGI, StGI and StGI-like1 proteins. Protein sequences of StGI and StGI-like1 were obtained from *StGI* (chr12:54737061..54723121) and *StGI-like1* (chr04:61226774..61193170) predicted coding sequences.

A

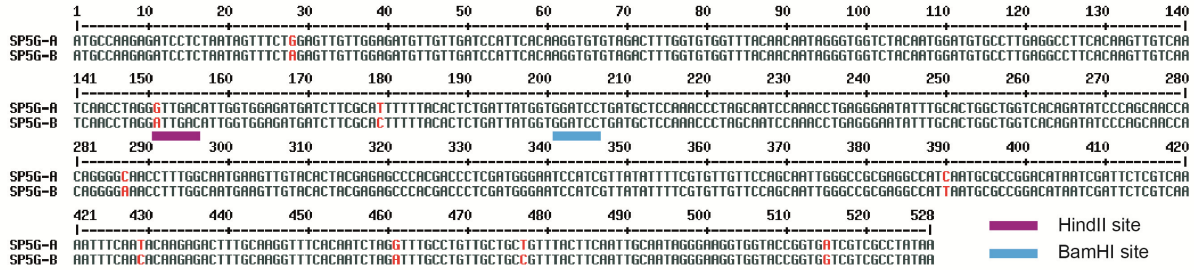

B

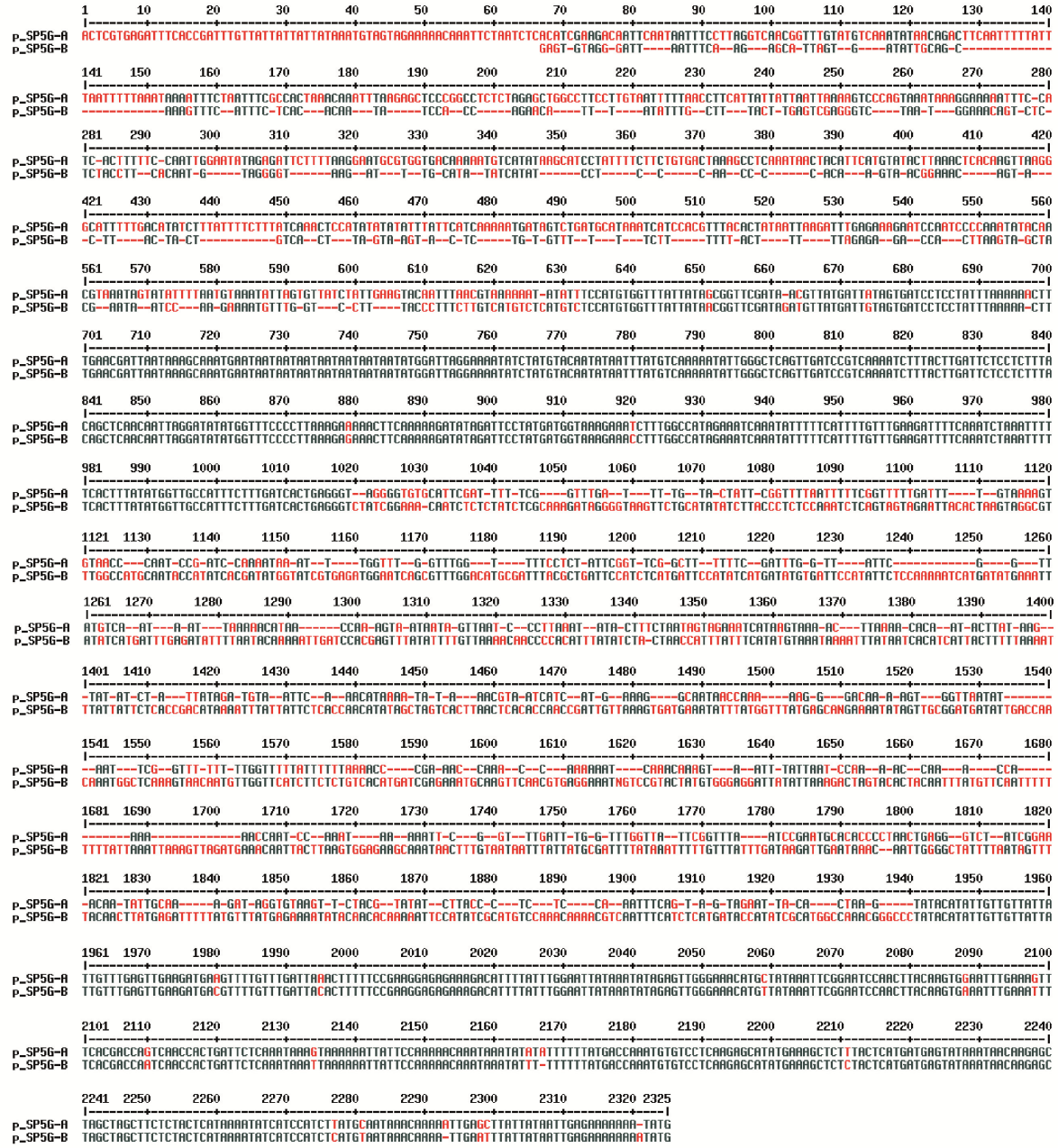

Figure S2. *StSP5G-A* and *StSP5G-B* sequence comparison. (A) Nucleotide sequence alignment of *StSP5G-A* and *StSP5G-B* coding DNA sequences. HindII and BamHI restriction sites are underlined in purple and blue respectively. (B) Nucleotide sequence alignment of *StSP5G-A* and *StSP5G-B* promoter sequences. Gene promoter regions were defined as 2007 bp up-stream of the start codon.

Annex 2: Publications